



# Biodegradable Polymersomes for Drug Delivery

Circulation Kinetics and Biodistribution,  
Modulated Drug Delivery and Cellular Uptake

Jung Seok Lee

# **BIODEGRADABLE POLYMERSOMES FOR DRUG DELIVERY**

**CIRCULATION KINETICS AND BIODISTRIBUTION, MODULATED DRUG  
DELIVERY AND CELLULAR UPTAKE**

**Jung Seok Lee**

The research described in this thesis was financially supported by the portfolio program 2004 of the University of Twente.

## Biodegradable Polymersomes for Drug Delivery

Circulation Kinetics and Biodistribution, Modulated Drug Delivery and Cellular Uptake

Jung Seok Lee

PhD Thesis, with references; with summary in English and in Dutch

University of Twente, Enschede, The Netherlands

May 2011

ISBN 978-90-365-3188-7

Copyright © 2011 by Jung Seok Lee. All rights reserved.

Cover pages were designed by Jung Seok Lee. The background for the cover pages was created by Peter Allen, UC Santa Barbara: [convergence.ucsb.edu](http://convergence.ucsb.edu).

Printed by Wöhrmann Print Service, Zutphen, The Netherlands

The printing of this thesis was sponsored by the Dutch Society for Biomaterials and Tissue Engineering (NBTE).

# **BIODEGRADABLE POLYMERSOMES FOR DRUG DELIVERY**

**CIRCULATION KINETICS AND BIODISTRIBUTION, MODULATED DRUG  
DELIVERY AND CELLULAR UPTAKE**

**DISSERTATION**

**to obtain  
the degree of doctor at the University of Twente,  
on the authority of the rector magnificus,  
prof. dr. H. Brinksma,  
on account of the decision of the graduation committee,  
to be publicly defended  
on Friday the 20<sup>th</sup> of May 2011 at 16:45**

**by**

**Jung Seok Lee**

**born on the 12<sup>th</sup> of December 1978  
in Mokpo, South Korea**

This dissertation has been approved by:

Promotor: Prof. Dr. J. Feijen

## Table of Contents

<b>Chapter 1.</b> General introduction	3
<b>Chapter 2.</b> Formation, Characterization and Design of Polymersomes for Drug Delivery	11
<b>Chapter 3.</b> Biodegradable Polymersomes as Carriers and Release Systems for Paclitaxel Using Oregon Green <sup>®</sup> 488 Labeled Paclitaxel as a Model Compound	45
<b>Chapter 4.</b> Thermosensitive Hydrogel-containing Polymersomes for Controlled Drug Delivery	69
<b>Chapter 5.</b> Time-Resolved Fluorescence and Fluorescence Anisotropy of Fluorescein Labeled Poly ( <i>N</i> -isopropylacrylamide) incorporated in Polymersomes	93
<b>Chapter 6.</b> Lysosomally Cleavable Peptide-containing Polymersomes Modified with anti-EGFR Antibody for Systemic Cancer Chemotherapy	109
<b>Chapter 7.</b> Circulation Kinetics and Biodistribution of Dual-Labeled Polymersomes with Modulated Surface Charge in Tumor-Bearing Mice: Comparison with Stealth Liposomes	135
<b>Conclusions and Future Perspectives</b>	155
<b>Summary</b>	157
<b>Samenvatting</b>	160
<b>Acknowledgements</b>	163
<b><i>Curriculum Vitae</i></b>	166





# Chapter 1

## General introduction

A well designed drug delivery system (DDS) is as important as the pharmacological activity of a drug since the therapeutic efficacy of many drugs is often limited in the administration by their bioavailability, solubility, stability and safety [1]. After administration of a drug only a very small fraction of the dose actually arrives at the target receptors or sites of action and usually most of the dose is wasted either by being taken up by other tissues or by decomposition before arrival [2]. DDS is used to administer a pharmaceutical compound to achieve an optimal therapeutic effect. This technology may involve control of drug release rate, improvement of therapeutic index, minimization of drug degradation and reduction of drug toxicity in the body offering means of optimizing therapy with established drugs [3]. In recent years, drug delivery is becoming a further demanding science because of the substantial decline in the rate of appearance of new drug entities [4]. For the development of new DDSs, strategies to improve patient acceptance or compliance have to be considered [5]. Common routes of DDSs include intravenous/muscular (injection), non-invasive peroral (through the mouth), topical (skin), transmucosal (nasal, buccal/sublingual, vaginal, ocular and rectal) and inhalation administration as shown in Fig. 1.1.



Figure 1.1. Examples of drug delivery systems



Polymers have gained a worldwide interest in DDS applications as the most versatile class of materials. Classically, they have mainly performed a valuable function as excipients in tablet and capsule formations [6]. However, the possibilities for polymers in the biomedical field changed drastically with the rapid development of polymer science, modern biochemistry and biomedicine after the 1950s [7]. The evolution moved the paradigm of polymers from synthetic plastic materials to pharmacologically active systems. Polymers are now capable of offering advanced and sophisticated functions, for instance, long circulation times in blood, local drug delivery, specific recognition and controlled cellular uptake of medicines [8]. Numerous types and structures of polymers can basically be synthesized providing a variety in design and development of advanced DDS. Functional multiblock copolymers, highly branched macromolecules, dendrimers with a wide variation of surface characteristics, biodegradable or stimuli-responsive systems have opened new possibilities [6, 8, 9]. So far, a large number of various polymers have been used to develop drug delivery devices such as patches, scaffolds, hydrogels, micro- or nanoparticulates, polymer-drug conjugates and micelles [10-17].

As a new generation of the polymer-based colloidal carriers, polymersomes (Ps) have attracted rapidly growing interest [18, 19]. Ps are artificial vesicles that contain an aqueous solution in the core surrounded by a bi-layer membrane. The bi-layer membrane is composed of hydrated hydrophilic coronas (e.g. poly(ethylene glycol (PEG)) both at the inside and outside of hydrophobic middle part of the membrane (Fig. 1.2). The aqueous core can be utilized for the encapsulation of therapeutic hydrophilic molecules and the membrane can integrate hydrophobic drugs within its hydrophobic part [20]. Due to the relatively thick membranes, Ps can be rather stable [21]. The presence of a hydrophilic PEG brush on the surface will reduce the protein adsorption onto the Ps during the blood circulation [22, 23]. Permeability, rate of degradation and stimuli-sensitivity of the membranes can be varied by using various biodegradable and/or stimuli-responsive block copolymers to modulate the release of the encapsulated drugs [24]. End groups of the PEG can be used to immobilize homing moieties like antibodies or RGD-containing peptides, which are able to recognize target cells or tissues [25, 26].

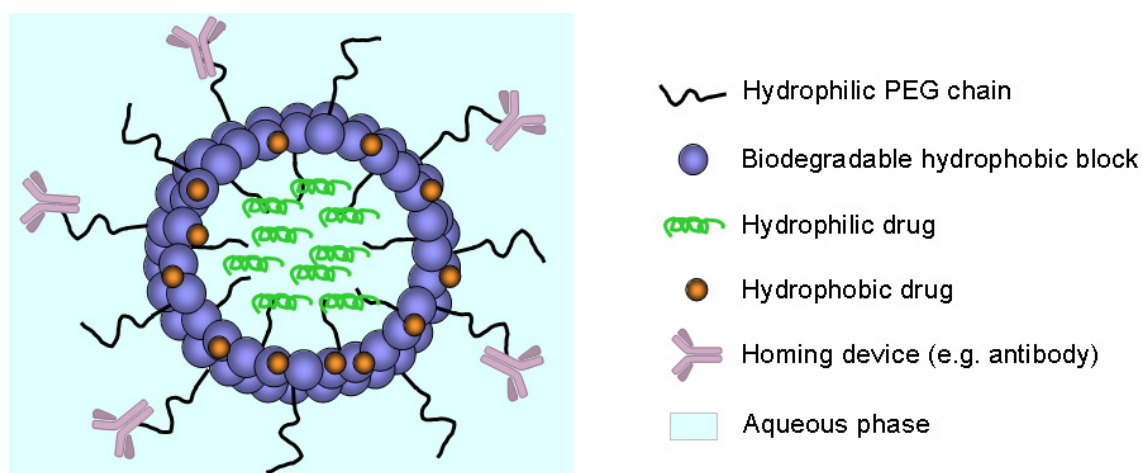


Figure 1.2. 2D cross-sectional schematic representation of a biodegradable polymersome modified by homing devices (antibody) and containing hydrophilic and/or hydrophobic drugs. The polymersome is composed of a bi-layer membrane surrounding an aqueous core. The bi-layer membrane has hydrated hydrophilic layers (PEG) both at the in- and outside of the biodegradable hydrophobic inner layer (in blue). Hydrophilic and hydrophobic compounds can be loaded in the aqueous core and in the membrane, respectively.

### Aim of the thesis

The aims of work described in this thesis are:

- to modulate the release of drugs from biodegradable polymersomes by varying the membrane composition or by introducing thermo-sensitive hydrogels
- to evaluate the circulation kinetics, organ distribution and tumor accumulation of polymersomes as a function of the surface charge in comparison with stealth liposomes
- to design, prepare and characterize lysosomally destabilizable polymersomes that contain a cleavable peptide sequence within the membrane and to immobilize targeting molecules (e.g. antibody) on the surface of the polymersomes.

## Structure of the thesis

In this thesis, the development and characterization of new polymersomes systems are described. To explore their feasibility as drug delivery systems, these polymersomes were used for the release of model drugs, *in vitro* cell experiments as well as *in vivo* animal studies.

A general introduction is presented in **Chapter 1**, providing the aim and general background of the work, and the structure of the thesis. In **Chapter 2**, criteria for the formation of polymersomes, their characterization as well as an overview of previously studied polymersomes is given. Also various block copolymers that are responsive to pH, temperature, redox conditions, light, magnetic field, ionic strength and the concentration of glucose and that are used to prepare biodegradable and/or stimuli-responsive polymersomes are discussed in this chapter.

In **Chapters 3 and 4**, strategies to modulate the release of drugs from polymersomes by modification of the membrane permeability and the formation of a hydrogel inside the polymersomes are described. Two biodegradable block copolymers, methoxy PEG-b-poly(*D,L*-lactide) (mPEG-PDLLA) and mPEG-b-poly( $\epsilon$ -caprolactone) (mPEG-PCL), were used to prepare three types of polymersomes to investigate the loading and release of fluorescent labeled paclitaxel (**Chapter 3**). A thermosensitive hydrogel based on poly(*N*-isopropylacrylamide) (PNIPAAm) was introduced into polymersomes to modify the interior properties and the membrane permeability (**Chapter 4**). The effect of the hydrogel on the release of the model compound, fluorescein isothiocyanate labeled dextran (MW 4000 g/mol, FD4) from the gel-containing polymersomes (hydrosomes) was studied and presented in the chapter. In order to characterize the temperature dependent formation of a PNIPAAm hydrogel inside polymersomes, the photo-physical properties of fluorescein isothiocyanate (FITC) covalently bound to PNIPAAm and located in the polymersomes was monitored in time by using time-resolved fluorescence techniques. The results of this study are presented in **Chapter 5**.

In **Chapter 6**, novel polymersomes based on a block copolymer of mPEG and PDLLA in which a peptide sequence, Phe-Gly-Leu-Phe-Gly (FGLFG), was introduced in between the two blocks (mPEG-pep-PDLLA) are presented. The peptide sequence is cleavable by lysosomal enzymes either present in extracellular tumor tissue or in the lysosomal compartments of tumor cells. Anti-epidermal growth factor receptor antibody (abEGFR) was coupled onto polymersomes prepared by using mPEG-pep-PDLLA to enhance the endocytic uptake into SKBR3 breast cancer cells. FD with a molecular weight of 40,000 g/mol (FD40) was

encapsulated into the polymersomes and the intracellular release was investigated by using confocal laser scanning microscopy.

In **Chapter 7**, the circulation kinetics and biodistribution of polymersomes with modulated surface charge in tumor-bearing mice are reported. For the study, dual labeled polymersomes were prepared by encapsulating  $^3\text{H}$ -dextran (70,000 g/mol) in the aqueous core and by post-coupling of  $^{14}\text{C}$ -thioglycolic acid onto acrylamide PEG chains of the polymersomes. The surface charge of the polymersomes was modulated by coupling of thioglycolic acid onto polymersomes containing different molar ratios of acrylamide PEG. Dipalmitoyl phosphatidylcholine (DPPC)/cholesterol based stealth liposomes with 7.5 % of PEG distearoyl phosphatidylethanolamine (PEG-DSPE) were also included in the study as a reference. The work described in this thesis has either been published or has been submitted or to be submitted for publication [27-31].

## References

- [1] A.S. Hoffman, The origins and evolution of "controlled" drug delivery systems. *J. Control. Release* 132(3) (2008) 153-163.
- [2] J. Kreuter, *Colloidal Drug Delivery Systems*, Marcel Dekker, New York, 1994.
- [3] M. Malmsten, *Surfactants and polymers in drug delivery*, Marcel Dekker, New York, 2002.
- [4] P. Johnson, J.G. Lloyed-Jones, *Drug Delivery System: Fundamental and Techniques*, Ellis Horwood, Chichester, 1987.
- [5] J.R. Robinson, V.H.L. Lee, *Controlled Drug Delivery: Fundamentals and Applications*, Marcel Dekker, New York, 1987.
- [6] O. Pillai, R. Panchagnula, Polymers in drug delivery. *Curr. Opin. Chem. Biol.* 5(4) (2001) 447-451.
- [7] I.F. Uchegbu, A.G. Schatzlein, *Polymers in Drug Delivery*, CRC Press, Boca Raton, 2006.
- [8] W.B. Liechty, D.R. Kryscio, B.V. Slaughter, N.A. Peppas, Polymers for Drug Delivery Systems. *Annu. Rev. Chem. Biomolec. Eng.* 1 (2010) 149-173.
- [9] C.M. Paleos, D. Tsiourvas, Z. Sideratou, L.A. Tziveleka, Drug delivery using multifunctional dendrimers and hyperbranched polymers. *Expert Opin. Drug Deliv.* 7(12) (2010) 1387-1398.
- [10] A.D. Keith, Polymer Matrix Considerations for Transdermal Devices. *Drug Dev. Ind. Pharm.* 9(4) (1983) 605-625.
- [11] J.H. Park, M.G. Allen, M.R. Prausnitz, Biodegradable polymer microneedles: Fabrication, mechanics and transdermal drug delivery. *J. Control. Release* 104(1) (2005) 51-66.
- [12] H.Y. Cheung, K.T. Lau, T.P. Lu, D. Hui, A critical review on polymer-based bio-engineered materials for scaffold development. *Compos. Pt. B-Eng.* 38(3) (2007) 291-300.
- [13] N.S. Satarkar, D. Biswal, J.Z. Hilt, Hydrogel nanocomposites: a review of applications as remote controlled biomaterials. *Soft Matter* 6(11) (2010) 2364-2371.
- [14] S. Ahmed, F.R. Jones, A Review of Particulate Reinforcement Theories for Polymer Composites. *J. Mater. Sci.* 25(12) (1990) 4933-4942.
- [15] J. Kopecek, P. Kopeckova, HEMA copolymers: Origins, early developments, present, and future. *Adv. Drug Deliv. Rev.* 62(2) (2010) 122-149.
- [16] H. Maeda, Review on the development of a polymer conjugate drug: SMANCS. *Med. Chem.* (1997) 197-204.
- [17] K. Kataoka, A. Harada, Y. Nagasaki, Block copolymer micelles for drug delivery: design, characterization and biological significance. *Adv. Drug Deliv. Rev.* 47(1) (2001) 113-131.
- [18] F. Ahmed, P.J. Photos, D.E. Discher, Polymersomes as viral capsid mimics. *Drug Dev. Res.* 67(1) (2006) 4-14.
- [19] D.E. Discher, A. Eisenberg, Polymer vesicles. *Science* 297(5583) (2002) 967-973.
- [20] M. Antonietti, S. Forster, Vesicles and liposomes: A self-assembly principle beyond lipids. *Adv. Mater.* 15(16) (2003) 1323-1333.
- [21] H. Bermudez, A.K. Brannan, D.A. Hammer, F.S. Bates, D.E. Discher, Molecular weight dependence of polymersome membrane structure, elasticity, and stability. *Macromolecules* 35(21) (2002) 8203-8208.
- [22] F.H. Meng, G.H.M. Engbers, A. Gessner, R.H. Muller, J. Feijen, Pegylated polystyrene particles as a model system for artificial cells. *J. Biomed. Mater. Res. Part A* 70A(1) (2004) 97-106.
- [23] P.J. Photos, L. Bacakova, B. Discher, F.S. Bates, D.E. Discher, Polymer vesicles in vivo: correlations with PEG molecular weight. *J. Control. Release* 90(3) (2003) 323-334.

- [24] F.H. Meng, Z.Y. Zhong, J. Feijen, Stimuli-Responsive Polymersomes for Programmed Drug Delivery. *Biomacromolecules* 10(2) (2009) 197-209.
- [25] Z.Y. Hu, F. Luo, Y.F. Pan, C. Hou, L.F. Ren, J.J. Chen, J.W. Wang, Y.D. Zhang, Arg-Gly-Asp (RGD) peptide conjugated poly(lactic acid)-poly(ethylene oxide) micelle for targeted drug delivery. *J. Biomed. Mater. Res. Part A* 85A(3) (2008) 797-807.
- [26] M. Pechar, K. Ulbrich, M. Jelinkova, B. Rihova, Conjugates of antibody-targeted PEG multiblock polymers with doxorubicin in cancer therapy. *Macromol. Biosci.* 3(7) (2003) 364-372.
- [27] J.S. Lee, M. Ankone, E. Pieters, R.M. Schiffelers, W.E. Hennink, J. Feijen, Circulation Kinetics and Biodistribution of Dual-Labeled Polymersomes with modulated Surface Charge in Tumor-Bearing Mice: Comparison with Stealth Liposomes. submitted to *J. Control. Release*.
- [28] J.S. Lee, C. Cusan, T. Groothuis, J. Feijen, Lysosomally Cleavable Peptide-containing Polymersomes modified with anti-EGFR Antibody for Systemic Cancer Chemotherapy. to be submitted to *Macromolecules*.
- [29] J.S. Lee, J. Feijen, Biodegradable Polymersomes as Carriers and Release Systems for Paclitaxel Using Fluorescein Labeled Paclitaxel as a Model Compound. to be submitted to *J. Control. Release*.
- [30] J.S. Lee, R.B.M. Koehorst, H. Amerongen, J. Feijen, Time-Resolved Fluorescence and Fluorescence Anisotropy of Fluorescein Labeled Poly (N-isopropylacrylamide) incorporated in Polymersomes. to be submitted to *J. Phys. Chem. B*.
- [31] J.S. Lee, W. Zhou, F.H. Meng, D.W. Zhang, C. Otto, J. Feijen, Thermosensitive hydrogel-containing polymersomes for controlled drug delivery. *J. Control. Release* 146(3) (2010) 400-408.





# *Chapter 2*

## **Formation, Characterization and Design of Polymersomes for Drug Delivery**

### **Introduction**

Polymersomes (Ps) are a class of artificial vesicles made from synthetic amphiphilic block copolymers [1-3]. Typical Ps are hollow spheres that contain an aqueous solution in the core surrounded by a bi-layer membrane. The bi-layer membrane is composed of hydrated hydrophilic coronas both at the inside and outside of the hydrophobic middle part of the membrane separating and protecting the fluidic core from the outside medium (Fig. 2.1). The aqueous core can be utilized for the encapsulation of therapeutic molecules such as drugs, enzymes, other proteins and peptides, and DNA and RNA fragments [4-9]. The membrane can integrate hydrophobic drugs within its hydrophobic core [10-12]. The possibility to load drugs into Ps has been highlighted for a number of applications in medicine, pharmacy, and biotechnology.

It is well known that Ps are rather stable and that they may have rather long blood circulation times [13-15]. In general, synthetic block copolymers have been used for the preparation of Ps [16, 17]. The composition and molecular weight of these polymers can be varied, which allows not only the preparation of Ps with different properties and responsiveness to stimuli but also Ps with different membrane thicknesses and permeabilities [18-20]. Usually, Ps have relatively thick and robust membranes (2-50 nm) formed by amphiphilic block copolymers with a relatively high molecular weight [3, 21-24]. Relatively long blood circulation times of Ps can be accomplished by the introduction of a hydrophilic surface layer for instance by poly(ethylene glycol) (PEG) blocks [14, 25, 26]. Carriers with a PEG brush on the surface are generally considered to have “stealth character” due to minimization of the interfacial free energy and the steric repulsion provided by the PEG molecules [27-29].

Based on their multi drug loading capacity, membrane robustness and stealth properties Ps are highly interesting for drug delivery applications. A lot of work has been directed to develop Ps for targeted drug delivery [30-34]. In particular, the development of stimuli-responsive Ps to further control the release of drugs by switching the stability and permeability of the membrane has attracted a lot of interest. Up to now, various block copolymers that are responsive to pH, temperature, redox conditions, light, magnetic field, ionic strength and concentration of glucose have been synthesized and used to prepare biodegradable and/or stimuli-responsive Ps. For site-specific drug delivery, it is also important to guide Ps to the specific target area and to enhance their interaction with specific cells in this area [35-38]. This can be achieved by introducing targeting moieties, for example, antibodies, antibody fragments, or RGD-containing peptides on the surface of the Ps [30, 39-41]. These Ps can release drugs by external stimuli after arrival at the target site enhancing the therapeutic efficacy and minimizing possible side effects. In order to design such Ps, it is necessary to understand the requirements for the polymers to be used and the techniques for the formation of Ps. In this chapter, criteria for the formation of Ps, their characterization as well as an overview of Ps that have been previously studied as drug delivery systems will be given.

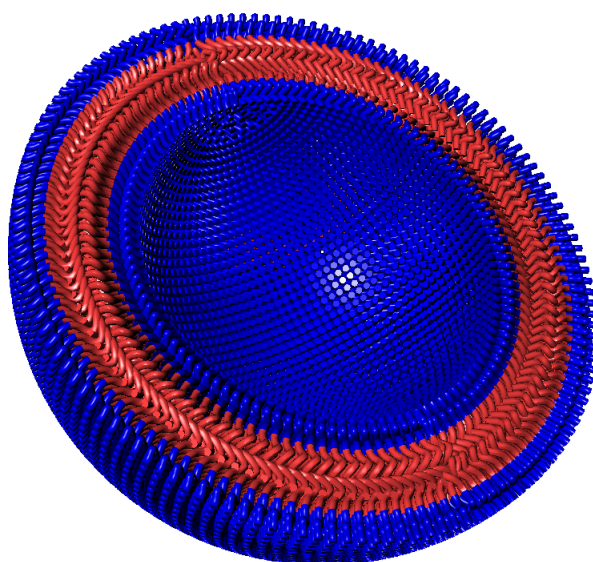


Figure 2.1. Schematic illustration of a 3D cross-section of a polymersome with a bi-layer membrane based on block copolymers. The membrane is composed of hydrated hydrophilic coronas (in blue) both at the in- and outside of the hydrophobic polymer core of the membrane (in red), which separates and protects the aqueous core from the surrounding environment.

### **Preparation methods for polymersomes**

Many techniques can be used to prepare Ps by self-assembly of amphiphilic block copolymers. The most important preparation methods are generally classified into two groups: solvent-switching techniques and polymer rehydration techniques [2, 3, 42-44]. Using the solvent-switch techniques, Ps are formed by first dissolving block copolymers in an organic solvent, which is a good solvent for all the blocks present, followed by hydration of the solution. The hydration can be done by either slowly adding water to the organic polymer solution or by injecting the organic solution into water. This procedure renders the hydrophobic blocks insoluble, triggering copolymer self-assembly into Ps as a result of increasing interfacial tension between the hydrophobic blocks and water [45-47]. Therefore, this technique is also called as 'phase inversion'. The size and size distribution of the vesicles can be varied by selecting different organic solvents [48].

Polymer rehydration techniques are based on the hydration of amphiphilic block copolymer films to induce self-assembly. Polymers are first dissolved in an organic solvent and then a thin film is prepared by evaporation of the organic solvent. Subsequently, the film is hydrated by the addition of water. The steps in the formation of Ps by the hydration procedure are water permeation through defects in the polymer layers driven by hydration forces, inflation of polymer layers and formation of bulges, which finally yield vesicles upon separation from the surface [42, 43]. Typically, this method produces Ps with a broad size distribution and therefore the Ps obtained are subsequently sized by sequential extrusion through filters with different pore sizes using a high pressure [44, 49]. To produce Ps with a relatively narrow size distribution, an electrical field (AC) has been applied [50-52]. The rate of water diffusion across the polymer film can be enhanced by the application of an alternating current and in this way control of the hydration rate of the amphiphilic polymer film is possible [53].

In principle, amphiphilic block copolymers can self-assemble into a wide range of morphologies upon hydration of the copolymer including spherical, cylindrical micelles or vesicles [1, 2, 54]. The mass or volume fraction of the hydrophilic block of the block copolymer ( $f$ ) and the interaction parameter of its hydrophobic block with H<sub>2</sub>O ( $\chi$ ) are known to be critical parameters to determine the morphology of the self-assembled system [55, 56]. For block copolymers with a high  $\chi$ , vesicular structures are favored when  $f$  of PEG ( $f_{\text{PEG}}$ ) is 10-40 %. At  $f_{\text{PEG}} = 45-55$  %, cylindrical micelles tend to form, and at  $f_{\text{PEG}} = 55-70$  %, spherical micelles are

predominantly formed. In the classical description, the curvature of the hydrophobic-hydrophilic interface as described by its mean curvature ( $H$ ) and its Gaussian curvature ( $K$ ) are related to the packing parameter ( $p$ ), equations 2.1 and 2.2, in which  $v$  is the volume of the hydrophobic part of the polymer,  $a$  the interfacial area per molecule and  $l$  the chain length of the hydrophobic part of the polymer normalized to the interface [1, 2, 57, 58].

$$\frac{v}{al} = 1 + Hl + \frac{Kl^2}{3}, \quad p = v/(al) \quad (2.1 \text{ and } 2.2)$$

Different morphologies correspond to different values of  $p$ , for instance,  $p \leq 1/3$  (spheres),  $1/3 \leq p \leq 1/2$  (cylinders) and  $1/2 \leq p \leq 1$  (vesicles).

However, vesicular formation can also be influenced by the preparation methods and conditions like polymer concentration, the type of organic solvent and the volume ratio of solvent and water [59-61]. Fig. 2.2 represents a phase diagram for poly(styrene)-*b*-poly(acrylic acid), (PS-PAA) in dioxane/water [62]. For PS<sub>310</sub>-PAA<sub>52</sub>, the concentration of the polymer was varied from approximately 0.1 to 10 wt.% . The solid lines are the phase boundaries determined from TEM pictures, while the dotted line is the micellization curve obtained by static light scattering (SLS) measurements. The upper graph (Fig. 2.2A) shows regions of stable morphologies by plotting the logarithm of the polymer concentration versus the water content. The lower graph (Fig. 2.2B) is part of the classical ternary phase diagram. At relatively high water contents, the formation of vesicles is favored. The addition of water increases the interfacial tension and drives the aggregation of the hydrophobic PS blocks. Changing the composition of the solvent mixture, like increasing the water concentration, leads to morphological changes from spheres to rods to vesicles. The characteristics of polymers to be used also have to be considered for the choice of the preparation technique. For example, block copolymers of which the hydrophobic blocks have a high glass transition temperature ( $T_g$ ) cannot directly form Ps by using the polymer rehydration method [63]. An organic solvent has to be used to lower the  $T_g$  to provide sufficient chain mobility [34].

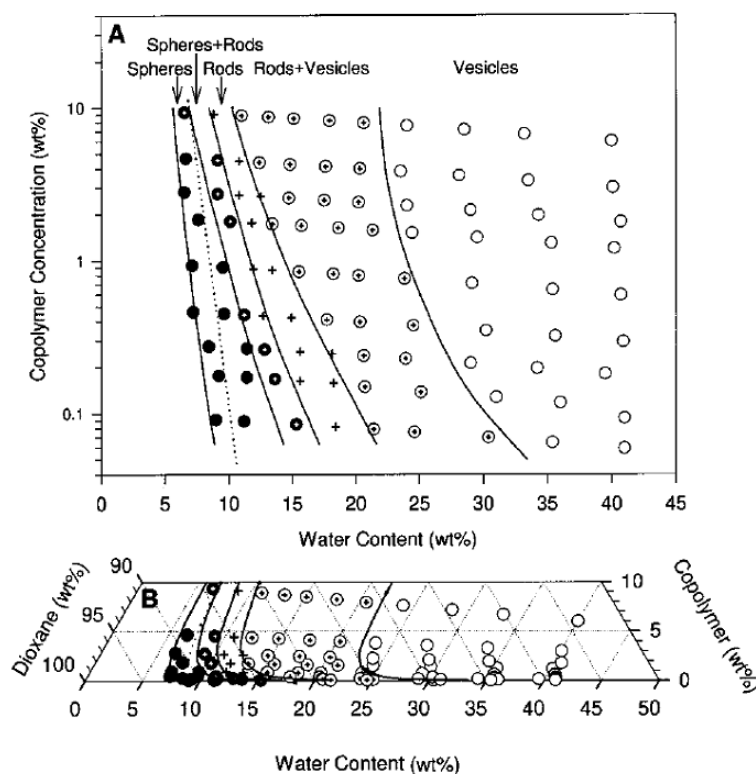


Figure 2.2. Phase diagram of the fractionated copolymer PS<sub>310</sub>-PAA<sub>52</sub> in dioxane/H<sub>2</sub>O mixture [62]. The symbols indicate morphologies, i.e., closed circles for spheres, closed circles with plus sign for mixtures of spheres and rods, plus sign for rods, open circles with plus sign for mixtures of rods and vesicles, open circles for vesicles. The solid lines are the phase boundaries determined by TEM. The dotted line is the micellization curve obtained by static light scattering (SLS) measurements. (A) (top) shows the regions of stable morphologies by plotting the logarithm of the polymer concentration versus the water content. (B) (bottom) is part of a ternary phase diagram.

### Amphiphilic block copolymers for vesicle formation

Block copolymers comprise two or more homopolymer blocks. Each block is polymerized with a specific monomer or a combination of monomers that have unique physico-chemical properties in the polymers [64-67]. Block copolymers are used for creating self-constructing Ps with a variety of properties and potential applications. Ps with a range of properties can be produced by applying block copolymers with different molecular weights, functionalities, compositions and molecular architectures [68-70]. A summary of degradable or nondegradable block copolymers, which have been explored for the formation of Ps, is given in Tables 2.1 and 2.2. As a hydrophobic part of the block copolymers, non-biodegradable poly(ethyl ethylene) (PEE) [18], poly(butadiene) (PBD) [11, 18, 31, 63, 71], poly(dimethylsiloxane) (PDMS) [72, 73],

and poly(styrene) (PS) [60, 62, 74] as well as biodegradable poly(lactide) (PLA) [41, 48, 75-77], poly( $\epsilon$ -caprolactone) (PCL) [41, 48] and poly(trimethylene carbonate) (PTMC) [48] have been applied. Degradable polymers undergo hydrolytic cleavage of their ester or carbonate linkages in the main chains with a rate of hydrolysis depending on the character of the block, the molecular weight of the block, the pH and sometimes the presence of enzymes [78-81]. Poly (acrylic acid) (PAA) [60, 62, 82], poly(*L*-glutamic acid) (PGA) [31, 63, 71, 83] and PEG [11, 12, 18, 41, 48, 74, 76, 77, 84-88] have been frequently selected as water-soluble blocks. PEG has been used most frequently as a hydrophilic block because of the resistance it provides in surface layers to blood protein adsorption [89-93]. It is possible to prepare diblock, triblock and multiblock copolymers and these different architectures can be exploited for the design of Ps with membranes with various degrees of entanglements and sub-structures.

Fig. 2.3 schematically illustrates the possible bi-layer assemblies in an aqueous environment for AB diblock, and ABA, BAB and ABC triblock copolymers, where A and C are different hydrophilic polymer blocks and B is a hydrophobic block. The geometric shapes of the amphiphiles in the aqueous environment are driven by complementary hydrophobic/hydrophobic interactions between the polymer chains [3, 44]. For AB and BAB copolymers, there is only one molecular conformation that can lead to bi-layered membrane formation (cylindrical shape for AB and curved shape for BAB). The hydrophobic chains will be entangled in the middle of the membrane to minimize the interfacial area with water and the hydrophilic block should be positioned to the out side of the membranes. On the other hand, ABA copolymers can have two possible conformations. The hydrophobic block can either form a curved loop so as both hydrophilic chains are toward the outside of the membrane or they can stretch forming a cylindrical shape with the two hydrophilic blocks at the opposite sides of the membrane. Interestingly, ABC copolymers can self-assemble into Ps with asymmetric membranes in such a way that the character of the internal and external surfaces differs from each other. Due to the difference in MW, charge and solubility of the hydrophilic blocks (A or C), one of the polymer chains with a relatively larger fraction is preferentially segregated to the outer surface of the Ps [50, 54]. Depending on the environmental conditions (i.e. pH and temperature), changes in the fraction of the hydrophilic chains can lead to spontaneous inversion or rearrangement of the membrane, which is of interest both in fundamental research of Ps and for drug delivery applications.

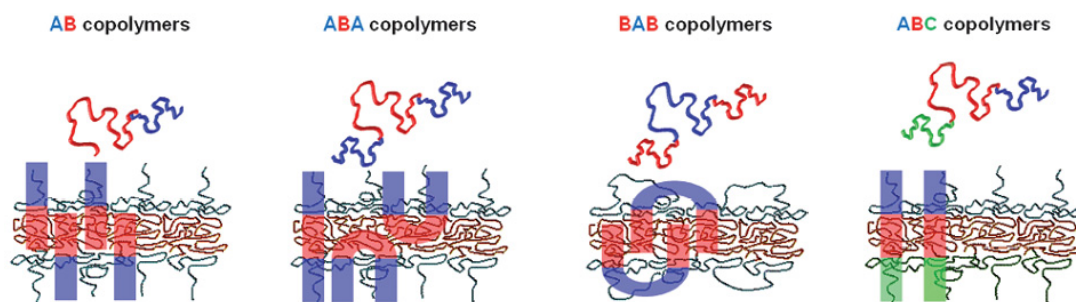


Figure 2.3. Membrane conformation of polymersomes formed by diblock and triblock copolymers [3, 44].

In case of using stimuli-sensitive polymers, Ps can be formed by increasing the hydrophobicity of the polymer by changing the temperature or pH (Table 2.3). Poly(*N*-isopropylacrylamide) (PNIPAAm) is the most frequently used thermosensitive polymer, which can be applied as a hydrophobic building block [94-102]. Various applications are based on the thermal properties of PNIPAAm due to its sharp transition behavior and its lower critical solution temperature (LCST) range between 30-50 °C [103-105]. Below the LCST, this polymer is completely soluble in aqueous solutions, but becomes non-soluble above the LCST [106-109], which allows PNIPAAm based block copolymers to self-assemble into micelles or Ps above the LCST. Block copolymers of PEG and PNIPAAm forming thermosensitive micelles were reported for the first time by Feijen *et al.* [110]. Later on thermosensitive Ps have been prepared from poly(*N*-(3-aminopropyl)-methacrylamide hydrochloride)-*b*-PNIPAAm (PAMPA-PNIPAAm), poly(2-cinnamoyl ethyl methacrylate)-*b*-PNIPAAm (PCEMA-PNIPAAm), and also from PEG-PNIPAAm prepared in a different way as by Feijen *et al.*

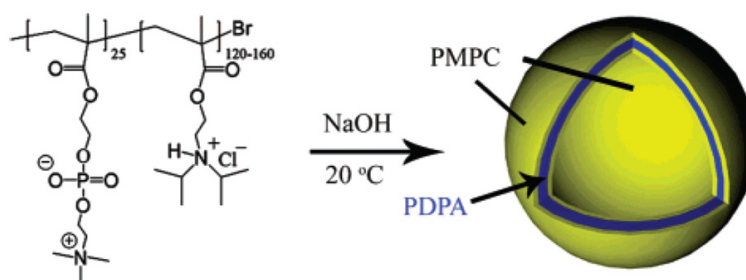


Figure 2.4. Formation of Ps by using PMPC-PDPA block copolymer [111].



The solubility of pH sensitive polymers in aqueous solutions can be modulated by change of the pH. Normally, these polymers have titratable functional groups and they can be protonated or deprotonated by changing the pH in relation to the pKa of the groups [112-115]. For instance, poly(2-(methacryloyloxy) ethyl phosphorylcholine)-b-poly(2-(diisopropylamino) ethyl methacrylate) (PMPC-PDPA) formed vesicles spontaneously by changing the pH of the solution from 2 to 6 due to deprotonation of the tertiary amine groups (pKa 6.3) of PDPA (Fig. 2.4) [4, 116]. PDPA becomes relatively hydrophobic at physiological pH. PBD-PGA at basic conditions can also form vesicular structures with a diameter of 100-150 nm by the presence of deprotonated PGA in the corona. The size of the Ps was tunable by changing the pH of the solution due to the coil-helix transition of PGA [31, 63]. It has also been reported that due to the pH responsiveness of both blocks in poly(*L*-lysine)-b-PGA (PLys-PGA) “schizophrenic” Ps can be formed in which PGA forms the hydrophobic core of the membranes at pH < 4, whereas PLys forms the hydrophobic part of the bi-layer at pH > 10 (Fig. 2.5) [83].

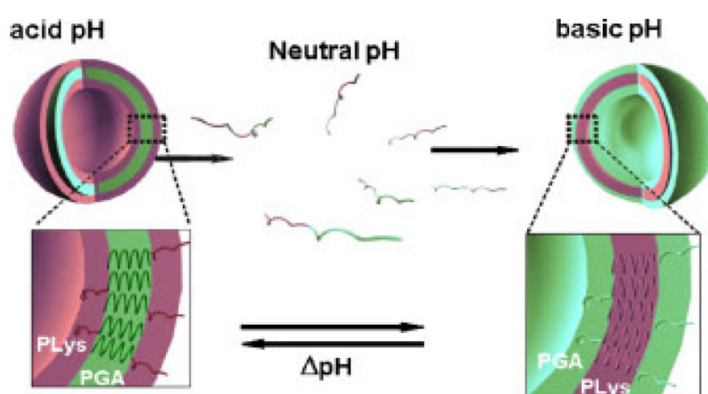


Figure 2.5. Schematic representation of the self-assembly of the di-block copolymer PLys-PGA into “schizophrenic vesicles” [83].

Secondary interactions or crosslinking of polymers can stabilize the bi-layer structure of Ps membranes. Poly(2-methyl-2-oxazoline) (PMOXA)-b-PDMS-b-PMOXA (PMOXA-PDMS-PMOXA) triblock copolymers can form a vesicular structure and UV irradiation of the vesicular dispersion led to the formation of covalently cross-linked Ps (Fig. 2.6) [72, 73]. The colloidal stability of the cross-linked Ps increased and the vesicles were stable during several weeks in the

dark. Kukula *et al.* prepared stable vesicles based on PGA-PBD probably driven by the packing of the  $\alpha$ -helical PGA blocks [63]. Magnetism was used for the formation of oligolamellar Ps. Hydrophobic Fe<sub>3</sub>O<sub>4</sub> nanoparticles were incorporated in the membranes of Ps prepared by using PEG-b-poly(isoprene) (PEG-PI) or PEG-P2VP and oligolamellar vesicle formation was observed using appropriate magnetic fields as a result of the bridging effect of adjacent magnetic particles [117].

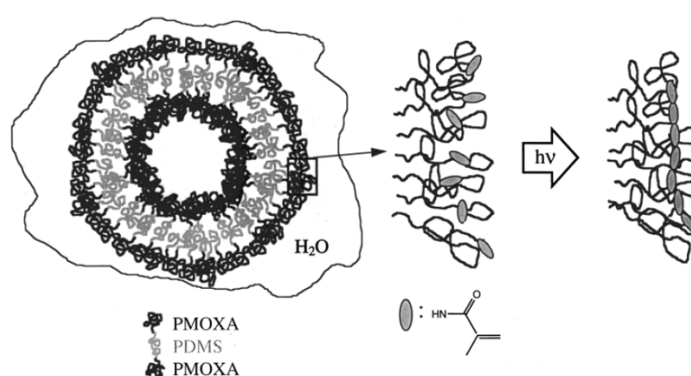


Figure 2.6. Schematic illustration of a PMOXA-PDMS-PMOXA tri-block copolymer vesicle in water and of the intravesicular cross-linking of the individual polymer molecules to a nanocapsule through UV irradiation of the polymerizable end groups of the block copolymer [72, 73].

Table 2.1. Examples of non-degradable polymersomes

Polymers	formation method	drug / stimulus for release	ref.
PEG-PEE	film rehydration	none reported	[18]
PEG-PBD	film rehydration	paclitaxel, doxorubicin	[11, 18]
PMOXA-PDMS-PMOXA	phase inversion, UV crosslinking	calcein	[72, 73]
PEG-PS	phase inversion	none reported	[74]
PAA-PS	phase inversion	none reported	[60, 62]

**PEG-PEE:** poly(ethylene glycol)-b-poly(ethyl ethylene), **PEG-PBD:** poly(ethylene glycol)-b-poly(butadiene), **PMOXA-PDMS-PMOXA:** poly(2-methyl-2-oxazoline)-b-poly(dimethylsiloxane)-b-poly(2-methyl-2-oxazoline), **PEG-PS:** poly(ethylene glycol)-b-poly(styrene), **PAA-PS:** poly(acrylic acid)-b-poly(styrene).

Table 2.2. Examples of degradable polymersomes

Polymers	formation method	drug / stimulus for release	ref.
PEG-PLA	phase inversion	carboxyl fluorescein	[41, 48, 76, 77]
PEG-PCL	phase inversion	carboxyl fluorescein	[41, 48]
PEG-PTMC	phase inversion	none reported	[48]
PEG-PTMBPEC	phase inversion	paclitaxel, doxorubicin / pH-triggered hydrolysis	[12]

**PEG-PLA:** poly(ethylene glycol)-b-poly(lactide), **PEG-PCL:** poly(ethylene glycol)-b-poly( $\epsilon$ -caprolactone), **PEG-PTMC:** poly(ethylene glycol)-b-poly(trimethylene carbonate), **PEG-PTMBPEC:** poly(ethylene glycol)-b-poly(2,4,6-trimethoxybenzylidene-pentaerythritol carbonate).

Table 2.3. Examples of stimuli-sensitive polymersomes

Polymers	formation method	degradability	drug / stimulus for release	ref.
PGA-PBD	basic solution	no	pH-triggered size change	[31, 63]
PEG-(PG2MA-IND)	pH 2.0-3.5	no	pH-triggered hydrolysis	[85]
PEG-P2VP	phase inversion	no	fluorescein / pH-triggered deformation	[84]
PLys-PLE	water or phase inversion	yes	Fura-2 / pH-triggered deformation	[118]
PMPC-PDPA	water, pH 2-6	no	DNA / release at pH < 6	[4, 111]
PEG-PS-PDEAMA	phase inversion	no	pH-tunable membrane permeability	[88]
PLys-PGA	pH < 4 or pH > 10	yes	pH (schizophrenic)	[83]
PAMPA-PNIPAAm	water, heating	no	temperature	[119]
PCEMA-PNIPAAm	water, heating	no	temperature	[120]
PEG-PNIPAAm	water, heating	no	doxorubicin / temperature	[87]
PLA-PNIPAAm	water	no	temperature	[75]
PEG-PPS-PEG	phase inversion	no	oxidation	[86]
PEG-SS-PPS	film rehydration	no	calcein / reduction	[121]
PAA-PAzoMA	phase inversion	no	deformation by UV light	[82]
PGA -PBD	$\gamma$ -Fe <sub>2</sub> O <sub>3</sub> in water	no	magnetic field	[71]
PEG-PI / PEG-P2VP	Fe <sub>3</sub> O <sub>4</sub> , magnetic field	no	magnetic field	[122]

**PGA-PBD:** poly(*L*-glutamic acid)-b-poly(butadiene), **PEG-(PG2MA-IND):** poly(ethylene glycol)-b-poly(glycerol monomethacrylate)-IND, **PEG-P2VP:** poly(ethylene glycol)-b-poly(2-vinylpyridine), **PLys-PLE:** poly(*L*-lysine)-b-poly(leucine), **PMPC-PDPA:** poly(2-(methacryloyloxy) ethyl phosphorylcholine)-b-poly(2-(diisopropylamino) ethyl methacrylate), **PEG-PS-PDEAMA:** poly(ethylene glycol)-b-poly(styrene)-b-(poly(2-diethylaminoethyl methacrylate)), **PLys-PGA:** poly(*L*-lysine)-b-poly(*L*-glutamic acid), **PAMPA-PNIPAAm:** poly(*N*-(3-aminopropyl)-methacrylamide hydrochloride)-b-poly(*N*-isopropylacrylamide), **PCEMA-PNIPAAm:** poly(2-cinnamoyl ethyl methacrylate)-b-poly(*N*-isopropylacrylamide), **PEG-PNIPAAm:** poly(ethylene glycol)-b-poly(*N*-isopropylacrylamide), **PLA-PNIPAAm:** poly(lactide)-b-poly(*N*-isopropylacrylamide), **PEG-PPS-PEG:** poly(ethylene glycol)-b-poly(propylene sulfide)-b-poly(ethylene glycol), **PEG-SS-PPS:** poly(ethylene glycol)-disulfide bond-poly(propylene sulfide), **PAA-PAzoMA:** poly(acrylic acid)-b-poly(methacrylate) containing a side-chain of azobenzene, **PEG-PI:** poly(ethylene glycol)-b-poly(isoprene).

### **Characterization of polymersomes**

The most common tool to investigate Ps in an aqueous dispersion is dynamic/static light scattering [42, 43]. This technique has been mainly used to determine vesicle size and size distribution (polydispersity index) [123-127], but also for determining the critical aggregation concentration [72, 128], vesicle disruption and change in the size with variation of pH or temperature [129, 130]. The zeta potential of Ps can be determined through dynamic light scattering by measuring the electrophoretic mobility of Ps in a capillary cell [77, 131]. In order to directly visualize Ps, light or electron microscopy is most frequently applied. By using microscopy, many important characteristics of Ps such as size, morphology and homogeneity can be evaluated [7, 13, 33, 45, 54, 56]. Optical microscopy provides relatively straightforward visualization after fast and easy sample preparation. Ps in aqueous dispersions can be applied without drying, staining or freezing. However, the resolution, magnification and contrast of the specimens are rather limited and only giant Ps with a diameter larger than 1  $\mu\text{m}$  are suitable for microscopical evaluation [132-134]. Scanning electron microscopy (SEM) or transmission electron microscopy (TEM) (Fig. 2.7a) [48] allow to investigate nanovesicles with a high resolution ( $> 1 \text{ nm}$ ), but the specimens need to be dried and optionally stained to enhance the contrast [135]. On the other hand, Ps in the hydrated state have been studied by using cryogenic TEM (Cryo-TEM) after rapid freezing of specimens (Fig. 2.7b) [18]. Freeze-fracture TEM can be used to study the internal structure of Ps by fracturing and etching the frozen samples [136, 137]. However, electrons cannot deeply penetrate into membrane of Ps and the quality of the photographs is dependent on the optical properties of the polymers applied [138-141].

Fluorescence microscopy has some benefits over electron microscopy [142, 143]. Specific labeling of parts of the Ps with fluorochromes gives information about their position in the Ps and multiple staining with different probes allows the visualization of the presence of individual molecules in compartments of the Ps. Confocal laser scanning microscopy (CLSM) is one of the popular tools for visualization of Ps (Fig. 2.7c) [48]. Optical slices of Ps in the z-direction can be obtained by using CLSM and in principle the slices can be combined providing a 3D stacked vesicular image [144, 145]. One of the interesting possibilities of fluorescence technique is to study the dynamics such as diffusion, rotational mobility and fluorescence lifetime of fluorophores in Ps by time-resolved measurements. By tracking of the photophysical properties of a molecular probe in Ps, dye-carrier interactions as well as changes in the local environment

can be detected [146]. These techniques have been previously used for better understanding of protein-substrate, protein-receptor and lipid-protein interactions [147-150] as well as for probing the local environment of a dye in micelles [151-153] or liposomes [154, 155] and to characterize sol-gel transitions [156-159].

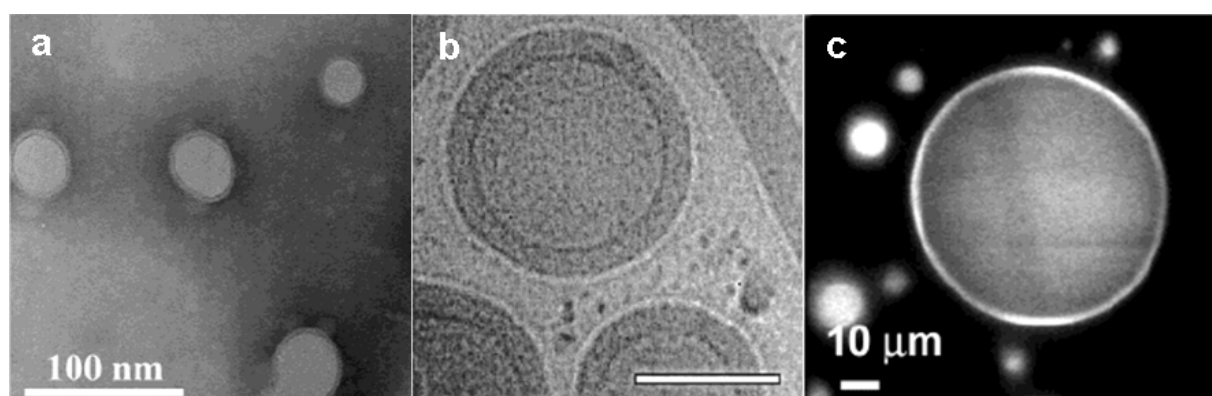


Figure 2.7. Microscopic images of Ps. (a) TEM micrograph of Ps made from PEG-PLA by injecting an acetone solution of the polymer into DI water. Ps on a carbon-coated copper grid were stained with phosphotungstic acid (2 wt.%) solution [48]. (b) Cryo-TEM image of Ps based on PEG-PBD. The hydrophobic cores of PBD are the darker areas. Scale bar is 100 nm [18]. (c) CLSM image of giant Ps prepared by adding a solution of PEG-PLA in chloroform to PBS in the presence of Nile red as a fluorescent probe [48].

### **Polymersomes for drug loading and release.**

In general, Ps are more stable in the circulation than liposomes [14, 15, 77]. Hydrophilic, hydrophobic or amphiphilic compounds can be loaded in Ps using either the aqueous core or the bi-layer membrane, which makes them very attractive vesicles for various applications in drug delivery, biomedical imaging and diagnostics [3].

The membrane of Ps can be considered as a reservoir system for both hydrophobic and amphiphilic molecules similar to cell membranes, which incorporate cholesterol and membrane proteins. It has been reported that highly lipophilic anticancer drugs [10, 12], dyes [14] and quantum dots [160, 161] as well as amphiphilic dyes (i.e. octadecyl rhodamine B [50, 51]) and membrane proteins (i.e. OmpF, LamB and FhuA [162]) can be integrated within the membrane of Ps while maintaining their functionality. These molecules can be incorporated in Ps by first dissolving or dispersing them together with the membrane-forming polymer building blocks in an organic solvent after which the organic solution/dispersion is added to water or an aqueous solution. In this way, paclitaxel (PTX) or doxorubicin (DOX) could be loaded into the

membranes of Ps with comparable loading amounts and efficiencies as compared to other self-assembled carriers (i.e. micelles and liposomes) [10, 12]. However, the Ps formulations obtained were much more stable than those based on the other carriers. The aqueous core of the Ps like that of liposomes can be utilized for encapsulation of hydrophilic therapeutic molecules [4-6, 33]. Membranes of such vesicles provide physical barriers that isolate the encapsulated molecules from the external environment, which is similar to natural vesicles found in the body. Several methods are currently used for the loading of hydrophilic molecules, but the most common methods are direct encapsulation during formation of Ps or diffusive loading methods using a pH or salt gradient over the membrane of already formed Ps [10, 163-165]. However, relatively hydrophilic drugs can also be incorporated in the core of the Ps by introducing the drug into the organic phase together with the polymer and using this mixture for Ps formation in contact with water [77].

In principle, drug release from Ps is governed by the diffusion of the drug through the membrane. The driving force is a concentration gradient of the drug between Ps and the surrounding medium [166-168]. When the drug is diffusing from the core of the Ps to the surrounding medium the release rate is a function of the square root of time. The size distribution of the Ps will also play a role in the overall release rate [169, 170]. Based on the theoretical approach suitable Ps for the delivery of specific drugs can be designed and the release kinetics may be predicted. Nevertheless, in many cases, rate and spatial control for drug release can not be adjusted to the desired level because the properties of the Ps membranes cannot be varied to a large extent due to constraints for the composition of block copolymers, which can be used to form Ps [171].

To achieve controlled drug delivery, significant efforts have been devoted to develop smart Ps. The physical and chemical properties of some Ps membranes are changeable in response to external stimuli. Various polymers, which are responsive to pH, temperature, redox conditions, light, magnetic field, ionic strength and concentration of glucose, have been used to form Ps for programmed drug delivery [34]. Some of these stimuli are able to trigger the disintegration of Ps for instance by a change in the hydrophilic/hydrophobic properties of the block copolymers or by poration of the membrane as a result of the preferred cleavage of covalent bonds in the polymer chains of one polymer component of the membrane. These possibilities in changing the properties of Ps by external stimuli are promising for the controlled release of drugs from the Ps

after arrival at the target site, where the stimulus is present. In this way, the efficacy of the drugs at the site of action can be enhanced and side effects reduced.

The pH responsiveness of Ps is very interesting because the pH in different tissues and cell compartments in the body varies from 2 to 8. In oral drug delivery, the change of the pH along the GI tract (pH 2 in the stomach, pH 5-8 in the intestine) has been mostly utilized [172-174]. The acidic environment of cancerous tissues (pH 6.5-7.2) [175, 176], endosomes (pH 5.0-6.5) [177-179] and lysosomes (pH 4.5-5.0) [180, 181] has been utilized for anticancer drug delivery and intracellular drug delivery. A general strategy for targeted drug delivery is based on carriers, in which drugs remain encapsulated during circulation in blood at physiological pH (7.4), but are rapidly released upon arrival in the acidic target site. Usually, polymers employed for pH sensitive systems are polyacids or polybases, which have titratable functionalities in the pendant groups or in the polymer back bone. The titratable moieties can be either ionized or deionized upon change of the pH depending on their pKa. The shift in the charge density of the polymers affects the hydrophilic/hydrophobic balance of the membrane, which may lead to a relatively fast disintegration of Ps. Non-ionized hydrophobic blocks will become more water-soluble after ionization and dissolution of the Ps may take place. Ps can aggregate and precipitate by deionization of hydrophilic blocks because the block copolymer becomes less water-soluble. For example, PEG-b-poly(2-vinylpyridine) (PEG-P2VP) vesicles (1-10  $\mu\text{m}$ ) can be completely solubilized at a pH below 5 [84]. P2VP is insoluble in water under neutral and alkaline conditions, but soluble at acidic conditions. Similarly, PLys-b-poly(leucine) (PLys-PLC) vesicles showed a pH-dependent solubility and eventually a pH-triggered release of encapsulated Fura-2 dye [118]. Upon lowering the pH, PLys becomes protonated, leading to the solubilization of the membrane and the instantaneous release of the encapsulated Fura-2.

In addition, a pH-dependent degradation or permeability of the Ps membrane can be used to modulate drug release. Ps based on PEG-b-poly(2,4,6-trimethoxybenzylidenepentaerythritol carbonate) (PEG-PTMBPEC) were reported by Chen *et al.* and *in vitro* studies demonstrated that the release of paclitaxel (PTX) as well as doxorubicin (DOX) from these Ps was faster at mildly acidic conditions than at physiological pH due to the faster degradation of PTMBPEC at mildly acidic conditions [12]. The pH-dependent release of indomethacin (IND) from Ps based on PEG-b-poly(glycerol monomethacrylate)-IND conjugates (PEG-(PG2MA-IND)) was also demonstrated [85]. IND was bound to the copolymer via an ester bond and rapid release of IND



was detected at acidic conditions, owing to hydrolysis of ester bonds. The group of Eisenberg reported pH-responsive permeable Ps consisting of the triblock copolymer PEG-b-PS-b-(poly(2-diethylaminoethyl methacrylate), PDEAMA) [88]. After the formation of Ps at pH 10.4, a decrease in pH induced a change in vesicle size. This was a result of the fact that the initially hydrophobic PDEAMA domain became protonated and therefore turned into a hydrophilic structure, attracting water. The concurrent phase separation between PS and protonated PDEAMA yielded a rigid PS layer in between the PDEAMA and PEG domains, keeping the self-assembled structure together (Fig. 2.8).

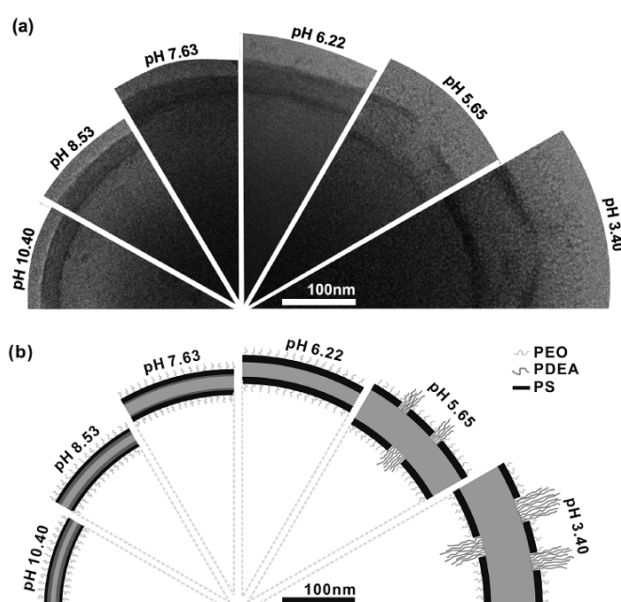


Figure 2.8. Reversible change of the PEG-PS-PDEAMA membrane upon pH change [88]. (a) Cryo-TEM images of the vesicle wall structure at several pH values. (b) Schematic illustration of the presumed membrane structure at corresponding pH values.

Thermo-sensitivity has also been employed as a stimulus. Block copolymers based on PNIPAAm were frequently used for the preparation of thermo-sensitive Ps [75, 87, 119, 120]. At the lower critical solution temperature (LCST), the conformation of PNIPAAm will change and below the LCST, PNIPAAm is soluble in aqueous environments. Qin *et al.* prepared temperature-sensitive Ps by dissolving PEG-PNIPAAm in water below the LCST of the polymer and forming Ps above the LCST (Fig. 2.9) [87]. The Ps were stable at body temperature, but they disassembled upon cooling because the PNIPAAm polymer chains in the Ps membranes became soluble. Local drug release can be achieved with the Ps either by applying simple ice packs or

deeply penetrating cryoprobes. The occurrence of oxidation-reduction (redox) reactions in the body has also been reported as a means to control spatial drug release in the body [182, 183]. Oxidative conditions exist in extracellular fluids and inflamed or tumor tissues, while intracellular compartments are known to be reductive [184-189]. Hubbell and co-workers developed oxidation responsive Ps based on PEG-b-poly(propylene sulfide)-b-PEG (PEG-PPS-PEG) [86]. The hydrophobic PPS was oxidized and transformed within 2 h into hydrophilic poly(sulfoxides) and poly(sulfones) upon exposure to hydrogen peroxide in the glucose-oxidase (GOx)/glucose/oxygen system, leading to destabilization of the vesicular structure. Reduction-sensitive disulfide block copolymer, PEG-SS-PPS was used to prepare Ps that can protect therapeutics in the extracellular environment but releasing their contents within the early endosome when the Ps are taken up by cells [121].

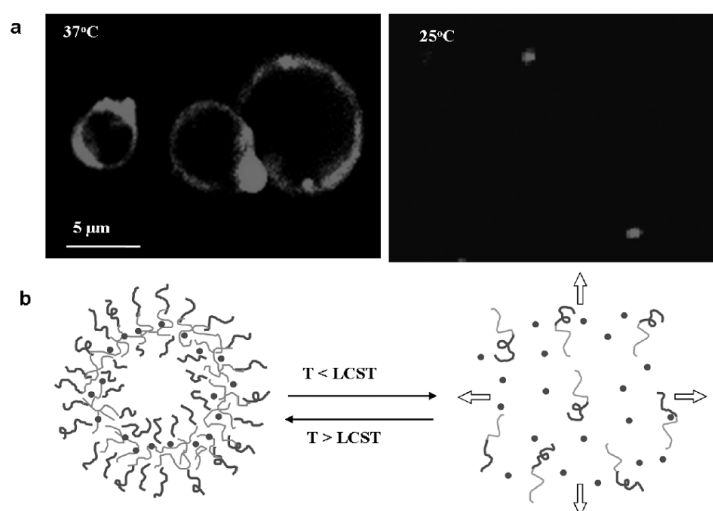


Figure 2.9. a) Fluorescence images and b) schematic illustration of vesicles from PEG-PNIPAAm copolymer at 37 °C and 25 °C, respectively [87]. The membrane was labeled with PKH 26 (5 mg/ml).

As external stimuli of the body, light and magnetism have also been explored to modulate local drug delivery. Tong *et al.* prepared Ps based on diblock copolymer composed of a side-chain azobenzene containing poly(methacrylate) and PAA (PAA-PAzoMa), which are photolyzable by UV light (Fig. 2.10) [82]. The polymer has UV labile azobenzene groups on the side chains of the hydrophobic block. Reversible changes in the structure of the vesicles were observed when they were alternately illuminated with UV or visible light for about 20 s.

Magnetically sensitive Ps have been developed for applications for targeted and triggered release of drugs and for diagnostic purposes [190-192]. Deformation or transformation of Ps can also be induced by the incorporation of magnetic particles. Lecommandoux *et al.* reported magnetic Ps formed by entrapping hydrophobically modified  $\gamma\text{-Fe}_2\text{O}_3$  nanoparticles [71]. Magnetic particles were incorporated in the membrane of Ps based on PGA-PBD during the self-assembly process. The deformation of these vesicles by applying an external magnetic field gradient (at the length scale of the membrane thickness) was reported. The application of a magnetic field could trigger the transient opening of the bi-layer and the release of an encapsulated content.

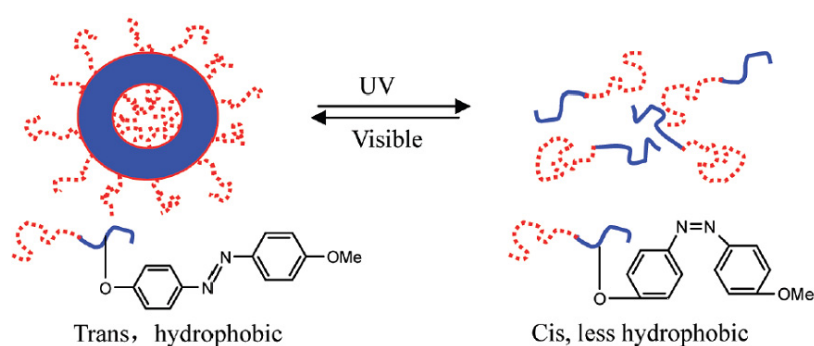


Figure 2.10. Reversible polymersome formation by UV/visible illumination [34, 82].

Novel approaches to control the release of drugs from Ps are to use different biodegradable polymer compositions to prepare Ps or to modify the interior of the Ps. By selecting different biodegradable polymers, the permeability of the Ps membrane can be varied and the release of drugs from the Ps may be controlled [41, 193] since each biodegradable polymer has a unique hydrolysis rate in contact with water or enzymes. Biodegradable block copolymers based on PLA, PCL and PTMC, and hydrophilic blocks like PEG have already been used to prepare biodegradable Ps. Ps with membranes based on different biodegradable polymers may be very challenging to further control the rate of degradation and consequently drug release. Either block copolymers with a hydrophobic block consisting of comonomers or simple blends of different degradable block copolymers are of interest. On the other hand, stimuli-sensitive hydrogels can be introduced in Ps to modulate the release of drugs from the Ps [76]. Polymers, which are sensitive to various stimuli (i.e. temperature, pH and etc) can be encapsulated with drugs or proteins in Ps and this may change the morphology of the interior of the Ps. Hydrogels in the Ps can form by external stimuli and will influence the diffusion rate of drugs from the interior of the

Ps to the surroundings. It can be concluded that at present the release of drugs from Ps can be tuned by the use of different stimuli-responsive and/or biodegradable polymers for the formation of Ps and by modifying the interior of the Ps with hydrogels.

### **Interactions of polymericosomes with proteins and cells**

Nanocarriers have been explored for the delivery of therapeutic and diagnostic agents [194]. However, a number of questions of whether the properties of carriers are suitable for biomedical applications are still remaining. One of the main problems encountered with the application of nanocarriers is the rapid clearance of carriers by mononuclear phagocytes (MPS) *in vivo* [195]. MPS is a part of the immune system that consists of phagocytic cells located in reticular connective tissue [196, 197]. It is generally known that the clearance of nanocarriers starts with adhesion of proteins, especially opsonins (opsonization) [198, 199]. The carrier-protein complex can be bound to appropriate receptors on the phagocytes including immunoglobulin G (IgG) and complement components allowing subsequent adhesion of the complex to the phagocytic cells and eventually internalization of the carriers.

Protein adsorption can be reduced by introducing various natural or synthetic hydrophilic polymers including polysaccharides [200, 201], poly(amino acid)s [202, 203], poly(hydroxyethyl methacrylate) (PHMA) [204-206] and PEG on the surface of carriers. PEG is one of the most popular polymers as a hydrophilic block of amphiphilic block copolymers and Ps prepared by PEG-based amphiphiles have a dense PEG brush on the surface. PEG is known to be very effective for inducing “stealth properties” by preventing interactions with blood components [36, 207-209]. The protein resistant character is generally ascribed to a combination of the low interfacial free energy of PEG with water, its steric stabilization effect and high mobility. The decrease in protein adsorption normally depends on the molecular weight, surface concentration and molecular conformation of PEG [90, 210, 211]. This is illustrated in Fig. 2.11, showing the reduction in protein adsorption onto PS particles as a function of the surface concentration of amino PEG [27]. Less protein adsorption takes place when the surface concentration of PEG is increased. The use of longer amino PEG (MW > 3400 g/mol) was more efficient to prevent protein adsorption than shorter amino PEG (MW 1500 g/mol). Nevertheless, the relationship may depend on the properties of the starting particles (nature of the particle matrix), immobilization chemistry and the surface charge [212].

Due to the stealth properties of the PEG brush, pegylated carriers may be expected to have relatively long circulation times as compared to non-pegylated carriers. However, the PEG coating can also diminish the uptake of these carriers by cells since the PEG brush reduces cell-carrier interactions. It has been reported by Vertut-Doi *et al.* that the presence of 5 mol% of PEG (8800 g/mol)-cholesterol in liposomes decreased the binding of the liposomes to J774 cells to 30 % of that obtained by liposomes without a PEG layer [213]. Therefore, one of the challenging topics has been the design of drug carriers with targeting moieties, resulting in high intracellular drug concentrations in a selective manner. For pegylated Ps, end groups of the PEG can be used to anchor homing moieties like antibodies, antibody fragments, or RGD-containing peptides. For example, PEG-PLA or PEG-PCL based Ps with antihuman IgG or antihuman serum albumin showed specific binding to human IgG or human serum albumin coated SPR disks [41]. An anti-intercellular adhesion molecule 1 (anti-ICAM-1) immobilized Ps prepared from PEG-PBD could be targeted to vascular endothelial cells [30].

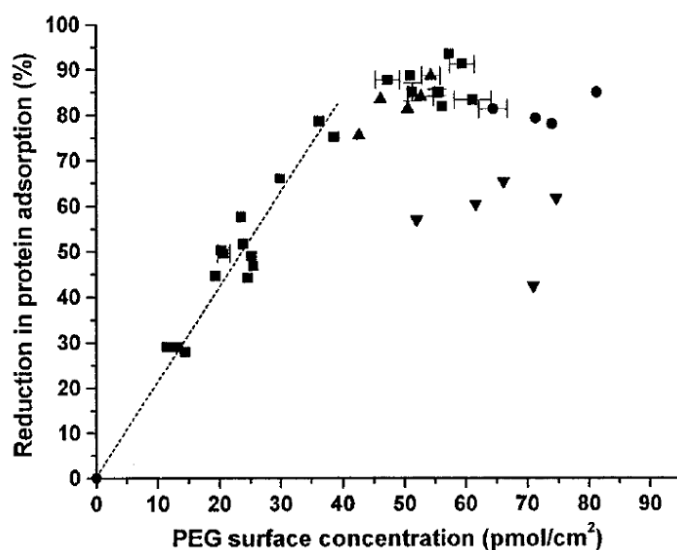


Figure 2.11. The influence of PEG surface concentration on polystyrene (PS) particles and length of the PEG on the reduction in protein adsorption from human plasma dilutions (85 v.%) as compared to bare PS particles. The % reduction for PS particles modified with amino PEG 3400 g/mol (■), amino PEG 1500 g/mol (▼), hydroxyl PEG 3400 g/mol (●) and methoxy PEG 5000 g/mol (▲) are shown. The dotted line is the fit for data of amino PEG (3400 g/mol) coated PS below 40 % in the surface concentration of PEG ( $Y=3.021X$ ,  $R=0.966$ ) [27].

### **Circulation kinetics and biodistribution of Polymersomes**

Although there is little known about the opsonization process of nanocarriers due to the complexity of the biological events, surface coating, charge and size of nanocarriers are undoubtedly playing important roles in the blood clearance [25, 214-217]. As previously discussed, opsonization processes can be influenced by the variation of MW and surface concentration of PEG molecules. Discher and colleagues investigated the effect of PEG on the circulation time of Ps based on PEG-PBD with different PEG MW in rats [14]. Ps with a PEG of MW 2300 g/mol exhibited a half lifetime of  $28 \pm 10$  h, while a half lifetime of  $15.8 \pm 2.2$  h was obtained when PEG with a MW of 1200 g/mol was used. Stealth liposomes coated with PEG (MW 1900 g/mol) (7.5-10 mol%) had shorter half lifetimes of 10-15 h in rats when compared to Ps with a similar MW of PEG. It has been suggested that the surface of Ps may adsorb less and/or different plasma proteins due to a higher surface concentration of PEG as compared to the liposomes.

Ps are known to accumulate primarily in the liver [14, 77]. Adsorption of liver specific opsonins probably enhances the uptake of Ps by liver macrophages, Kupffer cells and this process may play a major role in the hepatic uptake of the vesicles [216]. Interactions with the opsonins can be reduced by introduction of a slightly negative or positive charge on the surface of Ps, yielding prolonged blood circulation times [218, 219]. However, it has been reported that either high negative or positive charge lead to more rapid clearance of carriers due to enhanced hepatic uptake [203, 219, 220]. Likewise, a range of optimal sizes for specific nanocarriers has been suggested to establish long circulation times (e.g. stealth liposomes with diameters from 70 to 200 nm). For example, pegylated liposomes with diameters greater than 200 nm showed a significant accumulation in the spleen as a result of mechanical filtration followed by phagocytosis [221]. In contrast, pegylated liposomes with diameters below approximately 70 nm showed an increased accumulation in the liver, possibly also due to changes in protein adsorption related to the high curvature of such small liposomes [222]. Tumor accumulation can be achieved by passive accumulation via the enhanced permeability and retention (EPR) effect depending on the shape and size of the carriers [223]. Therefore, spherical Ps with a diameter less than 200 nm may exhibit a high accumulation in the tumor upon long circulating times. Nevertheless, despite the high expectations for Ps as a rational choice in pharmaceutical applications, more *in vivo* studies are required.

### **Conclusions and perspectives**

Polymersomes are able to encapsulate hydrophilic, hydrophobic and amphiphilic molecules like any other vesicular structure, but their thick and tough membrane provides them with superior stability *in vitro* and probably also *in vivo*. The presence of a dense PEG brush with relatively long PEG polymers on the surface of polymersomes may increase their biological stability (stealthiness) and prolong the circulation times in blood. Polymersomes are versatile systems and their overall properties and drug release profiles can be easily tuned by applying various block copolymers that are possibly biodegradable and/or stimuli-responsive. All these advantages make polymersomes one of the most interesting supramolecular structures for potential applications in delivery of drugs, genes and proteins. However, most polymersome systems reported so far are lacking specific cellular interactions and therefore their targetability to specific cells or tissues can be substantially improved. Therefore, it would be interesting to design novel stimuli-responsive Ps that are provided with biologically active homing devices as transport vesicles for drugs to further increase the concentration of drugs at specific target sites.



## References

- [1] M. Antonietti, S. Forster, Vesicles and liposomes: A self-assembly principle beyond lipids. *Adv. Mater.* 15(16) (2003) 1323-1333.
- [2] J.Z. Du, R.K. O'Reilly, Advances and challenges in smart and functional polymer vesicles. *Soft Matter* 5(19) (2009) 3544-3561.
- [3] M. Massignani, H. Lomas, G. Battaglia, Polymersomes: A Synthetic Biological Approach to Encapsulation and Delivery. *Adv. Polym. Sci.* 229 (2010) 115-154.
- [4] H. Lomas, I. Canton, S. MacNeil, J. Du, S.P. Armes, A.J. Ryan, A.L. Lewis, G. Battaglia, Biomimetic pH sensitive polymersomes for efficient DNA encapsulation and delivery. *Adv. Mater.* 19(23) (2007) 4238-4243.
- [5] T.O. Pangburn, M.A. Petersen, B. Waybrant, M.M. Adil, E. Kokkoli, Peptide- and Aptamer-Functionalized Nanovectors for Targeted Delivery of Therapeutics. *J. Biomech. Eng.-Trans. ASME* 131(7) (2009) 1-20.
- [6] D.A. Christian, S. Cai, D.M. Bowen, Y. Kim, J.D. Pajerowski, D.E. Discher, Polymersome carriers: From self-assembly to siRNA and protein therapeutics. *Eur. J. Pharm. Biopharm.* 71(3) (2009) 463-474.
- [7] K.T. Kim, S.A. Meeuwissen, R.J.M. Nolte, J.C.M. van Hest, Smart nanocontainers and nanoreactors. *Nanoscale* 2(6) (2010) 844-858.
- [8] H. Lomas, J.Z. Du, I. Canton, J. Madsen, N. Warren, S.P. Armes, A.L. Lewis, G. Battaglia, Efficient Encapsulation of Plasmid DNA in pH-Sensitive PMPC-PDPA Polymersomes: Study of the Effect of PDPA Block Length on Copolymer-DNA Binding Affinity. *Macromol. Biosci.* 10(5) (2010) 513-530.
- [9] O. Onaca, R. Enea, D.W. Hughes, W. Meier, Stimuli-Responsive Polymersomes as Nanocarriers for Drug and Gene Delivery. *Macromol. Biosci.* 9(2) (2009) 129-139.
- [10] F. Ahmed, R.I. Pakunlu, A. Brannan, F. Bates, T. Minko, D.E. Discher, Biodegradable polymersomes loaded with both paclitaxel and doxorubicin permeate and shrink tumors, inducing apoptosis in proportion to accumulated drug. *J. Control. Release* 116(2) (2006) 150-158.
- [11] S.L. Li, B. Byrne, J. Welsh, A.F. Palmer, Self-assembled poly(butadiene)-b-poly(ethylene oxide) polymersomes as paclitaxel carriers. *Biotechnol. Prog.* 23(1) (2007) 278-285.
- [12] W. Chen, F.H. Meng, R. Cheng, Z.Y. Zhong, pH-Sensitive degradable polymersomes for triggered release of anticancer drugs: A comparative study with micelles. *J. Control. Release* 142(1) (2010) 40-46.
- [13] D.E. Discher, A. Eisenberg, Polymer vesicles. *Science* 297(5583) (2002) 967-973.
- [14] P.J. Photos, L. Bacakova, B. Discher, F.S. Bates, D.E. Discher, Polymer vesicles in vivo: correlations with PEG molecular weight. *J. Control. Release* 90(3) (2003) 323-334.
- [15] B.M. Discher, Y.Y. Won, D.S. Ege, J.C.M. Lee, F.S. Bates, D.E. Discher, D.A. Hammer, Polymersomes: Tough vesicles made from diblock copolymers. *Science* 284(5417) (1999) 1143-1146.
- [16] H.K. Cho, I.W. Cheong, J.M. Lee, J.H. Kim, Polymeric nanoparticles, micelles and polymersomes from amphiphilic block copolymer. *Korean J. Chem. Eng.* 27(3) (2010) 731-740.
- [17] K. Letchford, H. Burt, A review of the formation and classification of amphiphilic block copolymer nanoparticulate structures: micelles, nanospheres, nanocapsules and polymersomes. *Eur. J. Pharm. Biopharm.* 65(3) (2007) 259-269.

- [18] H. Bermudez, A.K. Brannan, D.A. Hammer, F.S. Bates, D.E. Discher, Molecular weight dependence of polymersome membrane structure, elasticity, and stability. *Macromolecules* 35(21) (2002) 8203-8208.
- [19] F. Ahmed, P.J. Photos, D.E. Discher, Polymersomes as viral capsid mimics. *Drug Dev. Res.* 67(1) (2006) 4-14.
- [20] G. Battaglia, A.J. Ryan, S. Tomas, Polymeric vesicle permeability: A facile chemical assay. *Langmuir* 22(11) (2006) 4910-4913.
- [21] H. Aranda-Espinoza, H. Bermudez, F.S. Bates, D.E. Discher, Electromechanical limits of polymersomes. *Phys. Rev. Lett.* 8720(20) (2001) 1-4.
- [22] B.M. Discher, D.A. Hammer, F.S. Bates, D.E. Discher, Polymer vesicles in various media. *Curr. Opin. Colloid Interface Sci.* 5(1-2) (2000) 125-131.
- [23] D.E. Discher, F. Ahmed, Polymersomes. *Annu. Rev. Biomed. Eng.* 8 (2006) 323-341.
- [24] R. Dimova, U. Seifert, B. Pouligny, S. Forster, H.G. Dobereiner, Hyperviscous diblock copolymer vesicles. *Eur. Phys. J. E* 7(3) (2002) 241-250.
- [25] V.D. Awasthi, D. Garcia, R. Klipper, B.A. Goins, W.T. Phillips, Neutral and anionic liposome-encapsulated hemoglobin: Effect of postinserted poly(ethylene glycol)-distearoylphosphatidylethanolamine on distribution and circulation kinetics. *J. Pharmacol. Exp. Ther.* 309(1) (2004) 241-248.
- [26] M.L. Immordino, F. Dosio, L. Cattel, Stealth liposomes: review of the basic science, rationale, and clinical applications, existing and potential. *Int. J. Nanomed.* 1(3) (2006) 297-315.
- [27] F.H. Meng, G.H.M. Engbers, A. Gessner, R.H. Muller, J. Feijen, Pegylated polystyrene particles as a model system for artificial cells. *J. Biomed. Mater. Res. Part A* 70A(1) (2004) 97-106.
- [28] S.I. Jeon, J.H. Lee, J.D. Andrade, P.G. Degennes, Protein Surface Interactions in the Presence of Polyethylene Oxide 1. Simplified Theory. *J. Colloid Interface Sci.* 142(1) (1991) 149-158.
- [29] S.I. Jeon, J.D. Andrade, Protein Surface Interactions in the Presence of Polyethylene Oxide 2. Effect of Protein Size. *J. Colloid Interface Sci.* 142(1) (1991) 159-166.
- [30] J.J. Lin, P. Ghoroghchian, Y. Zhang, D.A. Hammer, Adhesion of antibody-functionalized polymersomes. *Langmuir* 22(9) (2006) 3975-3979.
- [31] F. Checot, S. Lecommandoux, H.A. Klok, Y. Gnanou, From supramolecular polymersomes to stimuli-responsive nano-capsules based on poly(diene-b-peptide) diblock copolymers. *Eur. Phys. J. E* 10(1) (2003) 25-35.
- [32] F. Ahmed, G. Srinivas, M.L. Klein, T. Minko, D.E. Discher, Polymersomes for drug delivery through target-controlled release. *Abstracts of Papers of the Amer. Chemical Soc.* 230 (2005) U1233-U1234.
- [33] O. Onaca, R. Enea, D.W. Hughes, W. Meier, Stimuli-Responsive Polymersomes as Nanocarriers for Drug and Gene Delivery. *Macromol. Biosci.* 9(2) (2009) 129-139.
- [34] F.H. Meng, Z.Y. Zhong, J. Feijen, Stimuli-Responsive Polymersomes for Programmed Drug Delivery. *Biomacromolecules* 10(2) (2009) 197-209.
- [35] O. Soga, C.F. van Nostrum, M. Fens, C.J.F. Rijcken, R.M. Schiffelers, G. Storm, W.E. Hennink, Thermosensitive and biodegradable polymeric micelles for paclitaxel delivery. *J. Control. Release* 103(2) (2005) 341-353.
- [36] A. VertutDoi, H. Ishiwata, K. Miyajima, Binding and uptake of liposomes containing a poly(ethylene glycol) derivative of cholesterol (stealth liposomes) by the macrophage cell

- line J774: Influence of PEG content and its molecular weight. *Biochim. Biophys. Acta-Biomembr.* 1278(1) (1996) 19-28.
- [37] R. Sharma, J.S. Lee, R.C. Bettencourt, C. Xiao, S.F. Konieczny, Y.Y. Won, Effects of the Incorporation of a Hydrophobic Middle Block into a PEG-Polycation Diblock Copolymer on the Physicochemical and Cell Interaction Properties of the Polymer-DNA Complexes. *Biomacromolecules* 9(11) (2008) 3294-3307.
- [38] S.E. Dunn, A. Brindley, S.S. Davis, M.C. Davies, L. Illum, Polystyrene-Poly(Ethylene Glycol) (Ps-Peg2000) Particles as Model Systems for Site-Specific Drug-Delivery .2. The Effect of Peg Surface-Density on the in-Vitro Cell-Interaction and in-Vivo Biodistribution. *Pharm. Res.* 11(7) (1994) 1016-1022.
- [39] T. Noh, Y.H. Kook, C. Park, H. Youn, H. Kim, E.T. Oh, E.K. Choi, H.J. Park, C. Kim, Block Copolymer Micelles Conjugated with anti-EGFR Antibody for Targeted Delivery of Anticancer Drug. *J. Polym. Sci. Pol. Chem.* 46(22) (2008) 7321-7331.
- [40] R.S. Herbst, D.M. Shin, Monoclonal antibodies to target epidermal growth factor receptor-positive tumors - A new paradigm for cancer therapy. *Cancer* 94(5) (2002) 1593-1611.
- [41] F.H. Meng, G.H.M. Engbers, J. Feijen, Biodegradable polymersomes as a basis for artificial cells: encapsulation, release and targeting. *J. Control. Release* 101(1-3) (2005) 187-198.
- [42] Biomimetic Block Copolymer Membranes, in W.P. Meier, W. Knoll (Eds.), *Polymer Membranes/Biomembranes*, Springer, 2010.
- [43] K. Kita-Tokarczyk, J. Grumelard, T. Haefele, W. Meier, Block copolymer vesicles - using concepts from polymer chemistry to mimic biomembranes. *Polymer* 46(11) (2005) 3540-3563.
- [44] C. LoPresti, H. Lomas, M. Massignani, T. Smart, G. Battaglia, Polymersomes: nature inspired nanometer sized compartments. *J. Mater. Chem.* 19(22) (2009) 3576-3590.
- [45] L.F. Zhang, A. Eisenberg, Multiple Morphologies of Crew-Cut Aggregates of Polystyrene-B-Poly(Acrylic Acid) Block-Copolymers. *Science* 268(5218) (1995) 1728-1731.
- [46] L.B. Luo, A. Eisenberg, Thermodynamic size control of block copolymer vesicles in solution. *Langmuir* 17(22) (2001) 6804-6811.
- [47] L.B. Luo, A. Eisenberg, Thermodynamic stabilization mechanism of block copolymer vesicles. *J. Am. Chem. Soc.* 123(5) (2001) 1012-1013.
- [48] F.H. Meng, C. Hiemstra, G.H.M. Engbers, J. Feijen, Biodegradable polymersomes. *Macromolecules* 36(9) (2003) 3004-3006.
- [49] G. Battaglia, S. Tomas, A.J. Ryan, Lamellarsomes: metastable polymeric multilamellar aggregates. *Soft Matter* 3(4) (2007) 470-475.
- [50] G. Battaglia, A.J. Ryan, Bilayers and interdigitation in block copolymer vesicles. *J. Am. Chem. Soc.* 127(24) (2005) 8757-8764.
- [51] H. Lomas, M. Massignani, K.A. Abdullah, I. Canton, C. Lo Presti, S. MacNeil, J.Z. Du, A. Blanz, J. Madsen, S.P. Armes, A.L. Lewis, G. Battaglia, Non-cytotoxic polymer vesicles for rapid and efficient intracellular delivery. *Faraday Discuss.* 139 (2008) 143-159.
- [52] G. Battaglia, A.J. Ryan, Pathways of polymeric vesicle formation. *J. Phys. Chem. B* 110(21) (2006) 10272-10279.
- [53] M.I. Angelova, D.S. Dimitrov, Liposome Electroformation. *Faraday Discuss.* 81(81) (1986) 303-311.

- [54] A. Blanz, S.P. Armes, A.J. Ryan, Self-Assembled Block Copolymer Aggregates: From Micelles to Vesicles and their Biological Applications. *Macromol. Rapid Commun.* 30(4-5) (2009) 267-277.
- [55] Y.Y. Won, A.K. Brannan, H.T. Davis, F.S. Bates, Cryogenic transmission electron microscopy (cryo-TEM) of micelles and vesicles formed in water by poly(ethylene oxide)-based block copolymers. *J. Phys. Chem. B* 106(13) (2002) 3354-3364.
- [56] Y.Y. Won, H.T. Davis, F.S. Bates, Giant wormlike rubber micelles. *Science* 283(5404) (1999) 960-963.
- [57] S.T. Hyde, A. Fogden, B.W. Ninham, Self-Assembly of Linear Block-Copolymers - Relative Stability of Hyperbolic Phases. *Macromolecules* 26(25) (1993) 6782-6788.
- [58] J.N. Israelachvili, D.J. Mitchell, B.W. Ninham, Theory of Self-Assembly of Lipid Bilayers and Vesicles. *Biochim. Biophys. Acta-Biomembr.* 470(2) (1977) 185-201.
- [59] P.L. Soo, A. Eisenberg, Preparation of block copolymer vesicles in solution. *J. Polym. Sci. Pt. B-Polym. Phys.* 42(6) (2004) 923-938.
- [60] H.W. Shen, A. Eisenberg, Block length dependence of morphological phase diagrams of the ternary system of PS-*b*-PAA/dioxane/H<sub>2</sub>O. *Macromolecules* 33(7) (2000) 2561-2572.
- [61] G.E. Yu, A. Eisenberg, Multiple morphologies formed from an amphiphilic ABC triblock copolymer in solution. *Macromolecules* 31(16) (1998) 5546-5549.
- [62] H.W. Shen, A. Eisenberg, Morphological phase diagram for a ternary system of block copolymer PS<sub>310</sub>-*b*-PAA<sub>52</sub>/dioxane/H<sub>2</sub>O. *J. Phys. Chem. B* 103(44) (1999) 9473-9487.
- [63] H. Kukula, H. Schlaad, M. Antonietti, S. Forster, The formation of polymer vesicles or "peptosomes" by polybutadiene-block-poly(L-glutamate)s in dilute aqueous solution. *J. Am. Chem. Soc.* 124(8) (2002) 1658-1663.
- [64] C. Allen, D. Maysinger, A. Eisenberg, Nano-engineering block copolymer aggregates for drug delivery. *Colloid Surf. B-Biointerfaces* 16(1-4) (1999) 3-27.
- [65] K. Kataoka, G.S. Kwon, M. Yokoyama, T. Okano, Y. Sakurai, Block-Copolymer Micelles as Vehicles for Drug Delivery. *J. Control. Release* 24(1-3) (1993) 119-132.
- [66] G.S. Kwon, Block copolymer micelles as drug delivery systems. *Adv. Drug Deliv. Rev.* 54(2) (2002) 167-167.
- [67] G.S. Kwon, M.L. Forrest, Amphiphilic block copolymer micelles for nanoscale drug delivery. *Drug Dev. Res.* 67(1) (2006) 15-22.
- [68] J.A. Opsteen, J.J.L.M. Cornelissen, J.C.M. van Hest, Block copolymer vesicles. *Pure Appl. Chem.* 76(7-8) (2004) 1309-1319.
- [69] L. Ma, A. Eisenberg, Relationship between Wall Thickness and Size in Block Copolymer Vesicles. *Langmuir* 25(24) (2009) 13730-13736.
- [70] W. Muller, M. Maskos, D. Metzke, P. Lob, Synthesis of block copolymer vesicles in a micromixer. *Houille Blanche-Rev. Int.* (6) (2009) 125-128.
- [71] S.B. Lecommandoux, O. Sandre, F. Checot, J. Rodriguez-Hernandez, R. Perzynski, Magnetic nanocomposite micelles and vesicles. *Adv. Mater.* 17(6) (2005) 712-718.
- [72] C. Nardin, T. Hirt, J. Leukel, W. Meier, Polymerized ABA triblock copolymer vesicles. *Langmuir* 16(3) (2000) 1035-1041.
- [73] C. Nardin, S. Thoeni, J. Widmer, M. Winterhalter, W. Meier, Nanoreactors based on (polymerized) ABA-triblock copolymer vesicles. *Chem. Commun.*(15) (2000) 1433-1434.
- [74] A.V. Kabanov, T.K. Bronich, V.A. Kabanov, K. Yu, A. Eisenberg, Spontaneous formation of vesicles from complexes of block ionomers and surfactants. *J. Am. Chem. Soc.* 120(38) (1998) 9941-9942.

- [75] M. Hales, C. Barner-Kowollik, T.P. Davis, M.H. Stenzel, Shell-cross-linked vesicles synthesized from block copolymers of poly(D,L-lactide) and poly (N-isopropyl acrylamide) as thermoresponsive nanocontainers. *Langmuir* 20(25) (2004) 10809-10817.
- [76] J.S. Lee, W. Zhou, F.H. Meng, D.W. Zhang, C. Otto, J. Feijen, Thermosensitive hydrogel-containing polymersomes for controlled drug delivery. *J. Control. Release* 146(3) (2010) 400-408.
- [77] J.S. Lee, M. Ankone, E. Pieters, R.M. Schiffelers, W.E. Hennink, J. Feijen, Circulation Kinetics and Biodistribution of Dual-Labeled Polymersomes with Modulated Surface Charge in Tumor-Bearing Mice: Comparison with Stealth Liposomes Submitted to *J. Control. Release* (Special issue).
- [78] I. Armentano, M. Dottori, E. Fortunati, S. Mattioli, J.M. Kenny, Biodegradable polymer matrix nanocomposites for tissue engineering: A review. *Polym. Degrad. Stabil.* 95(11) (2010) 2126-2146.
- [79] K. Leja, G. Lewandowicz, Polymer Biodegradation and Biodegradable Polymers - a Review. *Pol. J. Environ. Stud.* 19(2) (2010) 255-266.
- [80] B. Asplund, J. Sperens, T. Mathisen, J. Hilborn, Effects of hydrolysis on a new biodegradable co-polymer. *J. Biomater. Sci.-Polym. Ed.* 17(6) (2006) 615-630.
- [81] H.S. Kim, H.J. Kim, D. Cho, Thermal analysis of hydrolysis and degradation of biodegradable polymer and bio-composites. *J. Therm. Anal. Calorim.* 96(1) (2009) 211-218.
- [82] X. Tong, G. Wang, A. Soldera, Y. Zhao, How can azobenzene block copolymer vesicles be dissociated and reformed by light? *J. Phys. Chem. B* 109(43) (2005) 20281-20287.
- [83] F. Checot, J. Rodriguez-Hernandez, Y. Gnanou, S. Lecommandoux, Responsive micelles and vesicles based on polypeptide diblock copolymers. *Polym. Adv. Technol.* 17(9-10) (2006) 782-785.
- [84] U. Borchert, U. Lipprandt, M. Bilang, A. Kimpfler, A. Rank, R. Peschka-Suss, R. Schubert, P. Lindner, S. Forster, pH-induced release from P2VP-PEO block copolymer vesicles. *Langmuir* 22(13) (2006) 5843-5847.
- [85] C. Giacomelli, V. Schmidt, R. Borsali, Nanocontainers formed by self-assembly of poly(ethylene oxide)-b-poly(glycerol monomethacrylate) - Drug conjugates. *Macromolecules* 40(6) (2007) 2148-2157.
- [86] A. Napoli, M.J. Boerakker, N. Tirelli, R.J.M. Nolte, N.A.J.M. Sommerdijk, J.A. Hubbell, Glucose-oxidase based self-destructing polymeric vesicles. *Langmuir* 20(9) (2004) 3487-3491.
- [87] S.H. Qin, Y. Geng, D.E. Discher, S. Yang, Temperature-controlled assembly and release from polymer vesicles of poly(ethylene oxide)-block-poly(N-isopropylacrylamide). *Adv. Mater.* 18(21) (2006) 2905-2909.
- [88] S.Y. Yu, T. Azzam, I. Rouiller, A. Eisenberg, "Breathing" Vesicles. *J. Am. Chem. Soc.* 131(30) (2009) 10557-10566.
- [89] A.J. Coukell, C.M. Spencer, Polyethylene glycol-liposomal doxorubicin - A review of its pharmacodynamic and pharmacokinetic properties, and therapeutic efficacy in the management of AIDS-related Kaposi's sarcoma. *Drugs* 53(3) (1997) 520-538.
- [90] R. Gref, M. Luck, P. Quellec, M. Marchand, E. Dellacherie, S. Harnisch, T. Blunk, R.H. Muller, 'Stealth' corona-core nanoparticles surface modified by polyethylene glycol (PEG): influences of the corona (PEG chain length and surface density) and of the core

- composition on phagocytic uptake and plasma protein adsorption. *Colloid Surf. B-Biointerfaces* 18(3-4) (2000) 301-313.
- [91] P. Kim, D.H. Kim, B. Kim, S.K. Choi, S.H. Lee, A. Khademhosseini, R. Langer, K.Y. Suh, Fabrication of nanostructures of polyethylene glycol for applications to protein adsorption and cell adhesion. *Nanotechnology* 16(10) (2005) 2420-2426.
- [92] M.E. Price, R.M. Cornelius, J.L. Brash, Protein adsorption to polyethylene glycol modified liposomes from fibrinogen solution and from plasma. *Biochim. Biophys. Acta-Biomembr.* 1512(2) (2001) 191-205.
- [93] R.W. Wang, Y. Zhang, G.H. Ma, Z. Su, Modification of poly(glycidyl methacrylate-divinylbenzene) porous microspheres with polyethylene glycol and their adsorption property of protein. *Colloid Surf. B-Biointerfaces* 51(1) (2006) 93-99.
- [94] J.E. Chung, M. Yokoyama, M. Yamato, T. Aoyagi, Y. Sakurai, T. Okano, Thermo-responsive drug delivery from polymeric micelles constructed using block copolymers of poly(N-isopropylacrylamide) and poly(butylmethacrylate). *J. Control. Release* 62(1-2) (1999) 115-127.
- [95] D.C. Coughlan, O.I. Corrigan, Drug-polymer interactions and their effect on thermoresponsive poly(N-isopropylacrylamide) drug delivery systems. *Int. J. Pharm.* 313(1-2) (2006) 163-174.
- [96] F. Eeckman, A.J. Moes, K. Amighi, Poly(N-isopropylacrylamide) copolymers for constant temperature controlled drug delivery. *Int. J. Pharm.* 273(1-2) (2004) 109-119.
- [97] Y.X. Gao, X.M. Ji, Y.H. Yin, H. Dong, H. Zheng, Poly(N-isopropylacrylamide), poly(methacrylic acid) and their copolymers for oral colon-specific drug delivery. *J. Wuhan Univ. Technol.-Mat. Sci. Edit.* 24(4) (2009) 571-574.
- [98] E. Khodaverdi, O. Rajabi, F. Farhadi, A. Jalali, F.S.M. Tekie, Preparation and Investigation of Poly (N-isopropylacrylamide-acrylamide) Membranes in Temperature Responsive Drug Delivery. *Iran. J. Basic Med. Sci.* 13(3) (2010) 102-110.
- [99] Y.Y. Lang, S.M. Li, W.S. Pan, L.Y. Zheng, Thermo- and pH-sensitive drug delivery from hydrogels constructed using block copolymers of poly(N-isopropylacrylamide) and Guar gum. *J. Drug Deliv. Sci. Technol.* 16(1) (2006) 65-69.
- [100] A.S. Mathews, C.S. Ha, W.J. Cho, I. Kim, Drug delivery system based on covalently bonded poly[N-isopropylacrylamide-co-2-hydroxyethylacrylate]-based nanoparticle networks. *Drug Deliv.* 13(4) (2006) 245-251.
- [101] H. Yan, K. Tsujii, Potential application of poly(N-isopropylacrylamide) gel containing polymeric micelles to drug delivery systems. *Colloid Surf. B-Biointerfaces* 46(3) (2005) 142-146.
- [102] X. Zhu, J. DeGraaf, F.M. Winnik, D. Leckband, pH-dependent mucoadhesion of a poly(N-isopropylacrylamide) copolymer reveals design rules for drug delivery. *Langmuir* 20(24) (2004) 10648-10656.
- [103] C. Boutris, E.G. Chatzi, C. Kiparissides, Characterization of the LCST behaviour of aqueous poly(N-isopropylacrylamide) solutions by thermal and cloud point techniques. *Polymer* 38(10) (1997) 2567-2570.
- [104] M.V. Deshmukh, A.A. Vaidya, M.G. Kulkarni, P.R. Rajamohanam, S. Ganapathy, LCST in poly(N-isopropylacrylamide) copolymers: high resolution proton NMR investigations. *Polymer* 41(22) (2000) 7951-7960.
- [105] I. Shechter, O. Ramon, I. Portnaya, Y. Paz, Y.D. Livney, Microcalorimetric Study of the Effects of a Chaotropic Salt, KSCN, on the Lower Critical Solution Temperature (LCST)

- of Aqueous Poly(N-isopropylacrylamide) (PNIPA) Solutions. *Macromolecules* 43(1) (2010) 480-487.
- [106] Y. Kaneko, S. Nakamura, K. Sakai, A. Kikuchi, T. Aoyagi, Y. Sakurai, T. Okano, Synthesis and swelling-deswelling kinetics of poly(N-isopropylacrylamide) hydrogels grafted with LCST modulated polymers. *J. Biomater. Sci.-Polym. Ed.* 10(11) (1999) 1079-1091.
- [107] Y. Okada, F. Tanaka, Cooperative hydration, chain collapse, and flat LCST behavior in aqueous poly(N-isopropylacrylamide) solutions. *Macromolecules* 38(10) (2005) 4465-4471.
- [108] F.M. Winnik, Fluorescence Studies of Aqueous-Solutions of Poly(N-Isopropylacrylamide) Below and above Their Lcst. *Macromolecules* 23(1) (1990) 233-242.
- [109] M. Annaka, C. Tanaka, T. Nakahira, M. Sugiyama, T. Aoyagi, T. Okano, Fluorescence study on the swelling behavior of comb-type grafted poly(N-isopropylacrylamide) hydrogels. *Macromolecules* 35(21) (2002) 8173-8179.
- [110] M.D.C. Topp, P.J. Dijkstra, H. Talsma, J. Feijen, Thermosensitive micelle-forming block copolymers of poly(ethylene glycol) and poly(N-isopropylacrylamide). *Macromolecules* 30(26) (1997) 8518-8520.
- [111] J.Z. Du, S.P. Armes, pH-responsive vesicles based on a hydrolytically self-cross-linkable copolymer. *J. Am. Chem. Soc.* 127(37) (2005) 12800-12801.
- [112] M. Barea, M. Jenkins, R. Bridson, Polymer-coated liposomal formulations for pH-responsive drug release. *J. Pharm. Pharmacol.* 61 (2009) A78-A79.
- [113] Q. Gao, Y. Xu, D. Wu, Y.H. Sun, X.A. Li, pH-Responsive Drug Release from Polymer-Coated Mesoporous Silica Spheres. *J. Phys. Chem. C* 113(29) (2009) 12753-12758.
- [114] J. Jung, I.H. Lee, E. Lee, J. Park, S. Jon, pH-Sensitive polymer nanospheres for use as a potential drug delivery vehicle. *Biomacromolecules* 8(11) (2007) 3401-3407.
- [115] K.S. Soppimath, D.C.W. Tan, Y.Y. Yang, pH-triggered thermally responsive polymer core-shell nanoparticles for drug delivery. *Adv. Mater.* 17(3) (2005) 318-323.
- [116] J.Z. Du, Y.P. Tang, A.L. Lewis, S.P. Armes, pH-sensitive vesicles based on a biocompatible zwitterionic diblock copolymer. *J. Am. Chem. Soc.* 127(51) (2005) 17982-17983.
- [117] M. Krack, H. Hohenberg, A. Kornowski, P. Lindner, H. Weller, S. Forster, Nanoparticle-loaded magnetophoretic vesicles. *J. Am. Chem. Soc.* 130(23) (2008) 7315-7320.
- [118] E.G. Bellomo, M.D. Wyrsta, L. Pakstis, D.J. Pochan, T.J. Deming, Stimuli-responsive polypeptide vesicles by conformation-specific assembly. *Nat. Mater.* 3(4) (2004) 244-248.
- [119] Y. Li, B.S. Lokitz, C.L. McCormick, Thermally responsive vesicles and their structural "locking" through polyelectrolyte complex formation. *Angew. Chem.-Int. Edit.* 45(35) (2006) 5792-5795.
- [120] X.R. Chen, X.B. Ding, Z.H. Zheng, Y.X. Peng, Thermosensitive cross-linked polymer vesicles for controlled release system. *New J. Chem.* 30(4) (2006) 577-582.
- [121] S. Cerritelli, D. Velluto, J.A. Hubbell, PEG-SS-PPS: Reduction-sensitive disulfide block copolymer vesicles for intracellular drug delivery. *Biomacromolecules* 8(6) (2007) 1966-1972.
- [122] M. Krack, H. Hohenberg, A. Kornowski, P. Lindner, H. Weller, S. Forster, Nanoparticle-loaded magnetophoretic vesicles. *J. Am. Chem. Soc.* 130(23) (2008) 7315-7320.

- [123] M. Kocifaj, A review of the effects of light scattering on the dynamics of irregularly shaped dust grains in the Solar System. *J. Quant. Spectrosc. Radiat. Transf.* 110(11) (2009) 879-888.
- [124] F.W. Peaker, Light-Scattering Methods for the Chemical Characterisation of Polymers - a Review. *Analyst* 85(1009) (1960) 235-244.
- [125] N. Robinson, Molecular Size and Shape a Review of the Light-Scattering Method Applied to Some Important Biological and Other Macromolecules .2. *J. Pharm. Pharmacol.* 12(4) (1960) 193-218.
- [126] N. Robinson, Molecular Size and Shape a Review of the Light-Scattering Method Applied to Some Important Biological and Other Macromolecules .1. *J. Pharm. Pharmacol.* 12(3) (1960) 129-149.
- [127] C.M. Sorensen, Light scattering by fractal aggregates: A review. *Aerosol Sci. Technol.* 35(2) (2001) 648-687.
- [128] C. Nardin, M. Winterhalter, W. Meier, Giant free-standing ABA triblock copolymer membranes. *Langmuir* 16(20) (2000) 7708-7712.
- [129] M. Sauer, T. Haefele, A. Graff, C. Nardin, W. Meier, Ion-carrier controlled precipitation of calcium phosphate in giant ABA triblock copolymer vesicles. *Chem. Commun.*(23) (2001) 2452-2453.
- [130] M. Sauer, W. Meier, Responsive nanocapsules. *Chem. Commun.*(01) (2001) 55-56.
- [131] T. Miyanishi, Effects of Zeta Potential on Dynamic Flocculation in Microparticle Systems. *Papermakers Conference* (1995) 499-512.
- [132] P. Blattner, H.P. Herzig, R. Dandliker, Scanning near-field optical microscopy: transfer function and resolution limit. *Opt. Commun.* 155(4-6) (1998) 245-250.
- [133] J. Enderlein, Breaking the diffraction limit with dynamic saturation optical microscopy. *Appl. Phys. Lett.* 87(9) (2005) 1-3.
- [134] I.I. Smolyaninov, Optical microscopy beyond the diffraction limit. *HFSP J.* 2(3) (2008) 129-131.
- [135] D.R. Clarke, Review - Transmission Scanning Electron-Microscopy. *J. Mater. Sci.* 8(2) (1973) 279-285.
- [136] D.M.D. Landis, T.S. Reese, Membrane-Structure in Mammalian Astrocytes - a Review of Freeze-Fracture Studies on Adult, Developing, Reactive and Cultured Astrocytes. *J. Exp. Biol.* 95(Dec) (1981) 35-48.
- [137] N.J. Severs, Freeze-Fracture Cyto-Chemistry - Review of Methods. *J. Electron Microsc. Tec.* 13(3) (1989) 175-203.
- [138] M. Laue, N. Bannert, Detection limit of negative staining electron microscopy for the diagnosis of bioterrorism-related micro-organisms. *J. Appl. Microbiol.* 109(4) (2010) 1159-1168.
- [139] P.D. Nellist, B.C. Mccallum, J.M. Rodenburg, Resolution Beyond the Information Limit in Transmission Electron-Microscopy. *Nature* 374(6523) (1995) 630-632.
- [140] M. Tsuji, K. Katayama, Resolution Limit Due to Radiation-Damage in Transmission Electron-Microscopy of Polymer Crystals. *J. Electron Microsc.* 39(4) (1990) 312-312.
- [141] S. Van Aert, J.H. Chen, D. Van Dyck, Linear versus non-linear structural information limit in high-resolution transmission electron microscopy. *Ultramicroscopy* 110(11) (2010) 1404-1410.



- [142] A.Y. Kobitski, C.D. Heyes, G.U. Nienhaus, Total internal reflection fluorescence microscopy - a powerful tool to study single quantum dots. *Appl. Surf. Sci.* 234(1-4) (2004) 86-92.
- [143] P. Rech, J. Grima-Pettenati, A. Jauneau, Fluorescence microscopy: a powerful technique to detect low GUS activity in vascular tissues. *Plant J.* 33(1) (2003) 205-209.
- [144] M. Ferrando, W.E.L. Spiess, Review: Confocal scanning laser microscopy. A powerful tool in food science. *Food Sci. Technol. Int.* 6(4) (2000) 267-284.
- [145] D.V. Patel, C.N.J. McGhee, Contemporary in vivo confocal microscopy of the living human cornea using white light and laser scanning techniques: a major review. *Clin. Exp. Ophthalmol.* 35(1) (2007) 71-88.
- [146] H. Schneckenburger, H.K. Seidlitz, J. Eberz, New Trends in Photobiology (Invited Review) - Time-Resolved Fluorescence in Photobiology. *J. Photochem. Photobiol. B-Biol.* 2(1) (1988) 1-19.
- [147] U. Blaszczyk, A. Polit, A. Guz, Z. Wasylewski, Interaction of cAMP receptor protein from *Escherichia coli* with cAMP and DNA studied by dynamic light scattering and time-resolved fluorescence anisotropy methods. *J. Protein Chem.* 20(8) (2001) 601-610.
- [148] A. Frolov, F. Schroeder, Acyl coenzyme a binding protein: Ligand-protein interaction as monitored by time-resolved fluorescence. *Biophys. J.* 74(2) (1998) A145-A145.
- [149] P. Hazra, D. Chakrabarty, A. Chakraborty, N. Sarkar, Probing protein-surfactant interaction by steady state and time-resolved fluorescence spectroscopy. *Biochem. Biophys. Res. Commun.* 314(2) (2004) 543-549.
- [150] D. Maurel, J. Kniazeff, G. Mathis, E. Trinquet, J.P. Pin, H. Ansanay, Cell surface detection of membrane protein interaction with homogeneous time-resolved fluorescence resonance energy transfer technology. *Anal. Biochem.* 329(2) (2004) 253-262.
- [151] M. Almgren, J.E. Lofroth, Determination of Micelle Aggregation Numbers and Micelle Fluidities from Time-Resolved Fluorescence Quenching Studies. *J. Colloid Interface Sci.* 81(2) (1981) 486-499.
- [152] P.C. Griffiths, A. Paul, R.K. Heenan, J. Penfold, R. Ranganathan, B.L. Bales, Role of counterion concentration in determining micelle aggregation: Evaluation of the combination of constraints from small-angle neutron scattering, electron paramagnetic resonance, and time-resolved fluorescence quenching. *J. Phys. Chem. B* 108(12) (2004) 3810-3816.
- [153] R. Ranganathan, M. Peric, B.L. Bales, Time-resolved fluorescence quenching measurements of the aggregation numbers of normal sodium alkyl sulfate micelles well above the critical micelle concentrations. *J. Phys. Chem. B* 102(43) (1998) 8436-8439.
- [154] R.B.M. Koehorst, R.B. Spruijt, M.A. Hemminga, Site-directed fluorescence labeling of a membrane protein with BADAN: Probing protein topology and local environment. *Biophys. J.* 94(10) (2008) 3945-3955.
- [155] P.A. Vanparidon, J.K. Shute, K.W.A. Wirtz, A.J.W.G. Visser, A Fluorescence Decay Study of Parinaroyl-Phosphatidylinositol Incorporated into Artificial and Natural Membranes. *Eur. Biophys. J. Biophys. Lett.* 16(1) (1988) 53-63.
- [156] N.M. Eleftheriou, J.D. Brennan, Probing the dynamics of domain III of human serum albumin entrapped in sol-gel derived silica using a Sudlow's site II specific fluorescent ligand. *J. Sol-Gel Sci. Technol.* 50(2) (2009) 184-193.
- [157] N.J. Flint, S. Gardebrecht, L. Swanson, Fluorescence Investigations of "Smart" Microgel Systems. *J. Fluoresc.* 8(4) (1998) 343-353.

- [158] I. Pastor, M.L. Ferrer, M.P. Lillo, J. Gomez, C.R. Mateo, Structure and dynamics of lysozyme encapsulated in a silica sol-gel matrix. *J. Phys. Chem. B* 111(39) (2007) 11603-11610.
- [159] B. Rangarajan, L.S. Coons, A.B. Scranton, Characterization of hydrogels using luminescence spectroscopy. *Biomaterials* 17(7) (1996) 649-661.
- [160] N.M. Correa, H.G. Zhang, Z.A. Schelly, Preparation of AgBr quantum dots via electroporation of vesicles. *J. Am. Chem. Soc.* 122(27) (2000) 6432-6434.
- [161] Z.A. Schelly, Subnanometer size uncapped quantum dots via electroporation of synthetic vesicles. *Colloid Surf. B-Biointerfaces* 56(1-2) (2007) 281-284.
- [162] R. Stoenescu, A. Graff, W. Meier, Asymmetric ABC-triblock copolymer membranes induce a directed insertion of membrane proteins. *Macromol. Biosci.* 4(10) (2004) 930-935.
- [163] H. Lomas, I. Canton, S. MacNeil, J. Du, S.P. Armes, A.J. Ryan, A.L. Lewis, G. Battaglia, Biomimetic pH sensitive polymersomes for efficient DNA encapsulation and delivery. *Adv. Mater.* 19(23) (2007) 4238-4243.
- [164] F.H. Meng, G.H.M. Engbers, J. Feijen, Biodegradable polymersomes as a basis for artificial cells: encapsulation, release and targeting. *J. Control. Release* 101(1-3) (2005) 187-198.
- [165] C.P. O'Neil, T. Suzuki, D. Demurtas, A. Finka, J.A. Hubbell, A Novel Method for the Encapsulation of Biomolecules into Polymersomes via Direct Hydration. *Langmuir* 25(16) (2009) 9025-9029.
- [166] D.M. Saylor, C.S. Kim, D.V. Patwardhan, J.A. Warren, Diffuse-interface theory for structure formation and release behavior in controlled drug release systems. *Acta Biomater.* 3(6) (2007) 851-864.
- [167] M. Grassi, N. Cocceani, L. Magarotto, Mathematical modeling of drug release from microemulsions: Theory in comparison with experiments. *J. Colloid Interface Sci.* 228(1) (2000) 141-150.
- [168] K. Kubota, E.H. Twizell, H.I. Maibach, Drug-Release from a Suspension with a Finite Dissolution Rate - Theory and Its Application to a Betamethasone 17-Valerate Patch. *J. Pharm. Sci.* 83(11) (1994) 1593-1599.
- [169] N.S. Berchane, K.H. Carson, A.C. Rice-Ficht, M.J. Andrews, Effect of mean diameter and polydispersity of PLG microspheres on drug release: Experiment and theory. *Int. J. Pharm.* 337(1-2) (2007) 118-126.
- [170] J. Siepmann, N. Faisant, J. Akiki, J. Richard, J.P. Benoit, Effect of the size of biodegradable microparticles on drug release: experiment and theory. *J. Control. Release* 96(1) (2004) 123-134.
- [171] A. Mecke, C. Dittrich, W. Meier, Biomimetic membranes designed from amphiphilic block copolymers. *Soft Matter* 2(9) (2006) 751-759.
- [172] S. Ganta, D. Deshpande, A. Korde, M. Amiji, A review of multifunctional nanoemulsion systems to overcome oral and CNS drug delivery barriers. *Mol. Membr. Biol.* 27(7) (2010) 260-273.
- [173] K. Ainaoui, E.M. Ouriemchi, J.M. Vergnaud, Drug formulation for oral delivery with controlled release. *Abstracts of Papers of the Amer. Chemical Soc.* 216 (1998) U241-U242.
- [174] P. Li, S.R. Hynes, T.F. Haefele, M. Pudipeddi, A.E. Royce, A.T.M. Serajuddin, Development of Clinical Dosage Forms for a Poorly Water-Soluble Drug II: Formulation and Characterization of a Novel Solid Microemulsion Preconcentrate System for Oral Delivery of a Poorly Water-Soluble Drug. *J. Pharm. Sci.* 98(5) (2009) 1750-1764.

- [175] K. Engin, D.B. Leeper, J.R. Cater, A.J. Thistlethwaite, L. Tupchong, J.D. Mcfarlane, Extracellular Ph Distribution in Human Tumors. *Int. J. Hyperthermia* 11(2) (1995) 211-216.
- [176] A.J. Thistlethwaite, D.B. Leeper, D.J. Moylan, R.E. Nerlinger, Ph Distribution in Human-Tumors. *Int. J. Radiat. Oncol. Biol. Phys.* 11(9) (1985) 1647-1652.
- [177] J. Kneipp, H. Kneipp, B. Wittig, K. Kneipp, Following the Dynamics of pH in Endosomes of Live Cells with SERS Nanosensors. *J. Phys. Chem. C* 114(16) (2010) 7421-7426.
- [178] D. Liebl, F. Difato, L. Hornikova, P. Mannova, J. Strokrova, J. Forstova, Mouse polyomavirus enters early endosomes, requires their acidic pH for productive infection, and meets transferrin cargo in rab11-positive endosomes. *J. Virol.* 80(9) (2006) 4610-4622.
- [179] H.H. Sun, T.L. Andresen, R.V. Benjaminsen, K. Almdal, Polymeric Nanosensors for Measuring the Full Dynamic pH Range of Endosomes and Lysosomes in Mammalian Cells. *J. Biomed. Nanotechnol.* 5(6) (2009) 676-682.
- [180] E. Kucharz, M. Drozd, Role of Lysosomes in Diseases of Connective-Tissue - Review. *Folia Histochem. Cytochem.* 15(2) (1977) 63-78.
- [181] J.P. Luzio, V. Poupon, M.R. Lindsay, B.M. Mullock, R.C. Piper, P.R. Pryor, Membrane dynamics and the biogenesis of lysosomes (Review). *Mol. Membr. Biol.* 20(2) (2003) 141-154.
- [182] N. Bodor, Redox Drug Delivery Systems for Targeting Drugs to the Brain. *Ann.NY Acad.Sci.* 507 (1987) 289-306.
- [183] A. Corti, T.L. Duarte, A. Paolicchi, S. Dominici, G.D.D. Jones, P. Dilda, P.J. Hogg, A. Pompella, Gamma-Glutamyltransferase of Cancer Cells at the Crossroads of Redox Regulation, Tumor Progression, Drug Resistance and Drug Targeting. *Anticancer Res.* 28(5C) (2008) 3451-3452.
- [184] G.I. Giles, N.M. Giles, Organochalcogenides As Redox Activated Anti Cancer Drugs. *Free Radic. Biol. Med.* 47 (2009) S142-S142.
- [185] J.D. Pennington, K.M. Jacobs, L. Sun, G. Bar-Sela, M. Mishra, D. Gius, Thioredoxin and thioredoxin reductase as redox-sensitive molecular targets for cancer therapy. *Curr. Pharm. Design* 13(33) (2007) 3368-3377.
- [186] G. Powis, D. Mustacich, A. Coon, The role of the redox protein thioredoxin in cell growth and cancer. *Free Radic. Biol. Med.* 29(3-4) (2000) 312-322.
- [187] K.D. Tew, F. Ali-Osman, Redox pathways in cancer drug discovery. *Curr. Opin. Pharmacol.* 7(4) (2007) 353-354.
- [188] S. Toyokuni, Oxidative stress and cancer: The role of redox regulation. *Biotherapy* 11(2-3) (1998) 147-154.
- [189] T. Grundl, A Review of the Current Understanding of Redox Capacity in Natural, Disequilibrium Systems. *Chemosphere* 28(3) (1994) 613-626.
- [190] J. Dobson, Magnetic nanoparticles for drug delivery. *Drug Dev. Res.* 67(1) (2006) 55-60.
- [191] C. Sun, J.S.H. Lee, M.Q. Zhang, Magnetic nanoparticles in MR imaging and drug delivery. *Adv. Drug Deliv. Rev.* 60(11) (2008) 1252-1265.
- [192] O. Veiseh, J.W. Gunn, M.Q. Zhang, Design and fabrication of magnetic nanoparticles for targeted drug delivery and imaging. *Adv. Drug Deliv. Rev.* 62(3) (2010) 284-304.
- [193] F. Ahmed, D.E. Discher, Self-porating polymersomes of PEG-PLA and PEG-PCL: hydrolysis-triggered controlled release vesicles. *J. Control. Release* 96(1) (2004) 37-53.
- [194] B. Mishra, B.B. Patel, S. Tiwari, Colloidal nanocarriers: a review on formulation technology, types and applications toward targeted drug delivery. *Nanomed.-Nanotechnol. Biol. Med.* 6(1) (2010) 9-24.

- [195] H. Koide, T. Asai, K. Hatanaka, K. Shimizu, M. Yokoyama, T. Ishida, H. Kiwada, N. Oku, Elucidation of Accelerated Blood Clearance Phenomenon Caused by Repeat Injection of PEGylated Nanocarriers. *Yakugaku Zasshi-J. Pharm. Soc. Jpn.* 129(12) (2009) 1445-1451.
- [196] E.R. Unanue, Secretory Function of Mononuclear Phagocytes - Review. *Am. J. Pathol.* 83(2) (1976) 395-417.
- [197] P.C. Wilkinson, Recognition and Response in Mononuclear and Granular Phagocytes - Review. *Clin. Exp. Immunol.* 25(3) (1976) 355-366.
- [198] H. Harm, L. Renwartz, The Inhibition of Serum Opsonins by a Carbohydrate and the Opsonizing Effect of Purified Agglutinin on the Clearance of Non-Self Particles from the Circulation of Helix-Pomatia. *J. Invertebr. Pathol.* 36(1) (1980) 64-70.
- [199] C.R. Jenkin, D. Rowley, Role of Opsonins in Clearance of Living and Inert Particles by Cells of Reticuloendothelial System. *J. Exp. Med.* 114(3) (1961) 363-374.
- [200] C. Houga, J.F. Le Meins, R. Borsali, D. Taton, Y. Gnanou, Synthesis of ATRP-induced dextran-b-polystyrene diblock copolymers and preliminary investigation of their self-assembly in water. *Chem. Commun.*(29) (2007) 3063-3065.
- [201] L.C. You, H. Schlaad, An easy way to sugar-containing polymer vesicles or glycosomes. *J. Am. Chem. Soc.* 128(41) (2006) 13336-13337.
- [202] B. Romberg, J.M. Metselaar, L. Baranyi, C.J. Snel, R. Bunger, W.E. Hennink, J. Szebeni, G. Storm, Poly(amino acid)s: Promising enzymatically degradable stealth coatings for liposomes. *Int. J. Pharm.* 331(2) (2007) 186-189.
- [203] B. Romberg, C. Oussoren, C.J. Snel, W.E. Hennink, G. Storm, Effect of liposome characteristics and dose on the pharmacokinetics of liposomes coated with poly(amino acid)s. *Pharm. Res.* 24(12) (2007) 2394-2401.
- [204] A.K. Bajpai, Blood protein adsorption onto macroporous semi-interpenetrating polymer networks (IPNs) of poly(ethylene glycol) (PEG) and poly(2-hydroxyethyl methacrylate) (PHEMA) and assessment of in vitro blood compatibility. *Polym. Int.* 56(2) (2007) 231-244.
- [205] G.P. Lopez, B.D. Ratner, R.J. Rapoza, T.A. Horbett, Plasma Deposition of Ultrathin Films of Poly(2-Hydroxyethyl Methacrylate) - Surface-Analysis and Protein Adsorption Measurements. *Macromolecules* 26(13) (1993) 3247-3253.
- [206] J.H. Teichroeb, J.A. Forrest, L.W. Jones, J. Chan, K. Dalton, Quartz crystal microbalance study of protein adsorption kinetics on poly(2-hydroxyethyl methacrylate). *J. Colloid Interface Sci.* 325(1) (2008) 157-164.
- [207] D. Bazile, C. Prudhomme, M.T. Bassoullet, M. Marlard, G. Spenlehauer, M. Veillard, Stealth Me.Peg-Pla Nanoparticles Avoid Uptake by the Mononuclear Phagocytes System. *J. Pharm. Sci.* 84(4) (1995) 493-498.
- [208] G.S. He, L.L. Ma, J. Pan, S. Venkatraman, ABA and BAB type triblock copolymers of PEG and PLA: A comparative study of drug release properties and "stealth" particle characteristics. *Int. J. Pharm.* 334(1-2) (2007) 48-55.
- [209] T. Niidome, M. Yamagata, Y. Okamoto, Y. Akiyama, H. Takahashi, T. Kawano, Y. Katayama, Y. Niidome, PEG-modified gold nanorods with a stealth character for in vivo applications. *J. Control. Release* 114(3) (2006) 343-347.
- [210] B. Shi, C. Fang, Y.Y. Pei, Stealth PEG-PHDCA niosomes: Effects of chain length of PEG and particle size on niosomes surface properties, in vitro drug release, phagocytic uptake, in vivo pharmacokinetics and antitumor activity. *J. Pharm. Sci.* 95(9) (2006) 1873-1887.

- [211] T. Waku, M. Matsusaki, T. Kaneko, M. Akashi, PEG brush peptide nanospheres with stealth properties and chemical functionality. *Macromolecules* 40(17) (2007) 6385-6392.
- [212] G. Yin, Z. Liu, J. Zhan, F.X. Ding, N.J. Yuan, Impacts of the surface charge property on protein adsorption on hydroxyapatite. *Chem. Eng. J.* 87(2) (2002) 181-186.
- [213] A. VertutDoi, H. Ishiwata, K. Miyajima, Binding and uptake of liposomes containing a poly(ethylene glycol) derivative of cholesterol (stealth liposomes) by the macrophage cell line J774: Influence of PEG content and its molecular weight. *Biochim. Biophys. Acta-Biomembr.* 1278(1) (1996) 19-28.
- [214] A. Gabizon, D. Papahadjopoulos, The Role of Surface-Charge and Hydrophilic Groups on Liposome Clearance In vivo. *Biochim. Biophys. Acta-Biomembr.* 1103(1) (1992) 94-100.
- [215] G.S. Kwon, K. Kataoka, Block-Copolymer Micelles as Long-Circulating Drug Vehicles. *Adv. Drug Deliv. Rev.* 16(2-3) (1995) 295-309.
- [216] S. Stolnik, L. Illum, S.S. Davis, Long Circulating Microparticulate Drug Carriers. *Adv. Drug Deliv. Rev.* 16(2-3) (1995) 195-214.
- [217] H. Takeuchi, H. Kojima, H. Yamamoto, Y. Kawashima, Polymer coating of liposomes with a modified polyvinyl alcohol and their systemic circulation and RES uptake in rats. *J. Control. Release* 68(2) (2000) 195-205.
- [218] Y. Yamamoto, Y. Nagasaki, Y. Kato, Y. Sugiyama, K. Kataoka, Long-circulating poly(ethylene glycol)-poly(D,L-lactide) block copolymer micelles with modulated surface charge. *J. Control. Release* 77(1-2) (2001) 27-38.
- [219] H. Aoki, T. Tottori, F. Sakurai, K. Fuji, K. Miyajima, Effects of positive charge density on the liposomal surface on disposition kinetics of liposomes in rats. *Int. J. Pharm.* 156(2) (1997) 163-174.
- [220] B. Romberg, C. Oussoren, C.J. Snel, M.G. Carstens, W.E. Hennink, G. Storm, Pharmacokinetics of poly(hydroxyethyl-L-asparagine)-coated liposomes is superior over that of PEG-coated liposomes at low lipid dose and upon repeated administration. *Biochim. Biophys. Acta-Biomembr.* 1768(3) (2007) 737-743.
- [221] S.M. Moghimi, H. Hedeman, I.S. Muir, L. Illum, S.S. Davis, An Investigation of the Filtration Capacity and the Fate of Large Filtered Sterically-Stabilized Microspheres in Rat Spleen. *Biochim. Biophys. Acta-Gen. Subj.* 1157(3) (1993) 233-240.
- [222] D.C. Litzinger, A.M.J. Buiting, N. Vanrooijen, L. Huang, Effect of Liposome Size on the Circulation Time and Intraorgan Distribution of Amphipathic Poly(Ethylene Glycol)-Containing Liposomes. *Biochim. Biophys. Acta-Biomembr.* 1190(1) (1994) 99-107.
- [223] H. Maeda, J. Wu, T. Sawa, Y. Matsumura, K. Hori, Tumor vascular permeability and the EPR effect in macromolecular therapeutics: a review. *J. Control. Release* 65(1-2) (2000) 271-284.

## *Chapter 3*

### **Biodegradable Polymersomes as Carriers and Release Systems for Paclitaxel using Oregon Green<sup>®</sup> 488 Labeled Paclitaxel as a Model Compound\***

Jung Seok Lee, Jan Feijen

*Department of Polymer Chemistry and Biomaterials, Institute for Biomedical Technology and Technical Medicine, MIRA, Faculty of Science and Technology, University of Twente, Enschede, The Netherlands*

---

\* Submitted to Journal of Controlled Release

### Abstract

Oregon Green<sup>®</sup> 488 labeled paclitaxel (Flutax) loaded biodegradable polymersomes (Flutax-Ps) based on methoxy poly(ethylene glycol)-b-poly(*D,L*-lactide) (mPEG-PDLLA), methoxy poly(ethylene glycol)-b-poly( $\epsilon$ -caprolactone) (mPEG-PCL) or a mixture of the block copolymers (50:50, w/w) were prepared (abbreviated as Flutax-Ps (L), Flutax-Ps (C) and Flutax-Ps (LC), respectively). For the formation of the Ps, the corresponding block copolymers and Flutax were dissolved in THF and the THF solution was injected into an aqueous phase. Flutax-Ps with a size less than 150 nm were obtained, which had Flutax entrapment efficiencies higher than 55 % (polymer concentration: 1 mg/ml; Flutax concentration up to 100  $\mu$ g/ml). A sustained and complete release of Flutax was observed for Flutax-Ps (L) over one month with no initial burst. Flutax was released much slower from Ps (C) than from Ps (L) (49.9 % after one month), which is probably due to differences in the crystallinity and rate of degradation of the consisting copolymers. The release rate of Flutax from Ps (LC) was in between those of Ps (L) and Ps (C). The *in vitro* cytotoxicity of Flutax-Ps (L) using cultured SKBR3 breast cancer cells was compared with that of empty Ps (L) and a Cremophor<sup>®</sup> EL/ethanol formulation (50:50, v/v) with Flutax (FCE) or without Flutax (CE). At a Flutax concentration of 5  $\mu$ g/ml, about 67 % reduction in the viability of SKBR3 cells was observed for Flutax-Ps (L) after 3 d exposure, while the FCE formulation reduced the cell viability for more than 90 % under the same conditions. Empty Ps (L) showed a low toxicity of about 10 % and the CE formulation exhibited a cytotoxicity higher than 54 % without Flutax, indicating that the high reduction in SKBR3 cell viability for FCE is associated with the toxicity of the Cremophor<sup>®</sup> EL formulation.

## **Introduction**

During the past few decades, nanocarriers have been developed as prime candidates for the delivery of hydrophobic therapeutic agents. Polymersomes (Ps), self-assembled polymeric vesicles, have attracted rapidly growing interest as a novel class of nanocarriers, partly based on their good colloidal stability and long circulation times [1-4]. Ps may have relatively thick membranes (up to 40 nm), which are formed by synthetic amphiphilic block copolymers. In general, Ps have rather long circulation times due to the presence of a hydrophilic surface layer like poly(ethylene glycol) (PEG) [5]. PEG surface brushes reduce protein adsorption onto the Ps by minimizing the interfacial free energy between the Ps and the aqueous environment and the steric hindrance exerted by the mobile PEG molecules [6-8].

The use of paclitaxel (PTX), a microtubule stabilizing agent, has been indicated by the National Cancer Institute (NCI) as the most significant advance in chemotherapy of the past 20 years. PTX exhibits strong cytotoxic activity against various cancer types, especially breast and ovarian cancer [9]. However, effective administration of PTX has been hindered by its low solubility in water (~0.4 µg/ml) since it is highly lipophilic [10]. Currently, PTX is formulated in a mixture of Cremophor<sup>®</sup> EL (a polyethoxylated castor oil) and dehydrated ethanol (50:50, v/v) and is on the market with the trademark TAXOL<sup>®</sup>. In this formulation, the Cremophor<sup>®</sup> EL required to solubilize PTX may cause serious side effects, including hypersensitivity, nephrotoxicity and neurotoxicity [11, 12]. Problems encountered with TAXOL<sup>®</sup> have led to the development of alternative formulations to reduce side effects like Abraxane<sup>®</sup>, in which PTX is bound to albumin.

New formulations of PTX also include polymeric micelles [13-17], emulsions [18-20], nanoparticles [21, 22], dendrimers [23], hydrogels [24-26] and liposomes [27-31]. These carriers have not only been developed to enhance the concentration of PTX in aqueous solutions and dispersions, but also to deliver PTX in a controlled manner. Zhang *et al.* incorporated PTX into the core of micelles based on mPEG-PDLLA. Concentrations of PTX in these aqueous micellar systems up to 50 mg/ml could be reached [32]. Star-branched PEG-PDLLA copolymers were investigated to form PTX loaded micelles and the release of PTX from these micelles was controlled over a 2 week period [33]. PTX-loaded liposomes have been reported, which could be used to increase the concentration of PTX in aqueous systems to 0.44 mg/ml [34].



However, these formulations were not very stable either *in vitro* or *in vivo*. mPEG-PDLLA micelles and liposomes containing PTX were only stable for several days upon storage at 4 °C after which precipitation of PTX took place [34, 35]. *In vivo* studies showed that PTX rapidly dissociated from mPEG-PDLLA micelles in blood and that it was eliminated as free paclitaxel, while the micelles were rapidly removed by the kidneys with a circulation half lifetime of less than 3 h [36]. In view of their stability and long circulation time, Ps may be good candidates as stable carriers for PTX. Li *et al.* demonstrated that PTX could be loaded into the hydrophobic part of the membranes of non-biodegradable Ps based on PEG-b-poly(butadiene) (PEG-PBD). The PTX-loaded Ps were stable for periods over 4 months at 4 °C, which offers a means to obtain PTX formulations with a rather high aqueous PTX concentration (up to 0.69 mg/ml) [37]. At the moment, no *in vivo* studies with PTX-loaded Ps have been reported.

The aim of this study is to develop biodegradable Ps for PTX delivery and to study the release of PTX from these Ps in aqueous systems. In principle, the release of PTX from Ps can be controlled by using amphiphilic block copolymers with different hydrophobic blocks. Bermudez *et al.* and Ahmed *et al.* prepared Ps based on block copolymers such as PEG-PBD, PEG-b-poly(ethylene) (PEG-PEE), PEG-b-poly(lactic acid) (PEG-PLA) and PEG-PCL. The latter two copolymers are biodegradable and it was shown that the mechanical properties and the rate of degradation of these Ps membranes depend on the character and length of the hydrophobic blocks [2, 38, 39].

In this study, two amphiphilic di-block copolymers were used to prepare three types of drug-loaded and non-loaded Ps. Ps were prepared by injecting THF solutions of mPEG-PDLLA, mPEG-PCL or a mixture of the block copolymers (50:50, w/w) with or without a model drug for PTX into PBS or DI water. Ps made of mPEG-PDLLA, mPEG-PCL and a mixture of two block copolymers have been abbreviated as Ps (L), Ps (C) and Ps (LC), respectively. Oregon Green<sup>®</sup> 488 labeled PTX (Flutax) was employed as the model drug (Fig. 3.1). Flutax in aqueous solutions can be directly quantified by fluorescence spectroscopy. Flutax exhibits a comparable activity as native PTX since Oregon Green<sup>®</sup> 488 is bound to the hydroxyl group at position 7 of PTX, which is known to be not essential for the anticancer activity [40]. Flutax has also been used for unraveling the cellular targets of the drug and studying details of drug-microtubule interactions at the molecular level [40-42]. However, it has to be realized that Flutax may slightly differ from PTX with respect to water solubility and cytotoxicity.

As illustrated in Fig. 3.2, Flutax will be mostly incorporated in the hydrophobic part of the membrane of Ps and subsequently released into the medium. Ps before and after loading of Flutax were compared with respect to their size and morphology by DLS and TEM, respectively. Flutax-loaded Ps (Flutax-Ps) were imaged by CLSM and the stability in a PBS dispersion at 37 °C was evaluated by determining the size, count rate and polydispersity index (PDI) with DLS as a function of time. Fluorescence spectroscopy was used to determine the Flutax loading capacity of different Ps and to monitor the release of Flutax from the Ps. The *in vitro* cytotoxicity of Flutax-Ps was studied using cultured SKBR3 breast cancer cells and compared with the cytotoxicity of empty Ps as well as that of a Cremophor<sup>®</sup> EL/ethanol formulation with or without Flutax.

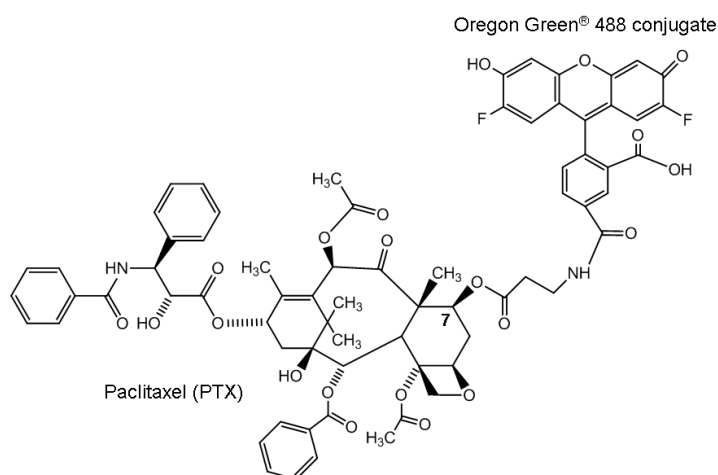


Figure 3.1. Structure of Oregon Green<sup>®</sup> 488 conjugated paclitaxel (Flutax)

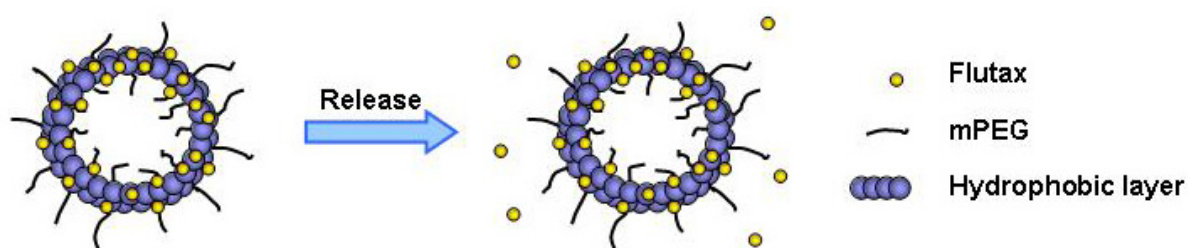


Figure 3.2. Schematic 2D-cross sectional illustration of the release of Flutax from Ps, in which Flutax was incorporated in the Ps membrane.

## Materials and methods

### *Materials*

*D,L*-lactide (DLLA) was obtained from Purac Biochem b.v. (The Netherlands) and recrystallized from toluene.  $\epsilon$ -Caprolactone (CL, Sigma-Aldrich, The Netherlands) was distilled over calcium hydride. Monomethoxy poly(ethylene glycol) with a molecular weight of 5000 g/mol (mPEG, Iris Biotech, Germany) was dried by dissolution in anhydrous toluene followed by azeotropic distillation under  $N_2$ . Stannous octoate,  $Sn(Oct)_2$  (Sigma, UK) and uranyl acetate dihydrate (Fluka, USA) were used as received. Oregon Green<sup>®</sup> 488 conjugated paclitaxel (Flutax) was purchased from Invitrogen (The Netherlands). Deionized water (DI water) was obtained from a Milli-Q water purification system (Millipore, France) and phosphate buffered saline (PBS, 0.01M, pH 7.4, containing 0.02 wt.%  $NaN_3$ , B. Braun, USA) were used for release experiments and cell studies. Dulbecco's Modified Eagle Medium (DMEM, Invitrogen, The Netherlands), Foetal Bovine Serum (FCS, Invitrogen, The Netherlands) and Penicillin-Streptomycin (PS, Invitrogen, The Netherlands) were used to prepare the medium for SKBR3 cells. CellTiter 96<sup>®</sup> Aqueous Non-Radioactive cell Proliferation Assay kit was purchased from Promega Benelux b.v. (The Netherlands) and used for the MTS assay.

### *Synthesis of mPEG-PDLLA or mPEG-PCL*

mPEG-PDLLA or mPEG-PCL was synthesized by ring-opening polymerization (ROP) using mPEG as an initiator. mPEG (0.50 g, 0.1 mmol), DLLA (4.2 g, 29.2 mmol) or CL (4.2 g, 36.8 mmol),  $Sn(Oct)_2$  (0.04 g, 0.1 mmol) and toluene (30.0 ml) were charged in that order in a reaction vessel. The reaction was performed at 110 °C for 26 h under stirring. After cooling, a drop of HCl (37 wt.%) was added to the reaction mixture to hydrolyze the tin-oxygen bond. The copolymer was isolated by precipitation in methanol. After filtration and washing with methanol, the copolymer was dissolved in dichloromethane (DCM) and precipitated in diethyl ether. Subsequently, the polymer was isolated by filtration, washed several times with diethyl ether, and dried under vacuum. The monomer conversion and the number average molecular weight of block copolymers ( $M_n$ ) were determined by <sup>1</sup>H-NMR (Inova 300 MHz, Varian, USA).

### *Preparation of Flutax-loaded Ps*

Three types of Flutax-Ps were prepared by using mPEG-PDLLA, mPEG-PCL or a mixture of the block copolymers (50:50 w/w) (abbreviated as Flutax-Ps (L), Flutax-Ps (C) and Flutax-Ps (LC), respectively). The amphiphilic block copolymer or a block copolymer mixture (10 mg/ml) with Flutax (0.1, 0.5 or 1.0 mg/ml) was dissolved in THF (1 ml), and the THF solution was injected either into 50 ml of PBS (pH 7.4) or in DI water (TEM experiments). After 15 min without shaking, the vial containing the mixture was turned upside down several times, resulting in a turbid dispersion. To remove the organic solvent from the solution, the Flutax-Ps dispersion was transferred into a dialysis bag (cut-off 50,000 g/mol, Spectra/Por, CA), which was placed in a 4 l flask with PBS or DI water. The dialysis was performed for 2 d by replacing the PBS or DI water for at least 5 times. Subsequently, the dispersion was ultrafiltrated through a membrane (cut-off 100,000 g/mol, Ultracel Ultrafiltration Disc, Millipore, USA) for 1 d to remove non-encapsulated Flutax. The purified samples were concentrated 5 times during the ultrafiltration step. Flutax-Ps prepared with 10 µg/ml of Flutax in the feed were considered as standard Ps and used for the characterization with DLS, TEM, CLSM and for *in vitro* release and cell studies. For comparison, empty Ps (L), Ps (C) and Ps (LC) were also prepared using a similar method as for the preparation of Flutax-Ps (L, C and LC), but in the absence of Flutax. Flutax-Ps (L) and Flutax-Ps (C) were also blended to yield Flutax-Ps (L+C), which was also used for the release study.

### *Dynamic light scattering and transmission electron microscopy*

The stability of Flutax-Ps in time was investigated by measuring the size, count rate and polydispersity index (PDI) with DLS (Zetasizer Nano ZS, Malvern Instruments, Malvern, UK). Samples were prepared by filtering the solutions through a 0.45 µm Millipore filter into cuvettes. Flutax-Ps suspensions in PBS were prepared and monitored for 4 weeks at 37 °C. Data were collected at different incubation times by measuring DLS 30 times. The size and PDI of Flutax-Ps before the incubation were compared to those of empty Ps. Transmission electron microscopy (TEM, Philips CM30, Hillsboro, USA) was performed to elucidate the morphology and membrane thickness of Ps as well as Flutax-Ps. A dispersion of empty Ps (2 µl) was placed on a 200 mesh carbon grid without using a staining agent and dried at room temperature. A Flutax-Ps dispersion was deposited onto a 300 mesh carbon grid. After 30 s, the dispersion was stained

with an uranyl acetate solution (2 wt.%) for 1 min. The excess solution was removed and the sample was dried at room temperature. Ps and Flutax-Ps in DI water were used for TEM studies.

#### *Confocal laser scanning microscopy*

Fluorescence images were obtained by CLSM (LSM 510, Zeiss, Germany) equipped with a Zeiss Axiovert 100 M Inverted Microscope for Nomarski DIC and Epi-Fluorescence. To evaluate the co-localization of Flutax and Ps, 1 ml of the Flutax-Ps (L) suspension was introduced into homemade thin-glass-bottomed cuvettes and an Ar laser was employed for excitation of Oregon Green<sup>®</sup> 488.

#### *Loading of Flutax in Ps and release*

Flutax-loaded Ps were prepared by injecting the appropriate THF solution into PBS. In order to determine the amount of loaded Flutax, Ps were solubilized using Triton X-100 [43]. After adding Triton X-100 to the Ps dispersion with a final concentration of 2 wt.%, the mixture was heated for 3 h at 80 °C. The release of Flutax from suspensions of Ps placed in a microdialysis system was monitored by periodic withdrawal of PBS samples. The release was studied by placing a dispersion of Flutax-Ps (1 ml, 10 µg/ml of Flutax in the feed) into a dialysis bag (cut-off 20,000 g/mol) and immersing the bag into a large vial containing PBS. The total volume of PBS was 100 ml, which is enough to solubilize the Flutax when 100 % of loaded Flutax is released into the medium (~ 0.08 µg/ml). The experiments were carried out in three-fold. The release of free Flutax from an empty dialysis bag was also measured to evaluate the effect of the dialysis membrane on release kinetics of Flutax in the experiment. At appropriate times, 1 ml of the release medium was collected from the vials and the medium was replaced by fresh PBS. Concentrations of released Flutax were determined by fluorescence spectroscopy (Safire<sup>2</sup>, Tecan, CA) at an emission wavelength of 516 nm and an excitation wavelength of 495 nm. In this way, the loaded amounts of Flutax as well as the release kinetics were obtained.

#### *In vitro cytotoxicity of Flutax-Ps*

Flutax-loaded Ps or non-loaded Ps prepared using PBS were applied for the study. For comparison, Flutax solubilized in Cremophor<sup>®</sup> EL (FCE) was prepared as a model formulation of TAXOL<sup>®</sup>. In detail, 120 µg of Flutax was dissolved in 0.01 ml of ethanol and to this solution

0.01 mL Cremophor<sup>®</sup> EL was added. Then this mixture was sonicated for 30 min. A Cremophor<sup>®</sup> EL formulation without Flutax (CE) was also prepared as a control. The four stock solutions were further stepwise diluted with PBS to give Flutax concentrations ranging from 10 to 0.1 µg/ml. To evaluate the cytotoxicity of these formulations, SKBR3 cells were used, which were seeded in a 96-well plate at a density of  $5 \times 10^3$  cells per well and cultured at 37 °C in a humidified atmosphere with 5 % CO<sub>2</sub>. After 2 d, the cell medium was removed and 100 µl of fresh cell medium was added. The different Flutax formulations (100 µl) were added to the medium in the wells resulting in Flutax concentrations varying from 0.05 to 5 µg/ml. As a reference, 100 µl of PBS was added to the medium. The cells were incubated for 72 h and the number of viable cells was determined using an MTS colorimetric assay. The well plate was incubated for 4 h and the absorbance at 490 nm was recorded using a plate reader (Safire<sup>2</sup>, Tecan, CA).

## **Results and discussion**

### *Characterization of block copolymers*

In principle, amphiphilic block copolymers can self-assemble in an aqueous environment into structures with various morphologies including spherical micelles, cylindrical micelles and vesicles. The morphology of the self-assembled systems will be determined by the volume fraction of hydrophilic block ( $f$ ) and the molecular weight (MW) of the block copolymer [4, 44]. Di-block copolymers with an  $f$  between 10 and 40 % and a MW ranging from ~2700 to 50,000 g/mol have been used to prepare various Ps as previously reported in the literature [1, 39, 45, 46]. In this study, mPEG-PDLLA and mPEG-PCL with a MW about 42,000 g/mol and 40,000 g/mol, respectively, were synthesized by ROP of *D,L*-lactide and  $\epsilon$ -caprolactone, respectively using mPEG (5000 g/mol) as an initiator with high monomer conversions ( $\geq 96$  %) and further used to form Ps (L), Ps (C), and Ps (LC). Calculated volume fractions of the mPEG blocks ( $f_{PEG}$ ) were 11.8 % for mPEG-PDLLA and 12.5 % for mPEG-PCL according to the <sup>1</sup>H-NMR analysis (Table 3.1).

Table 3.1. Characterization of mPEG-PDLLA and mPEG-PCL

	Monomer conversion <sup>a</sup> (%)	Mn (theor.) <sup>b</sup> (PDLLA or PCL) (g/mol)	Mn ( <sup>1</sup> H-NMR) <sup>c</sup> (PDLLA or PCL) (g/mol)	$f_{\text{PEG}}^{\text{d}}$ (%)
mPEG <sub>5k</sub> -PDLLA	99	42,000	41,800	11.8
mPEG <sub>5k</sub> -PCL	96	42,000	40,100	12.5

<sup>a</sup> Determined by <sup>1</sup>H NMR.

<sup>b</sup> Calculated from the initial ratio of monomer to PEG hydroxyl groups.

<sup>c</sup> Determined from <sup>1</sup>H-NMR analysis by calculating the ratio of the PEG methylene peak to the main peak of the polyester.

<sup>d</sup> Calculated volume fraction of PEG in block copolymers.

### Preparation of Ps and Flutax-Ps

Prior efforts have been undertaken to assemble polymer vesicles from block copolymers with relatively high molecular weights and low hydrophilic volume fractions ( $f_{\text{PEG}} < 20\%$ ). It was reported that these types of block copolymers can form Ps by either injecting a solution of the polymer in an organic solvent into an aqueous phase [39, 46] or by adding water to the organic polymer solution [47, 48]. In this study, a series of Ps and Flutax-Ps were prepared by injecting THF solutions of mPEG-PDLLA or mPEG-PCL in the absence or the presence of Flutax into PBS (or DI water for TEM). Flutax-Ps with average diameters less than 150 nm were obtained with narrow size distributions, while Ps without Flutax were smaller ( $< 93$  nm) (Table 3.2). In principle, the hydrodynamic diameters of the Flutax-Ps obtained will be suitable to localize these Ps in tumor tissue by the enhanced permeability and retention (EPR) effect since the size of the pores of leaky blood vessels in tumor tissue is known to be about 200 nm [49, 50]. Effective passive targeting of Ps to a tumor can be achieved by extravasation of the vesicles in the tumor provided that the Ps have sufficient long circulation times. The Flutax-Ps have an external PEG layer, which will reduce protein adsorption from blood and subsequent uptake by the reticuloendothelial system (RES).

Table 3.2. Average diameters and PDI of Ps with or without loaded Flutax

	Ps (L)	Ps (C)	Flutax-Ps (L)	Flutax-Ps (C)	Flutax-Ps (LC)
Diameter <sup>a</sup> (nm)	90.9	92.9	143.2	133.5	142.2
PDI <sup>b</sup>	0.15	0.09	0.13	0.19	0.11

<sup>a</sup> Measurements were performed 30 times and averaged.

<sup>b</sup> Polydispersity index.

To prove that Flutax was co-localized with the Ps, CLSM combining both fluorescence- and bright field microscopy of Flutax-Ps (L) was carried out. Fig. 3.3 shows the green fluorescence image of Flutax, the bright field image of Ps (L) and the combined image. As indicated with arrows in the combined image, it can be observed that Flutax and Ps (L) are co-localized. TEM was performed to directly visualize the morphology and to evaluate the membrane thickness of Ps and Flutax-Ps. Figs. 3.4a, 3.4b and 3.4c show TEM images of empty Ps. Figs. 3.4d, 3.4e and 3.4f represent TEM images of Flutax-loaded Ps. It can be seen that all types of Ps are spherical nanovesicles with a membrane thickness of about 15 nm and the thickness was not dependent on the size and the type of the vesicles.

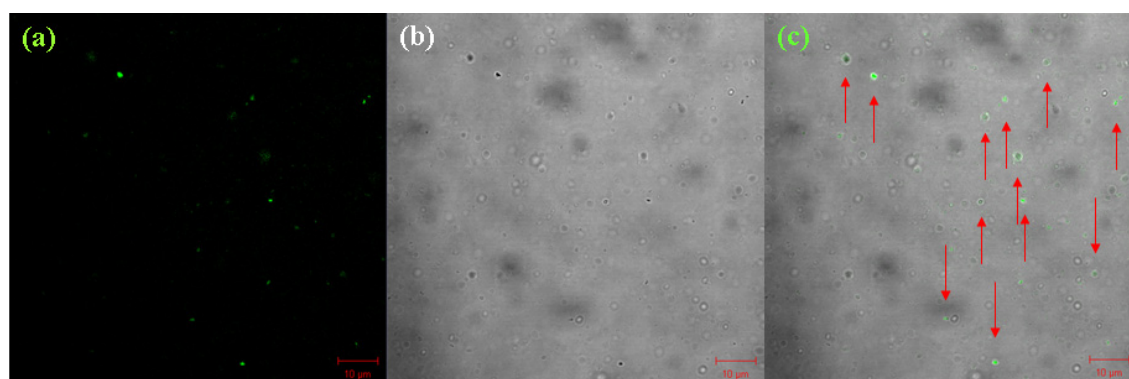


Figure 3.3. CLSM images of Flutax-Ps (L). Fluorescence image (a), bright field image (b) and the combined image (c). Size bars are 10  $\mu\text{m}$  and arrows mark the co-localization of Flutax and Ps (L).



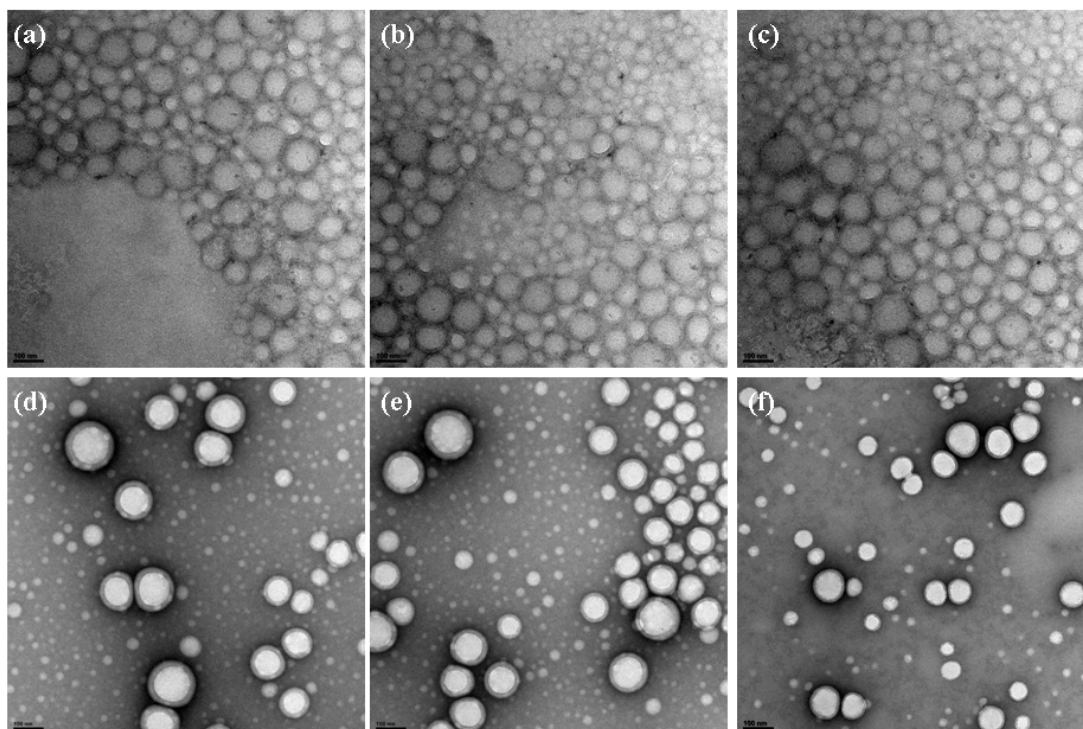


Figure 3.4. TEM images of empty Ps (a, b and c) and Flutax-loaded Ps (d, e and f) on carbon grids. A dispersion of empty Ps was placed on a 200 mesh normal carbon grid without using a staining agent and dried at room temperature, (a) Ps (L), (b) Ps (C) and (c) Ps (LC). A drop of Flutax loaded Ps dispersion was deposited onto a 300 mesh porous carbon grid and stained by uranyl acetate (2 wt.%), (d) Flutax-Ps (L), (e) Flutax-Ps (C) and (f) Flutax-Ps (LC). Size bars represent 100 nm.

#### *Loading of Ps with Flutax*

The amount of Flutax loaded in different types of Ps was determined by fluorescence spectroscopy and the entrapment efficiency was calculated based on the amount of Flutax in the feed used for the preparation of Flutax-Ps (Eq. 3.1).

$$\text{Entrapment efficiency (\%)} = \frac{\text{mass of drug in polymersomes}}{\text{mass of drug used for formulation}} \times 100 \quad (3.1)$$

In general, the entrapment efficiencies of Flutax for the three types of formulations were comparable and quite high (> 75 %) when 10 µg/ml of Flutax was used in the feed (Table 3.3). The loading capacity of Ps (C) was slightly higher than for Ps (L) and Ps (LC) probably due to the more hydrophobic character of PCL compared to PDLLA. This is in agreement with earlier

findings by Lin *et al*, who reported that hydrophobic drugs can be encapsulated with a higher efficiency in PCL-based carriers than in carriers based on PDLLA [51, 52].

The effect of the feed concentration of Flutax on the loading capacity of the Ps was also evaluated and summarized in Table 3.3. Flutax-Ps (L) were obtained from dispersions with three different concentrations of Flutax (10, 50 or 100 µg/ml) and one concentration of mPEG-PDLLA of 1.0 mg/ml in PBS. The Flutax uptake in Ps (L) dispersions (up to 55 µg/ml) increased with increasing concentrations of Flutax in the feed, but the entrapment efficiency decreased. This may indicate that the Flutax saturation level of the membrane of Ps (L) has not been reached with the Flutax concentration used. Entrapment efficiencies of Flutax in Ps (L) using 10 µg/ml and 50 µg/ml of Flutax in the feed were comparable and decreased at higher Flutax feed concentrations.

Table 3.3. Loading of Ps with Flutax

	Flutax-Ps (L)			Flutax-Ps (C)	Flutax-Ps (LC)
Flutax feed <sup>a</sup> (µg/ml)	10.0	50.0	100.0	10.0	10.0
Polymer <sup>b</sup> (mg/ml)	1.0	1.0	1.0	1.0	1.0
Loaded Flutax <sup>c</sup> (µg/ml)	7.6	38.5	55.3	8.1	7.7
Entrapment efficiency <sup>d</sup> (%)	75.6 ± 2.8	76.9 ± 1.5	55.3 ± 3.3	80.8 ± 4.1	77.0 ± 1.8

<sup>a</sup> Initial feed concentration of Flutax for the preparation of Flutax-Ps.

<sup>b</sup> Concentration of block copolymers used for the preparation of Flutax-Ps.

<sup>c</sup> Loading capacity of Ps dispersions for Flutax.

<sup>d</sup> Entrapment efficiency of Flutax in Ps. The experiments were carried out in triplicate.

#### *Colloidal stability of Flutax-Ps*

Nanocarriers based on micelles and liposomes are often reported to have poor colloidal stability in an aqueous solution after loading of hydrophobic drugs [34-36]. The low stability of these carriers may be attributed to binding of drugs to the hydrophobic blocks, which alters the curvature of the hydrophobic chains and thereby the chain packing parameter, eventually resulting in disintegration of the colloidal structures. In contrast, Ps have a relatively high colloidal stability because of the rather thick bi-layered membranes and therefore they can be considered as alternative carriers. In the literature, Li *et al*. compared the stability of worm-like micelles and Ps based on PEG-PBD after loading of paclitaxel in an aqueous environment. The worm-like micelles in PBS at 4 °C were only stable for 1 week. Aggregation of the micelles as

well as the formation of paclitaxel precipitates was observed after 1 week, while the PTX-loaded Ps were stable for 4 month at this temperature [53].

In our study, Ps consisting of mPEG-PDLLA or mPEG-PCL or a combination (50:50) both at 4 °C and 37 °C in PBS were also investigated with respect to their stability by DLS. The three types of Flutax-Ps, which have been studied here, exhibited an excellent stability for more than 2 month at 4 °C and no Flutax precipitates were observed (data not shown). The kilo count per second (Kcps) of the Flutax-Ps (L) in PBS at 37 °C did not change for 3 d, but decreased slowly within a period of 4 weeks (Fig. 3.5a). This can be mainly explained by hydrolysis of the PDLLA blocks, resulting in a very gradual disturbance of the hydrophilic/hydrophobic balance of the membranes. Initially, chains with comparatively short hydrophobic blocks will tend to gradually segregate and this ultimately may induce hydrophilic pores into the membranes, which eventually leads to destabilization of the bi-layer followed by the formation of aggregates [37]. The size and PDI of the remaining Flutax-Ps (L) in the dispersion did not significantly change in time since the aggregates resulting from hydrolysis were too big to be measured by DLS (> 10  $\mu\text{m}$ ). Flutax-Ps (C) and Flutax-Ps (LC) showed constant values for Kcps for a longer period than Flutax-Ps (L), reflecting a better stability in PBS than Flutax-Ps (L) (Figs. 3.5b and 3.5c). This is due to the difference in the rate of degradation of the block copolymers. PCL is more hydrophobic than PDLLA as previously discussed, lowering the accessibility of water to the Ps membrane resulting in a relatively lower rate of hydrolysis. Flutax-Ps with more PCL moieties showed slower degradation. No loss of Ps was observed during 2 weeks for Flutax-Ps (C) (100 % PCL) and for 1 week for Flutax-Ps (LC) (50 % PCL), whereas this was only the case for 3 d for Flutax-Ps (L).

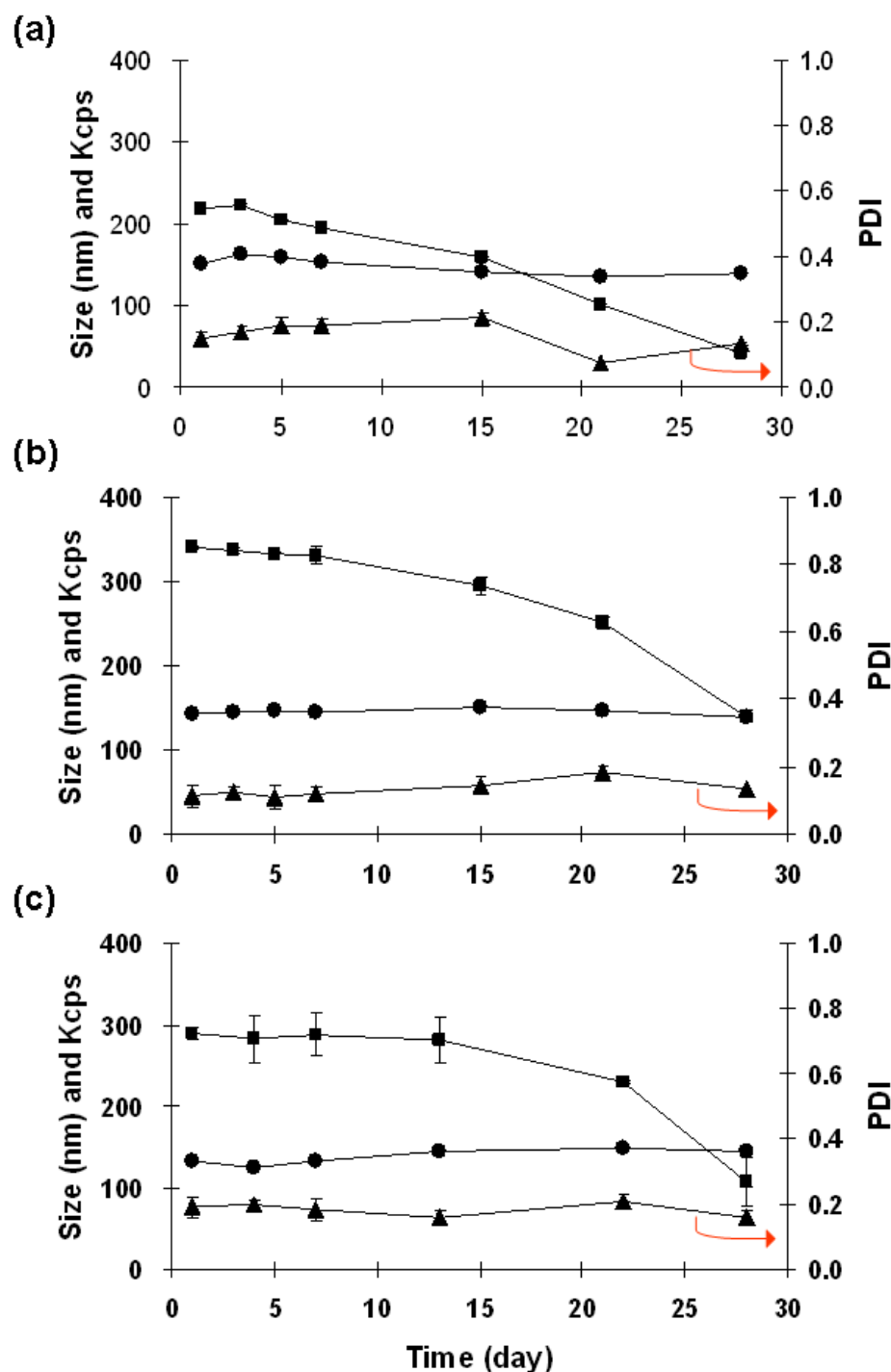


Figure 3.5. Stability of (a) Flutax-Ps (L), (b) Flutax-Ps (LC) and (c) Flutax-Ps (C) dispersions incubated at 37 °C in PBS measured by DLS. Diameter (●), Kcps (■) and PDI (▲). DLS measurements were performed 30 times per sample at each time point. The data given are mean values and the error bars are the standard deviations of the mean.

### *Release of Flutax from Ps*

Fluorescent paclitaxel (Flutax) was used as a model drug for PTX to study the release kinetics for four types of Ps formulations. Fig. 3.6 represents the release profiles of Flutax from the vesicles placed in a dialysis bag. All release profiles for the vesicles showed no initial burst because of the poor solubility of Flutax in the surrounding medium. A sustained release of Flutax was observed for Flutax-Ps (L) and complete release of the drug was accomplished after one month. Interestingly, it can be seen that the release kinetics of Flutax from Ps (L) approach a zero-order release. In order to explain this, it has to be considered that the membrane of the Ps (L) is biodegradable by bulk hydrolysis. Flutax is mainly incorporated in the PDLLA part of the membrane. The drug release from such matrix systems is governed by diffusion of the drug through the matrix. Upon degradation of the matrix the diffusion coefficient of the drug in the matrix may increase, compensating for the decrease in the concentration gradient. [54]. Similar shapes of release curves for PTX have been reported for various PDLLA-based micelles [14, 33, 55, 56]. The effects of aggregation of the Ps (L) in time during degradation on the release profile of Flutax are hard to describe.

Ps (C) released 49.9 % of the loaded Flutax over 1 month, which is much lower than the release from Ps (L). This can possibly be related to the crystallinity of the consisting copolymers. PDLLA is an amorphous polymer, whereas PCL is semi-crystalline reducing the diffusion rate of Flutax. Another possible reason is the difference in the rate of degradation of the membrane-forming polymers. PDLLA is degrading faster than PCL and therefore Flutax release from Ps (L) will also be faster. The release rate of Flutax from Ps (L+C), a mixture of Ps (L) and Ps (C) (50:50, v/v), was in between those for the constituting Ps. Ps (LC) showed similar release kinetics as Ps (L+C), but the release rate became slightly lower after 1 week. This may be due to the fact that a relatively slow release of Flutax is governed by PCL domains in the later stages, whereas a relatively fast release of Flutax from the PDLLA domains (probably located at the surface of the hydrophobic part of the membranes) occurs in the early stages. Malin *et al.* reported an increase of the crystallinity of PCL-PDLLA block copolymer during hydrolysis, which was explained by a relatively fast mass loss of the amorphous phase [57, 58]. The difference in the release rate of Flutax from Ps (L+C) and Ps (LC) may be an indication for the formation of individual Ps containing both mPEG-PDLLA and mPEG-PCL. Blends of PDLLA and PCL show two T<sub>gs</sub> close to the T<sub>gs</sub> of the individual polymers revealing that phase

separation occurs [59-61]. Ahmed and Discher have developed Ps based on mixtures of PEG-PLA and PEG-PBD or PEG-PCL and PEG-PBD. Both block copolymers were incorporated in single Ps, yielding Ps membranes with a variation in permeabilities and degradation properties [38]. The release of Flutax from the empty dialysis membrane (cut off 20,000 g/mol) was fast, but it may slightly influence the initial release data for the vesicles.

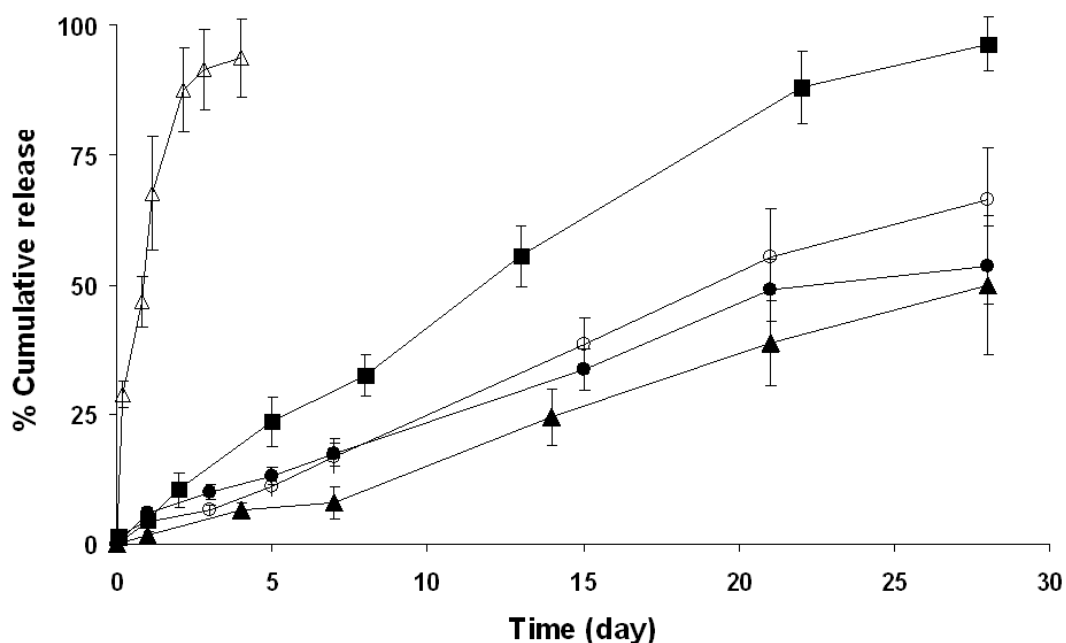


Figure 3.6. Release of Flutax from Ps at 37 °C in PBS measured by fluorescence spectroscopy. Flutax release from the dialysis bag ( $\Delta$ ), Ps (L) ( $\blacksquare$ ), Ps (C) ( $\blacktriangle$ ), Ps (LC) ( $\bullet$ ) and Ps (L+C) ( $\circ$ ). At different time intervals, 1 ml of the release medium was collected and analyzed. The experiments were carried out in triplicate.

#### *Cytotoxicity of Flutax-Ps with respect to cancer cells*

The *in vitro* cytotoxicity of Flutax-Ps (L) was studied using cultured SKBR3 breast cancer cells. For comparison, the cytotoxicity of empty Ps (L) as well as that of a Cremophor<sup>®</sup> EL/ethanol formulation (50:50, v/v) with Flutax (FCE) and without Flutax (CE) was also evaluated. Cells were incubated with formulations of Flutax with concentrations ranging from 0.05 to 5  $\mu\text{g/ml}$ . As shown in Fig. 3.7, about 67 % reduction in cell viability was observed when cells were exposed to Ps (L) with 5  $\mu\text{g/ml}$  of loaded Flutax for 3 d. However, the FCE formulation at a Flutax concentration of 5  $\mu\text{g/ml}$  resulted in a reduction of cell viability of more

than 90 %. It should be noted that this was apparently due to the combined effect of both Flutax and the Cremophor<sup>®</sup> EL formulation. The CE formulation exhibited a cell viability reduction higher than 54 %. This high cytotoxicity is in agreement with previous observations [62, 63]. In contrast, empty Ps (L) only induced a reduction in cell viability of about 10 % at the highest concentration tested (0.5 mg/ml). This may be related to a rather low interaction between the cells and Ps. Furthermore, it is well known that mPEG-PDLLA is biocompatible and therefore it has been employed for the preparation of various micro- or nanoparticles and micelles [64-66]. It is hypothesized that the cytotoxicity of Flutax-Ps (L) is associated with both Flutax released during the exposure time and possible internalization of Flutax-Ps (L) via endocytosis into SKBR3 cells. However, further studies are required to explain the mechanisms responsible for the observed cytotoxicity. At a Flutax concentration of 1 µg/ml, the results showed a similar trend for all formulations as observed at 5 µg/ml, but fewer differences between the samples were found because of the lower concentration of Flutax and materials applied.

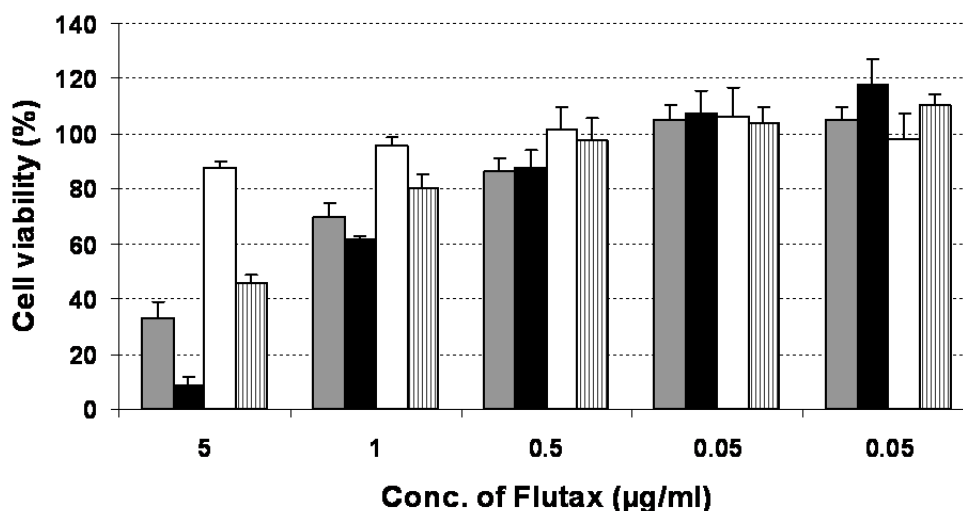


Figure 3.7. Cytotoxicity of Flutax formulations and controls for SKBR3 cells after 3 d exposure. Flutax-Ps (L) (■), Ps (L) (□), Cremophor<sup>®</sup> EL/ethanol formulation (50:50, v/v) with Flutax (■) and Cremophor<sup>®</sup> EL/ethanol formulation without Flutax (▣). The data given are mean values and the error bars are the standard deviations of the mean.

## **Conclusions**

A series of nano-sized polymersomes (Ps) based on mPEG-PDLLA or mPEG-PCL was prepared with a narrow size distribution. Fluorescent paclitaxel (Flutax) could be loaded into the membrane of the Ps with a high drug entrapment efficiency by using a simple solvent injection method. The release rate of Flutax from Ps can be varied by selecting Ps with membranes formed from different types or compositions of block copolymers. *In vitro* cytotoxicity studies using human breast cancer cells (SKBR3) revealed that Flutax loaded Ps may exhibit a chemotherapeutic efficacy comparable to that of a Flutax Cremophor<sup>®</sup> EL/ethanol formulation. By using Ps, the toxic Cremophor<sup>®</sup> EL formulation can be avoided and in principle passive targeting can be realized. Therefore, it is concluded that Ps based on biodegradable mPEG-PDLLA and/or mPEG-PCL are very promising nanocarriers for the controlled delivery of lipophilic drugs like paclitaxel for chemotherapeutic applications.

## **Acknowledgement**

The authors thank Mark Smithers (MESA<sup>+</sup>, University of Twente) for TEM measurements.



## References

- [1] F. Ahmed, P.J. Photos, D.E. Discher, Polymersomes as viral capsid mimics. *Drug Dev. Res.* 67(1) (2006) 4-14.
- [2] H. Bermudez, A.K. Brannan, D.A. Hammer, F.S. Bates, D.E. Discher, Molecular weight dependence of polymersome membrane structure, elasticity, and stability. *Macromolecules* 35(21) (2002) 8203-8208.
- [3] B.M. Discher, D.A. Hammer, F.S. Bates, D.E. Discher, Polymer vesicles in various media. *Curr. Opin. Colloid Interface Sci.* 5(1-2) (2000) 125-131.
- [4] D.E. Discher, A. Eisenberg, Polymer vesicles. *Science* 297(5583) (2002) 967-973.
- [5] P.J. Photos, L. Bacakova, B. Discher, F.S. Bates, D.E. Discher, Polymer vesicles in vivo: correlations with PEG molecular weight. *J. Control. Release* 90(3) (2003) 323-334.
- [6] S.I. Jeon, J.D. Andrade, Protein Surface Interactions in the Presence of Polyethylene Oxide 2. Effect of Protein Size. *J. Colloid Interface Sci.* 142(1) (1991) 159-166.
- [7] S.I. Jeon, J.H. Lee, J.D. Andrade, P.G. Degennes, Protein Surface Interactions in the Presence of Polyethylene Oxide 1. Simplified Theory. *J. Colloid Interface Sci.* 142(1) (1991) 149-158.
- [8] F.H. Meng, G.H.M. Engbers, A. Gessner, R.H. Muller, J. Feijen, Pegylated polystyrene particles as a model system for artificial cells. *J. Biomed. Mater. Res. Part A* 70A(1) (2004) 97-106.
- [9] R. Panchagnula, Pharmaceutical aspects of paclitaxel. *Int. J. Pharm.* 172(1-2) (1998) 1-15.
- [10] A.K. Singla, A. Garg, D. Aggarwal, Paclitaxel and its formulations. *Int. J. Pharm.* 235(1-2) (2002) 179-192.
- [11] Y.W. Lam, Chan, C.Y., Kuhn, J.G., Pharmacokinetics and pharmacodynamics of the taxanes. *J. Oncol. Pharm. Practice* 3 (1997) 76-93.
- [12] R.B. Weiss, Donehower, R.C., Wiernik, P.H., Ohnuma, T., Gralla, R.J., Trump, D.L., Baker, J.R., VanEcho, D.A., VonHoff, D.D., Leyland-Jones, B., Hypersensitivity reactions from taxol. *J. Clin. Oncol.* 8 (1990) 1263-1268.
- [13] Y.W. Cho, J. Lee, S.C. Lee, K.M. Huh, K. Park, Hydrotropic agents for study of in vitro paclitaxel release from polymeric micelles. *J. Control. Release* 97(2) (2004) 249-257.
- [14] K.M. Huh, S.C. Lee, Y.W. Cho, J.W. Lee, J.H. Jeong, K. Park, Hydrotropic polymer micelle system for delivery of paclitaxel. *J. Control. Release* 101(1-3) (2005) 59-68.
- [15] K.M. Huh, H.S. Min, S.C. Lee, H.J. Lee, S. Kim, K. Park, A new hydrotropic block copolymer micelle system for aqueous solubilization of paclitaxel. *J. Control. Release* 126(2) (2008) 122-129.
- [16] S. Kim, J.Y. Kim, K.M. Huh, G. Acharya, K. Park, Hydrotropic polymer micelles containing acrylic acid moieties for oral delivery of paclitaxel. *J. Control. Release* 132(3) (2008) 222-229.
- [17] S.C. Lee, K.M. Huh, J. Lee, Y.W. Cho, R.E. Galinsky, K. Park, Hydrotropic polymeric micelles for enhanced paclitaxel solubility: In vitro and in vivo characterization. *Biomacromolecules* 8(1) (2007) 202-208.
- [18] J. Han, C. Washington, S.S. Davis, Design and evaluation of an emulsion vehicle for paclitaxel. II. Suppression of the crystallization of paclitaxel by freeze-drying technique. *Drug Dev. Ind. Pharm.* 33(10) (2007) 1151-1157.
- [19] J.H. Han, S.S. Davis, C. Papandreou, C.D. Melia, C. Washington, Design and evaluation of an emulsion vehicle for paclitaxel. I. physicochemical properties and plasma stability. *Pharm. Res.* 21(9) (2004) 1573-1580.

- [20] P. Simamora, R.M. Dannenfelser, S.E. Tabibi, S.H. Yalkowsky, Emulsion formulations for intravenous administration of paclitaxel. *PDA J. Pharm. Sci. Technol.* 52(4) (1998) 170-172.
- [21] M.C. Pinder, N.K. Ibrahim, Nanoparticle albumin-bound paclitaxel for treatment of metastatic breast cancer. *Drugs Today* 42(9) (2006) 599-604.
- [22] W.J. Trickler, A.A. Nagvekar, A.K. Dash, A novel nanoparticle formulation for sustained paclitaxel delivery. *AAPS PharmSciTech* 9(2) (2008) 486-493.
- [23] T. Ooya, K.M. Huh, M. Saitoh, E. Tamiya, K. Park, Self-assembly of cholesterol-hydrotropic dendrimer conjugates into micelle-like structure: Preparation and hydrotropic solubilization of paclitaxel. *Sci. Technol. Adv. Mater.* 6(5) (2005) 452-456.
- [24] D.D. Guo, C.X. Xu, J.S. Quan, C.K. Song, H. Jin, D.D. Kim, Y.J. Choi, M.H. Cho, C.S. Cho, Synergistic anti-tumor activity of paclitaxel-incorporated conjugated linoleic acid-coupled poloxamer thermosensitive hydrogel in vitro and in vivo. *Biomaterials* 30(27) (2009) 4777-4785.
- [25] S.H. Ranganath, I. Kee, W.B. Krantz, P.K.H. Chow, C.H. Wang, Hydrogel Matrix Entrapping PLGA-Paclitaxel Microspheres: Drug Delivery with Near Zero-Order Release and Implantability Advantages for Malignant Brain Tumour Chemotherapy. *Pharm. Res.* 26(9) (2009) 2101-2114.
- [26] E. Ruel-Gariepy, M. Shive, A. Bichara, M. Berrada, D. Le Garrec, A. Chenite, J.C. Leroux, A thermosensitive chitosan-based hydrogel for the local delivery of paclitaxel. *Eur. J. Pharm. Biopharm.* 57(1) (2004) 53-63.
- [27] A. Cabanes, K.E. Briggs, P.C. Gokhale, J.A. Treat, A. Rahman, Comparative in vivo studies with paclitaxel and liposome-encapsulated paclitaxel. *Int. J. Oncol.* 12(5) (1998) 1035-1040.
- [28] A. Sharma, E. Mayhew, L. Bolcsak, C. Cavanaugh, P. Harmon, A. Janoff, R.J. Bernacki, Activity of paclitaxel liposome formulations against human ovarian tumor xenografts. *Int. J. Cancer* 71(1) (1997) 103-107.
- [29] J. Treat, C. Huang, N. Damjanov, S. Walker, P. Drobins, C. Bowden, G. Massimini, A. Rahman, Phase I trial in advanced malignancies with liposome encapsulated paclitaxel (LEP). *Clin. Cancer Res.* 6 (2000) 4492s-4492s.
- [30] X.H. Wang, H. Zheng, Z.Y. Zhu, Y.Q. Wei, L.J. Chen, Clinical Pharmacokinetics of Paclitaxel Liposome with a New Route of Administration in Human Based on the Analysis with Ultra Performance Liquid Chromatography. *J. Pharm. Sci.* 99(11) (2010) 4746-4752.
- [31] Q. Zhang, X.E. Huang, L.L. Gao, A clinical study on the premedication of paclitaxel liposome in the treatment of solid tumors. *Biomed. Pharmacother.* 63(8) (2009) 603-607.
- [32] X.C. Zhang, J.K. Jackson, H.M. Burt, Development of amphiphilic diblock copolymers as micellar carriers of taxol. *Int. J. Pharm.* 132(1-2) (1996) 195-206.
- [33] S.S. Venkatraman, P. Jie, F. Min, B.Y.C. Freddy, G. Leong-Huat, Micelle-like nanoparticles of PLA-PEG-PLA triblock copolymer as chemotherapeutic carrier. *Int. J. Pharm.* 298(1) (2005) 219-232.
- [34] M.L. Immordino, P. Brusa, S. Arpicco, B. Stella, F. Dosio, L. Cattel, Preparation, characterization, cytotoxicity and pharmacokinetics of liposomes containing docetaxel. *J. Control. Release* 91(3) (2003) 417-429.
- [35] P. Crosasso, M. Ceruti, P. Brusa, S. Arpicco, F. Dosio, L. Cattel, Preparation, characterization and properties of sterically stabilized paclitaxel-containing liposomes. *J. Control. Release* 63(1-2) (2000) 19-30.

- [36] H.M. Burt, X.C. Zhang, P. Toleikis, L. Embree, W.L. Hunter, Development of copolymers of poly(D,L-lactide) and methoxypolyethylene glycol as micellar carriers of paclitaxel. *Colloid Surf. B-Biointerfaces* 16(1-4) (1999) 161-171.
- [37] F. Ahmed, R.I. Pakunlu, A. Brannan, F. Bates, T. Minko, D.E. Discher, Biodegradable polymersomes loaded with both paclitaxel and doxorubicin permeate and shrink tumors, inducing apoptosis in proportion to accumulated drug. *J. Control. Release* 116(2) (2006) 150-158.
- [38] F. Ahmed, D.E. Discher, Self-porating polymersomes of PEG-PLA and PEG-PCL: hydrolysis-triggered controlled release vesicles. *J. Control. Release* 96(1) (2004) 37-53.
- [39] F.H. Meng, G.H.M. Engbers, J. Feijen, Biodegradable polymersomes as a basis for artificial cells: encapsulation, release and targeting. *J. Control. Release* 101(1-3) (2005) 187-198.
- [40] M.P. Lillo, O. Canadas, R.E. Dale, A.U. Acuna, Location and properties of the taxol binding center in microtubules: A picosecond laser study with fluorescent taxoids. *Biochemistry* 41(41) (2002) 12436-12449.
- [41] J.F. Diaz, I. Barasoain, J.M. Andreu, Fast kinetics of taxol binding to microtubules - Effects of solution variables and microtubule-associated proteins. *J. Biol. Chem.* 278(10) (2003) 8407-8419.
- [42] J.F. Diaz, I. Barasoain, A.A. Souto, F. Amat-Guerri, J.M. Andreu, Macromolecular accessibility of fluorescent taxoids bound at a paclitaxel binding site in the microtubule surface. *J. Biol. Chem.* 280(5) (2005) 3928-3937.
- [43] V. Pata, F. Ahmed, D.E. Discher, N. Dan, Membrane solubilization by detergent: Resistance conferred by thickness. *Langmuir* 20(10) (2004) 3888-3893.
- [44] F.H. Meng, Z.Y. Zhong, J. Feijen, Stimuli-Responsive Polymersomes for Programmed Drug Delivery. *Biomacromolecules* 10(2) (2009) 197-209.
- [45] J.C.M. Lee, H. Bermudez, B.M. Discher, M.A. Sheehan, Y.Y. Won, F.S. Bates, D.E. Discher, Preparation, stability, and in vitro performance of vesicles made with diblock copolymers. *Biotechnol. Bioeng.* 73(2) (2001) 135-145.
- [46] J.S. Lee, W. Zhou, F.H. Meng, D.W. Zhang, C. Otto, J. Feijen, Thermosensitive hydrogel-containing polymersomes for controlled drug delivery. *J. Control. Release* 146(3) (2010) 400-408.
- [47] K. Yu, A. Eisenberg, Bilayer morphologies of self-assembled crew-cut aggregates of amphiphilic PS-b-PEO diblock copolymers in solution. *Macromolecules* 31(11) (1998) 3509-3518.
- [48] L.F. Zhang, A. Eisenberg, Multiple Morphologies of Crew-Cut Aggregates of Polystyrene-B-Poly(Acrylic Acid) Block-Copolymers. *Science* 268(5218) (1995) 1728-1731.
- [49] S.K. Hobbs, W.L. Monsky, F. Yuan, W.G. Roberts, L. Griffith, V.P. Torchilin, R.K. Jain, Regulation of transport pathways in tumor vessels: Role of tumor type and microenvironment. *Proc. Natl. Acad. Sci. U. S. A.* 95(8) (1998) 4607-4612.
- [50] A. Lavasanifar, J. Samuel, G.S. Kwon, Poly(ethylene oxide)-block-poly(L-amino acid) micelles for drug delivery. *Adv. Drug Deliv. Rev.* 54(2) (2002) 169-190.
- [51] W.J. Lin, C.L. Wang, Y.C. Chen, Comparison of two pegylated copolymeric micelles and their potential as drug carriers. *Drug Deliv.* 12(4) (2005) 223-227.
- [52] D. Sutton, S.H. Wang, N. Nasongkla, J.M. Gao, E.E. Dormidontova, Doxorubicin and beta-lapachone release and interaction with micellar core materials: Experiment and modeling. *Exp. Biol. Med.* 232(8) (2007) 1090-1099.

- [53] S.L. Li, B. Byrne, J. Welsh, A.F. Palmer, Self-assembled poly(butadiene)-b-poly(ethylene oxide) polymersomes as paclitaxel carriers. *Biotechnol. Prog.* 23(1) (2007) 278-285.
- [54] A.W.L. Anya M. Hillery, *James Swarbrick Drug Delivery and Targeting: For Pharmacists and Pharmaceutical Scientists*, Taylor & Francis, London and New York, 2001.
- [55] W.S. Shim, S.W. Kim, E.K. Choi, H.J. Park, J.S. Kim, D.S. Lee, Novel pH sensitive block copolymer micelles for solvent free drug loading. *Macromol. Biosci.* 6(2) (2006) 179-186.
- [56] H.C. Shin, A.W.G. Alani, D.A. Rao, N.C. Rockich, G.S. Kwon, Multi-drug loaded polymeric micelles for simultaneous delivery of poorly soluble anticancer drugs. *J. Control. Release* 140(3) (2009) 294-300.
- [57] T. Karjalainen, M. HiljanenVainio, M. Malin, J. Seppala, Biodegradable lactone copolymers .3. Mechanical properties of epsilon-caprolactone and lactide copolymers after hydrolysis in vitro. *J. Appl. Polym. Sci.* 59(8) (1996) 1299-1304.
- [58] M. Malin, M. HiljanenVainio, T. Karjalainen, J. Seppala, Biodegradable lactone copolymers .2. Hydrolytic study of epsilon-caprolactone and lactide copolymers. *J. Appl. Polym. Sci.* 59(8) (1996) 1289-1298.
- [59] M.H. Huang, S.M. Li, M. Vert, Synthesis and degradation of PLA-PCL-PLA triblock copolymer prepared by successive polymerization of epsilon-caprolactone and (DL)-lactide. *Polymer* 45(26) (2004) 8675-8681.
- [60] N. Lopez-Rodriguez, A. Lopez-Arraiza, E. Meaurio, J.R. Sarasua, Crystallization, morphology, and mechanical behavior of polylactide/poly(epsilon-caprolactone) blends. *Polym. Eng. Sci.* 46(9) (2006) 1299-1308.
- [61] R.S.I. Serra, J.L.E. Ivirico, J.M.M. Duenas, A.A. Balado, J.L.G. Ribelles, M.S. Sanchez, Segmental Dynamics in Poly(epsilon-caprolactone)/Poly(L-lactide) Copolymer Networks. *J. Polym. Sci. Pt. B-Polym. Phys.* 47(2) (2009) 183-193.
- [62] S.C. Lee, C. Kim, I.C. Kwon, H. Chung, S.Y. Jeong, Polymeric micelles of poly(2-ethyl-2-oxazoline)-block-poly(epsilon-caprolactone) copolymer as a carrier for paclitaxel. *J. Control. Release* 89(3) (2003) 437-446.
- [63] O. Soga, C.F. van Nostrum, M. Fens, C.J.F. Rijcken, R.M. Schiffelers, G. Storm, W.E. Hennink, Thermosensitive and biodegradable polymeric micelles for paclitaxel delivery. *J. Control. Release* 103(2) (2005) 341-353.
- [64] C.C. Lin, K.S. Anseth, PEG Hydrogels for the Controlled Release of Biomolecules in Regenerative Medicine. *Pharm. Res.* 26(3) (2009) 631-643.
- [65] M. Nahar, T. Dutta, S. Murugesan, A. Asthana, D. Mishra, V. Rajkumar, M. Tare, S. Saraf, N.K. Jain, Functional polymeric nanoparticles: An efficient and promising tool for active delivery of bioactives. *Crit. Rev. Ther. Drug Carr. Syst.* 23(4) (2006) 259-318.
- [66] O. Onaca, R. Enea, D.W. Hughes, W. Meier, Stimuli-Responsive Polymersomes as Nanocarriers for Drug and Gene Delivery. *Macromol. Biosci.* 9(2) (2009) 129-139.



# Chapter 4

## Thermosensitive Hydrogel-containing Polymersomes for Controlled Drug Delivery<sup>\*</sup>

Jung Seok Lee<sup>a</sup>, Wei Zhou<sup>a</sup>, Fenghua Meng<sup>a,c</sup>, Dianwen Zhang<sup>b</sup>, Cees Otto<sup>b</sup>, Jan Feijen<sup>a</sup>

<sup>a</sup> *Department of Polymer Chemistry and Biomaterials, Institute for Biomedical Technology and Technical Medicine, MIRA, Faculty of Science and Technology, University of Twente, Enschede, The Netherlands*

<sup>b</sup> *MESA+ Institute for Nanotechnology, Biophysical Engineering Group, University of Twente, Enschede, The Netherlands*

<sup>c</sup> *Biomedical Polymers Laboratory, and Key Laboratory of Organic Synthesis of Jiangsu Province, College of Chemistry, Chemical Engineering and Materials Science, Soochow University, Suzhou, 215123, People's Republic of China,*

---

<sup>\*</sup> Journal of Controlled Release, 146 (2010) 400-408

### Abstract

PNIPAAm-containing polymersomes (N/Ps) were prepared by injecting a solution of poly(ethylene glycol)-*b*-poly(*D,L*-lactide) (mPEG-PDLLA) and poly(*N*-isopropylacrylamide) (PNIPAAm) in THF into water to incorporate PNIPAAm into polymersomes (Ps). At 37 °C, hydrogel-containing Ps (Hs, hydrosomes) with an average diameter of 127 nm as measured with dynamic light scattering (DLS) were obtained which may be used as potential novel carriers for anticancer drugs and proteins. Dual-labeled N/Ps (FITC-N/RB-Ps) were prepared analogously using rhodamine B tagged mPEG-PDLLA (mPEG-PDLLA-RB) and fluorescein isothiocyanate labeled PNIPAAm (FITC-N). The co-localization of RB-labeled Ps (RB-Ps) and FITC-N in RB-Ps was shown by dual fluorescence CLSM. Fluorescence correlation spectroscopy (FCS) and fluorescence anisotropy (FA) measurements with these systems gave further evidence for the colocalization of PNIPAAm and Ps. Micron-sized giant Ps with a diameter of 5-10  $\mu\text{m}$  containing FITC-N were prepared using  $\text{CHCl}_3$  as the organic phase. The presence of FITC-N in these giant Ps as well as the phase separation of the internal FITC-N solution above the lower critical solution temperature (LCST) was also shown by CLSM. The release of fluorescein isothiocyanate tagged dextran (FITC-dextran, MW 4000 g/mol, FD4) from Hs revealed that in the presence of the hydrogel at 37 °C a more sustained release of FD4 (up to 30 d) with a low initial burst effect was obtained as compared to the release from bare Ps.

## **Introduction**

Although a large number of drug delivery systems has been designed during the past few decades, there is still a need for further reduction of side effects, more convenient methods of administration and an improvement of patient compliance [1, 2]. Some of these requirements can be achieved by using injectable nanocarrier systems, providing a temporal modulated drug release for predefined periods as well as a spatial drug distribution control in the body [3].

Polymersomes (Ps), synthetic supramolecular-structures similar to liposomes but composed of amphiphilic block copolymers instead of lipids [4], have attracted a lot of attention among the various nanocarrier systems due to their outstanding stability and relatively long circulation times [5, 6]. Long circulation times of Ps can be accomplished by applying a poly(ethylene glycol) (PEG) layer on the surface of the Ps as previously reported by Lee *et al.* and Photos *et al.* [6, 7]. The presence of PEG reduces protein adsorption onto the Ps [8, 9], which is caused by the relatively low interfacial energy of the water containing PEG layer and water, and the steric hindrance provided by the PEG molecules [10-12].

Drug delivery from Ps can be controlled by varying the permeability of the bi-layer. Bermudez *et al.* and Ahmed *et al.* prepared Ps based on block copolymers such as PEG-b-poly(butadiene) (PEG-PBD), PEG-b-poly(ethylene) (PEG-PEE), PEG-b-poly(lactic acid) (PEG-PLA) and PEG-b-poly( $\epsilon$ -caprolactone) (PEG-PCL) and showed that the permeability, mechanical properties and the rate of degradation of the bi-layer membrane can be tuned by varying the length of the PEG as well as the character and length of the hydrophobic blocks [5, 13]. However, the range of variation in the properties is rather limited, because there are constraints for the block copolymers to form Ps such as the hydrophilic block volume fraction and a low glass transition temperature ( $T_g$ ) of the hydrophobic phase [4, 14].

Significant efforts have been devoted to further control the membrane permeability of Ps by using block copolymers which are temperature sensitive, pH-responsive and which may be chemically or physically crosslinked [15-19]. An alternative approach is to modify the properties of the interior of the nano-sized Ps for instance by the introduction of a gel. Jesorka *et al.* have reported giant liposomes containing a PNIPAAm hydrogel, which were prepared by direct injection of a PNIPAAm solution into the liposomes [20, 21]. It is obvious that this method is not practical for further applications.



The aim of this study is to develop a facile method for the introduction of a thermosensitive polymer solution, like PNIPAAm into Ps and to investigate the effect of the presence of the hydrogel inside the Ps on the release of a model compound. mPEG-PDLLA was used as a biodegradable and biocompatible amphiphilic block copolymer for the preparation of nano-sized Ps. PDLLA can be degraded by hydrolysis [22, 23] and PEG with a MW less than 50,000 g/mol can be excreted by the kidneys [24]. Aqueous solutions of PNIPAAm have a sharp phase transition behavior and an LCST of 32 °C [25]. PNIPAAm has also been used as a component for the preparation of thermosensitive hydrogels, micelles, liposomes and Ps [15, 26-30]. PNIPAAm containing Ps (N/Ps) were prepared by injecting a THF solution of the block copolymer and PNIPAAm into water. Gel containing Ps, further denoted as hydrosomes (Hs), were obtained by raising the temperature of N/Ps suspensions to 37 °C. After loading of N/Ps with drugs at room temperature and subsequent injection into the body, a prolonged delivery of the drug may be achieved because of the formation of a gel at 37 °C in the interior of the Ps (Fig. 4.1). The N/Ps and Hs were characterized by using dynamic light scattering (DLS), TEM and fluorescence studies. The release of the model compound, FITC-dextran (MW 4000 g/mol), from Ps and Hs was evaluated to study the effect of the presence of a hydrogel inside Ps on its release rate.

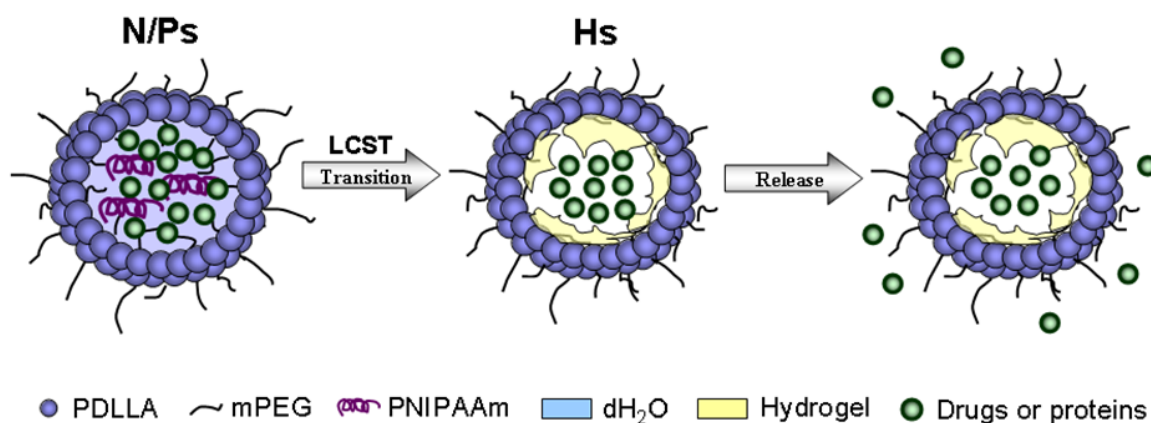


Figure 4.1. Schematic 2D-cross sectional illustration of Ps and Hs in which the PNIPAAm solution present in the core phase separates and partially turns into a gel at the LCST of the internal PNIPAAm aqueous solution, influencing the release rate of incorporated agents.

## **Materials and methods**

### *Materials*

*D,L*-lactide (DLLA, Purac Biochem b.v., The Netherlands), *N*-isopropylacrylamide (NIPAAm, Aldrich, USA), and 2,2'-azobisisobutyronitrile (AIBN, Fluka, Switzerland) were recrystallized from toluene, hexane, and methanol, respectively. Monomethoxy poly(ethylene glycol) with a molecular weight of 5000 g/mol (mPEG, Iris Biotech, Germany) was dried by dissolution in anhydrous toluene followed by azeotropic distillation under N<sub>2</sub>. Stannous octoate (SnOct), fluorescamine and FITC-dextran (MW 4000 g/mol) were obtained from Sigma (USA). Sodium tetraborate was supplied by Aldrich (USA). Rhodamine B (RB), fluorescein isothiocyanate (FITC), 2-aminoethanethiol (AET), *N,N'*-dicyclohexylcarbodiimide (DCC), 4-di(methylamino)pyridine (DMAP) and uranyl acetate dihydrate were purchased from Fluka (Switzerland) and used as received. Deionized water (DI water) was obtained from a Milli-Q water purification system (Millipore, France) and phosphate buffered saline (PBS, 0.01 M, pH 7.4, containing 0.02 wt.% NaN<sub>3</sub>, B. Braun, USA) were used in the model drug release experiments.

### *Synthesis of (fluorescently labeled) mPEG-PDLLA and PNIPAAm*

mPEG-PDLLA was synthesized by ring-opening polymerization (ROP) of DLLA using mPEG as an initiator (Fig. 4.2a). mPEG (0.50 g, 0.1 mmol), DLLA (4.11 g, 28.5 mmol), SnOct (0.04 g, 0.1 mmol) and toluene (16.5 ml) were charged in that order in a reaction vessel. The reaction was performed at 110 °C for 26 h under stirring. After cooling, a drop of HCl (37 wt.%) was added to the reaction mixture to hydrolyze the tin-oxygen bond. A sample was taken to determine the monomer conversion by <sup>1</sup>H-NMR (Inova 300 MHz, Varian, USA). The copolymer was isolated by precipitation in methanol. After filtration and washing with methanol, the copolymer was dissolved in dichloromethane (DCM) and precipitated in diethyl ether. Subsequently, the polymer was isolated by filtration, washed several times with diethyl ether, and dried under vacuum. <sup>1</sup>H-NMR analysis showed that the monomer conversion was 99 % and that the Mn of the PDLLA block was 42,000 g/mol. Area integrations of the  $\underline{\text{CH}}-\text{CH}_3$  peak (5.18 ppm) from PDLLA and the  $\underline{\text{CH}}_2-\underline{\text{CH}}_2-\text{O}$  peak (3.62 ppm) from mPEG were used for the calculation of the Mn.

Amine-terminated PNIPAAm (PNIPAAm-NH<sub>2</sub>) was prepared by free radical polymerization of NIPAAm using AET as a chain transfer agent (Fig. 4.2b) as previously reported [29]. NIPAAm (11.30 g, 100 mmol), AIBN (0.14 g, 1 mmol) and AET (0.08 g, 1 mmol) were dissolved in methanol and the reaction mixture was heated at 60 °C for 20 h in a nitrogen atmosphere. The copolymer was recovered by precipitation into cold diethyl ether. This procedure was repeated twice and the polymer was dried in a vacuum oven. The LCST of an aqueous PNIPAAm solution (5 wt.%) was 32 °C as determined using a UV-visible spectrophotometer (CARY 300 Bio, Varian, USA). The M<sub>n</sub> and M<sub>w</sub> of PNIPAAm were analyzed by gel permeation chromatography (GPC) as 39,200 g/mol and 56,000 g/mol, respectively. The GPC was equipped with an RI detector (RI 2414 detector, Waters, Germany), Waters 515 pump and  $\mu$ Styragel columns (300  $\times$  7.8 mm, 20  $\mu$ m particle size, Waters, Germany). A DMF containing LiCl (0.1 M) was used as an eluent (flow rate 1 ml/min) and PNIPAAm (0.5 wt.%) was dissolved in the DMF solution for the GPC analysis (injection volume 30  $\mu$ l). Poly(methyl methacrylate)s were used as calibration standards. The degree of functionalization of PNIPAAm with NH<sub>2</sub> was 96.0  $\pm$  4.7 % (n=3, ave  $\pm$  std) as obtained by using the fluorescamine assay [31] using PEG diamine (IRIS Biotech, Germany, M<sub>n</sub> 23,100 g/mol) as a standard.

mPEG-PDLLA-RB was prepared by reacting mPEG-PDLLA (2.35 g, 0.05 mmol) with RB (0.03 g, 0.06 mmol) using DCC (0.01 g, 0.06 mmol) and DMAP (0.01 g, 0.06 mmol) in DCM (200 ml) at room temperature for 24 h (Fig. 4.2c) [32]. Residual urea was removed by repeated filtration until the solution was clear. Free RB was separated by ultrafiltration (cut-off 10,000 g/mol, Stirred Cells, Millipore co., USA). The PNIPAAm-NH<sub>2</sub> was labeled using FITC according to literature [33] as shown in Fig. 4.2d. FITC (0.06 g, 0.15 mmol) was dissolved in 0.1 M sodium tetraborate buffer (pH 9.0, 150 ml) containing 10 % (v/v) acetone. Aminated PNIPAAm (3.50 g, 0.10 mmol) was then dispersed in the resulting solution. The dispersion was stirred at room temperature for 6 h in the dark and free FITC was removed by ultrafiltration (cut-off 10,000 g/mol).

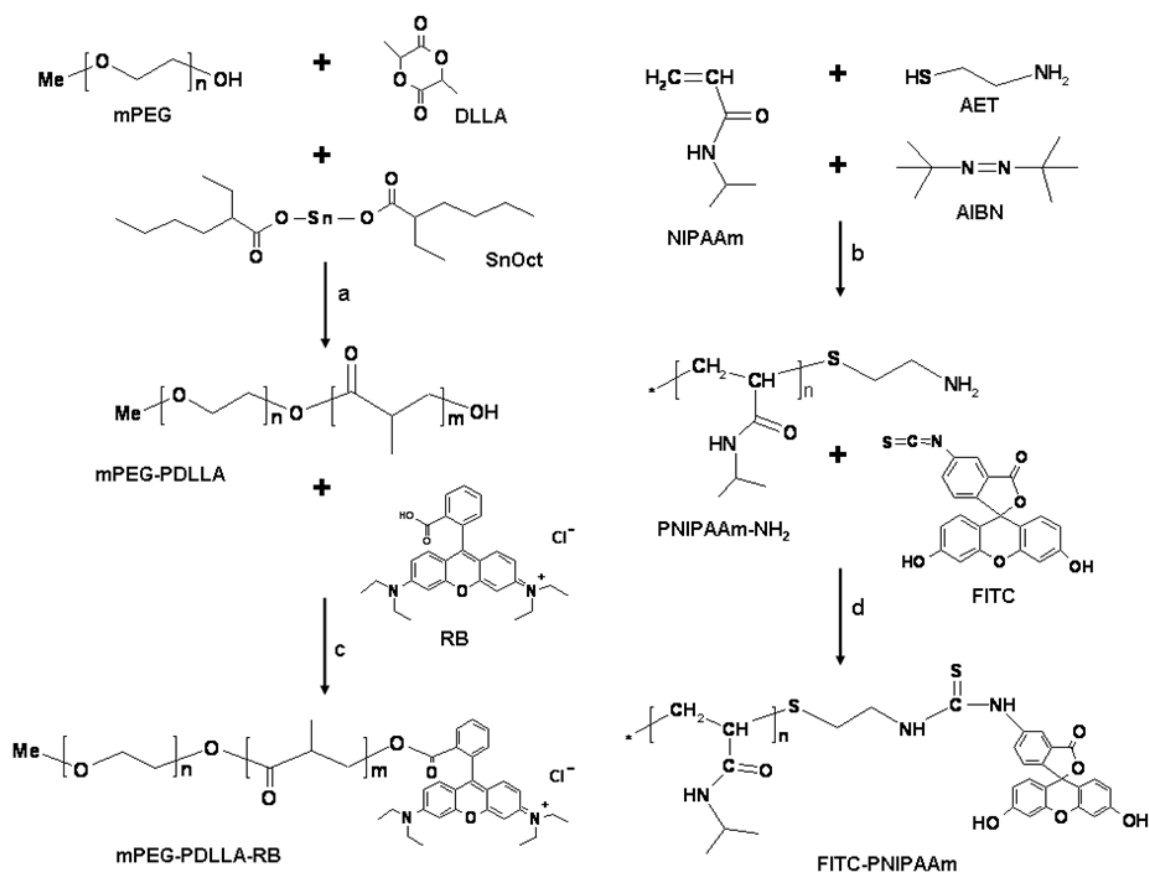


Figure 4.2. Synthesis of (fluorescently labeled) mPEG-PDLLA and PNIPAAm

#### Preparation of N/Ps and FITC-N/Ps

Nano-sized N/Ps and FITC-N/Ps were prepared using the solvent injection method, allowing large-scale production of Ps [34]. In brief, the amphiphilic block copolymer (10 mg/ml) and PNIPAAm with or without the FITC label (50 mg/ml) were dissolved in THF (3 ml), and the THF solution was injected into an aqueous phase (50 ml). After 15 min without shaking, the vial containing the mixture was turned upside down several times, resulting in a turbid dispersion. To remove the organic solvent from the solution, the Ps dispersion was transferred into a dialysis bag (cut-off 50,000 g/mol, Spectra/Por, CA), which was placed in a 4 l flask with DI water for 2 d. DI water was replaced for at least 5 times. Subsequently, the dispersion was ultrafiltrated through a membrane (cut-off 100,000 g/mol, Ultracel Ultrafiltration Disc, Millipore, USA) for 5 h to remove non-encapsulated PNIPAAm. The purified solutions were concentrated 10 times during the ultrafiltration step. All procedures were carried out at room temperature.

*DLS measurements and TEM*

Size measurements of N/Ps and Hs were performed with a Zetasizer Nano ZS (Malvern Instruments, Malvern, UK) using a wavelength of 532 nm with a step-wise increase and subsequent decrease in temperature to examine the influence of the temperature on the size and a stability of the bi-layer membrane structure. The hydrodynamic radius ( $R_H$ ) was measured by back-scattering at a detection angle of  $173^\circ$  using the Stokes-Einstein equation (Eq. 4.1):

$$R_H = \frac{k_B T}{6\pi\eta D_0} \quad (4.1)$$

where  $k_B$  = Boltzmann constant,  $T$  = absolute temperature,  $\eta$  = solvent viscosity,  $D_0$  = diffusion coefficient at infinite dilution. Bare Ps were prepared by the same method as mentioned above and used as a comparison. All samples were prepared by filtering the solutions through a  $0.45 \mu\text{m}$  Millipore filter into cuvettes, which were subsequently mounted in a thermostated cell. The measurements were repeated five times.

Transmission electron microscopy (TEM, Philips CM30, Hillsboro, USA) was performed to elucidate the morphology and membrane thickness of Ps. For TEM, Ps dispersions were prepared by injecting a THF solution into an aqueous solution. A dispersion of empty Ps ( $2 \mu\text{l}$ ) was placed on a 200 mesh carbon grid without using a staining agent and dried at room temperature. An N/Ps dispersion was kept at  $37^\circ\text{C}$  to form Hs and  $2 \mu\text{l}$  of the dispersion was deposited onto a 300 mesh carbon grid. After 30 s, Hs were stained with an uranyl acetate solution (2 wt.%) for 1 min. The excess solution was removed and the sample was dried at  $37^\circ\text{C}$ .

*Dual channel CLSM using FITC and RB*

Fluorescence images were obtained by CLSM (LSM 510, Zeiss, Germany) equipped with a Zeiss Axiovert 100 M Inverted Microscope for Nomarski DIC and Epi-Fluorescence. FITC-N/RB-Ps were prepared using mPEG-PDLLA-RB and FITC-N by injecting a polymer solution (THF) into DI water. To observe the co-localization of the two different fluorescence markers, a double-illumination system consisting of an Ar laser and a He-Ne laser was employed for excitation of FITC and RB, respectively.

### *Fluorescence correlation spectroscopy*

FCS has emerged as a sensitive technique operating at the level of single fluorescent molecules diffusing in and out of the confocal volume created by a focused laser beam. FCS of aqueous solutions of FITC, FITC-N and FITC-N/Ps was carried out at room temperature. Solutions of FITC and FITC-N were used as controls. FCS was carried out on a home-built set up [35], which can be briefly described as follows. Linearly polarized laser light with a wavelength of 488 nm was used to excite FITC. Light passed a dichroic mirror with a low-reflection/high-transmission (reflection < 5 %, transmission > 95 %) beam splitter and an objective. The fluorescence emission was collected by the same objective and > 95 % of fluorescent light passed through the dichroic mirror towards the detectors. The detection path consisting of a notch filter and folding mirrors were used to direct the fluorescent light to an avalanche photodiode for FCS measurements or to a single-prism spectrometer equipped with a liquid nitrogen cooled charged-coupled device camera (SPEC-10 System, Princeton Instruments, Trenton, NJ) for spectral measurements. Spectral data were acquired frame by frame with the help of WINSPEC (Roper Scientific).

### *Fluorescence anisotropy measurements*

For steady-state anisotropy measurements, a fluorescent sample was excited with linearly polarized light, yielding fluorescent light emission from the sample. FA data were determined with a fluorescence spectrophotometer (CARY Eclipse, Varian, USA) equipped with polarizers in the right-angle configuration and a temperature controller. The fluorescence anisotropy,  $r(\lambda)$ , was calculated directly from the uncorrected, polarized fluorescence,  $I(\lambda)$ , as follows:

$$r(\lambda) = \frac{I(\lambda)_{VV} - G(\lambda)I(\lambda)_{VH}}{I(\lambda)_{VV} + 2G(\lambda)I(\lambda)_{VH}}, \quad G(\lambda) = \frac{I(\lambda)_{HV}}{I(\lambda)_{HH}} \quad (4.2)$$

where the subscript-values refer to the horizontal or vertical settings of the excitation and emission polarizers, respectively.  $G(\lambda)$  compensates for the wavelength-dependent, polarizing effects of the instrument. In FA, a higher value of  $r$  relates to a more restricted motion of the fluorophore during its fluorescence lifetime. In turbid media light scattering may also contribute to the measured anisotropy [36, 37]. A solution of FITC-N/Ps was placed in a 1-mm-thin quartz

cell and recorded at 25 °C (FITC-N/Ps) and 37 °C (FITC-labeled Hs, FITC-Hs) with an excitation wavelength of 495 nm. Solutions of FITC and FITC-N were used as controls.

#### *CLSM of giant FITC-N/Ps and FITC-Hs*

To further study the formation of a PNIPAAm hydrogel in the Ps, giant FITC-N/Ps were prepared using FITC-N (50 mg/ml) and mPEG-PDLLA (10 mg/ml) by injecting solutions of these polymers in CHCl<sub>3</sub> (3 ml) as a water immiscible organic solvent into an aqueous solution (50 ml) and by evaporating CHCl<sub>3</sub> at ambient conditions for 3 d. To reveal the Ps with encapsulated FITC-N, the Ps dispersion was diluted 1:1 with DI water just before the CLSM analysis in order to decrease the fluorescence of the aqueous medium outside the Ps. For the CLSM studies, 1 ml of the FITC-N/Ps suspensions was introduced in homemade thin-glass-bottomed cuvettes, which were placed in the thermostated incubator at 25 °C and 37 °C (TC-202A Bipolar Temperature Controller, Harvard Apparatus, USA).

#### *Release of FD4 from Ps, N/Ps and Hs*

FITC-dextran (MW 4000 g/mol, FD4)-loaded N/Ps (FD4-N/Ps) were prepared by injecting the appropriate THF solution into DI water as previously mentioned. In this case, FD4 (500 mg/ml) was added to a DI water solution (50 ml) while PNIPAAm (50 mg/ml) and mPEG-PDLLA (10 mg/ml) were dissolved in THF (3 ml). Free FD4 and free PNIPAAm were removed by ultrafiltration (cut-off 100,000 g/mol) for 24 h at room temperature. To determine the amount of loaded FD4, Ps were solubilized using Triton X-100 [38]. After adding Triton X-100 to the Ps dispersion with a final concentration of 2 wt.%, the mixture was heated for 3 h at 80 °C. The release of FD4 both at 25 °C and 37 °C from suspensions of Ps placed in a microdialysis system was monitored by periodic withdrawals of PBS samples. The release of FD4 from Ps filled with either gel or sol was studied by placing a dispersion of Ps (1 ml) into a dialysis bag (cut-off 100,000 g/mol) and immersing the bag into a large vial containing 29 ml of PBS. The experiments were carried out in three-fold. The release of free FD4 from an empty dialysis bag was also measured to confirm that the dialysis membrane was not rate controlling in the release experiment. At appropriate times, 1 ml of the release medium was collected from the vials and the medium was replaced by fresh PBS. Concentrations of released FD4 were determined by fluorescence spectroscopy (Safire<sup>2</sup>, Tecan, CA) at an emission wavelength of 516 nm and an

excitation wavelength of 495 nm. In this way, the loaded amounts of FD4 as well as the release kinetics were obtained. The stability of the FD4-containing Hs (FD4-Hs) during drug delivery was evaluated by measuring the size, count rate and polydispersity index (PDI) by DLS at 37 °C. FD4-Hs suspensions were incubated using the same method and conditions as used for FD4 release experiments. Data were collected at different incubation times.

## **Results and discussion**

### *Formation of nano-sized Ps, N/Ps and Hs*

Drug delivery systems based on self-assembled carriers have received widespread interest since the 1980s [39]. The design and evaluation of micelles and liposomes as drug delivery carriers have received a lot of attention. A drawback of these systems is that they often accumulate in the liver and spleen via a rapid uptake by the reticuloendothelial system (RES). Moreover these systems are often not stable in the circulation [3]. In contrast, Ps can be designed to have a stable membrane and a relatively bioinert surface. The uptake of Ps with a size lower than 200 nm by the RES can be reduced, while extravasation from leaky capillaries is enhanced [40].



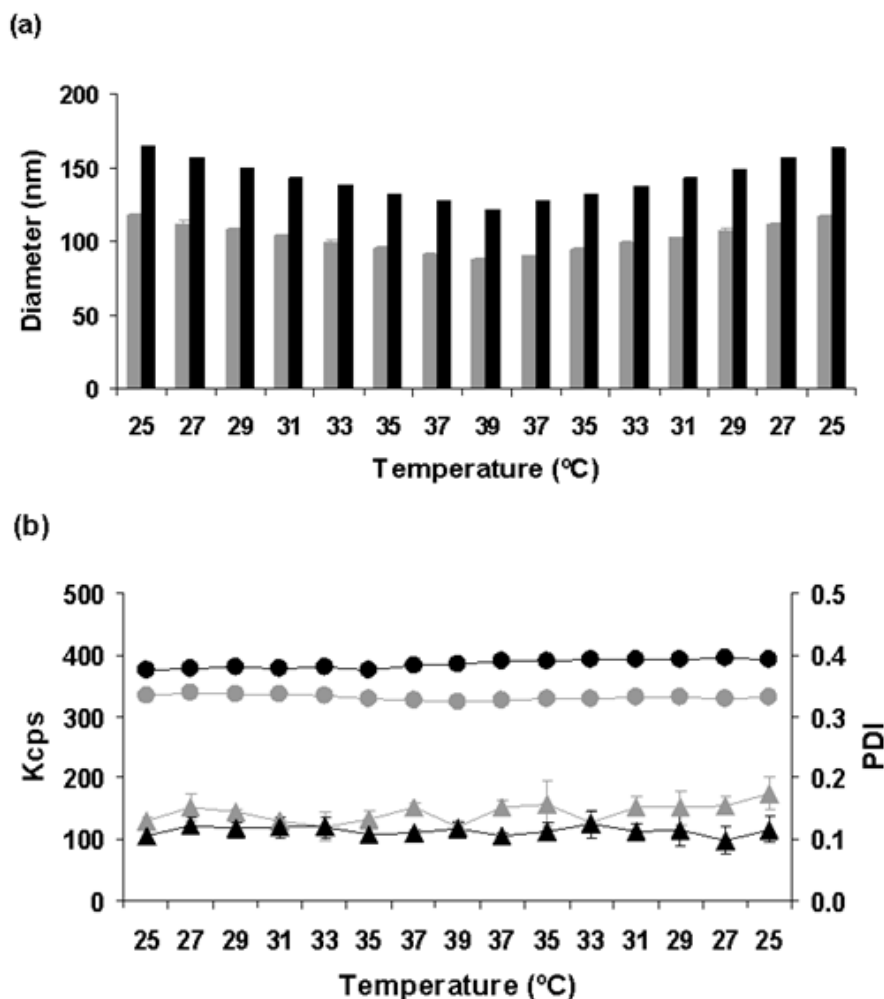


Figure 4.3. DLS measurements of Ps prepared with or without PNIPAAm as a function of temperature (heating and cooling in a step-wise manner). Ps ( $\bullet$ ,  $\blacktriangle$  and gray bars), N/Ps and Hs ( $\bullet$ ,  $\blacktriangle$  and black bars). Diameter (gray and black bars), kilo count per second (Kcps) ( $\bullet$  and  $\bullet$ ) and polydispersity index (PDI) ( $\blacktriangle$  and  $\blacktriangle$ ). Measurements were performed 30 times and averaged. Error bars represent standard deviations.

Ps can be prepared by sonication of an aqueous copolymer dispersion, hydration of a copolymer film and rehydration using various solvent compositions (organic solvent / water mixtures) [6]. However, these techniques have substantial shortcomings, including rather complicated preparation and filtration procedures. In this study, Ps containing PNIPAAm with an average diameter of 163 nm (25 °C) and a narrow size distribution (Fig. 4.3) were prepared by a simple solvent injection method [41] using a THF solution of the copolymer and PNIPAAm. The corresponding Ps without PNIPAAm had a diameter of 120 nm at 25 °C (Fig. 4.3a). The larger size of N/Ps as compared to the Ps is possibly due to an increase of the interfacial free energy at

the interior surface of the N/Ps. Both the size of the N/Ps and Ps decrease with increasing the temperature to 37 °C and the original sizes were obtained again by cooling to 25 °C. These effects may be due to partial dehydration of ethylene oxide groups in the PEG blocks with increasing temperature [42]. DLS measurements show that the Kcps and PDI of the N/Ps are not changing during the temperature cycle. Based on these data and the thermoreversible changes in size of the N/Ps, it can be concluded that the expected hydrogel formation of the PNIPAAm solution inside the Ps did not disrupt the membrane of the Ps (Fig. 4.3b).

TEM was performed to directly visualize the morphology and to evaluate the membrane thickness of Ps. Fig. 4.4a shows a TEM image of empty Ps. Fig. 4.4b represents a TEM image of Hs, which were deposited onto a carbon grid at 37 °C after pre-equilibration at 37 °C. It can be seen that the Hs are spherical nanocapsules after the phase transition of the incorporated PNIPAAm solution. Vesicles with a diameter varying from 50 to 150 nm can be observed, which corresponds well with the size distribution obtained from the DLS analysis as shown in Fig. 4.3a. The membrane thickness was about 15 nm for both Ps and Hs, and the thickness was not dependent on the size of the vesicles.

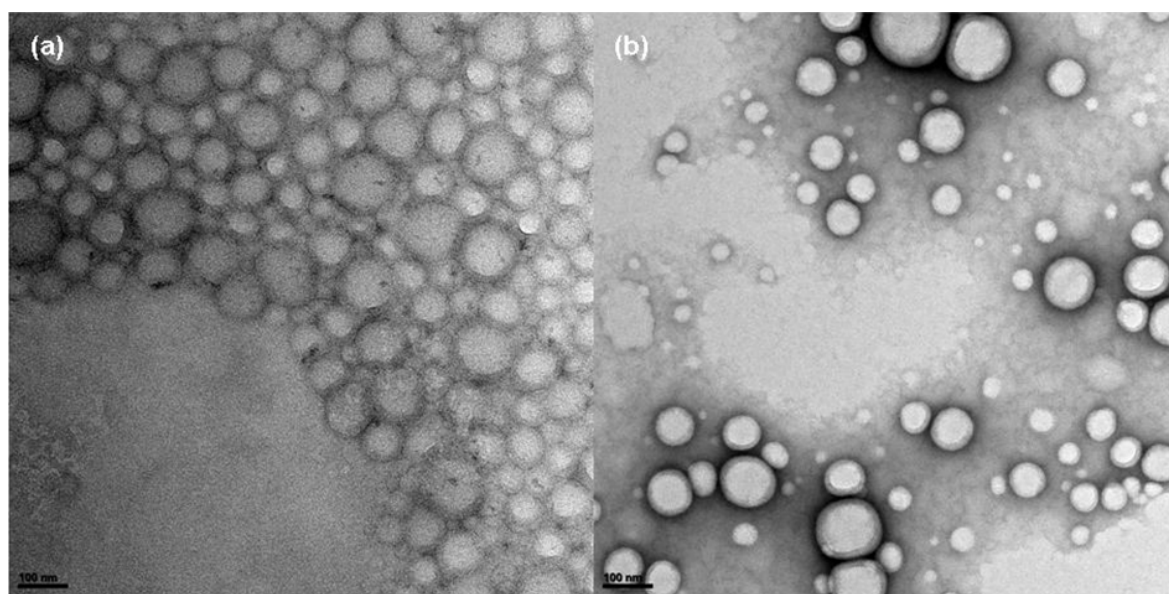


Figure 4.4. TEM images of empty Ps (a) and nano-sized Hs (b) on carbon grids. (a): A dispersion of empty Ps was placed on a 200 mesh normal carbon grid without using a staining agent and dried at room temperature. (b): A drop of the pre-equilibrated Hs dispersion at 37 °C was deposited onto a 300 mesh porous carbon grid and stained by uranyl acetate. Size bars represent 100 nm.

*Co-localization of PNIPAAm and Ps: dual fluorescence CLSM*

To prove that PNIPAAm was co-localized with Ps, FITC-N and RB-labeled Ps (RB-Ps) were used for dual fluorescence CLSM. Fig. 4.5 shows images of the green fluorescence of the FITC label, the red fluorescence of the RB label and the combination of both fluorescent labels. The combined image indicates that FITC-N and RB-Ps were co-localized.

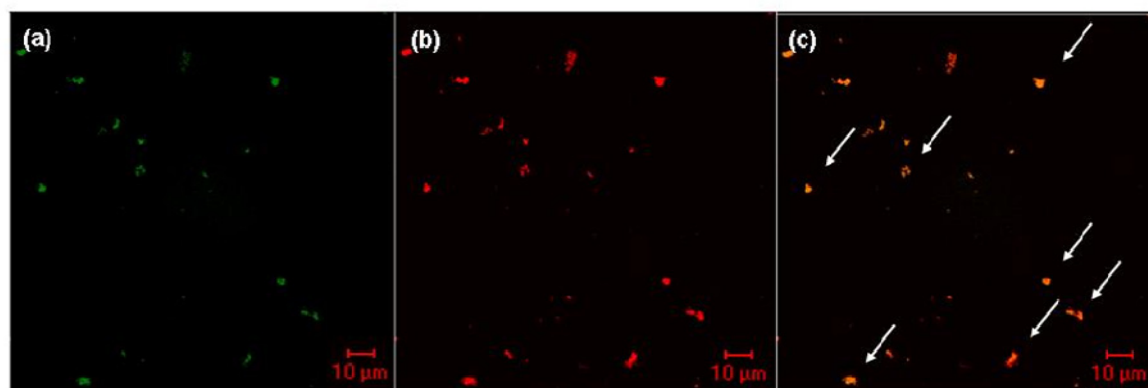


Figure 4.5. Dual fluorescence CLSM images of FITC-N and RB-Ps prepared by the injection of a THF solution of labeled polymers into water. FITC and RB were illuminated using two different laser channels resulting in a green color (a) and a red color (b), respectively. The combined image of panel (a) and panel (b) is represented in panel (c). Size bars are 10  $\mu\text{m}$  and arrows mark the co-localization of FITC-N and RB-Ps.

*Co-localization of PNIPAAm and Ps: fluorescence correlation spectroscopy*

To further investigate the association of PNIPAAm and Ps, fluorescence correlation spectroscopy (FCS) measurements were carried out on Ps containing FITC-N at room temperature. FCS of the free FITC solution and the FITC-N solution were used as controls. Fluorescence intensity fluctuations due to the diffusion of fluorescent molecules in and out of the excitation volume were monitored. Fig. 4.6a shows intense bursts of fluorescence from FITC-N/Ps. Long residence times ( $8.82 \pm 7.71$  ms) are associated with the relatively slow diffusion of Ps with co-localized FITC-N (Table 4.1). FITC-N had a short residence time, which reflects a relatively fast diffusion of the FITC coupled PNIPAAm molecules (Fig. 4.6c). As expected, the diffusion of free FITC was even faster (residence time of  $0.04 \pm 0.01$  ms) than that of FITC-N in which FITC was coupled to a relatively high molecular weight PNIPAAm polymer (Fig. 4.6b). Non-labeled PNIPAAm and Ps were used as controls (Figs. 4.6d and 4.6e). These results confirm again that PNIPAAm is co-localized with Ps.

Table 4.1. Residence times of FITC, FITC-N and FITC-N/Ps obtained by FCS

	Free FITC <sup>a</sup>	FITC-N <sup>a</sup>	FITC-N/Ps
Residence time (ms)	0.04 ± 0.01	0.08 ± 0.03	8.82 ± 7.71

<sup>a</sup> 10 μM aqueous solution.

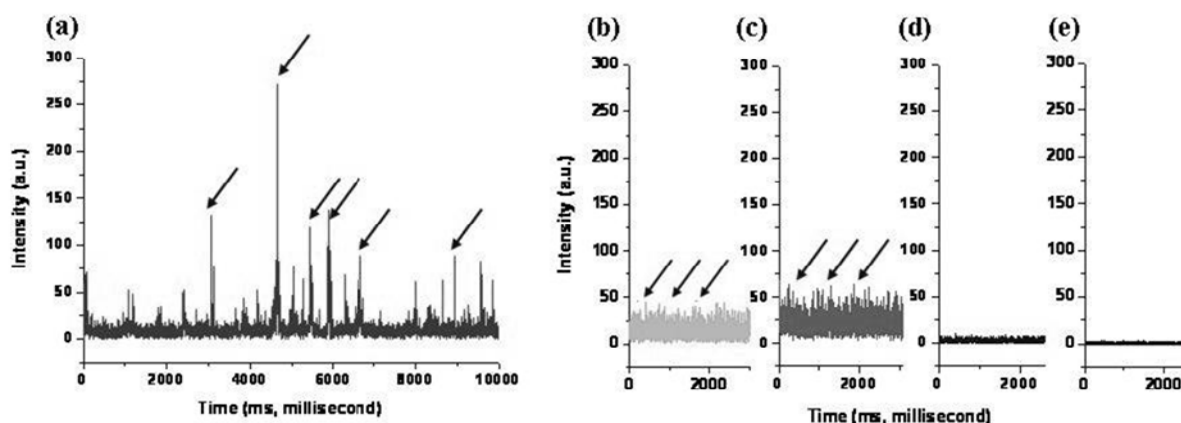


Figure 4.6. FCS of FITC, FITC-N and FITC-N/Ps at 25 °C. Non-labeled Ps and PNIPAAm were used as controls. (a) FITC-N/Ps, (b) free FITC (10 μM), (c) FITC-N (10 μM), (d) Ps and (e) PNIPAAm. Arrows represent fluorescence bursts indicating the passage of fluorescent molecules in and out of the laser detection area.

*Internal PNIPAAm hydrogel formation: steady state fluorescence anisotropy*

To get information on the sol-gel transition of internalized PNIPAAm solution with Ps, steady state FA measurements on FITC-N/Ps and -Hs were performed and compared with free FITC and FITC-N. The  $r$  values of solutions of these compounds and Ps dispersions were recorded as a function of the wavelength (Fig. 4.7). At  $\lambda < 520$  nm, the anisotropy measurements are affected by light scattering. Average  $r$  values were calculated from the measurements at  $\lambda > 520$  nm and given in Table 4.2. Aqueous solutions (10 μM) of both free FITC at 25 °C and 37 °C, and FITC-N at 25 °C showed a low  $r$  value of  $\sim 0.012$  (Figs. 4.7a and 4.7b) reflecting a high rotational freedom of FITC. The  $r$  value of FITC-N/Ps was 7 times higher than that of free FITC-N and free FITC indicating that the FITC label of PNIPAAm internalized in the Ps was strongly hindered in its rotational motion. A possible local high concentration of the PNIPAAm solution in the Ps could also contribute to a decrease of the rotational freedom of FITC. However, at the moment it is not possible to calculate the exact PNIPAAm concentration in the Ps. Based on the

$r$  values of FITC-N and free FITC, the translational and rotational diffusion of the label were similar at 25 °C.

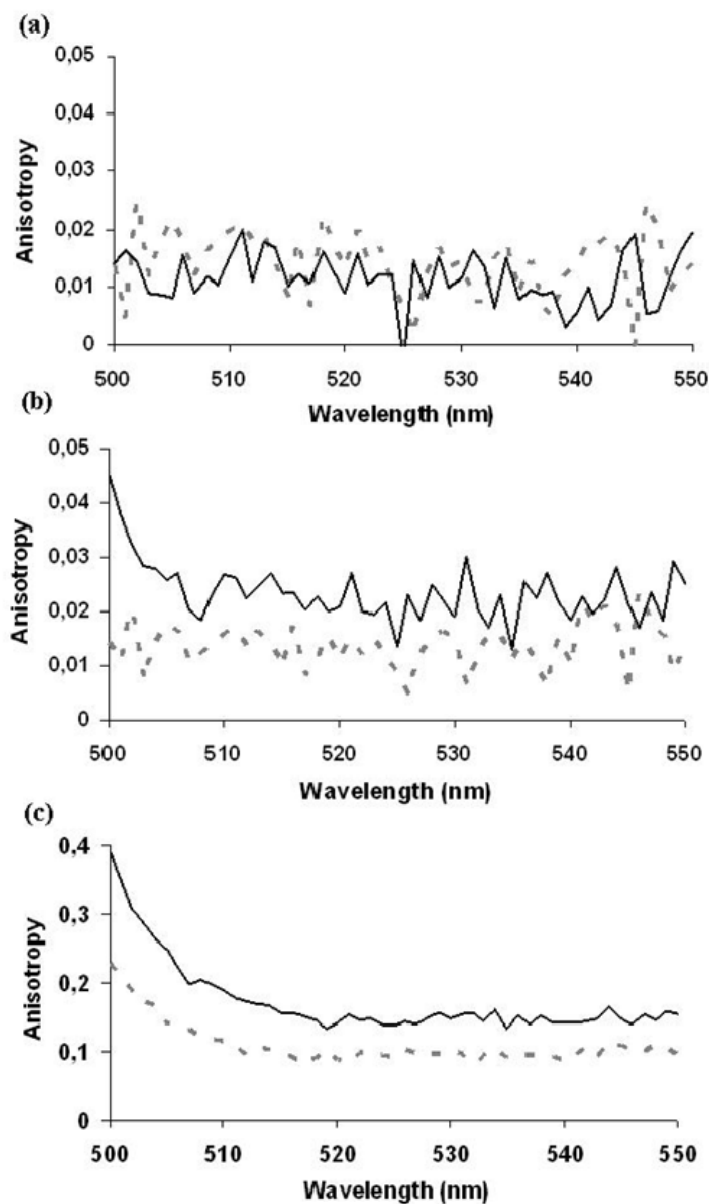


Figure 4.7. Temperature-dependent fluorescent anisotropy ( $r$ ) values of FITC, FITC-N and FITC-N in Ps at 25 °C (gray dashed lines) and 37 °C (black solid lines). (a) free FITC (10 μM), (b) FITC-N (10 μM), and (c) FITC-N/Ps (25 °C) and -Hs (37 °C).

When the temperature was increased to 37 °C, an increase of  $r$  was observed for the FITC-N solution. This was a result of the coil to globular transition of PNIPAAm and possible

subsequent self-aggregation of PNIPAAm chains as a result of intramolecular dehydration [43]. We also noted an increase in the  $r$  below a wavelength of 520 nm due to a slight increase in (polarized) light scattering. Upon increasing the temperature from 25 °C to 37 °C, the  $r$  value was increased significantly from 0.096 to 0.148 (Fig. 4.7c). These results demonstrate that the PNIPAAm concentration of the internal solution was high enough to form a hydrogel, which suppresses the rotational freedom of the FITC label.

Table 4.2. Average  $r$  values monitored from 520 to 550 nm

	Free FITC <sup>a</sup>	FITC-N <sup>a</sup>	FITC-N/Ps (25 °C) and -Hs (37 °C)
25 °C	0.013 ± 0.006	0.013 ± 0.005	0.096 ± 0.007
37 °C	0.011 ± 0.005	0.022 ± 0.004	0.148 ± 0.007

<sup>a</sup> 10 μM aqueous solution.

*Internal PNIPAAm hydrogel formation: CLSM using giant N/Ps and Hs*

In order to establish the presence of a PNIPAAm hydrogel and its formation after phase separation in Ps, giant FITC-N/Ps and -Hs were used for CLSM. The FITC-N/Ps with a diameter of 5-10 μm were prepared using CHCl<sub>3</sub> instead of THF as a organic phase. The gel formation and phase separation of the PNIPAAm solution in the giant Hs could be observed using CLSM combining both fluorescence- and bright field microscopy. Fig. 4.8c provides evidence of the presence of FITC-N inside the Ps below the LCST of the FITC-N solution. Above this temperature, phase separation of the solution took place leading to a fluorescent PNIPAAm hydrogel in the vicinity of the membrane and an aqueous phase in the center of the giant Ps (Figs. 4.8f and 4.8g). It should be noted that a solution of PNIPAAm can phase-separate into an aqueous phase and a gel phase with a volume of 10-20 % of the total volume when the concentration of the initial PNIPAAm solution is high enough to form a hydrogel [44, 45]. Phase separation is further corroborated by the data on the anisotropy measurements of the Ps containing FITC-N. Finally, Figs. 4.8b and 4.8e confirm the hollow sphere structure before and after the internal hydrogel formation, respectively, indicating that the membrane of the giant Ps is not disrupted during the sol-gel transition. Disruption of the membrane of nano-sized N/Ps during the phase transition also did not take place according to the DLS results (Fig. 4.3).

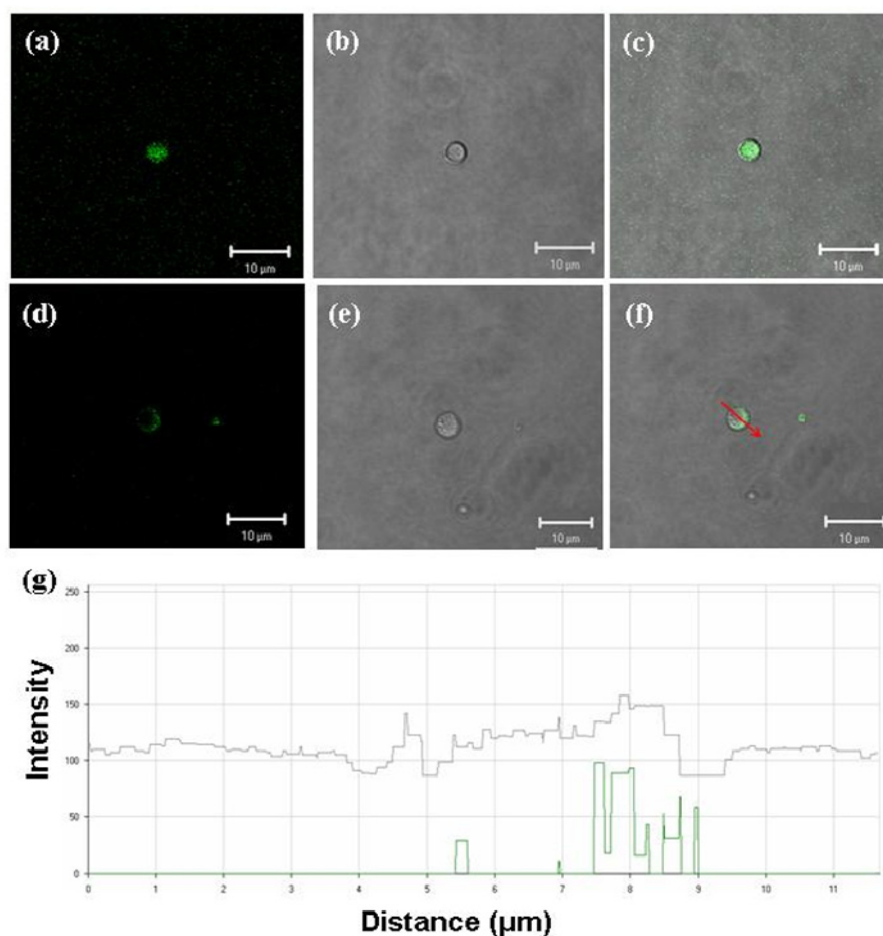


Figure 4.8. FITC-N containing giant Ps and Hs were imaged using CLSM at different temperatures to visualize internal gelation of the FITC-N solution. Giant FITC-N/Ps were prepared by injection of a chloroform solution of the copolymer and FITC-N into water. Fluorescence images (a and d), bright field images (b and e) and combined images (c and f) were taken at two different temperatures (upper panels: FITC-N/Ps at 25 °C and lower panels: FITC-N/Hs at 37 °C). White light and fluorescence intensities were scanned as indicated by a red arrow in (f). Gray lines and green lines show white light and fluorescence profiles, respectively (g). Size bars represent 10 μm.

#### *Release of FITC-dextran (FD4) from Ps, N/Ps and Hs*

FD with a molecular weight of 4000 (FD4) was used as a model compound to investigate the release kinetics from Ps at different temperatures. Figs. 4.9a and 4.9b represent the release profiles of FD4 from different vesicles at 25 °C and 37 °C placed in a dialysis bag. The release of FD4 from the empty dialysis membrane was fast and did hardly influence the release data for the vesicles. All release profiles for the vesicles showed an initial burst of 10-20 % followed by a gradual decrease of the release rate (Fig. 4.9b).

Fig. 4.9a shows that FD4 was completely released from the Hs at 37 °C after a month, while the release from Ps at 37 °C was already completed after 6 d. The difference in release rates has to be due to the presence of a hydrogel in the Hs. As discussed before, the PNIPAAm solution in the vesicles separates in two phases above the LCST forming a gel and an aqueous solution. Based on distribution studies of FD4 in a phase separated PNIPAAm system, it was estimated that about 80 % of encapsulated FD4 was in the aqueous phase and 20 % in the gel phase (data not shown). As shown before, the hydrogel was located very close to the membrane of the Hs. Therefore, the hydrogel forms an extra barrier for release of the FD4 and also limits the available free membrane area for permeation of FD4 from the aqueous solution inside the Hs. A possible interaction between the internal PEG chains and PNIPAAm chains may explain the localization of the gel in conjunction with the membrane of the Ps. This is further supported by the work of Polozova and Winnik [46] who concluded that the amide groups of PNIPAAm may form hydrogen bonds with ethylene oxide units. This not only can explain the image shown in Fig. 4.8f, but also the sustained FD4 release from Hs at 37 °C. Both Hs and empty Ps show a more rapid release of FD4 at 37 °C than at 25 °C due to an increase in the membrane permeability. Both N/Ps and empty Ps have similar FD4 release profiles at 25 °C, indicating that the presence of a PNIPAAm solution in Ps did not lead to a prolonged release of FD4. It can also be seen that at 37 °C the release of FD4 from Hs is faster than the release from N/Ps at 25 °C. Apparently, the increase of the permeability of the membrane with temperature has a stronger effect on the release than the formation of the membrane associated hydrogel.

In order to understand a possible influence of the degradation of the Ps membrane in time on the release of FD4 from Hs, DLS measurements of the FD4-Hs were carried out at different time points and the size distribution, K<sub>ps</sub> and PDI were monitored. FD4-Hs showed an excellent stability during 20 d based on their narrow and unimodal size distribution. After 20 d of incubation, Hs formed aggregates possibly facilitated by the presence of PNIPAAm (Fig. 4.9c). This can be explained by gradual hydrolysis of the PDLLA block, which eventually leads to destabilization of the bi-layer. Initially, chains with comparatively short hydrophobic blocks will tend to segregate and ultimately may induce hydrophilic pores in the membrane [13]. Therefore, the accelerated release rate of FD4 from Hs after 20 d at 37 °C can be explained by the gradual degradation of the PDLA blocks of the copolymer forming the membrane.



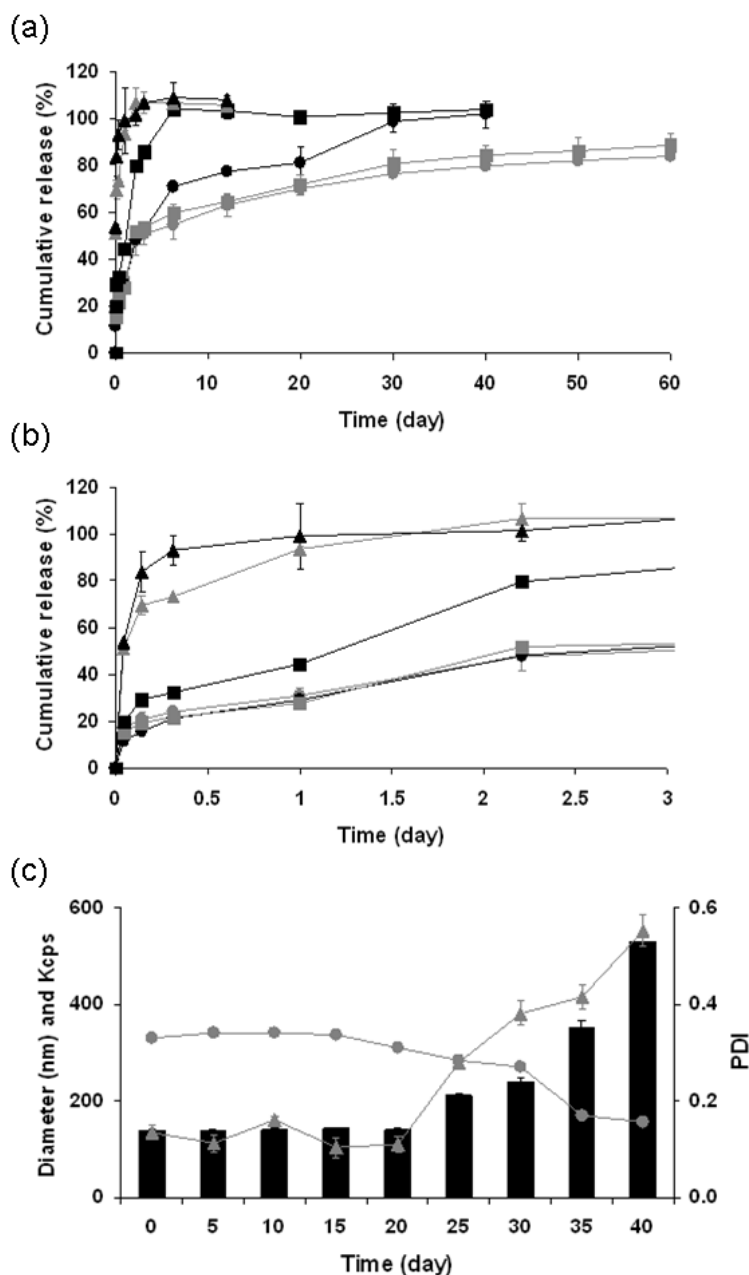


Figure 4.9. FD4 release from Ps at 25 °C and 37 °C, N/Ps and Hs measured with fluorescence spectroscopy. (a) FD4 release from the dialysis bag at 25 °C (▲) and at 37 °C (▲), FD4 release from Ps at 25 °C (■) and at 37 °C (■), and from N/Ps (25 °C, ●) and from Hs (37 °C, ●). At different time intervals, 1 ml of the release medium was collected and analyzed by fluorescence spectroscopy. The experiments were carried out in triplicate. (b) FD4 release data for the first 3 d (enlargement of Fig. 4.9a). The stability of the FD4-Hs vesicles at 37 °C was investigated over a period of 60 d by analyzing the samples for the release data with DLS. (c) DLS data of FD4-Hs as a function of time. Diameter (black bars), Kcps (●) and PDI (▲). DLS measurements were performed 30 times per sample. The data given are mean values and the error bars are the standard deviations of the mean.

## **Conclusions**

Novel bi-layer-enclosed nano-compartments containing a thermosensitive hydrogel, further named hydrosomes, were developed and characterized. This new controlled release system is composed of polymersomes (Ps) with a biodegradable mPEG-PDLLA membrane containing a PNIPAAm solution inside the reservoir at 25 °C. Above the LCST of the PNIPAAm solution in the Ps, phase separation takes place, and a hydrogel and an aqueous phase are formed. The presence of the PNIPAAm solution in the Ps was shown by dual fluorescence CLSM, FCS, FA and CLSM of PNIPAAm containing giant Ps. FITC-dextran with a molecular weight of 4000 (FD4) was released over a period of 4 weeks from Ps at 37 °C with a low initial burst, while the release from Ps not containing PNIPAAm was completed in 6 d. These results are explained by the formation of a membrane associated PNIPAAm hydrogel layer in the hydrosomes (Hs), which strongly reduces the release rate of FD4. In our current program, we further focus on the introduction of stimuli-sensitive nanogels in Ps to effectively control the site specific release of drugs and proteins.

## **Acknowledgement**

The authors thank Mark Smithers (MESA<sup>+</sup>, University of Twente) for TEM measurements and Clemens Padberg (MTP, University of Twente) for GPC analysis.

**References**

- [1] P.B. Malafaya, G.A. Silva, E.T. Baran, R.L. Reis, Drug delivery therapies I - General trends and its importance on bone tissue engineering applications. *Curr. Opin. Solid State Mat. Sci.* 6(4) (2002) 283-295.
- [2] V.R. Sinha, A. Trehan, Biodegradable microspheres for parenteral delivery. *Crit. Rev. Ther. Drug Carr. Syst.* 22(6) (2005) 535-602.
- [3] L.Y. Qiu, Y.H. Bae, Polymer architecture and drug delivery. *Pharm. Res.* 23(1) (2006) 1-30.
- [4] B.M. Discher, D.A. Hammer, F.S. Bates, D.E. Discher, Polymer vesicles in various media. *Curr. Opin. Colloid Interface Sci.* 5(1-2) (2000) 125-131.
- [5] H. Bermudez, A.K. Brannan, D.A. Hammer, F.S. Bates, D.E. Discher, Molecular weight dependence of polymersome membrane structure, elasticity, and stability. *Macromolecules* 35(21) (2002) 8203-8208.
- [6] J.C.M. Lee, H. Bermudez, B.M. Discher, M.A. Sheehan, Y.Y. Won, F.S. Bates, D.E. Discher, Preparation, stability, and in vitro performance of vesicles made with diblock copolymers. *Biotechnol. Bioeng.* 73(2) (2001) 135-145.
- [7] P.J. Photos, L. Bacakova, B. Discher, F.S. Bates, D.E. Discher, Polymer vesicles in vivo: correlations with PEG molecular weight. *J. Control. Release* 90(3) (2003) 323-334.
- [8] R. Gref, Y. Minamitake, M.T. Peracchia, V. Trubetskoy, V. Torchilin, R. Langer, Biodegradable Long-Circulating Polymeric Nanospheres. *Science* 263(5153) (1994) 1600-1603.
- [9] S. Stolnik, L. Illum, S.S. Davis, Long Circulating Microparticulate Drug Carriers. *Adv. Drug Deliv. Rev.* 16(2-3) (1995) 195-214.
- [10] S.I. Jeon, J.H. Lee, J.D. Andrade, P.G. Degennes, Protein Surface Interactions in the Presence of Polyethylene Oxide 1. Simplified Theory. *J. Colloid Interface Sci.* 142(1) (1991) 149-158.
- [11] S.I. Jeon, J.D. Andrade, Protein Surface Interactions in the Presence of Polyethylene Oxide 2. Effect of Protein Size. *J. Colloid Interface Sci.* 142(1) (1991) 159-166.
- [12] K.D. Park, Y.S. Kim, D.K. Han, Y.H. Kim, E.H.B. Lee, H. Suh, K.S. Choi, Bacterial adhesion on PEG modified polyurethane surfaces. *Biomaterials* 19(7-9) (1998) 851-859.
- [13] F. Ahmed, P.J. Photos, D.E. Discher, Polymersomes as viral capsid mimics. *Drug Dev. Res.* 67(1) (2006) 4-14.
- [14] A. Mecke, C. Dittrich, W. Meier, Biomimetic membranes designed from amphiphilic block copolymers. *Soft Matter* 2(9) (2006) 751-759.
- [15] L.Y. Chu, S.H. Park, T. Yamaguchi, S. Nakao, Preparation of thermo-responsive core-shell microcapsules with a porous membrane and poly(N-isopropylacrylamide) gates. *J. Membr. Sci.* 192(1-2) (2001) 27-39.
- [16] H.W. Duan, M. Kuang, G. Zhang, D.Y. Wang, D.G. Kurth, H. Mohwald, pH-Responsive capsules derived from nanocrystal templating. *Langmuir* 21(24) (2005) 11495-11499.
- [17] F.T. Liu, A. Eisenberg, Preparation and pH triggered inversion of vesicles from poly(acrylic acid)-block-polystyrene-block-poly(4-vinyl pyridine). *J. Am. Chem. Soc.* 125(49) (2003) 15059-15064.
- [18] F.H. Meng, Z.Y. Zhong, J. Feijen, Stimuli-Responsive Polymersomes for Programmed Drug Delivery. *Biomacromolecules* 10(2) (2009) 197-209.
- [19] C. Nardin, T. Hirt, J. Leukel, W. Meier, Polymerized ABA triblock copolymer vesicles. *Langmuir* 16(3) (2000) 1035-1041.

- [20] A. Jesorka, M. Markstrom, M. Karlsson, O. Orwar, Controlled hydrogel formation in the internal compartment of giant unilamellar vesicles. *J. Phys. Chem. B* 109(31) (2005) 14759-14763.
- [21] A. Jesorka, M. Markstrom, O. Orwar, Controlling the internal structure of giant unilamellar vesicles by means of reversible temperature dependent sol-gel transition of internalized poly (N-isopropyl acrylamide). *Langmuir* 21(4) (2005) 1230-1237.
- [22] J.M. Anderson, M.S. Shive, Biodegradation and biocompatibility of PLA and PLGA microspheres. *Adv. Drug Deliv. Rev.* 28(1) (1997) 5-24.
- [23] I. Grizzi, H. Garreau, S. Li, M. Vert, Hydrolytic Degradation of Devices Based on Poly(DI-Lactic Acid) Size-Dependence. *Biomaterials* 16(4) (1995) 305-311.
- [24] T. Yamaoka, Y. Tabata, Y. Ikada, Distribution and Tissue Uptake of Poly(Ethylene Glycol) with Different Molecular-Weights after Intravenous Administration to Mice. *J. Pharm. Sci.* 83(4) (1994) 601-606.
- [25] C. Boutris, E.G. Chatzi, C. Kiparissides, Characterization of the LCST behaviour of aqueous poly(N-isopropylacrylamide) solutions by thermal and cloud point techniques. *Polymer* 38(10) (1997) 2567-2570.
- [26] S. Cammas, K. Suzuki, C. Sone, Y. Sakurai, K. Kataoka, T. Okano, Thermo-responsive polymer nanoparticles with a core-shell micelle structure as site-specific drug carriers. *J. Control. Release* 48(2-3) (1997) 157-164.
- [27] F. Kohori, K. Sakai, T. Aoyagi, M. Yokoyama, Y. Sakurai, T. Okano, Preparation and characterization of thermally responsive block copolymer micelles comprising poly(N-isopropylacrylamide-b-DL-lactide). *J. Control. Release* 55(1) (1998) 87-98.
- [28] K. Kono, A. Henmi, H. Yamashita, H. Hayashi, T. Takagishi, Improvement of temperature-sensitivity of poly(N-isopropylacrylamide)-modified liposomes. *J. Control. Release* 59(1) (1999) 63-75.
- [29] D.E. Meyer, B.C. Shin, G.A. Kong, M.W. Dewhirst, A. Chilkoti, Drug targeting using thermally responsive polymers and local hyperthermia. *J. Control. Release* 74(1-3) (2001) 213-224.
- [30] S.H. Qin, Y. Geng, D.E. Discher, S. Yang, Temperature-controlled assembly and release from polymer vesicles of poly(ethylene oxide)-block-poly(N-isopropylacrylamide). *Adv. Mater.* 18(21) (2006) 2905-2909.
- [31] Udenfrie.S, S. Stein, P. Bohlen, W. Dairman, Fluorescamine - Reagent for Assay of Amino-Acids, Peptides, Proteins, and Primary Amines in Picomole Range. *Science* 178(4063) (1972) 871-872.
- [32] H.A. Klok, J.J. Hwang, S.N. Iyer, S.I. Stupp, Cholesteryl-(L-lactic acid)((n)over-bar) building blocks for self-assembling biomaterials. *Macromolecules* 35(3) (2002) 746-759.
- [33] B. Elmas, M. Tuncel, G. Yalcin, S. Senel, A. Tuncel, Synthesis of uniform, fluorescent poly(glycidyl methacrylate) based particles and their characterization by confocal laser scanning microscopy. *Colloid Surf. A-Physicochem. Eng. Asp.* 269(1-3) (2005) 125-134.
- [34] M.E. Yildiz, R.K. Prud'homme, I. Robb, D.H. Adamson, Formation and characterization of polymersomes made by a solvent injection method. *Polym. Adv. Technol.* 18(6) (2007) 427-432.
- [35] D. Zhang, H. Lans, W. Vermeulen, A. Lenferink, C. Otto, Quantitative fluorescence correlation spectroscopy reveals a 1000-fold increase in lifetime of protein functionality. *Biophys. J.* 95(7) (2008) 3439-3446.

- [36] G. Hungerford, A.L.F. Baptista, P.J.G. Coutinho, E.M.S. Castanheira, M.E.C.D.R. Oliveira, Interaction of DODAB with neutral phospholipids and cholesterol studied using fluorescence anisotropy. *J. Photochem. Photobiol. A-Chem.* 181(1) (2006) 99-105.
- [37] B.R. Lentz, Use of Fluorescent-Probes to Monitor Molecular Order and Motions within Liposome Bilayers. *Chem. Phys. Lipids* 64(1-3) (1993) 99-116.
- [38] V. Pata, F. Ahmed, D.E. Discher, N. Dan, Membrane solubilization by detergent: Resistance conferred by thickness. *Langmuir* 20(10) (2004) 3888-3893.
- [39] H. Bader, H. Ringsdorf, B. Schmidt, Watersoluble Polymers in Medicine. *Angew. Makromolekulare Chemie* 123(Aug) (1984) 457-485.
- [40] A. Lavasanifar, J. Samuel, G.S. Kwon, Poly(ethylene oxide)-block-poly(L-amino acid) micelles for drug delivery. *Adv. Drug Deliv. Rev.* 54(2) (2002) 169-190.
- [41] F.H. Meng, G.H.M. Engbers, J. Feijen, Biodegradable polymersomes as a basis for artificial cells: encapsulation, release and targeting. *J. Control. Release* 101(1-3) (2005) 187-198.
- [42] S.Y. Park, B.R. Han, K.M. Na, D.K. Han, S.C. Kim, Micellization and gelation of aqueous solutions of star-shaped PLLA-PEO block copolymers. *Macromolecules* 36(11) (2003) 4115-4124.
- [43] R. Walter, J. Ricka, C. Quellet, R. Nyffenegger, T. Binkert, Coil-globule transition of poly(N-isopropylacrylamide): A study of polymer-surfactant association. *Macromolecules* 29(11) (1996) 4019-4028.
- [44] E. Ruel-Gariepy, J.C. Leroux, In situ-forming hydrogels - review of temperature-sensitive systems. *European Journal of Pharmaceutics and Biopharmaceutics* 58(2) (2004) 409-426.
- [45] Y. Suzuki, K. Tomonaga, M. Kumazaki, I. Nishio, Change in phase transition behavior of an NIPA gel induced by solvent composition: Hydrophobic effect. *Polym. Gels Netw.* 4(2) (1996) 129-142.
- [46] A. Polozova, F.M. Winnik, Contribution of hydrogen bonding to the association of liposomes and an anionic hydrophobically modified poly(N-isopropylacrylamide). *Langmuir* 15(12) (1999) 4222-4229.

# Chapter 5

## **Time-Resolved Fluorescence and Fluorescence Anisotropy of Fluorescein-Labeled Poly (*N*-isopropylacrylamide) incorporated in Polymersomes\***

Jung Seok Lee<sup>a</sup>, Rob B. M. Koehorst<sup>b, c</sup>, Herbert van Amerongen<sup>b, c</sup>, Jan Feijen<sup>a</sup>

<sup>a</sup> *Department of Polymer Chemistry and Biomaterials, Institute for Biomedical Technology and Technical Medicine, MIRA, Faculty of Science and Technology, University of Twente, Enschede, The Netherlands*

<sup>b</sup> *Laboratory of Biophysics, Wageningen University, Wageningen, The Netherlands*

<sup>c</sup> *MicroSpectroscopy Centre, Wageningen University, Wageningen, The Netherlands*

---

\* To be submitted to Journal of Physical Chemistry B

### Abstract

The phase behavior of fluorescein isothiocyanate (FITC) labeled poly(*N*-isopropylacrylamide) (PNIPAAm) incorporated in polymersomes (Ps) was studied by monitoring the fluorescence lifetime (FL) and the time-resolved fluorescence anisotropy (TRFA) as a function of temperature at pH 7.4. Ps containing FITC-labeled PNIPAAm with a diameter less than 200 nm were prepared by injecting a THF solution of poly(ethylene glycol)-*b*-poly(*D,L*-lactide) (mPEG-PDLLA) and FITC tagged PNIPAAm (FITC-N) into phosphate buffered saline (PBS, pH 7.4). Solutions of free FITC-N (2  $\mu$ M) in PBS were used as controls. The polarized fluorescence decay curves of FITC-N were fitted with two rotational correlation times ( $\phi_{1,2}$ ) and their corresponding amplitude ( $\beta_{1,2}$ ). Short rotational correlation times,  $\phi_1$ , correspond with the rotation of the FITC molecule itself whereas  $\phi_2$  corresponds to FITC-segmental rotation. FITC-N encapsulated in Ps (FITC-N/Ps) showed a decrease of the rotational motion upon increasing the temperature. The long rotational correlation time ( $\phi_2$ ) of FITC-N increased 3 fold, going from 15  $^{\circ}$ C to 40  $^{\circ}$ C, reflecting a reduced rotational mobility. The residual anisotropy ( $r_{\infty}$ ) of FITC-N/Ps at pH 7.4 showed a gradual increase, going from 15 to 25  $^{\circ}$ C followed by a gradual decrease at higher temperatures. These results are explained by a transition from coil to globule, a gradual increase of intermolecular aggregation and possibly phase separation and hydrogel formation.

## **Introduction**

Polymersomes (Ps), synthetic supramolecular-structures similar to liposomes but composed of amphiphilic block copolymers instead of lipids [1], have attracted a lot of attention for drug delivery applications due to their outstanding stability and relatively long residence times in the circulation [2, 3]. Significant efforts have been devoted to control drug delivery from Ps by varying the length and composition of the consisting block copolymers, by using block copolymers which are temperature sensitive, pH-responsive or block copolymers which are chemically or physically crosslinked [4, 5]. An alternative approach is to modify the interior of the Ps for instance by the introduction of a hydrogel. Poly(*N*-isopropylacrylamide) (PNIPAAm) may be used as a precursor of a thermo-sensitive hydrogel. PNIPAAm dissolved in water shows temperature induced dehydration of the polymer chains, which can be followed by the formation of a hydrogel depending on the molecular weight of the PNIPAAm and the concentration of the PNIPAAm solution [6]. Above the low critical solution temperature (LCST) of the PNIPAAm solution, aggregation of the PNIPAAm polymer chains takes place by intermolecular hydrophobic interaction, leading to phase separation into an aqueous phase and a hydrogel [7]. This behavior of PNIPAAm has been used to form a hydrogel either in liposomes or in Ps [8, 9].

In recent years, tracking of the photo-physical properties of a molecular probe by fluorescence spectroscopy has become a versatile technique to detect changes in the local environment of the probe. Fluorescently labeled compounds located in a heterogeneous environment can be followed in time by using time-resolved fluorescence techniques. These techniques have been used for better understanding of protein-substrate, protein-receptor and lipid-protein interactions as well as for probing the local environment of a dye in micelles or liposomes [10, 11] and to characterize sol-gel transitions [12]. It has also been reported that a sol-gel transition of PNIPAAm to form microgels and the sol-gel transition to form a silica gel matrix could be followed by fluorescence analysis [13-15]. Based on these findings, we assume that a time-resolved fluorescence study may also allow us to characterize the temperature dependent formation of a PNIPAAm hydrogel inside Ps.

In principle, this can be achieved by incorporation of a fluorescent dye labeled PNIPAAm into the Ps. Fluorescence anisotropy and fluorescence lifetime studies of this labeled PNIPAAm may give information about temperature induced changes in the interior of the Ps. Fluorescein isothiocyanate (FITC), a derivative of fluorescein which can be easily reacted with amine groups,



was selected as a fluorophore to label PNIPAAm because of its high quantum yield and adequate photo-stability. The fluorescent properties of FITC derivatives are strongly affected by the environment [16]. Therefore, it will be very useful for monitoring physical parameters like local mobility of the environment and rotational dynamics of labeled PNIPAAm in Ps.

The aim of this work is to investigate the thermo-responsive behavior of FITC-labeled PNIPAAm (FITC-N) in Ps by measuring the time-resolved fluorescence anisotropy (TRFA) and fluorescence lifetime profiles (FL). For this study, FITC was first coupled to PNIPAAm (FITC-N) and then incorporated into Ps by injecting a THF solution of the Ps forming polymer and FITC-N into PBS (pH 7.4). Poly(ethylene glycol)-*b*-poly(*D,L*-lactide), mPEG-PDLLA, was used as a biodegradable and biocompatible amphiphilic block copolymer for the formation of the Ps. A schematic picture of Ps containing a FITC labeled hydrogel and the chemical structure of the polymers used for the system is given in Fig. 5.1. TRFA and FL of FITC-N in Ps were measured as a function of temperature and the results were compared with those for the corresponding free solutions of FITC-N.

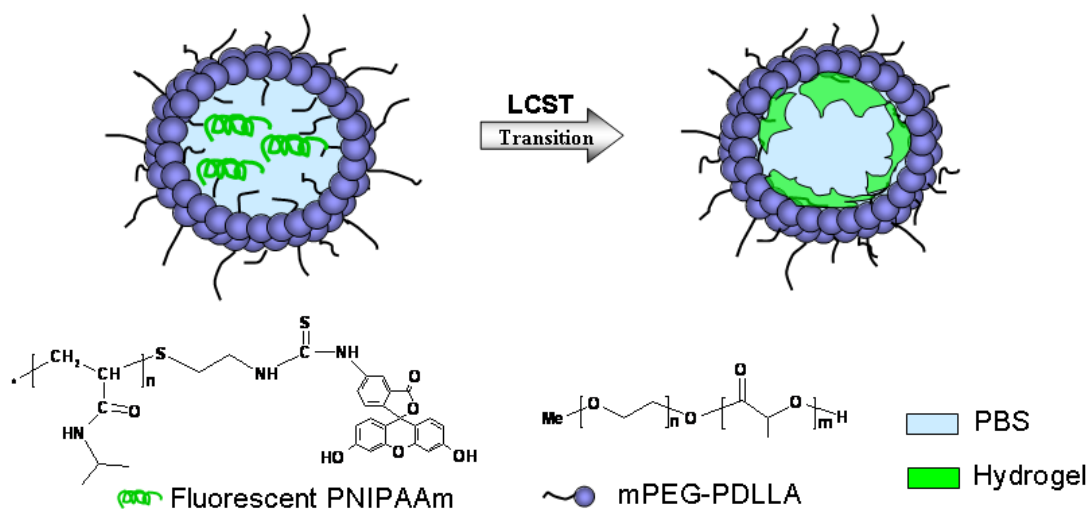


Figure 5.1. Schematic 2D-cross sectional illustration of FITC-N/Ps. At the LCST, phase separation of the FITC-N solution present in the core of Ps into an aqueous phase and a hydrogel takes place.

## **Materials and methods**

### *Materials*

*D,L*-lactide (DLLA, Purac Biochem b.v., The Netherlands), *N*-isopropylacrylamide (NIPAAm, Aldrich, USA), and 2,2'-azobisisobutyronitrile (AIBN, Fluka, Switzerland) were recrystallized from toluene, hexane, and methanol, respectively. Monomethoxy poly(ethylene glycol) with a molecular weight of 5000 g/mol (mPEG, Iris Biotech, Germany) was dried by dissolution in anhydrous toluene followed by azeotropic distillation under N<sub>2</sub>. Stannous octoate, Sn(Oct)<sub>2</sub> was obtained from Sigma (USA). Fluorescein isothiocyanate (FITC) and 2-aminoethanethiol (AET) were purchased from Fluka (Switzerland) and used as received. Phosphate buffered saline (PBS, 0.01M, pH 7.4, B. Braun, USA) was used as a medium for the FL and TRFA experiments.

### *Synthesis of polymers and preparation of FITC-labeled PNIPAAm-containing Ps*

mPEG-PDLLA and FITC-labeled PNIPAAm (FITC-N) were prepared as previously reported [8]. mPEG-PDLLA was synthesized by ring-opening polymerization (ROP) of DLLA using mPEG as an initiator. Amino terminated PNIPAAm was synthesized by free radical polymerization of NIPAAm using AET as a chain transfer agent and the resulting polymer was reacted with FITC. <sup>1</sup>H-NMR analysis (Inova 300 MHz, Varian, USA) showed that the monomer conversion of DLLA was 99 % and the Mn of the PDLLA block was 42,000 g/mol. Mn and Mw of PNIPAAm were analyzed by gel permeation chromatography (GPC) as 39,200 g/mol and 56,000 g/mol, respectively. The labeling efficiency of PNIPAAm with FITC was determined by fluorescence spectroscopy using FITC-dextran (Fluka, 40,000 g/mol) as a standard.

Polymersomes with encapsulated FITC-N, FITC-N/Ps, were prepared using the solvent injection method. In brief, mPEG-PDLLA (10 mg/ml) and FITC-labeled PNIPAAm (FITC-N, 50 mg/ml) were dissolved in THF (1 ml) and the resulting solution was injected into PBS (50 ml). After 15 min without shaking, the vial containing the mixture was turned upside down several times, resulting in a turbid dispersion. THF was removed by dialysis using a dialysis membrane (cut-off 50,000 g/mol, Spectra/Por, CA) in PBS for 2 d and subsequently non-encapsulated FITC-N was removed by ultrafiltration through a membrane (cut-off 100,000 g/mol, Ultracel Ultrafiltration Disc, Millipore, USA) for 5 h.

### Data acquisition

Time-resolved polarized fluorescence experiments were carried out using the time-correlated single-photon counting technique (TCSPC) [17]. The TCSPC setup and the measurement procedures used were described in detail elsewhere [18], and will only briefly be outlined below. A mode-locked CW Nd:YLF laser was used for the synchronous pumping of a cavity-dumped, dye laser (Rhodamine 6G) providing after frequency-doubling excitation at 300 nm. The samples were excited with vertically polarized light pulses (4 ps FWHM) at an excitation frequency of 591 kHz and both parallel and perpendicularly polarized fluorescence were detected. At 470 nm, excitation FITC fluorescence was detected using a Schott OG515nm cut-off filter in combination with a Balzers K55 broadband interference filter (550 nm). The data were collected using a multi-channel analyzer with a maximum time window of 4096 channels typically at 5 ps/channel. The dynamic instrumental response function of the setup was approximately 40-50 ps FWHM, and was obtained at the FITC emission wavelength using a solution of erythrosine B in de-ionized water as reference compound ( $\tau_{ref} = 80$  ps). One complete experiment for a fluorescence decay measurement consisted of the recording of data sets of the reference compound, the FITC-N or FITC-N/Ps samples, the background (buffer) and again the reference compound.

### Data analysis

Data analysis was performed using a model of discrete exponential terms [19]. Global analysis of the experimental data was performed using the ‘TRFA Data Processing Package’ of the Scientific Software Technologies Center (Belarusian State University, Minsk, Belarus) [20, 21]. The total fluorescence intensity decay  $I(t)$  was obtained from the measured parallel  $I_{||}(t)$  and perpendicular  $I_{\perp}(t)$  fluorescence intensity components through the relation:

$$I(t) = I_{||}(t) + 2I_{\perp}(t) \quad (5.1)$$

The fluorescence lifetime profile consisting of a sum of discrete exponentials with lifetime  $\tau_i$  and amplitude  $\alpha_i$  can be retrieved from the total fluorescence  $I(t)$  through the convolution product:

$$I(t) = E(t) \times \sum_{i=1}^N \alpha_i e^{-t/\tau_i} \quad (5.2)$$

where  $E(t)$  is the instrumental response function. The quality of the fit was judged by the chi-square value (below 1.1 was considered sufficient) and by the quality of the residuals and autocorrelation of these residuals. Average fluorescence lifetimes,  $\tau_{av}$ , were, calculated according to equation 3 [22].

$$\tau_{av} = \frac{\sum_{i=1}^n \alpha_i \tau_i^2}{\sum_{i=1}^n \alpha_i \tau_i} \quad (5.3)$$

The anisotropy decay  $r(t)$  is given by the following relation:

$$r(t) = \frac{I_{\parallel}(t) - I_{\perp}(t)}{I_{\parallel}(t) + 2I_{\perp}(t)} \quad (5.4)$$

In fluorescence anisotropy analysis, after deconvolution, the time-dependent fluorescence anisotropy  $r(t)$  is calculated from the parallel  $I_{\parallel}(t)$  and perpendicular  $I_{\perp}(t)$  components through the relations [23]:

$$I_{\parallel}(t) = \frac{I}{3} \sum_{i=1}^N \alpha_i e^{-t/\tau_i} \left\{ 1 + 2 \sum_{j=1}^M r_{0j} e^{-t/\phi_j} \right\} \quad (5.5)$$

$$I_{\perp}(t) = \frac{I}{3} \sum_{i=1}^N \alpha_i e^{-t/\tau_i} \left\{ 1 - \sum_{j=1}^M r_{0j} e^{-t/\phi_j} \right\} \quad (5.6)$$

in which  $i=j$  for correlated systems in which particular lifetime components  $\tau_i$  are associated with particular correlation times  $\phi_j$  (correlated or associative model), and  $i \neq j$  for systems in which all lifetimes equally contribute to the anisotropy (uncorrelated or non-associative model);  $r_{0j}$  is the fundamental anisotropy at time  $t=0$ .

## Results and discussion

Ps containing FITC-N, FITC-N/Ps, with a diameter less than 200 nm were prepared and characterized as previously reported [8]. The degree of functionalization of PNIPAAm with amine groups was  $96.0 \pm 4.7$  mol% and the labeling efficiency of PNIPAAm-NH<sub>2</sub> with FITC was  $94.0 \pm$

11.8 mol%. In order to acquire the internal dynamics of the label bound to PNIPAAm in Ps, FL profiles and TRFA of FITC-N in Ps were measured. Solutions of free FITC-N (2  $\mu$ M) in PBS were used for comparison.

In order to explain the FL and TRFA data which will be discussed later, first a model (Fig. 5.2) is presented which shows the possible temperature dependent changes in the local environment of the fluorescent probes. PNIPAAm in solution at relatively low concentrations exhibits a temperature induced coil to globule transition due to dehydration of the polymer chains. Depending on the molecular weight of PNIPAAm and at sufficiently high concentrations of the polymer solution, like in the Ps, the coil to globule transition can be followed by phase separation, leading to the formation of a hydrogel and an aqueous phase. The environment of FITC covalently linked to PNIPAAm will be changed both by the temperature induced coil to globule transition and hydrogel formation after phase separation of PNIPAAm present in the Ps. This may lead to restricted rotational mobility of the probe itself and/or the probe in conjunction with polymer segments. Fig. 5.2 gives a schematic picture of temperature and concentration dependent transitions of FITC-labeled PNIPAAm and associated rotational correlation times  $\phi_1$  and  $\phi_2$ .  $\phi_1$  is related to the rotation of individual FITC molecules, whereas  $\phi_2$  is related to the rotation of FITC in conjunction with PNIPAAm segments.

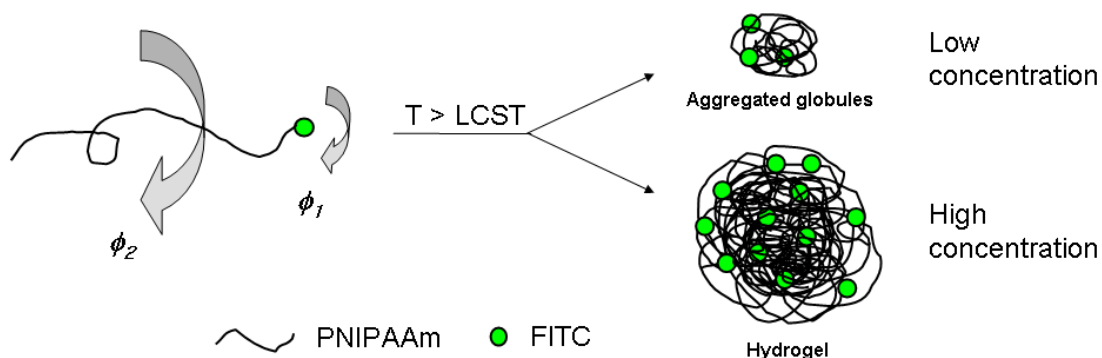


Figure 5.2. Schematic illustration of possible positions of FITC linked to PNIPAAm in the solution or incorporated in the PNIPAAm gel. PNIPAAm exhibits a coil to globule transition by increasing the temperature due to dehydration of the polymer chains. Depending on the molecular weight of PNIPAAm and the concentration of the polymer solution, the coil to globule transition can be followed by phase separation into a hydrogel and an aqueous phase (inside Ps). FITC will be associated either with the globular state of PNIPAAm or with the gel formed in the Ps at higher temperatures. A short rotational correlation time,  $\phi_1$ , and a long rotational correlation time,  $\phi_2$ , are presented.  $\phi_1$  relates to the rotation of individual FITC molecules, whereas  $\phi_2$  is related to the rotation of FITC in conjunction with PNIPAAm segments.

Fig. 5.3 shows a typical example of a fluorescence decay curve for FITC-N in PBS at 25 °C and the residuals corresponding to a 3-exponential fit. The fluorescence decay of FITC-labeled PNIPAAm (FITC-N) in PBS (pH 7.4) was fitted with 3 exponentials. This was also the case for that of buffered solutions (pH 7.4) of FITC-labeled PNIPAAm incorporated in polymersomes (FITC-N/Ps) and all fits were of good quality ( $\chi^2 < 1.1$ ).

In Table 5.1,  $\tau_{av}$  as a function of temperature is shown for a dilute solution of FITC-N in PBS at pH 7.4 and for FITC-N in polymersomes (FITC-N/Ps). For a dilute solution of FITC-N in PBS,  $\tau_{av}$  decreased from 3.77 to 3.46 ns upon increasing the temperature from 15 to 40 °C showing a normal temperature effect on fluorescence lifetimes. In general, the lifetimes of excited states are shortened with increasing temperature as a result of an increase of the non-radiative relaxation rate [24]. A coil to globule transition of PNIPAAm may not significantly influence the fluorescence lifetimes of FITC in the dilute solution because FITCs are conjugated at the end of PNIPAAm chains. In contrast,  $\tau_{av}$  of FITC-N in Ps increased upon increasing the temperature up to 30 °C. This may be indicative that FITC conjugated to PNIPAAm and localized in Ps exhibited different relaxation patterns most probably due to the relatively high concentration of PNIPAAm in the Ps.  $\tau_{av}$  of FITC-N in Ps was slightly longer than in dilute solution at the same temperature. Above 30 °C, a normal temperature effect on the fluorescence lifetimes of FITC-N in Ps was observed.

After deconvolution of the data obtained for dilute FITC-N solutions and for FITC-N/Ps, time-dependent fluorescence anisotropy  $r(t)$  data, calculated from the parallel  $I_{||}(t)$  and perpendicular  $I_{\perp}(t)$  components were obtained. A decay of the fluorescence anisotropy within 5 ns was seen. At relatively high temperatures ( $> 30$  °C), the fluorescence anisotropy decay curve of FITC-N shows a residual anisotropy,  $r_{\infty}$ , that increases upon further increase of temperature (Fig. 5.4a, Table 5.2). The polarized fluorescence decay curves of FITC-N were fitted with two rotational times ( $\phi_1, \phi_2$ ) and their corresponding amplitudes ( $\beta_1, \beta_2$ ) using the uncorrelated or non-associative model, in which all lifetimes equally contribute to the anisotropy (Table 5.2). The rotational times reflect a local mobility of FITC. However, rotational correlation times  $\phi_1$  and  $\phi_2$  did not increase during the coil-to-globule transition within the temperature range used. This can be explained by the fact that FITC is bound to the end of the PNIPAAm chains. The slight decrease of  $\phi_1$  and  $\phi_2$  above 30 °C can be considered as a common temperature effect. The increase of  $r_{\infty}$  with temperature for FITC-

N up to 0.09 can be explained by the earlier reported coil-to-globule transition of single PNIPAAm chains at high dilution [25]. In this respect, the global motion of a globule can be considered as ‘infinitely slow’ with the used time frame of 20 ns, resulting in a residual anisotropy,  $r_\infty$ . The contribution of  $r_\infty$  to the anisotropy decay increased with increasing temperature above 30 °C (Fig. 5.5a), indicating that a transition occurred at 30 °C.

For FITC-N/Ps, the data could also be fitted using the same uncorrelated or non-associative model (e.g. three fluorescence lifetimes in combination with two rotational correlation times). We observed rotational correlation times at relatively low temperatures that are close to the corresponding ones of the highly diluted reference FITC-N. FITC-N/Ps has already a high  $r_\infty$  (0.11) at 15 °C (Table 5.2). This may originate from reduced rotational motion of the dye possibly caused by interactions of the FITC-labeled PNIPAAm with PEG, which is present on the inner surface of Ps. This is supported by the work of Polozova and Winnik [26], stating that amide groups of PNIPAAm may form hydrogen bonds with ethylene oxide units of PEG. At 30 °C,  $\phi_2$  for FITC-N/Ps significantly increased as compared to  $\phi_2$  at relatively low temperatures, which is in contrast with the observed decrease of these parameters with increasing temperature for dilute FITC-N samples. These findings can be explained by an increase of the inter-chain aggregation of PNIPAAm with increasing temperature possibly in concert with phase separation and hydrogel formation. However, an initial increase of  $r_\infty$  from 0.11 to 0.21 upon raising the temperature of FITC-N/Ps from 15 to 25 °C is followed by a gradual decrease of  $r_\infty$  to 0.15 upon further increase of temperature. The increased dynamics at relatively high temperature can be explained by the fact that FITC is highly negatively charged at pH 7.4 [16] and may therefore be expelled from the relatively apolar, hydrogel forming globular structures and by that may reside in the more polar, less viscous aqueous phase. When the phase transition occurs the gel phase has a volume of 10-20 % of the original volume and the remainder forms an aqueous phase [27, 28].

Table 5.1.  $\tau_{av}^*$  of FITC-N dissolved in PBS or in Ps as a function of temperature

	15 °C	20 °C	25 °C	30 °C	35 °C	40 °C
FITC-N	3.77	3.73	3.72	3.70	3.61	3.46
FITC-N/Ps	3.90	3.96	3.96	4.03	4.01	3.97

\*Average fluorescence lifetime (ns).

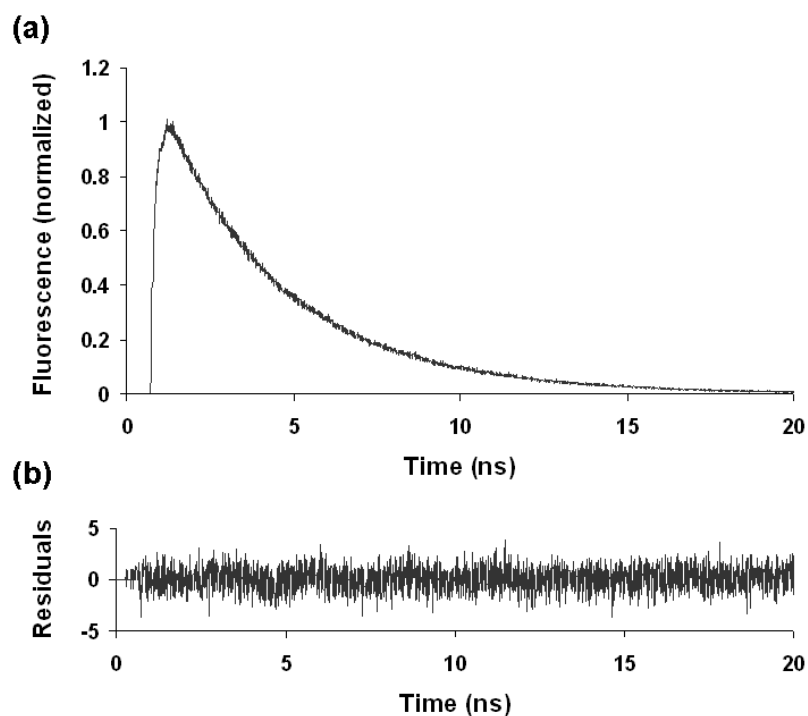


Figure 5.3. A fluorescence decay curve for FITC-N in PBS at 25 °C (a) and the residual of a 3-exponential fit (b).

Table 5.2 . Fluorescence anisotropy of FITC-N (2  $\mu$ M) and FITC-N/Ps

	temp.	$\beta_1^a$	$\phi_1^b$	$\beta_2^a$	$\phi_2^b$	$r_\infty^c$
FITC-N	15 °C	0.22	0.27	0.10	2.1	0.01
	20 °C	0.21	0.24	0.09	1.9	0.01
	25 °C	0.21	0.21	0.09	1.6	0.01
	30 °C	0.22	0.19	0.08	1.8	0.01
	35 °C	0.15	0.16	0.06	1.4	0.04
	40 °C	0.11	0.13	0.04	1.2	0.09
FITC-N/Ps	15 °C	0.14	0.20	0.11	1.4	0.11
	20 °C	0.11	0.26	0.08	1.7	0.15
	25 °C	0.06	0.40	0.07	2.8	0.21
	30 °C	0.07	0.45	0.07	3.9	0.19
	35 °C	0.07	0.30	0.09	3.4	0.17
	40 °C	0.09	0.34	0.09	4.2	0.15

<sup>a</sup> Fractional contribution to the fluorescence anisotropy decay.

<sup>b</sup> Rotational correlation time (ns).

<sup>c</sup> Residual anisotropy.



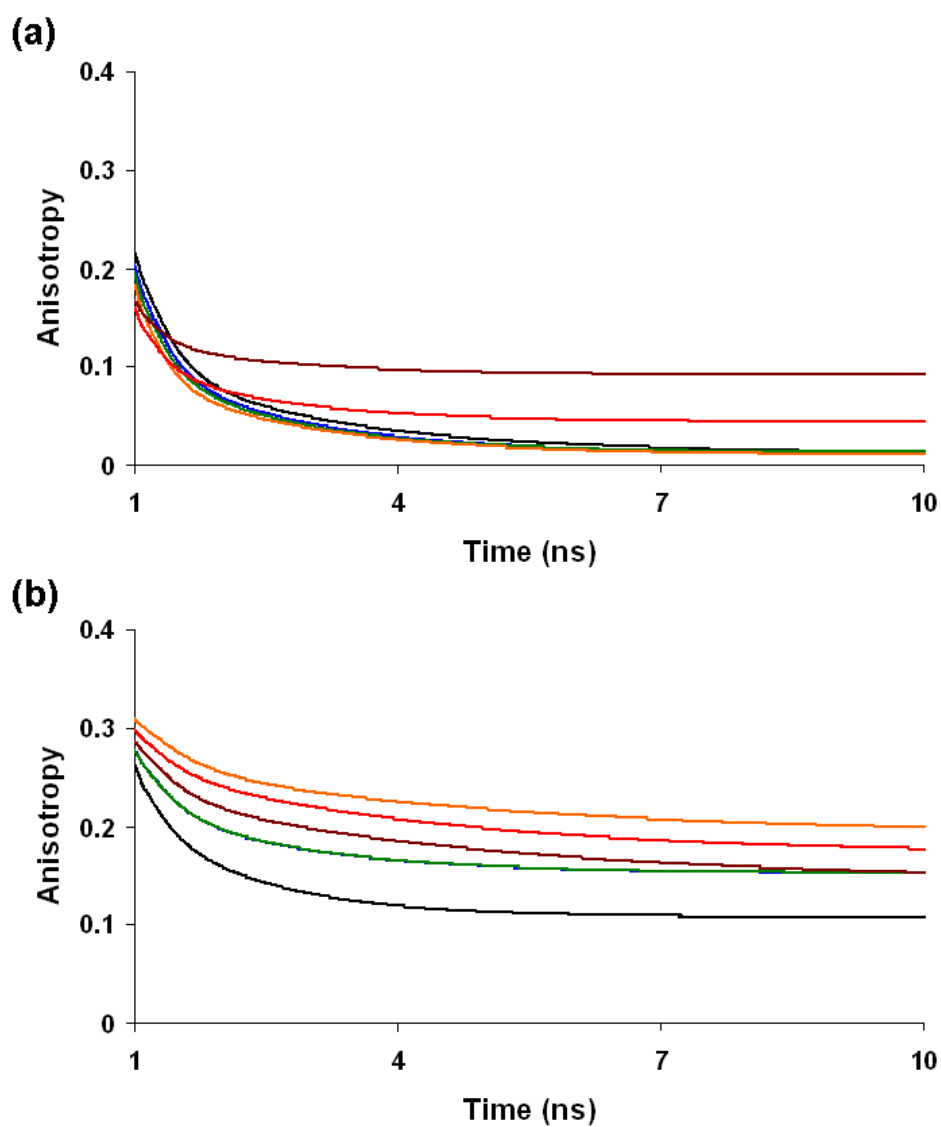


Figure 5.4. Fitted fluorescence anisotropy decay curves of FITC-N a) and FITC-N/Ps b) in PBS at 15 °C (black), 20 °C (blue), 25 °C (green), 30 °C (orange), 35 °C (red) and 40 °C (brown).

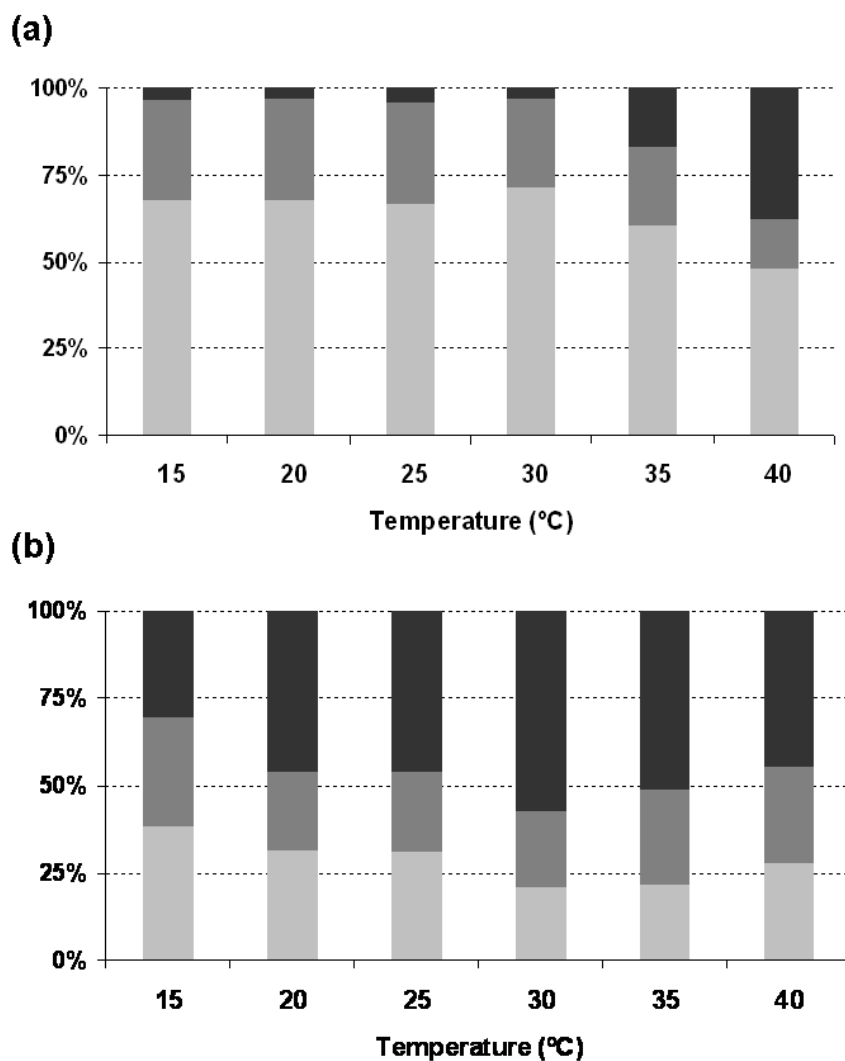


Figure 5.5. Contribution (%) of rotational correlation times and residual anisotropy to the fluorescence anisotropy decay for FITC-N (a) and FITC-N/Ps (b) as a function of temperature in PBS, relative to the total sum:  $\beta_1 + \beta_2 + r_\infty$  (which equals the initial anisotropy,  $r_0$ , at time zero). The contributions of the relatively short rotational correlation time,  $\phi_1$ , (light gray), the relatively long rotational correlation time,  $\phi_2$ , (dark gray) as well as the residual anisotropy,  $r_\infty$ , (black) are represented.

## Conclusions

PNIPAAm was labeled with FITC (FITC-N) and incorporated into polymersomes. The time-resolved fluorescence as well as the time-resolved fluorescence anisotropy of FITC-N in polymersomes were monitored in PBS as a function of temperature and compared with the results for FITC-N dissolved in PBS at pH 7.4. The results of the FL and TRFA measurements revealed that with increasing temperature PNIPAAm incorporated in Ps undergoes a coil to globule transition followed by intermolecular aggregation and possibly phase separation followed by hydrogel formation. In a future study, it would be interesting to use also other types of fluorescently labeled hydrogels to investigate the effect of the physico-chemical properties of the hydrogels on the time-resolved fluorescence and time-resolved fluorescence anisotropy.

## References

- [1] B.M. Discher, D.A. Hammer, F.S. Bates, D.E. Discher, Polymer vesicles in various media. *Curr. Opin. Colloid Interface Sci.* 5(1-2) (2000) 125-131.
- [2] J.C.M. Lee, H. Bermudez, B.M. Discher, M.A. Sheehan, Y.Y. Won, F.S. Bates, D.E. Discher, Preparation, stability, and in vitro performance of vesicles made with diblock copolymers. *Biotechnol. Bioeng.* 73(2) (2001) 135-145.
- [3] P.J. Photos, L. Bacakova, B. Discher, F.S. Bates, D.E. Discher, Polymer vesicles in vivo: correlations with PEG molecular weight. *J. Control. Release* 90(3) (2003) 323-334.
- [4] H. Bermudez, A.K. Brannan, D.A. Hammer, F.S. Bates, D.E. Discher, Molecular weight dependence of polymersome membrane structure, elasticity, and stability. *Macromolecules* 35(21) (2002) 8203-8208.
- [5] F.H. Meng, Z.Y. Zhong, J. Feijen, Stimuli-Responsive Polymersomes for Programmed Drug Delivery. *Biomacromolecules* 10(2) (2009) 197-209.
- [6] S. Furyk, Y.J. Zhang, D. Ortiz-Acosta, P.S. Cremer, D.E. Bergbreiter, Effects of end group polarity and molecular weight on the lower critical solution temperature of poly(N-isopropylacrylamide). *J. Polym. Sci. Pol. Chem.* 44(4) (2006) 1492-1501.
- [7] B. Jeong, S.W. Kim, Y.H. Bae, Thermosensitive sol-gel reversible hydrogels. *Adv. Drug Deliv. Rev.* 54(1) (2002) 37-51.
- [8] J.S. Lee, W. Zhou, F.H. Meng, D.W. Zhang, C. Otto, J. Feijen, Thermosensitive hydrogel-containing polymersomes for controlled drug delivery. *J. Control. Release* 146(3) (2010) 400-408.
- [9] A. Jesorka, M. Markstrom, M. Karlsson, O. Orwar, Controlled hydrogel formation in the internal compartment of giant unilamellar vesicles. *J. Phys. Chem. B* 109(31) (2005) 14759-14763.
- [10] R.B.M. Koehorst, R.B. Spruijt, M.A. Hemminga, Site-directed fluorescence labeling of a membrane protein with BADAN: Probing protein topology and local environment. *Biophys. J.* 94(10) (2008) 3945-3955.
- [11] P.A. Vanparidon, J.K. Shute, K.W.A. Wirtz, A.J.W.G. Visser, A Fluorescence Decay Study of Parinaroyl-Phosphatidylinositol Incorporated into Artificial and Natural Membranes. *Eur. Biophys. J. Biophys. Lett.* 16(1) (1988) 53-63.
- [12] B. Rangarajan, L.S. Coons, A.B. Scranton, Characterization of hydrogels using luminescence spectroscopy. *Biomaterials* 17(7) (1996) 649-661.
- [13] N.J. Flint, S. Gardebrecht, L. Swanson, Fluorescence Investigations of "Smart" Microgel Systems. *J. Fluoresc.* 8(4) (1998) 343-353.
- [14] N.M. Eleftheriou, J.D. Brennan, Probing the dynamics of domain III of human serum albumin entrapped in sol-gel derived silica using a Sudlow's site II specific fluorescent ligand. *J. Sol-Gel Sci. Technol.* 50(2) (2009) 184-193.
- [15] I. Pastor, M.L. Ferrer, M.P. Lillo, J. Gomez, C.R. Mateo, Structure and dynamics of lysozyme encapsulated in a silica sol-gel matrix. *J. Phys. Chem. B* 111(39) (2007) 11603-11610.
- [16] R. Sjoback, J. Nygren, M. Kubista, Absorption and Fluorescence Properties of Fluorescein. *Spectroc. Acta Pt. A-Molec. Biomolec. Spectr.* 51(6) (1995) L7-L21.
- [17] D.V. O' Connor, D. Phillips, Time Correlated Single Photon Counting. Academic Press, London, 1984.

- [18] J.W. Borst, M.A. Hink, A. van Hoek, A.J.W.G. Visser, Effects of refractive index and viscosity on fluorescence and anisotropy decays of enhanced cyan and yellow fluorescent proteins. *J. Fluoresc.* 15(2) (2005) 153-160.
- [19] N.V. Visser, A.H. Westphal, A. van Hoek, C.P.M. van Mierlo, A. Visser, H. van Amerongen, Tryptophan-tryptophan energy migration as a tool to follow apoflavodoxin folding. *Biophys. J.* 95(5) (2008) 2462-2469.
- [20] A.V. Digris, V.V. Skakoun, E.G. Novikov, A. van Hoek, A. Claiborne, A.J.W.G. Visser, Thermal stability of a flavoprotein assessed from associative analysis of polarized time-resolved fluorescence spectroscopy. *Eur. Biophys. J. Biophys. Lett.* 28(6) (1999) 526-531.
- [21] P.A.W. van den Berg, A. van Hoek, A.J.W.G. Visser, Evidence for a novel mechanism of time-resolved flavin fluorescence depolarization in glutathione reductase. *Biophys. J.* 87(4) (2004) 2577-2586.
- [22] Lakowicz, J. R., *Principles of Fluorescence Spectroscopy*, Springer, New York, 2006.
- [23] J.R. Lakowicz, *Principles of Fluorescence Spectroscopy*, R, Kluwer Academic/Plenum Publishers, New York, 1999.
- [24] C.K. Duan, A. Meijerink, R.J. Reeves, M.F. Reid, The unusual temperature dependence of the Eu<sup>2+</sup> fluorescence lifetime in CaF<sub>2</sub> crystals. *J. Alloy. Compd.* 408 (2006) 784-787.
- [25] C. Wu, S.Q. Zhou, Laser-Light Scattering Study of the Phase-Transition of Poly(N-Isopropylacrylamide) in Water .1. Single-Chain. *Macromolecules* 28(24) (1995) 8381-8387.
- [26] A. Polozova, F.M. Winnik, Contribution of hydrogen bonding to the association of liposomes and an anionic hydrophobically modified poly(N-isopropylacrylamide). *Langmuir* 15(12) (1999) 4222-4229.
- [27] Y. Suzuki, K. Tomonaga, M. Kumazaki, I. Nishio, Change in phase transition behavior of an NIPA gel induced by solvent composition: Hydrophobic effect. *Polym. Gels Netw.* 4(2) (1996) 129-142.
- [28] E. Ruel-Gariepy, J.C. Leroux, In situ-forming hydrogels - review of temperature-sensitive systems. *Eur. J. Pharm. Biopharm.* 58(2) (2004) 409-426.

## Chapter 6

### **Lysosomally Cleavable Peptide-containing Polymersomes Modified with anti-EGFR Antibody for Systemic Cancer Chemotherapy\***

Jung Seok Lee<sup>a</sup>, Claudia Cusan<sup>b</sup>, Tom Groothuis<sup>c</sup>, Jan Feijen<sup>a</sup>

<sup>a</sup> *Department of Polymer Chemistry and Biomaterials, MIRA Institute for Biomedical Technology and Technical Medicine, Faculty of Science and Technology, University of Twente, Enschede, The Netherlands*

<sup>b</sup> *DSM Pharmaceutical Products, Innovative Synthesis & Catalysis, Geleen, The Netherlands,*

<sup>c</sup> *Nanobiophysics, MIRA Institute for Biomedical Technology and Technical Medicine, Faculty of Science and Technology, University of Twente, Enschede, The Netherlands*

---

\* Submitted to Biomaterials

## Abstract

Novel polymersomes (Ps) based on a biodegradable and biocompatible block copolymer of methoxy poly(ethylene glycol) (mPEG) and poly(*D,L*-lactide) (PDLLA) in which a peptide sequence, Phe-Gly-Leu-Phe-Gly (FGLFG), was introduced in between the two blocks (mPEG-pep-PDLLA) were developed. The peptide linker is cleavable by the lysosomal enzyme cathepsin B (Cath B). Ps containing the peptide linker (Ps (pep)) with an average diameter of about 124 nm were prepared by injecting a THF solution of the block copolymer into DI water. The Ps had a membrane thickness of about 15 nm as determined by transmission electron microscopy (TEM). In order to investigate the enzymatic degradation of the Ps (pep), dynamic light scattering (DLS) measurements of Ps (pep) dispersions with different concentrations of Cath B at pH 5.5 and 7.4 were performed as a function of time. A gradual decrease in kilo counts per second (Kcps) of the Ps (pep) over 7 d was observed after incubation of the Ps (pep) dispersions with 5 units/ml of Cath B at pH 5.5 at 37 °C. The size distribution became also bimodal, indicating that aggregation and precipitation of Ps (pep) occurred by disintegration of the Ps (pep) as a result of cleavage of the peptide. The rate of disintegration of the Ps (pep) was depending on the concentration of Cath B and the pH. No changes by DLS were seen when the dispersions were incubated with the enzyme at pH 7.4. Acridine orange (AO) was encapsulated in Ps (pep) as a model drug and rapid release of AO triggered by Cath B degradation of Ps (pep) was observed at pH 5.5. Anti-epidermal growth factor receptor (anti-EGFR) antibody (abEGFR) was immobilized on the surface of Ps (pep) in order to enhance the cellular uptake of Ps (pep). Fluorescein isothiocyanate labeled dextran (40,000 g/mol) (FD40) was incorporated in the Ps (pep) for the cell study and Ps either without peptide or antibody or without both peptide and antibody were used as negative controls. After 3 d exposure to SKBR3 cells, abEGFR-conjugated Ps (pep) (abEGFR-Ps (pep)) were directly bound to the membrane of the cells and were endocytosed more rapidly as compared to Ps (pep) without abEGFR. Intracellular release of FD40 from Ps (pep) was observed, suggesting that the peptide linker in Ps (pep) was cleaved in the lysosomal compartments of the cells leading to Ps (pep) membrane disruption. An Alexa Fluor<sup>®</sup> 488 labeled fragment of anti-mouse IgG (F(ab')<sub>2</sub>A) was also coupled to Ps (pep). Specific binding of the Ps (pep) coupled IgG (F(ab')<sub>2</sub>A) onto SKBR3 cells treated with primary mouse antibody was observed, whereas no binding was found with SKBR3 cells treated with goat antibody.

## **Introduction**

Chemotherapy is an essential treatment for cancer. However, the efficacy of chemotherapy is often restricted by nonspecific body distribution of drugs ultimately followed by adverse systemic side effects. Therefore, it is necessary to generate a spatial drug distribution control, which can be achieved by drug targeting. Stimuli-responsive Ps as programmable delivery systems have recently attracted rapidly growing interest. Ps are self-assembled vesicles based on amphiphilic block copolymers and drug release from Ps can be modulated by exerting appropriate stimuli [1, 2]. Significant efforts have been devoted to develop Ps which are sensitive to stimuli like pH, temperature, redox potential, light, magnetic fields and ultrasound [2]. As one of the many examples, pH-dependent degradable Ps based on the diblock copolymer of PEG and poly(2,4,6-trimethoxybenzylidenepentaerythritol carbonate) (PTMBPEC) were reported by Chen *et al.* [3]. *In vitro* studies demonstrated that the release of paclitaxel (PTX) as well as doxorubicin (DOX) from these Ps was pH-dependent. The release of drugs at mildly acidic condition was faster than the release at physiological pH. This system may be useful for tumor-targeting applications because the pH of tumor tissues is about 6.5. Qin *et al.* reported temperature-sensitive Ps based on PEG-*b*-poly(*N*-isopropylacrylamide) (PEG-PNIPAAm) [4]. The Ps are only stable at higher temperatures and will disassemble at lower temperatures. In this way, local release of drugs can be achieved either by applying simple ice packs or deeply penetrating cryoprobes. Natural oxidation-reduction reactions (redox) have also been reported as a means for spatial drug release control within the body. Hubbell and co-workers developed oxidation responsive Ps based on PEG and poly(propylene sulfide) (PPS) [5]. The hydrophobic PPS block was oxidized and transformed within 2 h into hydrophilic poly(sulfoxides) and poly(sulfones) upon exposure to hydrogen peroxide in the glucose-oxidase (GOx)/glucose/oxygen system leading to destabilization of the vesicular structure. The reduction-sensitive disulfide group containing block copolymer, PEG-SS-PPS was used to prepare Ps that can protect therapeutics in the extracellular environment, but releasing their contents within the early endosome when the Ps are taken up by cells. These Ps may be also beneficial to increase the concentration of therapeutic drugs at target sites, enhancing the therapeutic efficacy and reducing side effects.

During the past few decades, the use of enzymes for targeted drug delivery has also been recognized as a very interesting approach. For instance, lysosomal enzymes like Cath B are



expressed at increased levels in tumor tissue as compared to normal tissue [6-8]. These enzymes can be used to cleave certain peptide sequences like the tetrapeptide sequence, Gly-Phe-Leu-Gly (GFLG) [9-12]. Structures containing these peptide sequences can be transformed by the cleavage of the peptide, resulting in the release of a covalently bound drug. For example, *N*-(2-hydroxypropyl) methacrylamide (HPMA) copolymer-DOX conjugates with GFLG linkers were produced in the early 1980s [13, 14]. Application of the water soluble conjugates containing GFLG in a mouse melanoma tumor model resulted in concentrations of approximately 70 times more DOX in the tumors than in normal tissues. Importantly, this approach also increased the maximum tolerated dose of the polymer/drug by up to ten times as compared to the free drug. The conjugates have been evaluated in clinical trials with encouraging results and further optimization of the design and structure to enhance the therapeutic efficacy seems feasible [15].

The aim of this study is to develop Ps, which contain peptide sequences that are cleavable by Cath B. Ps have received a lot of attention as a novel class of nanocarriers due to their good stability and long circulation times [16-19]. Usually, Ps based on amphiphilic block copolymers with a relatively high MW have relatively robust and thick membranes (up to 40 nm) [20]. Long circulation times of Ps can be obtained by the presence of a PEG brush on the Ps surface [19]. However, it should be noted that the PEG coating can also diminish the uptake of these carriers by cells since the PEG brush reduces cell-carrier interactions. It has been previously reported that the presence of PEG-cholesterol in liposomes inhibited the binding of the liposomes to J774 cells [21]. When liposomes contain 5 mol% of PEG (8800 g/mol)-cholesterol it was found that the adherence of these liposomes to cells was decreased to 30 % of that of liposomes without the PEG layer. Soga *et al.* reported the uptake of pegylated micelles by B16F10 cells. The uptake was time and concentration dependent, suggesting that the uptake had occurred via fluid state endocytosis rather than via interaction of the micelles with the cell membrane [22].

One of the solutions to enhance the cellular uptake of such pegylated systems can be the coupling of the PEG termini with cell-binding antigens. Anti-EGFR (ErbB-1; HER1 in humans) antibodies or fragments are very attractive candidates as cell binding molecules because they are very specific for the EGF receptor. This receptor is a normal cell-surface receptor for the members of the epidermal growth factor family (EGF-family). Interestingly, the receptor is over expressed on the surface of a number of different human cancer cells including colorectal, breast, and lung cancer cells [23]. This means that anti-EGFR antibodies or the fragments can be used

not only as cell-anchoring molecules to facilitate endocytic uptake, but also as targeting devices for specific cancer cells. In the literature, Noh *et al.* reported DOX loaded micelles conjugated with anti-EGFR antibodies, which showed a more than 2 fold enhanced uptake by RKO cells as compared to bare micelles, inducing an effective apoptosis of these cells [24].

In this study, we developed novel Ps based on a biodegradable and biocompatible diblock copolymer of PEG and PDLLA, in which the blocks are connected via a peptide sequence that is cleavable by lysosomal enzymes either present in extracellular tumor tissue or in the lysosomal compartments of tumor cells [7, 8]. Ps based on mPEG-pep-PDLLA, (Ps (pep)), were prepared by injecting a THF solution of the block copolymer into DI water. The morphology of the Ps (pep) was studied by TEM. Changes in size and numbers of the Ps during exposure to Cath B were studied by DLS. The release of AO from AO loaded Ps (pep) (AO-Ps (pep)) as well as the colloidal properties of these Ps (pep) were monitored to study the release of the model drug triggered by enzymatic degradation. For cell studies, F(ab')<sub>2</sub>A was post-conjugated with Ps (pep) (Fig. 6.1a, F(ab')<sub>2</sub>A-Ps (pep)). Anti-EGFR antibody (abEGFR) was also coupled onto Ps (pep), and fluorescein isothiocyanate labeled dextran (40,000 g/mol) (FD40) was encapsulated before the coupling reaction (Fig. 6.1b, FD40/abEGFR-Ps (pep)). The antibody-binding affinity of F(ab')<sub>2</sub>A-Ps (pep) and cellular uptake of FD40/abEGFR-Ps (pep) were studied using cultured human breast cancer cells (SKBR3).

A scheme for the targeted drug delivery to the tumor compartment using Ps (pep) with antibodies or antibody fragments is given in Fig. 6.2. Ps (pep) may have rather long circulation times due to their robustness and the presence of the PEG layer on the surface. The size of the Ps is proper to be passively localized in tumor tissue by the enhanced permeability and retention (EPR) effect. After the accumulation of Ps (pep) in the tumor, antibody-mediated endocytosis will take place and subsequently the Ps (pep) will be degraded by the action of lysosomal enzymes like Cath B either in endosomes or in lysosomes. In cells, Cath B normally exists as a membrane-associated protein in endosomes or free in lysosomes. Finally, encapsulated therapeutic drugs or proteins may be released rapidly by dissociation of the Ps (pep).

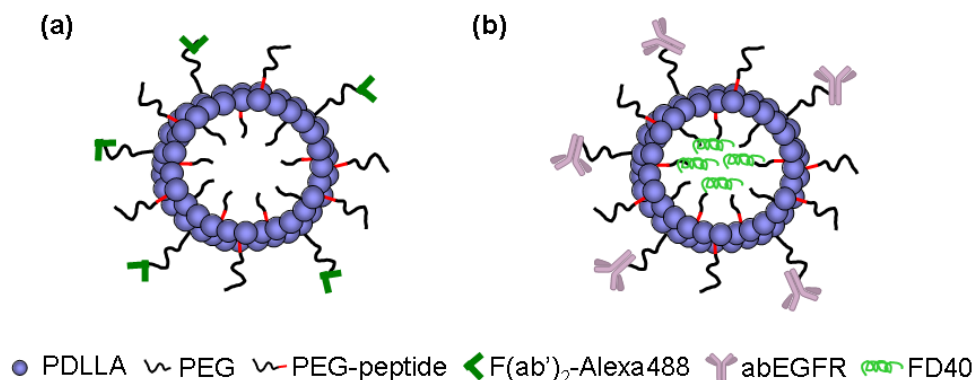


Figure 6.1. Schematic 2D-cross sectional illustration of Ps (pep) on which Alexa Fluor<sup>®</sup> 488 labeled antibody fragment (F(ab')<sub>2</sub>-Alexa488) (a) or anti-EGFR antibody (abEGFR) (b) was immobilized to PEG. Fluorescein dextran (40,000 g/mol, FD40) was encapsulated in abEGFR immobilized Ps (pep) (b) during the preparation for subsequent cell studies.

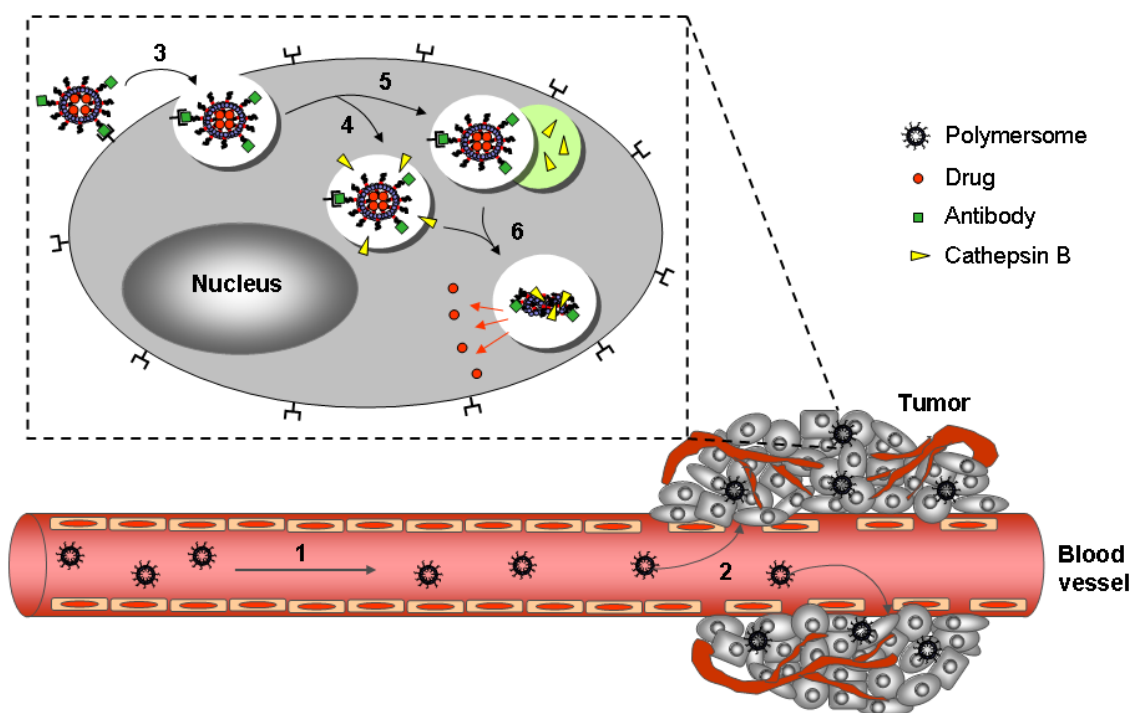


Figure 6.2. Schematic illustration of systemic targeting drug delivery by using antibody conjugated and peptide-containing Ps in which therapeutic drugs or proteins are present. Long circulating Ps can be passively localized in tumor tissue by the EPR effect (1 and 2). Antibody-mediated endocytosis (3) followed by enzymatic degradation of Ps either in endosomes (4) or in lysosomes (5) may occur especially when lysosomes fuse with endosomes. A rapid release of therapeutic drugs and proteins, which can be triggered by dissociation of Ps as a result of enzymatic degradation (6) will take place.

## **Materials and methods**

### *Materials*

*D,L*-lactide (DLLA) was obtained from Purac Biochem b.v. (The Netherlands) and recrystallized from toluene. Methoxy PEG (mPEG), methoxy amino PEG (mPEG-NH<sub>2</sub>) and carboxyl PEG (cPEG) with a molecular weight of 5000 g/mol (Iris Biotech, Germany) were dried by dissolution in anhydrous toluene followed by azeotropic distillation under N<sub>2</sub>. Stannous octoate (Sn(Oct)<sub>2</sub>), cathepsin B from human liver (≥ 2000 units/mg), monoclonal anti-EGFR antibody produced in mouse clone 29.1 and FITC-dextran (MW 40,000 g/mol) (FD40) were obtained from Sigma (UK) and used as received. Amino acids for the solid phase synthesis were supplied by Bachem. Trityl chloride, 1,8-diazabicyclo[5.4.0]undec-7-ene (DBU), *N,N*-diisopropylethylamine (DiPEA), 1-Hydroxy-7-azabenzotriazole (HOAt), *N*-(3-dimethylaminopropyl)-*N'*-ethylcarbodiimide hydrochloride (EDC·HCl) and *N*-hydroxysuccinimide (NHS) were purchased from Aldrich (USA). Ethylene diaminetetraacetic acid (EDTA), reduced *L*-glutathione (GT) and acridine orange hydrochloride hydrate (AO) were purchased from Sigma-Aldrich (The Netherlands). Alexa Fluor<sup>®</sup> 488 labeled F(ab')<sub>2</sub> fragment (F(ab')<sub>2</sub>A) of goat anti-mouse IgG was supplied by Invitrogen (The Netherlands). Deionized water (DI water) was obtained from a Milli-Q water purification system (Millipore, France) and phosphate buffered saline (PBS, 0.01M, pH 7.4, containing 0.02 wt.% NaN<sub>3</sub>, B. Braun, USA) was used for the cell study. Dulbecco's Modified Eagle Medium (DMEM, Invitrogen, The Netherlands), Foetal Bovine Serum (FCS, Invitrogen, The Netherlands) and Penicillin-Streptomycin (PS, Invitrogen, The Netherlands) were used to prepare the medium for SKBR3 cells. All other reagents used in the study were of analytical grade.

### *Synthesis of mPEG-peptide conjugate*

mPEG-peptide conjugate was prepared by coupling of pentapeptide, FGLFG, to mPEG-NH<sub>2</sub>. The peptide was prepared by solid phase synthesis according to the Merrifield protocol [25, 26] on chlorotriyl resin prior to the coupling reaction with mPEG-NH<sub>2</sub>. In brief, glycol methyl ester was protected by a trityl group (Trt) using 1.2 eq. of trityl chloride and 1.5 eq. of DBU in dichloromethane (DCM). The reaction was almost quantitative and the product was purified by flash column chromatography. Under basic conditions, the methyl ester was hydrolyzed, giving trityl glycolic acid in almost quantitative yield. The trityl glycolic acid was linked to the peptide

Phe-Gly-Leu-Phe-Gly as the last coupling step during the solid phase synthesis of the peptide. After the cleavage, trityl-glycolyl-peptide was recovered by precipitation. The reactions were followed by TLC and HPLC (HP 1090 Liquid Chromatography, Hewlett Packard, USA). Analytical HPLC was performed using a reversed-phase column (C18, particle size 5  $\mu\text{m}$ , 150  $\times$  4.6 mm internal diameter) at 40  $^{\circ}\text{C}$ . UV detection was carried out at 220 nm using a UV-VIS linear spectrometer (Spectra System UV 2000, Spectra Physics, Germany). The flow was 1 ml/min from 0-25.1 min and 2 ml/min from 25.2-29.8 min, after which the flow was reduced to 1 ml/min again until the end (30 min) of the chromatographic procedure. The injection volume of the samples was 20  $\mu\text{l}$ . The structure and the purity of the compounds were assessed by  $^1\text{H-NMR}$  (300 MHz, Bucher NMR spectrometer, USA). Trityl-glycolyl-peptide (2) was coupled to mPEG-NH<sub>2</sub> (1) in acetonitrile at 0  $^{\circ}\text{C}$  in a 3-fold excess with EDC·HCl, HOAt and DiPEA as coupling reagents (Fig. 6.3). The product (3) was purified by precipitation of the non-reacted peptide in diethyl ether and methyl tert butyl ether. Finally, the trityl protecting group was removed under acidic conditions, yielding mPEG-Phe-Gly-Leu-Phe-Gly (4). To confirm the complete cleavage of the trityl groups, the final deprotection in acetic acid was repeated again with an aliquot of the final compound and followed by analytic HPLC. The chemical structure of the final compound and the enantiomeric composition were analyzed by  $^1\text{H-NMR}$ .

#### *Synthesis of block copolymers*

mPEG-pep-PDLLA (5) or PEG-PDLLA was synthesized by ring-opening polymerization (ROP) using mPEG-peptide (4) or PEG (mPEG or cPEG) as an initiator. Functionalized PEG (0.50 g, 0.1 mmol), DLLA (4.2 g, 29.2 mmol), Sn(Oct)<sub>2</sub> (0.04 g, 0.1 mmol) and toluene (30.0 ml) were charged in that order in a reaction vessel. The reaction was performed at 110  $^{\circ}\text{C}$  for 26 h under stirring. After cooling, a drop of HCl (37 wt.%) was added to the reaction mixture to hydrolyze the tin-oxygen bond. The copolymer was isolated by precipitation in methanol. After filtration and washing with methanol, the copolymer was dissolved in DCM and precipitated in diethyl ether. Subsequently, the polymer was isolated by filtration, washed several times with diethyl ether, and dried under vacuum. The monomer conversion and the number average molecular weight ( $M_n$ ) of the block copolymers were determined by  $^1\text{H-NMR}$  (Inova 300 MHz, Varian, USA).

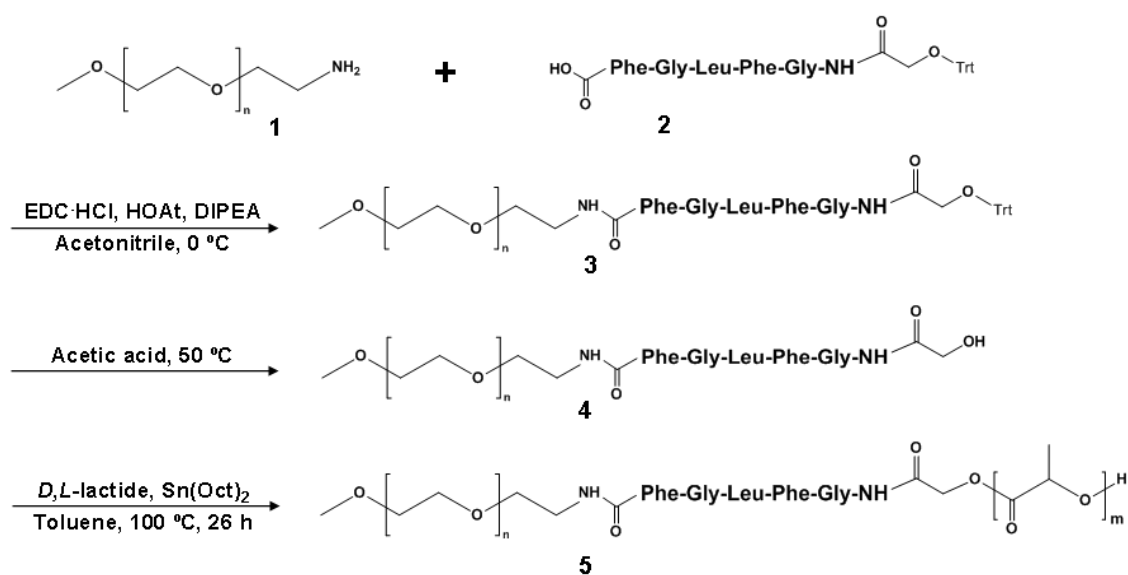


Figure 6.3. Synthesis of mPEG-peptide conjugate and mPEG-pep-PDLLA by ring-opening polymerization of *D,L*-lactide from the mPEG-peptide conjugate. mPEG-NH<sub>2</sub> (1), trityl-glycolyl-peptide (2), trityl-glycolyl-peptide-mPEG (3), mPEG-Phe-Gly-Leu-Phe-Gly (4) and mPEG-pep-PDLLA (5).

#### *Preparation of Ps (pep) and enzymatic degradation*

Ps (pep) were prepared by using mPEG-pep-PDLLA. The amphiphilic block copolymer (10 mg/ml) was dissolved in THF (1 ml), and the THF solution was injected into an aqueous phase (50 ml) [27]. After 15 min without shaking, the vial containing the mixture was turned upside down several times, resulting in a turbid dispersion. To remove the organic solvent from the solution, the Ps dispersion was transferred into a dialysis bag (cut-off 50,000 g/mol, Spectra/Por, CA), which was placed in a 4 l beaker filled with DI water. TEM (Philips CM30, Hillsboro, USA) was performed to elucidate the morphology and membrane thickness of Ps. A dispersion of Ps (2  $\mu$ l) was placed on a 200 mesh carbon grid without using a staining agent. The excess solution was removed and the sample was dried at room temperature.

The enzymatic degradation of Ps (pep) was performed using conditions previously reported [28, 29]. In brief, EDTA (1 mM) and GT (5 mM) were dissolved in a citrate phosphate buffer solution (pH 5.5, 0.05 M). The solution (100  $\mu$ l) was added into a dispersion of Ps (pep) (350  $\mu$ l). Different amounts of Cath B (0, 5, 10 and 20 units/ml) in 50  $\mu$ l of the buffer solution were applied to the solution and the resulting solutions were incubated at 37 °C. Kilo counts per second (Kcps) and size distribution of Ps (pep) in the dispersions were monitored by DLS

(Zetasizer Nano ZS, Malvern Instruments, Malvern) for a week. Ps (pep) dispersions with the same concentration of EDTA and GT were incubated with 5 units/ml of Cath B in PBS (pH 7.4) and also monitored by DLS as a control.

#### *Loading of AO into Ps and release of AO*

AO-Ps (pep) were prepared by injecting a THF solution (1 ml) of mPEG-pep-PDLLA (10 mg/ml) and AO (25 mg) into DI water (50 ml). In order to determine the amount of loaded AO, AO-Ps (pep) were solubilized using Triton X-100 [30]. After adding Triton X-100 to the AO-Ps (pep) dispersion with a final concentration of 2 wt.%, the mixture was heated for 3 h at 80 °C. The release of AO from Ps in the presence of Cath B was compared with that without Cath B. For the release experiment, a citrate phosphate buffer solution of EDTA and GT was added to dispersions of AO-Ps (pep), yielding a concentration of EDTA and GT of 0.1 mM and 0.5 mM, respectively. The samples (1 ml) with or without Cath B (10 units/ml) were placed in a microdialysis system (cut-off 20,000 g/mol) into a large vial containing a carbonate buffer solution and were monitored by periodic withdrawals of samples. The experiments were carried out in triplicate. The loading amount of AO and concentrations of released AO were determined by fluorescence spectroscopy (Safire<sup>2</sup>, Tecan, CA) at an emission wavelength of 525 nm and an excitation wavelength of 502 nm. The Kcps of the samples, which were used for the release experiments, were also measured by DLS.

#### *Immobilization of F(ab')<sub>2</sub>A or anti-EGFR antibody onto Ps (pep)*

For immobilization of the antibody or the F(ab')<sub>2</sub>A fragment, Ps (pep) were prepared by using a mixture of mPEG-pep-PDLLA and cPEG-PDLLA in 50:50 (w/w). F(ab')<sub>2</sub>A was coupled to the carboxyl groups of Ps (pep) by EDC/NHS chemistry. Briefly, 0.5 ml of Ps dispersion was mixed with MES buffer solution (0.5 ml, pH 6.0). EDC·HCl (0.015 mg) and NHS (0.012 mg) were added to the solution in that order and incubated for 30 min. F(ab')<sub>2</sub>A (0.3 mg/ml) was applied to the activated Ps (pep) dispersion and the mixture was titrated to pH 8.5. The reaction was performed for 2 h under mild stirring, yielding F(ab')<sub>2</sub>A-Ps (pep). abEGFR (1.1 mg/ml) was immobilized onto Ps (pep) using the same method as used for F(ab')<sub>2</sub>A, but FD40 was encapsulated prior to the coupling during the formation of Ps (pep) by dispersing FD40 (1.0 mg/ml) in THF especially for the CLSM study. The resulting dispersions of F(ab')<sub>2</sub>A-conjugated

Ps (pep), (F(ab')<sub>2</sub>A-Ps (pep)) or FD40-containing Ps (pep) modified with abEGFR (FD40/abEGFR-Ps (pep)) were purified by using a Sepharose 6B column twice with PBS as an eluent. The amounts of immobilized F(ab')<sub>2</sub>A and abEGFR were quantified by fluorescence spectroscopy and using a Nanodrop<sup>®</sup> spectrophotometer (ND-1000, Isogen Life Science), respectively. Size and PDI of F(ab')<sub>2</sub>A-Ps (pep) as well as FD40/abEGFR-Ps (pep) were measured by DLS and compared to Ps (pep).

#### *Antibody-binding assay of F(ab')<sub>2</sub>A-Ps (pep) on SKBR3 cells*

The binding affinity of F(ab')<sub>2</sub>A-Ps (pep) was evaluated by using SKBR3 cells incubated with mouse antibody. SKBR3 cells were seeded in 8-well homemade thin-glass-bottomed cuvettes at a density of  $2 \times 10^4$  cells/well and cultured at 37 °C in a humidified atmosphere with 5% CO<sub>2</sub> for 2 d. SKBR3 cells were first treated with mouse antibody and then fixed with a formaldehyde solution (4 wt.%) before adding F(ab')<sub>2</sub>A-Ps (pep). After 1 h, a dispersion of F(ab')<sub>2</sub>A-Ps (pep) (200 µl) was added to the cells and incubated for 72 h. All samples were washed a few times with PBS and imaged by fluorescence microscopy (ECLIPSE TE2000-U, Nikon). For the positive control, free F(ab')<sub>2</sub>A was applied to SKBR3 cells treated with a mouse antibody. For the negative control, SKBR3 cells were first treated with a goat antibody before F(ab')<sub>2</sub>A-Ps (pep) was added.

#### *Antibody-mediated endocytosis and intracellular model drug release using SKBR3 cells*

For this study, FD40/abEGFR-Ps (pep) and three control Ps were applied. The controls were FD40-Ps (pep) without abEGFR and FD40/abEGFR-Ps without the peptide sequence but with antibody in order to evaluate the effect of abEGFR or the peptide moiety on the endocytosis and model drug release. FD40-Ps, which does not contain either the abEGFR or the peptide sequence, was used as the negative control. For coupling of abEGFR, cPEG-PDLLA was mixed with mPEG-PDLLA or mPEG-pep-PDLLA in a weight ratio of 50:50. To introduce a comparable amount of peptide into FD40/abEGFR-Ps (pep), 50 wt.% of mPEG-PDLLA was used for the preparation of FD40-Ps (pep). The compositions of the block copolymers used for the four types of Ps are listed in Table 6.1. SKBR3 cells were seeded in 8-well homemade thin-glass-bottomed cuvettes at a density of  $2 \times 10^4$  cells/well and cultured at 37 °C in a humidified atmosphere with 5% CO<sub>2</sub> for 2 d. The cell medium was removed and 200 µl of fresh cell medium was added. Ps



(pep) or Ps containing FD40 either conjugated with abEGFR (200  $\mu$ l) or not was added to the medium. As a reference, 200  $\mu$ l of pure PBS was added to the medium. The cells were incubated for 3 d and fixed with a formaldehyde solution (4 wt.%) to be applied for CLSM.

Table 6.1. Compositions of the block copolymers used for preparation of Ps for the CLSM study

	Block copolymer compositions	abEGFR	FD40
FD40-Ps	mPEG-PDLLA	no	yes
FD40-Ps (pep) <sup>a</sup>	mPEG-pep-PDLLA + mPEG-PDLLA	no	yes
FD40/abEGFR-Ps <sup>a, b</sup>	mPEG-PDLLA + cPEG-PDLLA	yes	yes
FD40/abEGFR-Ps (pep) <sup>a, b</sup>	mPEG-pep-PDLLA + cPEG-PDLLA	yes	yes

<sup>a</sup> Block copolymers are dissolved in a weight ratio of 50:50 in THF with FD40 and the THF solution was injected into water.

<sup>b</sup> After the formation of Ps, abEGFR was coupled onto the cPEG of Ps.

## Results and discussion

### *Characterization of block copolymers*

mPEG-PDLLA or mPEG-pep-PDLLA was synthesized by ROP using mPEG or mPEG-peptide as an initiator. FGLFG was prepared by solid phase synthesis and conjugated with mPEG-NH<sub>2</sub> prior to the ROP reaction. The yield of mPEG-peptide conjugate after coupling of mPEG-NH<sub>2</sub> with the peptide and deprotection was 86 %. The conjugate contained 90 % of *L*-Phe and 10 % of *D*-Phe units. The starting peptide was enantiopure, but racemization occurred during coupling of the peptide with mPEG-NH<sub>2</sub> due to the C-terminal pegylation chemistry. The chemical structure of mPEG-pep-PDLLA was assessed by <sup>1</sup>H-NMR. The CH<sub>2</sub> peaks of PEG at 3.6 ppm and the methoxy groups at 3.3 ppm were found (Fig. 6.2a). The peaks of the isopropyl side chain of Leu appeared at 1.3 ppm (-CH<sub>2</sub>CH(CH<sub>3</sub>)<sub>2</sub>) and 1.7 ppm (-CH<sub>2</sub>CH(CH<sub>3</sub>)<sub>2</sub>) when FGLFG was conjugated to mPEG (Fig. 6.2b). The proton peaks of PDLLA blocks were observed at 5.2 ppm (-CH-) and 1.6 ppm (-CH<sub>3</sub>) (Fig. 6.2c). As determined by <sup>1</sup>H-NMR, the MW of the block copolymers was about 42,000 g/mol for PEG-PDLLA and 43,000 g/mol for mPEG-pep-PDLLA and the monomer conversions were more than 98 %. (Table 6.2). The hydrophilic volume fraction of PEG ( $f_{PEG}$ ) of the block copolymers ranged between 11.3 to 11.8 %, which is in the range required to form vesicles. It is known that block copolymers with a  $f_{PEG}$  between 10

and 40 % and a MW ranging from ~2700 to 50,000 g/mol are suitable for formation of nanovesicles [16, 27, 31, 32].

Table 6.2. Characterization of synthetic block copolymers

	Monomer conversion <sup>a</sup> (%)	Mn of PDLLA (theor.) <sup>b</sup> (g/mol)	Mn of PDLLA ( <sup>1</sup> H-NMR) <sup>c</sup> (g/mol)	$f_{PEG}^d$ (%)
mPEG <sub>5k</sub> -pep-PDLLA	99	42,000	43,000	11.3
mPEG <sub>5k</sub> -PDLLA	98	42,000	41,700	11.8
cPEG <sub>5k</sub> -PDLLA	99	42,000	42,200	11.7

<sup>a</sup> Determined by <sup>1</sup>H NMR.

<sup>b</sup> Calculated from the initial ratio of monomer to PEG hydroxyl groups.

<sup>c</sup> Determined from <sup>1</sup>H-NMR analysis by calculating the ratio of the PEG methylene peak to the main peak of the polyester.

<sup>d</sup> Calculated volume fraction of PEG in block copolymers.

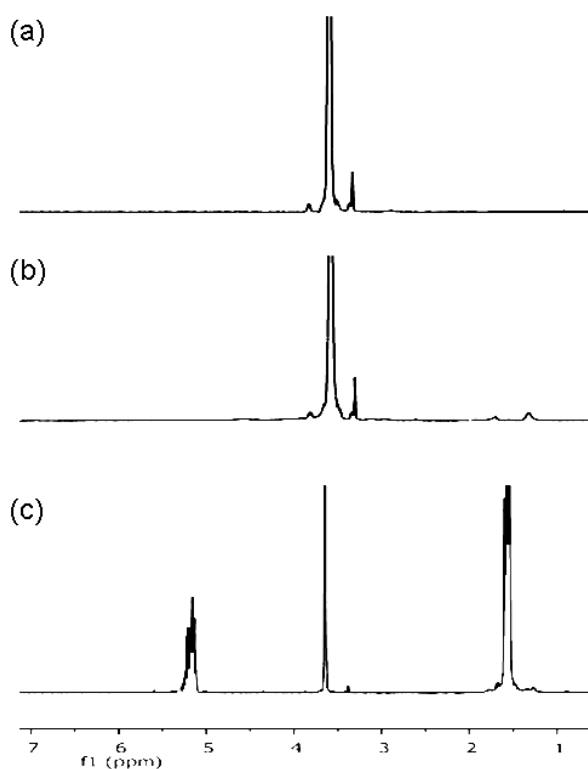


Figure 6.4. <sup>1</sup>H-NMR spectra of mPEG (a), mPEG-peptide (b) and mPEG-pep-PDLLA (c).

*Size and morphology of Ps (pep) and aggregation triggered by enzymatic activity*

Ps (pep) were prepared by injecting a polymer solution of THF into DI water. It has been reported that nano-sized Ps can be prepared using amphiphilic block copolymers with a relatively low  $f_{PEG}$  (10 ~ 20 %) by injecting the polymer-containing organic solvent into an aqueous phase [2, 33, 34]. Ps (pep) with an average diameter about 124 nm were obtained with a narrow size distribution (Table 6.3). Fig. 6.3 shows a TEM image of Ps (pep) and it can be seen that they are spherical nanovesicles with a membrane thickness of about 15 nm.

The Kcps of a Ps (pep) dispersion as a function of the concentration of Cath B at pH 5.5 and 7.4 was measured by DLS to investigate possible enzymatic degradation of the peptide sequence, resulting in destabilization of the Ps. Fig. 6.6a compares the Kcps in time of Ps (pep) dispersions under different conditions. Ps (pep) showed a gradual decrease in Kcps over 7 d when incubated with 5 units/ml of Cath B at pH 5.5 at 37 °C. The decrease in Kcps can be explained by the formation of precipitates after enzymatic cleavage of the peptide linker in the Ps (pep). Upon cleavage of the linker, PEG chains that are linked to PDLLA by the peptide linker will be dissociated from Ps (pep), which will disturb the hydrophilic/hydrophobic balance in the bi-layer membranes. Eventually, this may lead to the formation of aggregates and precipitates. The size distribution of Ps (pep) became bimodal in time, which can be expected when aggregates are formed (Fig. 6.6b). The enzymatic degradation was complete after one week and no Ps (pep) were detected by DLS. When more Cath B was applied the decrease of Kcps in time was faster, resulting in a rate of precipitation proportional to the concentration of Cath B. This result strongly suggests that the peptide linkers in the membrane of Ps (pep) are quite accessible to Cath B and that the interaction of Cath B with the peptide linkers is most probably membrane associated. In nature, Cath B is mainly found as a membrane-associated protein both in endosomes and cell membranes [35, 36].

As well known for the activity of enzymes, each enzyme has an optimal pH, at which the enzymatic activity is maximal. Cath B, one of the lysosomal enzymes, shows the highest activity at a pH between 5 and 6 [37-39]. This agrees with the finding that the activity of Cath B was very low at pH 7.4 and that the Kcps of Ps (pep) in the dispersion did not change after the incubation with 5 units/ml of Cath B for a week. This leads to the conclusion that Ps (pep) will not be enzymatically degraded in the circulation, which is in accordance with a report that this peptide sequence when used in drug conjugates is also stable in the circulation [40]. The

degradation of Ps (pep) was dependent on the concentration of Cath B. These Ps are interesting for cancer chemotherapy applications because of the tumor-specific distribution and activity of Cath B. The Kcps of a suspension of Ps (pep) without Cath B did not significantly change during a week indicating that normal hydrolysis of PDLLA blocks in Ps (pep) was very slow and did not influence the results.

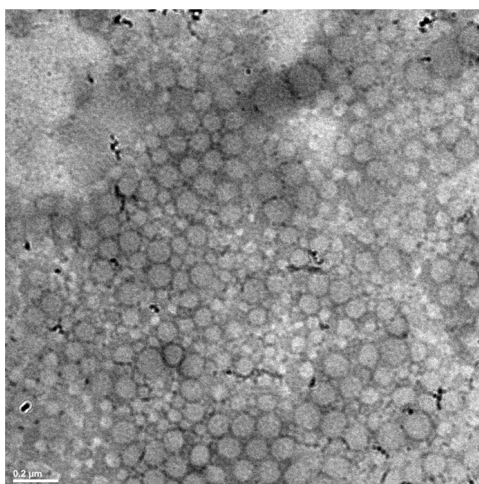


Figure 6.5. TEM images of Ps (pep) on a carbon grid. A dispersion of Ps (pep) was placed on a 200 mesh normal carbon grid without using a staining agent and dried at room temperature. Size bar represents 200 nm.

#### *Release of acridine orange from Ps (pep)*

AO release from Ps (pep) was investigated in the presence of Cath B (10 units/ml) and without Cath B. In order to correlate the release kinetics with enzymatic degradation of Ps (pep), the release of AO as well as the Kcps of AO-Ps (pep) was monitored at 37 °C at pH 5.5 for a week. In Fig. 6.7, the colloidal stability of AO-Ps (pep) and corresponding AO release in the presence of Cath B is compared with the same parameters in the absence of Cath B. At pH 5.5, AO is mostly cationically charged and in general charged molecules can not cross the membrane of Ps [41, 42]. However, about 40 % of AO was released from AO-Ps (pep) during 3 d at pH 5.5 and then the release discontinued (Fig. 6.7b). A possible explanation is that some fraction of AO was incorporated in the Ps membrane during the loading process and that this fraction of AO was released during the experiment. In this case, the release is mainly dependent on the concentration gradient of the dye between the membrane of Ps (pep) and surrounding media approaching a linear release as a function of  $\sqrt{t}$  ( $R^2 = 0.93$ ).

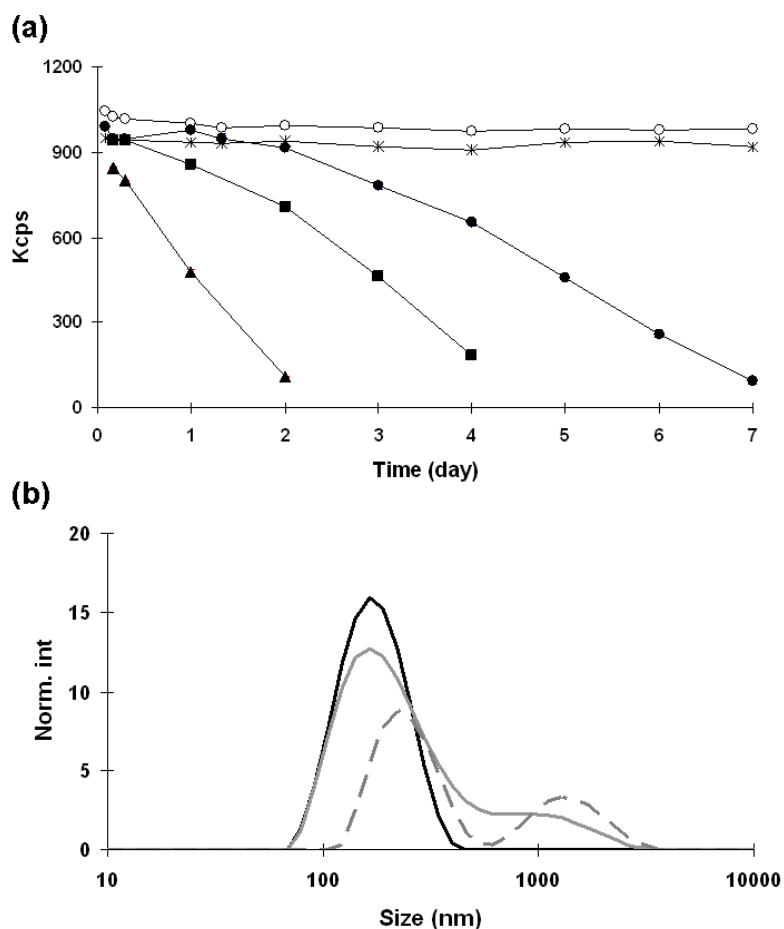


Figure 6.6. Kinetics of enzymatic degradation of Ps measured by DLS. (a) Kcps of a Ps (pep) dispersion as a function of time at different concentrations of Cath B at pH 5.5 and 7.4 at 37 °C. At pH 5.5: 0 unit/ml (○), 5 units/ml (●), 10 units/ml (■) and 20 units/ml (▲), at pH 7.4, 5 units/ml (\*) of Cath B was added into a dispersion of Ps and incubated at 37 °C. (b) The size distribution of Ps (pep) was measured at day 1 (black solid line), 4 (gray solid line) and 7 (gray dashed line) at a Cath B concentration of 5 units/ml. DLS measurements were performed 30 times per sample and the data given are mean values.

As may be expected in the presence of Cath B, AO was released relatively fast. The release of AO from Ps (pep) with Cath B was completed in 3 d (Fig. 6.7b) and it is clear that the release was associated with the degradation of Ps (pep) (Fig. 6.7a). AO-Ps (pep) were completely precipitated after 3 d. Disintegration of the membrane of AO-Ps (pep) took place due to the cleavage of peptide linkers leading to rapid and complete release of AO during the period. Interestingly, in the presence of Cath B, the shape of the release profile seems linear. This may

be explained by the fact that AO release from Ps (pep) is not only governed by diffusion of AO from the Ps membrane, but will also be affected by the disruption of the membrane and subsequent aggregation of the Ps. The rate of the diffusion decreases as the concentration of the dye incorporated in the membrane of the Ps (pep) decreases in time. In parallel, encapsulated dye in the aqueous core of the Ps (pep) will be also released as the membrane of the Ps (pep) is disrupted. Without Cath B, Ps (pep) were stable during the experimental period, showing a gradual decrease in release rate of AO.

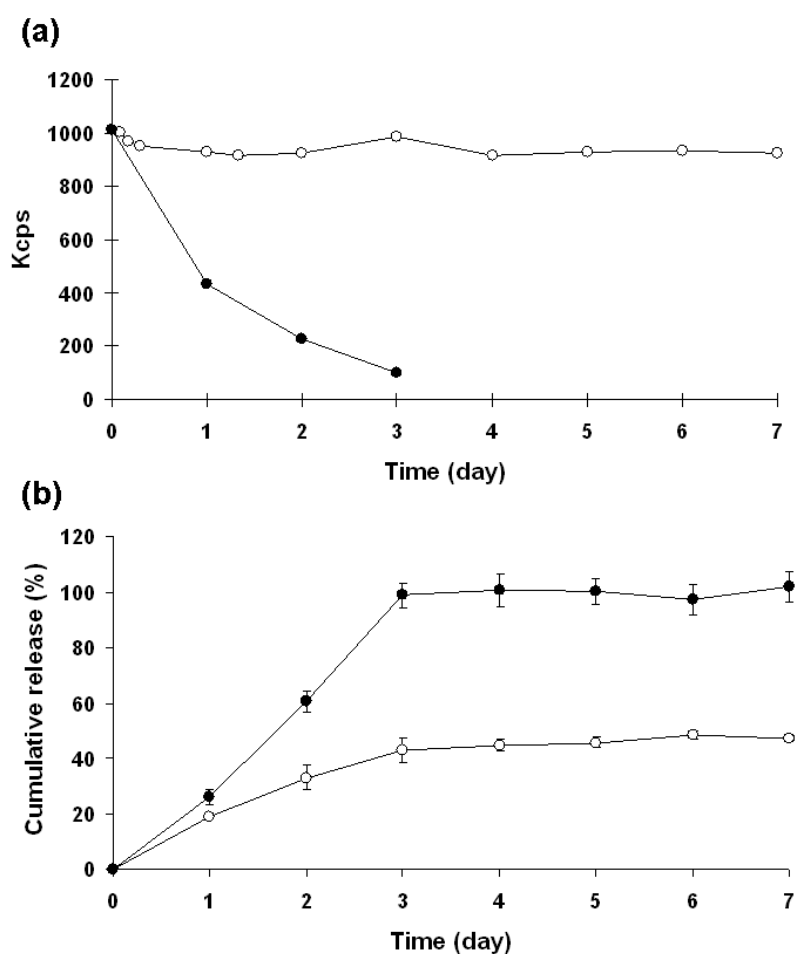


Figure 6.7. Stability of AO-Ps (pep) and AO release at 37 °C at pH 5.5. (a)  $K_{cps}$  of AO-Ps (pep) incubated with (●) (10 units/ml) or without (○) Cath B was determined by DLS. (b) AO was released from Ps in the presence (●) (10 units/ml) and the absence (○) of Cath B and measured by fluorescence spectroscopy. At different time intervals 1 ml of the release medium was collected and analyzed. The experiments were carried out in triplicate. The data given are mean values and the error bars are the standard deviations of the mean.

*Immobilization of F(ab')<sub>2</sub>-A488 or anti-EGFR antibody onto Ps (pep)*

Amine groups of F(ab')<sub>2</sub>A were used for the coupling with carboxyl groups on Ps (pep) using EDC/NHS. The coupling efficiency was about 23.3 % based on carboxyl groups on the external surface of the Ps and the amount of coupled F(ab')<sub>2</sub>A was 0.01 mg/mg (per mg of total block copolymer) after the appropriate purification. The size of Ps (pep) was slightly increased with about 5 nm due to the presence of F(ab')<sub>2</sub>A on the surface. The size of free F(ab')<sub>2</sub>A in PBS also measured by DLS was about 8 nm. To prepare FD40/abEGFR-Ps (pep), encapsulation of FD40 into Ps (pep) was performed followed by coupling of abEGFR. The amount of immobilized abEGFR was 0.05 mg/mg total block copolymer and 21.7 % of external surface carboxyl groups of the Ps (pep) was modified with abEGFR. An increment of about 30 nm in the diameter for FD40/abEGFR-Ps (pep) upon loading of FD40 and coupling of abEGFR was observed as compared to bare Ps (pep).

Table 6.3. Average diameters and PDI of Ps (pep) and modified Ps (pep)

	Ps (pep)	F(ab') <sub>2</sub> A-Ps (pep)	FD40/abEGFR-Ps (pep)
Diameter <sup>a</sup> (nm)	124.1	129.2	162.6
PDI <sup>b</sup>	0.11	0.11	0.14

<sup>a</sup> Measurements were performed 30 times and averaged.

<sup>b</sup> Polydispersity index.

*Antigen-binding affinity of F(ab')<sub>2</sub>A-Ps (pep)*

Alexa Fluor<sup>®</sup> 488 labeled F(ab')<sub>2</sub> fragment of goat anti-mouse IgG was immobilized onto Ps (pep) and incubated with SKBR3 cells for fluorescence microscopy. The SKBR3 cells were treated with goat antibody or mouse antibody and the cell membranes treated with the antibodies were fixed prior to the experiments. As shown in Fig. 6.8c, the cell membranes were fluorescent when modified with mouse antibody and incubated with F(ab')<sub>2</sub>A-Ps (pep). F(ab')<sub>2</sub>A was still showing the mouse-specific binding affinity when bound onto Ps (pep). F(ab')<sub>2</sub>A-Ps (pep) were not attached to cell membranes that were modified with goat antibody (Fig. 6.8e), which demonstrates that binding of F(ab')<sub>2</sub>A-Ps (pep) on mouse antibody-modified cells was not caused by any other nonspecific interaction. However, the binding efficiency of F(ab')<sub>2</sub>A-Ps (pep) onto the cells was lower than that of free F(ab')<sub>2</sub>A, which was incubated with the cells at

the same concentration as the immobilized  $F(ab')_2A$  (Fig. 6.8a). The lower affinity of  $F(ab')_2A$ -Ps (pep) indicates that the presence of Ps (pep) may influence the conformation of the  $F(ab')_2A$  fragments or that the receptors on the cells cannot be reached as easily due to the presence of the Ps (pep). Maruyama *et al.* reported that binding of an antibody to the antigen-binding site of target cells could be sterically hindered by its immobilization on polymeric carriers [43].

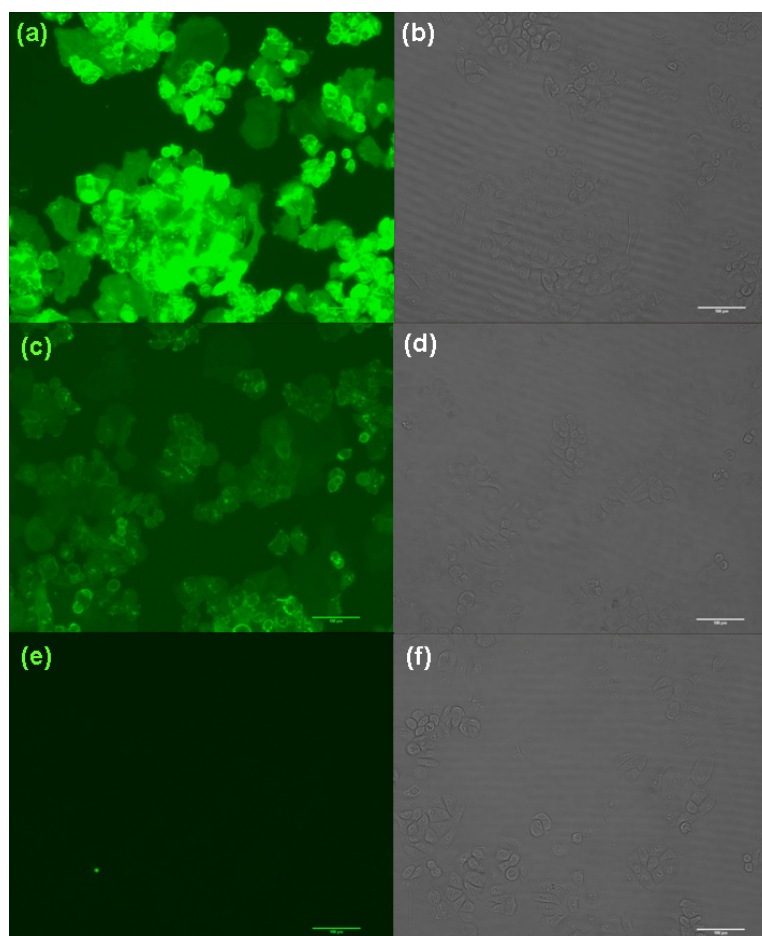


Figure 6.8. Fluorescence microscopic images of SKBR3 cells after 3 d incubation with  $F(ab')_2A$ -Ps (pep) at 37 °C. Fluorescence images (a, c and e) and bright images (b, d and f) from the same area of each sample are represented. Cells were incubated with mouse antibody (a-d) or goat antibody (e and f) prior to adding a PBS solution of free  $F(ab')_2A$  (a and b) or a dispersion of  $F(ab')_2A$ -Ps (pep) (c-f).  $F(ab')_2A$  immobilized on Ps (pep) was specifically bound to mouse antibodies on SKBR3 cells. Size bars represents 100  $\mu$ m.

#### *Enhanced cellular uptake of Ps and intracellular drug release*

In order to evaluate the effect of abEGFR on the endocytic uptake of Ps (pep), FD40-Ps (pep) with and without abEGFR were compared. FD40-Ps with or without antibody were also applied



to evaluate the effect of the presence of peptide linkers in the Ps on intracellular release of FD40. Fig. 6.9 represents fluorescence images, bright images and the combined images from each experiment. After 3 d exposure, abEGFR conjugated FD40-Ps were bound to the membranes of SKBR3 cells and incorporated in the cells, showing an enhanced endocytosis as compared to FD40-Ps (Figs. 6.9f and 6.9i). The enhanced endocytic uptake of FD40-Ps (L) can be explained by the antibody-mediated endocytosis generated by anchoring of the anti-EGFR antibody to EGF receptors on SKBR3 cell membranes. FD40-Ps without abEGFR were also internalized in SKBR3 cells, but at a slower rate. The slow endocytosis of FD40-Ps may be associated to pynocytic uptakes, “cell drinking”, which is in an agreement with previous reports. Cellular uptake of pegylated carriers (i.e. micelles and Ps) in cancer cells has been reported earlier and it was suggested that the endocytosis mainly occurred via fluid phase endocytosis [22, 44]. Likewise, FD40-Ps has a dense PEG brush probably reducing the interaction with the cell membranes. Fluorescently bright spots near around the nucleus in the cells may demonstrate that internalized FD40-Ps were mainly localized in lysosomal compartments of the cells. However, release of FD40 from the lysosomes was not observed during the experimental period.

The effect of the peptide linker in the Ps on the release of FD40 was very clear in the CLSM results. In Figs. 6.9l and 6.9o, it can be seen that intracellular release of FD40 in several cells took place after 3 d. When Ps (pep) were taken up by the cells either via fluid state or antibody-mediated endocytosis, the FGLFG linker in the membrane of Ps (pep) could be cleaved by lysosomal enzymes like Cath B. Disintegration of Ps (pep) may induce a burst release of FD40 into the cells, which was also seen by the release of AO from Ps (pep) in the presence of Cath B. An enhanced cellular uptake of FD40/abEGFR-Ps (pep) as compared to FD40-Ps (pep) was observed again, indicating that the presence of both abEGFR and peptide linker in the membrane had a synergistic effect on the intracellular delivery of FD40. Based on these results we suggest that Ps, which are equipped with a peptide linker in the membrane and an appropriate antibody to recognize tumor cells will be more effective for the delivery of cytostatic drugs in tumor cells than the corresponding Ps without a peptide linker and antibody. Notably, free FD40 in PBS was also incubated with SKBR3 cells under the same conditions, but the uptake after 3 d was negligible (data not shown). The intensity of the argon laser and measurement parameters for all CLSM pictures were kept the same. Auto-fluorescence caused by the blank cells was minimal (Fig. 6.9c).

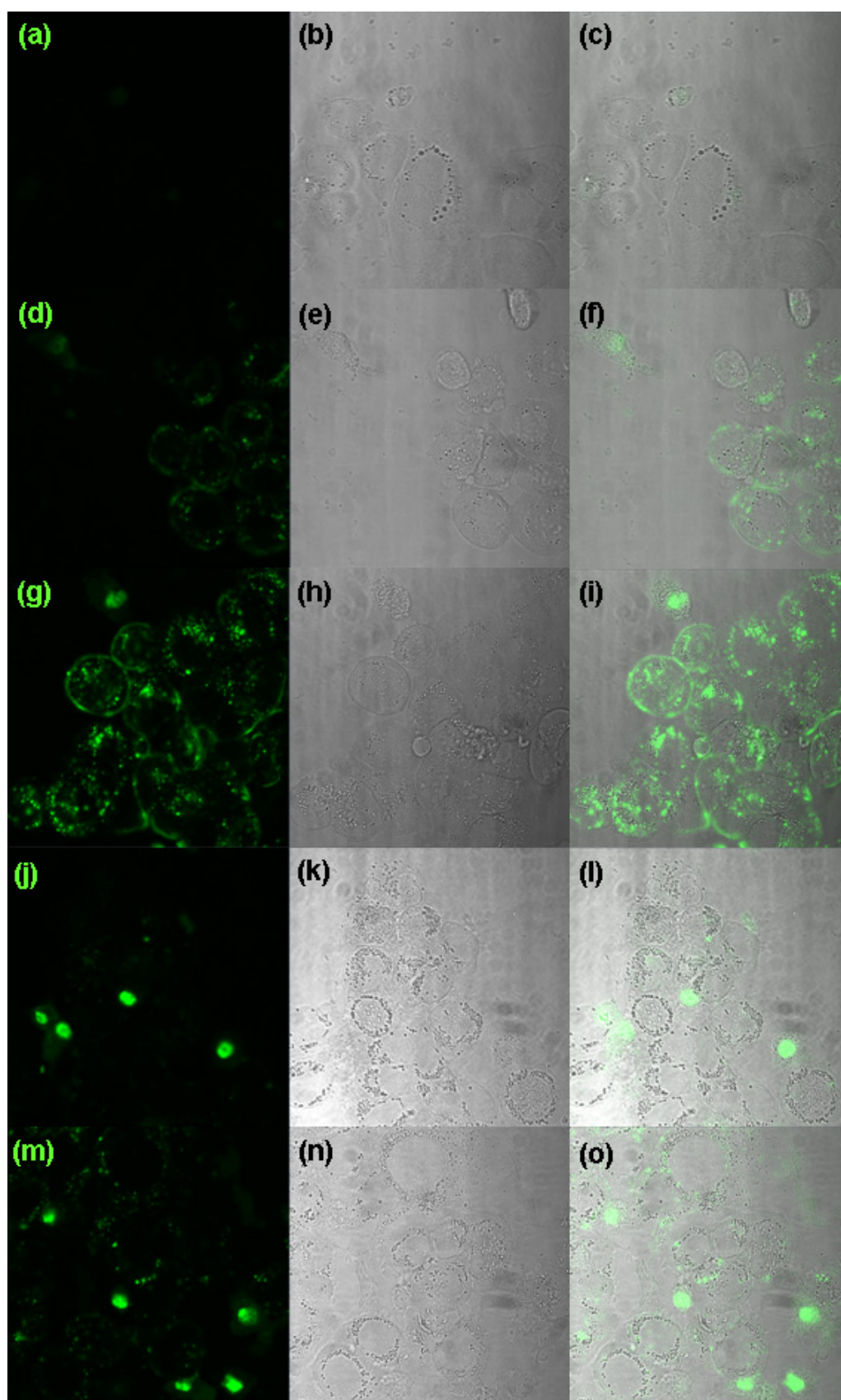


Figure 6.9. CLSM images of SKBR3 cells after 3 d exposure with Ps. Blank cells (a-c) were compared with cells incubated with FD40-Ps (d-f), FD40/abEGFR-Ps (g-i), FD40-Ps (pep) (j-l) and FD40/abEGFR-Ps (pep) (m-o). Fluorescence images of the cells are represented in the left column (a, d, g, j and m) and the bright images are shown in the middle (b, e, h, k and n). Combined images for fluorescence and bright images are represented in the right column (c, f, i, l and o). abEGFR conjugated Ps showed enhanced endocytosis mediated by the antibody bound on SKBR3 cells. Release of FD40 in SKBR3 cells was observed when Ps (pep) was applied.

## **Conclusions**

Novel polymersomes based on block copolymers of PEG and poly(*D,L*-lactide) with a peptide linker (Phe-Gly-Leu-Phe-Gly) between the PEG and poly(*D,L*-lactide) blocks, Ps (pep) were developed. This new carrier system showed relatively fast enzymatic destabilization at pH 5.5 in the presence of the lysosomal enzyme, cathepsin B (Cath B). A rapid release of the model drug acridine orange from the polymersomes was observed in the presence of cathepsin B at pH 5.5. Endocytosis of these polymersomes by SKBR3 cells was enhanced after conjugating anti-epidermal growth factor receptor antibody (abEGFR) on the surface of the polymersomes. Fluorescein isothiocyanate labeled dextran with a molecular weight of 40,000 g/mol was released from Ps (pep) inside the SKBR3 cells as a result of disintegration of the polymersomes in the lysosomal compartments. From these results, we conclude that peptide-containing polymersomes, which are modified with abEGFR, are extremely promising as systemic tumor targeting drug delivery systems because it is known that Cath B as well as the EGF receptor is over expressed in various tumors.

**References**

- [1] M. Antonietti, S. Forster, Vesicles and liposomes: A self-assembly principle beyond lipids. *Adv. Mater.* 15(16) (2003) 1323-1333.
- [2] F.H. Meng, Z.Y. Zhong, J. Feijen, Stimuli-Responsive Polymersomes for Programmed Drug Delivery. *Biomacromolecules* 10(2) (2009) 197-209.
- [3] W. Chen, F.H. Meng, R. Cheng, Z.Y. Zhong, pH-Sensitive degradable polymersomes for triggered release of anticancer drugs: A comparative study with micelles. *J. Control. Release* 142(1) (2010) 40-46.
- [4] S.H. Qin, Y. Geng, D.E. Discher, S. Yang, Temperature-controlled assembly and release from polymer vesicles of poly(ethylene oxide)-block-poly(N-isopropylacrylamide). *Adv. Mater.* 18(21) (2006) 2905-2909.
- [5] A. Napoli, M.J. Boerakker, N. Tirelli, R.J.M. Nolte, N.A.J.M. Sommerdijk, J.A. Hubbell, Glucose-oxidase based self-destructing polymeric vesicles. *Langmuir* 20(9) (2004) 3487-3491.
- [6] E. Elliott, B.F. Sloane, The cysteine protease cathepsin B in cancer. *Perspect. Drug Discov. Design* 6 (1996) 12-32.
- [7] B.F. Sloane, S.Q. Yan, I. Podgorski, B.E. Linebaugh, M.L. Cher, J.X. Mai, D. Cavallo-Medved, M. Sameni, J. Dosescu, K. Moin, Cathepsin B and tumor proteolysis: contribution of the tumor microenvironment. *Semin. Cancer Biol.* 15(2) (2005) 149-157.
- [8] S.Q. Yan, M. Sameni, B.F. Sloane, Cathepsin B and human tumor progression. *Biol. Chem.* 379(2) (1998) 113-123.
- [9] M. Hruby, T. Etrych, J. Kucka, M. Forsterova, K. Ulbrich, Hydroxybisphosphonate-containing polymeric drug-delivery systems designed for targeting into bone tissue. *J. Appl. Polym. Sci.* 101(5) (2006) 3192-3201.
- [10] M. Pechar, K. Ulbrich, M. Jelinkova, B. Rihova, Conjugates of antibody-targeted PEG multiblock polymers with doxorubicin in cancer therapy. *Macromol. Biosci.* 3(7) (2003) 364-372.
- [11] R. Satchi, T.A. Connors, R. Duncan, PDEPT: polymer-directed enzyme prodrug therapy I. HPMA copolymer-cathepsin B and PK1 as a model combination. *Br. J. Cancer* 85(7) (2001) 1070-1076.
- [12] R. Satchi-Fainaro, H. Hailu, J.W. Davies, C. Summerford, R. Duncan, PDEPT: Polymer-directed enzyme prodrug therapy. 2. HPMA copolymer-beta-lactamase and HPMA copolymer-C-Dox as a model combination. *Bioconjugate Chem.* 14(4) (2003) 797-804.
- [13] R. Satchi, R. Duncan, PDEPT: Polymer directed enzyme prodrug therapy - in vitro and in vivo characterisation. *Ann. Oncol.* 9 (1998) 83-83.
- [14] R. Satchi, R. Duncan, PDEPT: polymer-directed enzyme prodrug therapy. *Br. J. Cancer* 78(2) (1998) 149-150.
- [15] J. Kopecek, P. Kopeckova, HPMA copolymers: Origins, early developments, present, and future. *Adv. Drug Deliv. Rev.* 62(2) (2010) 122-149.
- [16] F. Ahmed, P.J. Photos, D.E. Discher, Polymersomes as viral capsid mimics. *Drug Dev. Res.* 67(1) (2006) 4-14.
- [17] H. Bermudez, A.K. Brannan, D.A. Hammer, F.S. Bates, D.E. Discher, Molecular weight dependence of polymersome membrane structure, elasticity, and stability. *Macromolecules* 35(21) (2002) 8203-8208.
- [18] D.E. Discher, A. Eisenberg, Polymer vesicles. *Science* 297(5583) (2002) 967-973.

- [19] P.J. Photos, L. Bacakova, B. Discher, F.S. Bates, D.E. Discher, Polymer vesicles in vivo: correlations with PEG molecular weight. *J. Control. Release* 90(3) (2003) 323-334.
- [20] B.M. Discher, D.A. Hammer, F.S. Bates, D.E. Discher, Polymer vesicles in various media. *Curr. Opin. Colloid Interface Sci.* 5(1-2) (2000) 125-131.
- [21] A. VertutDoi, H. Ishiwata, K. Miyajima, Binding and uptake of liposomes containing a poly(ethylene glycol) derivative of cholesterol (stealth liposomes) by the macrophage cell line J774: Influence of PEG content and its molecular weight. *Biochim. Biophys. Acta-Biomembr.* 1278(1) (1996) 19-28.
- [22] O. Soga, C.F. van Nostrum, M. Fens, C.J.F. Rijcken, R.M. Schiffelers, G. Storm, W.E. Hennink, Thermosensitive and biodegradable polymeric micelles for paclitaxel delivery. *J. Control. Release* 103(2) (2005) 341-353.
- [23] R.S. Herbst, D.M. Shin, Monoclonal antibodies to target epidermal growth factor receptor-positive tumors - A new paradigm for cancer therapy. *Cancer* 94(5) (2002) 1593-1611.
- [24] T. Noh, Y.H. Kook, C. Park, H. Youn, H. Kim, E.T. Oh, E.K. Choi, H.J. Park, C. Kim, Block Copolymer Micelles Conjugated with anti-EGFR Antibody for Targeted Delivery of Anticancer Drug. *J. Polym. Sci. Pol. Chem.* 46(22) (2008) 7321-7331.
- [25] A.R. Mitchell, S.B.H. Kent, M. Engelhard, R.B. Merrifield, New Synthetic Route to Tert-Butyloxycarbonylaminoacyl-4-(Oxymethyl)Phenylacetamidomethyl-Resin, an Improved Support for Solid-Phase Peptide-Synthesis. *J. Org. Chem.* 43(14) (1978) 2845-2852.
- [26] S.S. Wang, Merrifield, Rb, Solid Phase-Fragment Approach to Peptide Synthesis - Application of a T-Alkyloxycarbonylhydrazide Resin and a T-Alkyl Alcohol Resin. *Int. J. Pept. Protein Res.* 4(5) (1972) 309-318.
- [27] F.H. Meng, G.H.M. Engbers, J. Feijen, Biodegradable polymersomes as a basis for artificial cells: encapsulation, release and targeting. *J. Control. Release* 101(1-3) (2005) 187-198.
- [28] M. Pechar, J. Strohalm, K. Ulbrich, E. Schacht, Biodegradable drug carriers based on poly(ethylene glycol) block copolymers. *Macromol. Chem. Phys.* 198(4) (1997) 1009-1020.
- [29] P. Rejmanova, J. Kopecek, J. Pohl, M. Baudys, V. Kostka, Polymers Containing Enzymatically Degradable Bonds .8. Degradation of Oligopeptide Sequences in N-(2-Hydroxypropyl)Methacrylamide Co-Polymers by Bovine Spleen Cathepsin-B. *Macromol. Chem. Phys.* 184(10) (1983) 2009-2020.
- [30] V. Pata, F. Ahmed, D.E. Discher, N. Dan, Membrane solubilization by detergent: Resistance conferred by thickness. *Langmuir* 20(10) (2004) 3888-3893.
- [31] J.S. Lee, W. Zhou, F.H. Meng, D.W. Zhang, C. Otto, J. Feijen, Thermosensitive hydrogel-containing polymersomes for controlled drug delivery. *J. Control. Release* 146(3) (2010) 400-408.
- [32] J.C.M. Lee, H. Bermudez, B.M. Discher, M.A. Sheehan, Y.Y. Won, F.S. Bates, D.E. Discher, Preparation, stability, and in vitro performance of vesicles made with diblock copolymers. *Biotechnol. Bioeng.* 73(2) (2001) 135-145.
- [33] C. Nardin, T. Hirt, J. Leukel, W. Meier, Polymerized ABA triblock copolymer vesicles. *Langmuir* 16(3) (2000) 1035-1041.
- [34] H.W. Shen, A. Eisenberg, Block length dependence of morphological phase diagrams of the ternary system of PS-b-PAA/dioxane/H<sub>2</sub>O. *Macromolecules* 33(7) (2000) 2561-2572.
- [35] B.A. Frosch, I. Berquin, M.R. Emmert-Buck, K. Moin, B.F. Sloane, Molecular regulation, membrane association and secretion of tumor cathepsin B. *Apmis* 107(1) (1999) 28-37.

- [36] M. Linke, V. Herzog, K. Brix, Trafficking of lysosomal cathepsin B-green fluorescent protein to the surface of thyroid epithelial cells involves the endosomal/lysosomal compartment. *J. Cell Sci.* 115(24) (2002) 4877-4889.
- [37] I. Giusti, S. D'Ascenzo, D. Millimaggi, G. Taraboletti, G. Carta, N. Franceschini, A. Pavan, V. Dolo, Cathepsin B mediates the pH-dependent proinvasive activity of tumor-shed microvesicles. *Neoplasia* 10(5) (2008) 481-488.
- [38] J.W.J. vanderStappen, A.C. Williams, R.A. Maciewicz, C. Paraskeva, Activation of cathepsin B, secreted by a colorectal cancer cell line requires low pH and is mediated by cathepsin D. *Int. J. Cancer* 67(4) (1996) 547-554.
- [39] G.M. Zhao, G.H. Zhou, Y.L. Wang, X.L. Xu, Y.J. Huan, J.Q. Wu, Time-related changes in cathepsin B and L activities during processing of Jinhua ham as a function of pH, salt and temperature. *Meat Sci.* 70(2) (2005) 381-388.
- [40] J. Kopecek, P. Kopeckova, HPMA copolymers: Origins, early developments, present, and future. *Adv. Drug Deliv. Rev.* 62(2) (2010) 122-149.
- [41] S. Clerc, Y. Barenholz, A quantitative model for using acridine orange as a transmembrane pH gradient probe. *Anal. Biochem.* 259(1) (1998) 104-111.
- [42] M.G. Palmgren, Acridine-Orange as a Probe for Measuring Ph Gradients across Membranes - Mechanism and Limitations. *Anal. Biochem.* 192(2) (1991) 316-321.
- [43] K. Maruyama, T. Takizawa, N. Takahashi, T. Tagawa, K. Nagaike, M. Iwatsuru, Targeting efficiency of PEG-immunoliposome-conjugated antibodies at PEG terminals. *Adv. Drug Deliv. Rev.* 24(2-3) (1997) 235-242.
- [44] F. Ahmed, R.I. Pakunlu, A. Brannan, F. Bates, T. Minko, D.E. Discher, Biodegradable polymersomes loaded with both paclitaxel and doxorubicin permeate and shrink tumors, inducing apoptosis in proportion to accumulated drug. *J. Control. Release* 116(2) (2006) 150-158.

# Chapter 7

## **Circulation Kinetics and Biodistribution of Dual-Labeled Polymersomes with Modulated Surface Charge in Tumor-Bearing Mice: Comparison with Stealth Liposomes\***

Jung Seok Lee<sup>a</sup>, Marc Ankone<sup>a</sup>, Ebel Pieters<sup>b</sup>, Raymond M. Schiffelers<sup>b</sup>, Wim E. Hennink<sup>b</sup>, Jan Feijen<sup>a</sup>

<sup>a</sup> *Department of Polymer Chemistry and Biomaterials, Institute for Biomedical Technology and Technical Medicine, MIRA, Faculty of Science and Technology, University of Twente, Enschede, The Netherlands*

<sup>b</sup> *Department of Pharmaceutics, Utrecht Institute for Pharmaceutical Sciences, Utrecht University, Utrecht, The Netherlands*

---

\* Submitted to Journal of Controlled Release (special issue)



### Abstract

Polymersomes (Ps) based on poly(ethylene glycol)-*b*-poly(*D,L*-lactide) (PEG-PDLLA), with similar sizes (90-100 nm), but different zeta potentials (-7.6 to -38.7 mV) were prepared to investigate the effect of surface charge on blood circulation time and tissue distribution in tumor-bearing mice. For the *in vivo* studies, dual labeled Ps were applied, which were obtained by encapsulating <sup>3</sup>H-dextran 70k in the aqueous core of Ps and by post-coupling of <sup>14</sup>C-thioglycolic acid onto acrylated PEG chains of the Ps. Stealth liposomes (103 nm, -6 mV) were used as a control. A substantial longer half lifetime ( $\tau_{1/2}$ ) (47.3 h) and a reduced liver uptake (27.9 % of injected dose (% ID)) of Ps with a zeta potential of -7.6 mV were observed as compared to those of stealth liposomes (10.6 h, 39.8 % ID) most probably due to the presence of a relatively thicker and denser PEG brush of the Ps as compared to the liposomes. As a result of their longer circulation times a high tumor accumulation of 18.6 % ID was obtained for these Ps after 3 d circulation in mice, while only 11.2 % ID of stealth liposomes accumulated in the tumors as a result of their relatively short  $\tau_{1/2}$  in blood. By increasing the zeta potential on Ps, more rapid clearance of Ps from the blood circulation was found due to an enhanced uptake by the liver. Importantly, co-localization of the two labels of Ps was observed during circulation, indicating that dual labeled Ps were colloidally stable in blood without leakage of <sup>3</sup>H-dextran. In conclusion, the results show that Ps with a slightly negative surface charge (zeta potential -7.6 mV) are stable in the circulation and have longer circulation times and a higher tumor accumulation in mice than Ps with more negative zeta potentials or the stealth liposomes used as a control.

## **Introduction**

Polymersomes (Ps), synthetic polymer-based vesicles, have attracted rapidly growing interest as a novel class of nanocarriers. Ps based on amphiphilic block copolymers with a relatively high molecular weight (MW) have relatively thick and stable membranes (up to 40 nm) [1-3]. In order to design Ps with long circulation times, amphiphilic PEG block containing polymers can be applied. The presence of PEG at the surface of the Ps will reduce interactions with blood components [4] and increase their biological stability (stealth effect) [5]. These effects are dependent on the MW of the PEG and its surface concentration. The protein resistant character of a PEG brush on the surface of Ps is due to the conformation of PEG in aqueous media, minimization of the interfacial free energy and steric repulsion [6-8]. The influence of PEG on the surface of vesicular carriers on their circulation times has been previously demonstrated by comparing the circulation times of pegylated and non-pegylated liposomes. Non pegylated liposomes have very short blood circulation times due to a fast uptake by the reticulo-endothelial system (RES) [9]. Stealth liposomes, which are coated with PEG, exhibit much longer blood circulation times than non-pegylated liposomes. The PEG coating reduces protein adsorption onto the surface of the liposomes during the circulation [10].

Blood clearance of nanocarriers can be mediated by plasma proteins such as opsonins and dysopsonins that are adsorbed onto the surface of the carriers. Although there is little known about their effects on the opsonization process due to the complexity of the biological events, the surface charge and size of nanocarriers are undoubtedly also playing an important role in the adsorption of proteins to the surfaces [11-15]. It has been reported that the introduction of a slightly negative or positive charge on the surface of nanocarriers enhanced their blood circulation times and reduced the accumulation in the liver [16, 17]. However, carriers with either a high negative or high positive charge were cleared more rapidly from the blood circulation [17-19]. Based on these results it seems likely that there may be an optimal surface charge for a specific nanocarrier to reach the longest circulation time and lowest hepatic uptake. Likewise, a range of optimal sizes for specific nanocarriers has been suggested to establish long circulation times. For example, pegylated liposomes with diameters larger than 200 nm showed a significant accumulation in the spleen as a result of mechanical filtration, which was followed by phagocytosis [20]. On the other hand, pegylated liposomes with diameters below approximately

70 nm showed an increased accumulation in the liver, possibly also due to changes in protein adsorption related to the high curvature of such small liposomes [21].

So far, only one paper has been published on the blood circulation times and the biodistribution of Ps. Discher and his colleagues injected fluorescently labeled Ps based on PEG-b-poly(1,2-butadiene) (PEG-PBD) with varying lengths of the copolymer chains into rats [5]. They found that the Ps had half life circulation times ( $\tau_{1/2}$ ) up to 28 h and that the Ps accumulated primarily in the liver and the spleen. However, it can not be excluded that some of the label is released during blood circulation and transferred to blood components (e.g. albumin).

In this study, we have evaluated the effect of the surface charge of PEG-PDLLA based Ps with an average diameter of 100 nm on the circulation kinetics, organ distribution and tumor accumulation in tumor-bearing mice. In order to exclude possible transfer of labels, Ps dual labeled with  $^3\text{H}$  and  $^{14}\text{C}$  were used for the *in vivo* studies.  $^{14}\text{C}$ -thioglycolic acid was used to label the Ps membrane and  $^3\text{H}$ -dextran with a high molecular weight (70,000 g/mol) was co-localized with the Ps in the aqueous core. The zeta potential of the Ps was varied from -7.6 to -38.7 mV by coupling of thioglycolic acid onto Ps containing different molar ratios of acrylated PEG. Ps were prepared by using combinations of PEG-PDLLAs, of which one of the block copolymers had PEG blocks with methoxy end groups [22] and the other copolymer PEG blocks with acrylamide end groups. Dipalmitoyl phosphatidylcholine (DPPC)/cholesterol based stealth liposomes with 7.5 % of PEG distearoyl phosphatidylethanolamine (PEG-DSPE) were used as a reference. Ps containing non-labeled dextran and thioglycolic acid model systems were used for optimizing the dual labeling process and for characterizing the dual-labeled Ps with respect to the hydrodynamic diameter, polydispersity index (PDI) and zeta potential. The cytotoxicity of non-radioactive Ps for human umbilical vein endothelial cells (HUVEC) and HeLa cells was also evaluated.

## **Materials and methods**

### *Materials*

*D,L*-lactide (DLLA) was obtained from Purac Biochem b.v. (The Netherlands) and recrystallized from toluene. Monomethoxy poly(ethylene glycol) with a molecular weight of 5000 g/mol (mPEG, Iris Biotech, Germany) was dried by dissolution in anhydrous toluene followed by azeotropic distillation under N<sub>2</sub>. Stannous octoate, Sn(Oct)<sub>2</sub> (Sigma, UK) and mercapto PEG (5000 g/mol, Iris Biotech, Germany) were used as received. FITC-dextran (70,000 g/mol) (FD70), thioglycolic acid (TG), *N,N*-methylenebis(acrylamide) (MBA) and 5,5'-dithiobis-(2-nitrobenzoic acid) (DTNB) were obtained from Sigma (USA). <sup>3</sup>H-dextran (<sup>3</sup>H-D70, 70,000 g/mol) and <sup>14</sup>C-thioglycolic acid (<sup>14</sup>C-TG) were purchased from American Radiolabeled Chemicals (USA). DPPC and PEG-DSPE (2750 g/mol) were provided by Lipoid GmbH (Germany). Cholesterol was purchased from Sigma-Aldrich (The Netherlands). <sup>3</sup>H-cholesteryl oleylether was a product of Amersham (The Netherlands). Hionic-Fluor<sup>TM</sup> and Soluen<sup>®</sup>-350 were obtained from Perkin Elmer BioScience BV (The Netherlands). Deionized water (DI water), obtained from a Milli-Q water purification system (Millipore, The Netherlands) and 4-(2-hydroxyethyl)-1-piperazineethanesulfonic acid (HEPES, Sigma, USA) were used for cell and animal studies. EGM<sup>®</sup> endothelial cell growth medium and EX-CELL<sup>®</sup> medium were supplied by Lonza Ltd (USA) and used for HUVEC and HeLa cells, respectively. CellTiter 96<sup>®</sup> Aqueous Non-Radioactive cell Proliferation Assay kit was purchased from Promega Benelux BV (The Netherlands) and used for the MTS assay. All other reagents used in the study were of analytical grade.

### *Synthesis of block copolymers*

Two PEG-PDLLAs were synthesized by ring-opening polymerization (ROP) of DLLA using the hydroxyl groups of methoxy PEG (mPEG) or acrylamide PEG (aPEG) to initiate the polymerization. mPEG or aPEG (0.50 g, 0.1 mmol), DLLA (4.2 g, 29.2 mmol), Sn(Oct)<sub>2</sub> (0.04 g, 0.1 mmol) and toluene (30 ml) were charged in that order in a reaction vessel. The reaction was performed at 110 °C for 26 h under stirring. After cooling, a drop of HCl (37 wt.%) was added to the reaction mixture to hydrolyze the tin-oxygen bond. The copolymer was isolated by precipitation in methanol. After filtration and washing with methanol, the copolymer was dissolved in dichloromethane and precipitated in diethyl ether. Subsequently, the polymer was isolated by filtration, washed several times with diethyl ether, and dried under vacuum. The

monomer conversion and the number average molecular weight ( $M_n$ ) of block copolymers were determined by  $^1\text{H-NMR}$  (Inova 300 MHz, Varian).

aPEG was prepared prior to ROP by reacting mercapto PEG with MBA. HO-PEG-SH (0.5 g, 0.1 mmol) was dissolved in 5 ml of DI water and MBA (0.154 g, 1 mmol) in a carbonate buffer solution (pH 10) was added drop wise to this solution. After gentle stirring for 1 h at room temperature, the resulting solution was ultrafiltrated through a membrane with a cut-off of 1000 g/mol (Ultracel Ultrafiltration Disc, Millipore) for 2 d and lyophilized. An ELLMAN assay was carried out to determine the amount of unreacted thiol groups which indicated that less than 1 % of mercapto PEG had not reacted.

#### *Preparation and characterization of Ps*

FD70 was encapsulated in Ps during the formation of Ps. mPEG-PDLLA and aPEG-PDLLA were used to prepare self-assembled Ps by injecting a THF solution of the block copolymers into an aqueous solution. Ps based on aPEG-PDLLA and mPEG-PDLLA with a weight ratio of 10:90, 50:50 and 100:0 were prepared and abbreviated as Ps10, Ps50 and Ps100, respectively. In brief, the block copolymer or the mixture (10 mg/ml) was dissolved in THF (3 ml) and FD70 (0.1 mg/ml) was dispersed in the solution. The THF dispersion was injected into HEPES (50 ml, pH 7.4, 10 mM) to spontaneously form Ps. After 15 min without shaking, the vial containing the mixture was turned upside down several times, resulting in a turbid dispersion. To remove the organic solvent, the dispersion of FD70 loaded Ps (FD70-Ps) was transferred into a dialysis bag (cut-off 50,000 g/mol, Spectra/Por), which was placed in a 4 l flask with DI water. The dialysis was performed for 1 d by replacing the DI water for at least 5 times. After dialysis, the dispersion of FD70-Ps was filtrated with a syringe filter (pore size 100 nm, PES, Acrodisc, Pall) and concentrated to 10 ml using Vivaspin20 (Sartorius stedim biotech.).

TG was coupled onto the acrylamide groups of aPEG of Ps by a Michael addition reaction to introduce anionic charge on the Ps. For the reaction, carbonate buffer solution (1 ml, pH 10) was added to the dispersions (1 ml) of Ps10, Ps50 and Ps100. A stock solution of TG was prepared prior to the coupling by diluting TG (1 ml) with a carbonate buffer solution (9 ml). Different amounts of the stock solution were dropped into Ps dispersions (0.02 ml to Ps10, 0.20 ml to Ps50 and 1.00 ml to Ps100) under stirring and the reaction was carried out for 1 h at room temperature. Unreacted TG and free FD70 were removed by dialysis (cut-off 100,000 g/mol, Spectra/Por) in

DI water at 37 °C for 2 d. Dispersions of FD70-Ps coupled with TG (FD70/TG-Ps) were further concentrated 3 times. HEPES (2.4 mg/ml) was added to the dispersions and the samples were titrated to pH 7.4 with NaOH.

Size and PDI as well as zeta potential of FD70/TG-Ps10, FD70/TG-Ps50 and FD70/TG-Ps100 in HEPES (pH 7.4, 10 mM) were measured using a Zetasizer Nano ZS (Malvern Instruments, Malvern). Transmission electron microscopy (TEM, Philips CM30, Hillsboro, USA) was performed to elucidate the morphology and the membrane thickness of Ps. A dispersion of Ps (2  $\mu$ l, 6 mg/ml) was placed on a 200 mesh carbon grid without using a staining agent. The excess solution was removed and the sample was dried at room temperature. For TEM, Ps were prepared by injecting a THF solution of mPEG-PDLLA in DI water. Possible release of FD70 from Ps was monitored by placing a suspension of FD70/TG-Ps in HEPES in a microdialysis system (cut-off 100,000 g/mol). Periodic withdrawals of HEPES samples were monitored by fluorescence spectroscopy (Safire<sup>2</sup>, Tecan). Using DLS, the colloidal stability of the FD70/TG-Ps in HEPES at 37 °C was also monitored for 3 d.

#### *In vitro cytotoxicity of FD70/TG-Ps*

The cytotoxicity of FD70/TG-Ps10, FD70/TG-Ps50 and FD70/TG-Ps100 was investigated using HUVEC and HeLa cells. The cells of both lines were seeded into a 96-well plate at a density of  $5 \times 10^3$  cells per well and cultured at 37 °C in a humidified atmosphere with 5% CO<sub>2</sub>. After 1 d, the cell medium was changed with fresh cell medium (100  $\mu$ l) and dispersions of FD70/TG-Ps (100  $\mu$ l, 6 mg/ml) were added to the medium. The cells were incubated for 72 h and the number of viable cells was determined using an MTS colorimetric assay. The well plates were incubated for 4 h at 37 °C and the absorbance at 490 nm was recorded using a plate reader (Safire<sup>2</sup>, Tecan).

#### *Animal experiments*

For the circulation kinetics and biodistribution of Ps10, Ps50 and Ps100, Ps were dually labeled with <sup>3</sup>H-D70 (11.1 MBq) and <sup>14</sup>C-TG (0.5 MBq) using the THF injection method followed by the Michael addition reaction. <sup>3</sup>H-D70 was incorporated during the formation of Ps and <sup>14</sup>C-TG was post-coupled to acrylated PEG on the surface of the Ps. A schematic illustration of the dual labeled Ps is represented in Fig. 7.1. Stealth liposomes were used as a control. A film-

extrusion method [19, 23] was used to prepare the liposomes. In brief, DPPC, cholesterol and PEG-DSPE (2750 g/mol) (1.85:1.00:0.15) were dissolved in ethanol and  $^3\text{H}$ -cholesteryl oleylether (0.74 MBq) was added. A lipid film was obtained by evaporation of the solvent under a stream of nitrogen. The lipid film was hydrated in 3 ml of HEPES buffer solution, yielding a lipid concentration of 10  $\mu\text{mol}$  total lipid/ml. Liposomes were sized by sequential extrusion through two stacked polycarbonate filters (Poretics, Livermore, 400, 200 and 100 nm pore size) with a high pressure extrusion device.

C57Bl/6J female mice (20-25 g, 4-6 weeks old) were housed in groups of 4-8 animals and had free access to water and food. All animal studies were performed in compliance with guidelines set by national regulations and were approved by the local animal experiments ethical committee. Tumors were introduced in the flank of the mice by inoculation with  $1 \times 10^6$  of murine B16 melanoma tumor cells. Palpable subcutaneous tumors had developed over a period of approximately 10 d.

Three types of dual-labeled Ps (100 mg/kg) as well as the stealth liposomes (70 mg/kg) in HEPES (200  $\mu\text{l}$ ) were administered via the tail vein. Blood samples were obtained via cheek puncture after 1 h, 4 h and 8 h. After 24 h, 48 h and 72 h, mice were sacrificed to sample the blood, the organs and tumors, and the wet weight of the tissues was measured. Soluene<sup>®</sup>-350 (2 ml) was added to the blood and tissue samples, and the mixtures were incubated until the tissues were completely solubilized yielding yellowish solutions. To decolorize the samples, hydrogen peroxide (35 %) was added and these mixtures were incubated at room temperature overnight. Hionic-Fluor<sup>TM</sup> (10 ml) scintillation cocktail was added to these samples and the resulting mixture was counted for radioactivity. The total volume of blood in a mouse was estimated by the following equation [14]:

$$\text{Total blood volume (ml)} = \text{body weight (g)} \times 0.0845 \text{ ml/g} \quad (7.1)$$

The percent injected dose (% ID) and the percent ID per gram (% ID/g) values were calculated using the following equations:

$$\% \text{ ID} = \frac{\text{Dose in blood/tissue sample (Bq)}}{\text{Injected dose (Bq)}} \times 100 \quad (7.2)$$

$$\% \text{ ID/g} = \frac{\% \text{ ID}}{\text{Weight of tissue (g)}} \quad (7.3)$$

Pharmacokinetic parameters such as  $\tau_{1/2}$ , area under the curve (AUC), volume of distribution and clearance (Cl) for Ps and stealth liposomes were calculated using PKSolver [24].

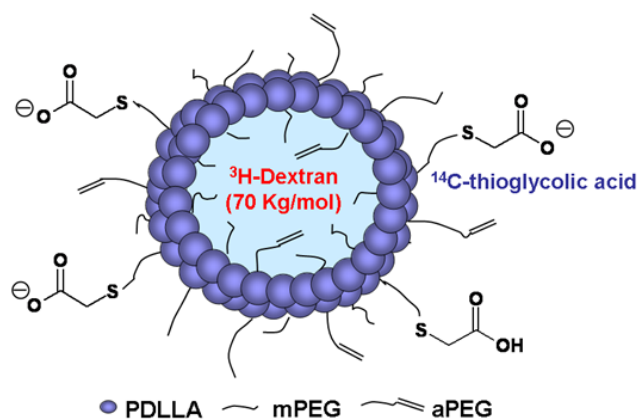


Figure 7.1. Schematic 2D-cross sectional illustration of dual-labeled Ps in which  $^3\text{H}$ -D70 was encapsulated in the core of Ps and  $^{14}\text{C}$ -TG coupled to acrylated PEG (aPEG).

## Results and discussion

### *Characterization of block copolymers and Ps*

mPEG-PDLLA and aPEG-PDLLA with number average molecular weights ( $M_n$ ) of 41,800 and 41,700 g/mol, respectively, were synthesized by ROP and used for the formation of polymeric vesicles (Table 7.1).  $^1\text{H}$ -NMR revealed that the length of the PDLLA blocks corresponded well with the feed amount as a result of the high monomer conversion. As previously reported, the volume fraction of hydrophilic polymer ( $f$ ) and the MW of the block copolymer will determine the shape of the self-assembled structures because the  $f$  and MW are influencing the curvature of the hydrophilic-hydrophobic interface of the self-assembled structures [25]. In previous studies, it was shown that amphiphilic di-block copolymers with an  $f$  between 10 and 40 % and a MW ranging from  $\sim 2700$  to 50,000 g/mol were able to form Ps [1, 26]. The volume fraction of the PEG block ( $f_{\text{PEG}}$ ) of both mPEG-PDLLA and aPEG-PDLLA was 11.8 % as calculated from the composition according to the  $^1\text{H}$ -NMR analysis.

Ps with an average diameter less than 100 nm and a narrow size distribution (Table 7.2) were spontaneously formed by the THF injection method. It has been previously reported that large block copolymers with small hydrophilic volume fractions ( $f < 20$  %) form Ps by injecting a



polymer-containing organic solvent into an aqueous phase [27]. Fig. 7.2 shows a TEM image of the Ps and it can be seen that the Ps are spherical nanovesicles with a membrane thickness of about 15 nm. The thickness of the membrane did not vary much with the size of the vesicles. In a control experiment, the release of encapsulated FD70 from Ps at 37 °C in PBS was monitored and less than 5 % of FD70 was released over a period of 3 d. This may be explained by the release of small amounts of FD70 incorporated in the Ps membrane during the encapsulation process. TG was coupled to the acrylamide groups of PEG on the surface of Ps and the zeta potential was well controlled by the molar ratio of mPEG-PDLLA and aPEG-PDLLA used for the preparation of the Ps and the amount of TG added to the Ps dispersion as -7.6 (FD70/TG-Ps10), -25.3 (FD70/TG-Ps50) and -38.7 mV (FD70/TG-Ps100). DLS experiments showed no significant change in mean diameter, PDI and Ps concentration before and after the labeling process and when FD70/TG-Ps dispersions were incubated for 3 d at 37 °C in HEPES, indicating that the FD70/TG-Ps were colloidally stable. For *in vivo* studies, the same method was used to prepare dual-labeled Ps but now the internal core of Ps was loaded with  $^3\text{H}$ -D70 and the shell was labeled with  $^{14}\text{C}$ -TG.

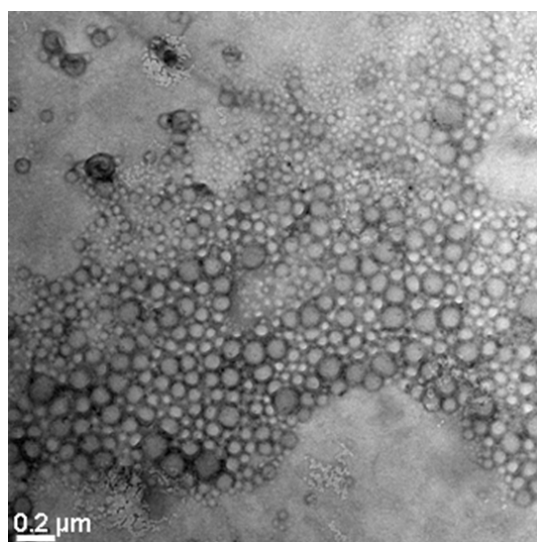


Figure 7.2. TEM images of Ps on carbon grids. mPEG-PDLLA was used to prepare Ps in DI water. A dispersion of Ps was placed on a 200 mesh normal carbon grid without using a staining agent and dried at room temperature. Size bar represents 200 nm.

Table 7.1. Characterization of mPEG-PDLLA and aPEG-PDLLA

	Monomer conversion <sup>a</sup> (%)	Mn of PDLLA (theor.) <sup>b</sup> (g/mol)	Mn of PDLLA ( <sup>1</sup> H-NMR) <sup>c</sup> (g/mol)	$f_{PEG}^d$ (%)
mPEG-PDLLA	99	42,000	41,800	11.8
aPEG-PDLLA	98	42,000	41,700	11.8

<sup>a</sup> Determined by <sup>1</sup>H NMR.

<sup>b</sup> Calculated from the initial ratio of monomer to PEG hydroxyl groups.

<sup>c</sup> Determined from <sup>1</sup>H-NMR analysis by calculating the ratio of the PEG methylene peak to the main peak of the polyester.

<sup>d</sup> Calculated volume fraction of PEG in block copolymers.

Table 7.2. Size and zeta potential of FD70/TG-Ps

	FD70/TG-Ps10	FD70/TG-Ps50	FD70/TG-Ps100
Size <sup>a</sup> (nm)	96.3 ± 6.6	95.5 ± 5.0	92.7 ± 1.8
PDI <sup>b</sup>	0.06	0.04	0.04
Zeta potential <sup>a</sup> (mV)	-7.6	-25.3	-38.7

<sup>a</sup> Measurements were performed 30 times and averaged.

<sup>b</sup> Polydispersity index.

#### Cell toxicity of Ps *in vitro*

The cytotoxicity of FD70/TG-Ps was studied using cultured HUVEC and HeLa cells. Cells were incubated with FD70/TG-Ps at the same concentrations as the samples used for *in vivo* mice experiments. As shown in Fig. 7.3, FD70/TG-Ps10, FD70/TG-Ps50 and FD70/TG-Ps100 showed no cytotoxicity for both HUVEC and HeLa cells after 3 d exposure. The Ps have an anionic PEGylated surface and the surface charge as well as the presence of the PEG chains at the surface of the Ps may contribute to a weak interaction with cells. An electrostatic repulsion between Ps and cell membranes, normally negatively charged, may occur and the PEG layer itself is well known to reduce the interaction with cells [28]. PEG-PDLLA, which was used to form Ps, is a biocompatible material and PEG-PDLLA with a wide range of MWs has been employed for the preparation of various nano and micro-sized drug delivery carriers.

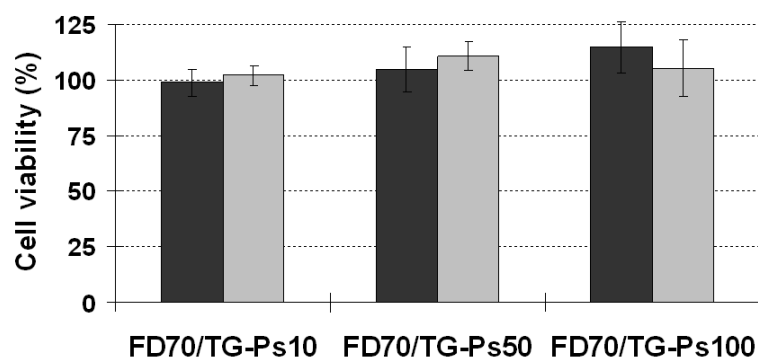


Figure 7.3. Cytotoxicity of FD/TG-Ps (3 mg/ml) for HUVEC and HeLa cells after 3 d exposure. HUVEC (■) and HeLa cells (■). The data given are mean values and the error bars are the standard deviations of the mean.

#### Blood circulation time

The circulation kinetics of Ps in mice was investigated and stealth liposomes with a diameter of  $103 \pm 8.0$  nm were used as a control. The % ID of tritium of the blood samples in time is presented in Fig. 7.4a and the pharmacokinetic parameters are listed in Table 7.3. Stealth liposomes exhibited a  $\tau_{1/2}$  of 10.6 h in the blood circulation, whereas Ps10 yielded a prolonged  $\tau_{1/2}$  of 47.3 h under the same conditions. Pharmacokinetic analysis revealed that the rate of clearance of Ps10 was more than two times lower as compared to stealth liposomes. This result may be related to the differences in MW and the surface concentration of PEG between Ps10 and stealth liposomes. Ps10 has a 100 % dense PEG brush with a MW of 5000 g/mol, whereas less than 10 mol % of PEG with a MW of 2000 g/mol was applied for the stealth liposomes. In principle, the clearance process of stealth liposomes from the circulation can be mediated by an array of blood components that interact with the stealth liposomes [29-31]. Similar blood components may also interact with Ps. Plasma proteins such as opsonins and dysopsonins that are adsorbed onto or incorporated in the PEG brush can interact with the hydrophobic core of the membranes [32]. However, this process can be influenced by the MW and surface concentration of PEG molecules. Previous studies showed that PEGs with a longer chain length at constant PEG surface concentration are more effective for reducing protein adsorption than PEGs with shorter chain lengths [33]. Meng *et al.* reported that long PEG molecules (3400 or 5000 g/mol) are much more effective in reducing protein adsorption than short PEG (1500 g/mol) [4]. When PEG with a similar length ( $2000 \pm 300$  g/mol) is introduced either on Ps or on liposomes, Ps exhibit a  $\tau_{1/2}$  of 28 h, while stealth liposomes show a  $\tau_{1/2}$  of 10-15 h in rats suggesting that the Ps

membranes adsorb less and/or different plasma proteins due to a higher surface concentration of PEG [5]. Although MW and surface concentration of PEG are important for the protein resistance, pegylation of liposomes is limited to PEGs with a MW lower than 2000 g/mol and a mole fraction of PEG lower than 11 % due to micellization [34].

Efficient drug carriers for intravenous administration have to increase the drug concentration at the target site. In order to accomplish this, the carrier should have a high drug retainability as well as colloidal stability in the blood circulation. To investigate the behavior of Ps *in vivo*, two radioactive molecules,  $^3\text{H}$ -D70 and  $^{14}\text{C}$ -TG, were used to dually label Ps. Figs. 7.4a and 7.4b represent the % ID of blood samples calculated by the measured radioactivity of  $^3\text{H}$  and  $^{14}\text{C}$ , respectively. Comparing Figs. 7.4a and 7.4b it can be concluded that for each sample the difference in the % ID either based on the radioactivity of  $^3\text{H}$  or on that of  $^{14}\text{C}$  was less than  $\pm 5\%$ . This is clear evidence that Ps used in the study maintained their colloidal stability during the circulation in blood because  $^3\text{H}$ -D70 was not or only to a very small extent released from the Ps. Free D70 has a relatively fast plasma clearance with a  $\tau_{1/2}$  less than 2 h in rats [35]. The colloidal stability of the Ps may be explained by the presence of a relatively thick membrane with a hydrophobic interior and the presence of a relatively long and dense PEG brush.

Table 7.3. Pharmacokinetic parameters for Ps and stealth liposomes

	Stealth liposomes	Ps10	Ps50	Ps100
$\tau_{1/2}$ (h)	$10.6 \pm 1.8$	$47.3 \pm 12.7$	$21.6 \pm 3.6$	$10.8 \pm 1.6$
AUC <sub>0-72h</sub> (% ID*h/ml)	$790 \pm 43$	$1666 \pm 141$	$1139 \pm 71$	$632 \pm 57$
AUC <sub>0-∞</sub> (% ID*h/ml)	$797 \pm 46$	$2634 \pm 258$	$1282 \pm 119$	$641 \pm 61$
Volume of distribution (ml)	$2.18 \pm 0.23$	$2.06 \pm 0.14$	$2.15 \pm 0.17$	$2.12 \pm 0.16$
Cl (ml/h)	$0.13 \pm 0.01$	$0.06 \pm 0.01$	$0.09 \pm 0.01$	$0.16 \pm 0.01$

Log-linear kinetics fit for all carriers  $r^2 > 0.9$ .

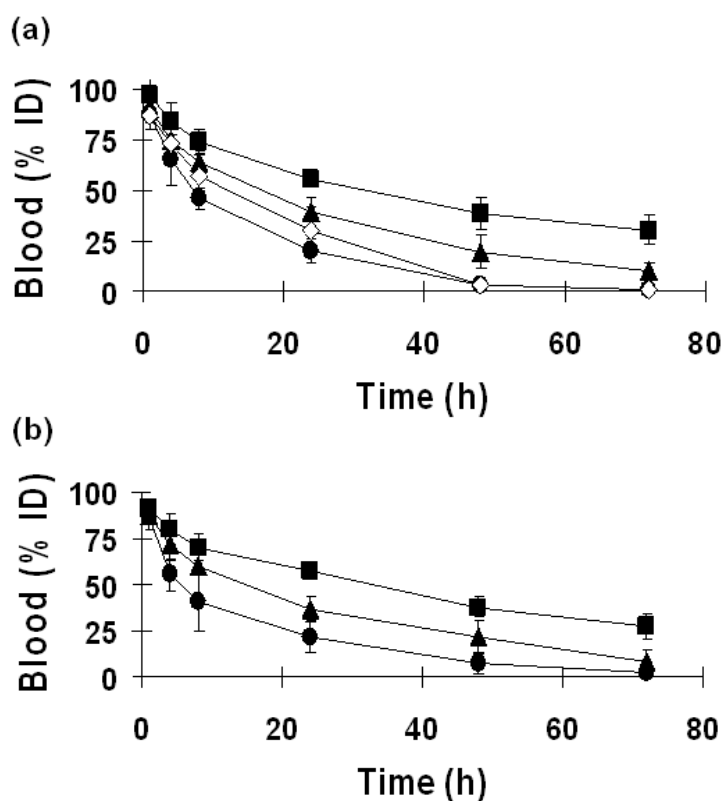


Figure 7.4. Circulation kinetics of anionic Ps and stealth liposomes in mice measured by radioactivity of  $^3\text{H}$  (a) or  $^{14}\text{C}$  (b) in blood samples. Ps were dual labeled with  $^3\text{H}$  and  $^{14}\text{C}$ , and stealth liposomes were labeled with  $^3\text{H}$ . Ps10 (■, -7.6 mV), Ps50 (▲, -25.3 mV), Ps100 (●, -38.7 mV) and stealth liposomes (◇, -6.0 mV). The experiments were carried out in triplicate. The data given are mean values and the error bars are the standard deviations of the mean.

#### *Tumor accumulation and organ distribution*

Tumor targeting can in principle be achieved by passive accumulation (EPR) of nanocarriers depending on their shape and size [36]. Spherical Ps with hydrodynamic diameters less than 200 nm are suitable to localize these Ps in tumor tissue by the EPR effect. The results of a biodistribution study with Ps with different surface charge using tumor-bearing mice are given in Fig. 7.5. Ps10 were taken up by the tumor with about 13.5 % ID/g after 1 d circulation and the uptake increased up to 18.6 % ID/g after 3 d, demonstrating that the tumor accumulation of Ps is relatively high. A maximal value of tumor accumulation of micelles and stealth liposomes of less than 15 % ID/g has been reported [14, 37, 38]. The relatively long circulating times of Ps led to a high accumulation in the tumor. This is in agreement with the results for poly(ethylene oxide)-b-poly(aspartic acid)-doxorubicin (PEO-PAsp-DOX) micelles and stealth liposomes, which show an enhanced tumor accumulation with prolonged circulation times [14, 39]. Stealth liposomes

with a shorter  $\tau_{1/2}$  in the blood circulation than Ps, were taken up by tumor tissues for about 11.2 % ID/g after 3 d under the same conditions.

Ps were found to accumulate primarily in the liver similar to stealth liposomes (Fig. 7.5). However, Ps10 showed a relatively low uptake of 28 % ID in the liver after 3 d as compared to stealth liposomes (40 % ID). It is known that adsorption of liver specific opsonins can enhance the uptake of vesicles by liver macrophages, Kupffer cells, and this process plays a major role in the hepatic uptake of the vesicles [15]. Therefore, it can be suggested that the relatively low hepatic uptake is associated with a diminished interaction with opsonins or an increased interaction with dysopsonins. Distributions of Ps and liposomes in the spleen, kidney and lung were comparable and very low % IDs were measured.

#### *Effect of surface charge of Ps on circulation and biodistribution*

Three anionic Ps (size ~100 nm) with different zeta potentials were applied to investigate the effect of surface charge on circulation times and biodistribution. Fig. 7.5 compares the % ID of Ps10, Ps50 and Ps100, which are calculated from blood samples in time. Ps100 was relatively rapidly removed from the circulation (0.16 ml/h, Table 7.3). Ps100 with a zeta potential of -38.7 mV had a  $\tau_{1/2}$  of 10.8 h and slightly negatively charged Ps10 (-7.6 mV) showed a more than 4-fold longer  $\tau_{1/2}$ . The  $\tau_{1/2}$  of Ps50 was 21.6 h in between the  $\tau_{1/2}$  of Ps10 and Ps100. It is a general view that an increase in the negative surface charge of carriers increases their clearance rate from the circulation due to a higher hepatic uptake [40]. This is in agreement with our finding that the highest liver uptake among Ps was observed for Ps100 (37.9 % after 3 d). Christian *et al.* have previously found an increased accumulation of anionic Ps in the liver of mice as compared to neutral Ps [41]. A mixture of two block copolymers, poly(acrylic acid)-b-poly(1,4-butadiene) (PAA-PBD, 5.4k-5.6k) and PEG-b-poly(1,2-butadiene) (PEG-PBD, 3.7k-6.8k) with a molar ratio of 10:90 was used to prepare the anionic Ps with a zeta potential of -13.3 mV. Neutral Ps, which were made of PEG-PBD in the absence of PAA-PBD, showed a reduction of the hepatic uptake of more than 30 % as compared to the anionic Ps. Similar findings have been reported by Romberg *et al.* for liposomes containing negatively charged phospholipids, which were very rapidly removed from the blood showing an enhanced hepatic uptake [18].

One explanation possibly related to this result is that leukocytes, unique for the liver have receptors which preferentially recognize anionic particles implying that the surface charge

influences the opsonization of the particle and so enhances their phagocytosis [42]. It has also been demonstrated that coating of negatively charged particles with a non-ionic polymer results in a reduction of the particle charge and a reduced liver uptake [43]. As a consequence, it seems likely that stealth properties may be optimized by introducing a low anionic charge on the surface of drug carriers, leading both to less interaction with blood components and low hepatic uptake. Takeuchi *et al.* and Yamamoto *et al.* previously suggested the role of a slight anionic charge of drug carriers in avoiding rapid blood clearance and high liver uptake. Liposomes with a surface charge of  $-4.4$  mV exhibited longer circulation times and lower hepatic uptake in rats as compared to highly anionic liposomes [13]. Tyrosyl-glutamic acid (Tyr-Glu) coated PEG-PDLLA micelles (Tyr-Glu-micelles) with a zeta potential of  $-10.6$  mV had similar circulation times as neutral Tyr-micelles, but a significantly lower uptake by the liver as compared to neutral ones [16]. Ps10 yielded the highest accumulation in the tumor due to the relatively long circulation time as previously discussed. Splenic uptake among Ps10, Ps50 and Ps100 were comparable ranging from 0.7 to 1.6 % ID and the uptake by the kidney and lung was less than 0.5 % ID.

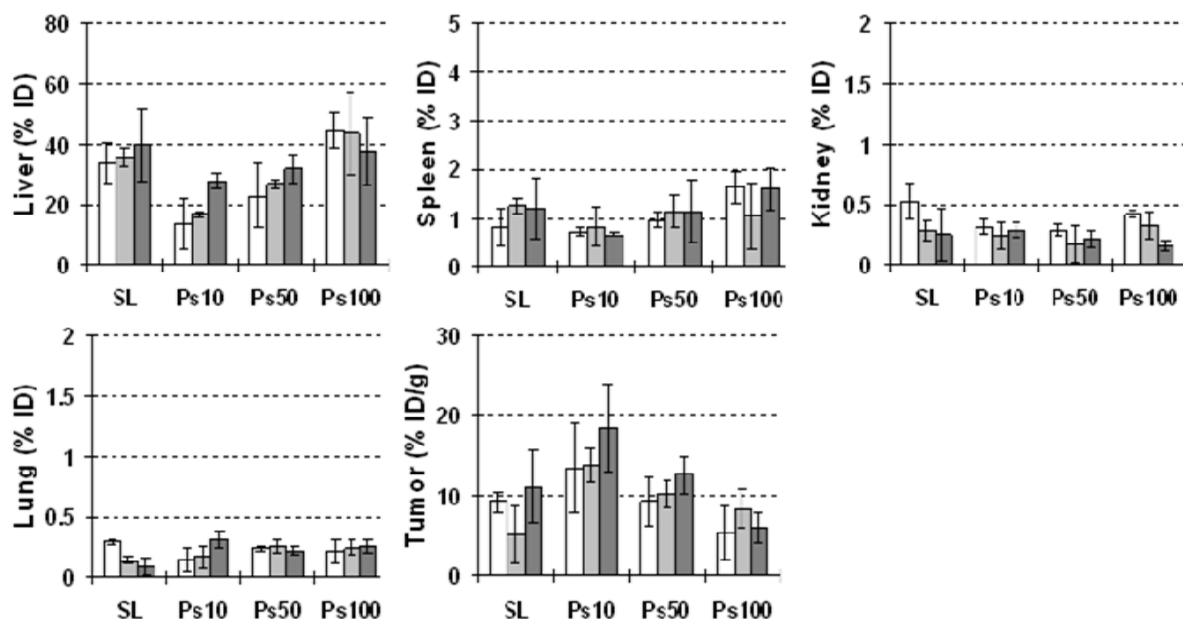


Figure 7.5. Biodistribution of dual-labeled Ps and stealth liposomes (SL) analyzed by the radioactivity of  $^3\text{H}$  in organs (% ID) and tumors (% ID/g). 24 h ( $\square$ , open), 48 h ( $\blacksquare$ , light gray) and 72 h after injection ( $\blacksquare$ , dark gray). The experiments were carried out in triplicate. The data given are mean values and the error bars are the standard deviations of the mean.

## **Conclusions**

PEG-PDLLA polymersomes with a low zeta potential (-7.6 mV) and a diameter of approximately 100 nm had a much longer half lifetime ( $\tau_{1/2}$  47 h) and a reduced liver uptake (28 % ID after 3 d) as compared to stealth liposomes ( $\tau_{1/2}$  10.6 h and 40 % ID after 3 d). A relatively high tumor accumulation of the polymersomes, probably via the EPR effect, was associated with a long circulation time. A dual-labeling technique was applied to investigate whether the polymersomes were able to carry an encapsulated high molecular weight model drug (dextran 70,000 g/mol) to the target site and whether the model drug remained encapsulated in the Ps during circulation. Co-localization of the two labels during circulation demonstrated that the model drug-loaded polymersomes were colloidally stable in blood and that no significant leakage of dextran occurred. The effects of the charge density of anionic polymersomes on circulation kinetics and biodistribution showed that polymersomes with a slightly negative surface charge are most suited for *in vivo* administration. It is concluded that long circulating polymersomes, which are stable in blood and which strongly accumulate in tumor tissue, are extremely promising as novel drug carriers. Further studies are required to evaluate the therapeutic efficacy of drug-loaded polymersomes as well as to study the detailed effects of surface structure and charge of polymersomes on opsonization and liver uptake processes.



**References**

- [1] F. Ahmed, P.J. Photos, D.E. Discher, Polymersomes as viral capsid mimics. *Drug Dev. Res.* 67(1) (2006) 4-14.
- [2] H. Bermudez, A.K. Brannan, D.A. Hammer, F.S. Bates, D.E. Discher, Molecular weight dependence of polymersome membrane structure, elasticity, and stability. *Macromolecules* 35(21) (2002) 8203-8208.
- [3] J.C.M. Lee, H. Bermudez, B.M. Discher, M.A. Sheehan, Y.Y. Won, F.S. Bates, D.E. Discher, Preparation, stability, and in vitro performance of vesicles made with diblock copolymers. *Biotechnol. Bioeng.* 73(2) (2001) 135-145.
- [4] F.H. Meng, G.H.M. Engbers, A. Gessner, R.H. Muller, J. Feijen, Pegylated polystyrene particles as a model system for artificial cells. *J. Biomed. Mater. Res. Part A* 70A(1) (2004) 97-106.
- [5] P.J. Photos, L. Bacakova, B. Discher, F.S. Bates, D.E. Discher, Polymer vesicles in vivo: correlations with PEG molecular weight. *J. Control. Release* 90(3) (2003) 323-334.
- [6] S.I. Jeon, J.D. Andrade, Protein Surface Interactions in the Presence of Polyethylene Oxide 2. Effect of Protein Size. *J. Colloid Interface Sci.* 142(1) (1991) 159-166.
- [7] S.I. Jeon, J.H. Lee, J.D. Andrade, P.G. Degennes, Protein Surface Interactions in the Presence of Polyethylene Oxide 1. Simplified Theory. *J. Colloid Interface Sci.* 142(1) (1991) 149-158.
- [8] K.D. Park, Y.S. Kim, D.K. Han, Y.H. Kim, E.H.B. Lee, H. Suh, K.S. Choi, Bacterial adhesion on PEG modified polyurethane surfaces. *Biomaterials* 19(7-9) (1998) 851-859.
- [9] H. Kiwada, T. Miyajima, Y. Kato, Studies on the Uptake Mechanism of Liposomes by Perfused-Rat-Liver .2. An Indispensable Factor for Liver Uptake in Serum. *Chem. Pharm. Bull.* 35(3) (1987) 1189-1195.
- [10] M.L. Immordino, F. Dosio, L. Cattel, Stealth liposomes: review of the basic science, rationale, and clinical applications, existing and potential. *Int. J. Nanomed.* 1(3) (2006) 297-315.
- [11] V.D. Awasthi, D. Garcia, R. Klipper, B.A. Goins, W.T. Phillips, Neutral and anionic liposome-encapsulated hemoglobin: Effect of postinserted poly(ethylene glycol)-distearoylphosphatidylethanolamine on distribution and circulation kinetics. *J. Pharmacol. Exp. Ther.* 309(1) (2004) 241-248.
- [12] A. Gabizon, D. Papahadjopoulos, The Role of Surface-Charge and Hydrophilic Groups on Liposome Clearance In vivo. *Biochim. Biophys. Acta-Biomembr.* 1103(1) (1992) 94-100.
- [13] H. Takeuchi, H. Kojima, H. Yamamoto, Y. Kawashima, Polymer coating of liposomes with a modified polyvinyl alcohol and their systemic circulation and RES uptake in rats. *J. Control. Release* 68(2) (2000) 195-205.
- [14] G.S. Kwon, K. Kataoka, Block-Copolymer Micelles as Long-Circulating Drug Vehicles. *Adv. Drug Deliv. Rev.* 16(2-3) (1995) 295-309.
- [15] S. Stolnik, L. Illum, S.S. Davis, Long Circulating Microparticulate Drug Carriers. *Adv. Drug Deliv. Rev.* 16(2-3) (1995) 195-214.
- [16] Y. Yamamoto, Y. Nagasaki, Y. Kato, Y. Sugiyama, K. Kataoka, Long-circulating poly(ethylene glycol)-poly(D,L-lactide) block copolymer micelles with modulated surface charge. *J. Control. Release* 77(1-2) (2001) 27-38.
- [17] H. Aoki, T. Tottori, F. Sakurai, K. Fuji, K. Miyajima, Effects of positive charge density on the liposomal surface on disposition kinetics of liposomes in rats. *Int. J. Pharm.* 156(2) (1997) 163-174.

- [18] B. Romberg, C. Oussoren, C.J. Snel, W.E. Hennink, G. Storm, Effect of liposome characteristics and dose on the pharmacokinetics of liposomes coated with poly(amino acid)s. *Pharm. Res.* 24(12) (2007) 2394-2401.
- [19] B. Romberg, C. Oussoren, C.J. Snel, M.G. Carstens, W.E. Hennink, G. Storm, Pharmacokinetics of poly(hydroxyethyl-L-asparagine)-coated liposomes is superior over that of PEG-coated liposomes at low lipid dose and upon repeated administration. *Biochim. Biophys. Acta-Biomembr.* 1768(3) (2007) 737-743.
- [20] S.M. Moghimi, H. Hedeman, I.S. Muir, L. Illum, S.S. Davis, An Investigation of the Filtration Capacity and the Fate of Large Filtered Sterically-Stabilized Microspheres in Rat Spleen. *Biochim. Biophys. Acta-Gen. Subj.* 1157(3) (1993) 233-240.
- [21] D.C. Litzinger, A.M.J. Buiting, N. Vanrooijen, L. Huang, Effect of Liposome Size on the Circulation Time and Intraorgan Distribution of Amphipathic Poly(Ethylene Glycol)-Containing Liposomes. *Biochim. Biophys. Acta-Biomembr.* 1190(1) (1994) 99-107.
- [22] F.H. Meng, G.H.M. Engbers, J. Feijen, Biodegradable polymersomes as a basis for artificial cells: encapsulation, release and targeting. *J. Control. Release* 101(1-3) (2005) 187-198.
- [23] S. Amselem, A. Gabizon, Y. Barenholz, A large-scale method for the preparation of sterile and non-pyrogenic liposomal formulation for defined size distributions for clinical use, in: G. Gregoriadis (Ed.), *Liposome Technology*, CRC press, Boca Raton, 1993, pp. 501-525.
- [24] Y. Zhang, M.R. Huo, J.P. Zhou, S.F. Xie, PKSolver: An add-in program for pharmacokinetic and pharmacodynamic data analysis in Microsoft Excel. *Comput. Meth. Programs Biomed.* 99(3) (2010) 306-314.
- [25] D.E. Discher, A. Eisenberg, Polymer vesicles. *Science* 297(5583) (2002) 967-973.
- [26] Y. Lee, J.B. Chang, H.K. Kim, T.G. Park, Stability studies of biodegradable polymersomes prepared by emulsion solvent evaporation method. *Macromol. Res.* 14(3) (2006) 359-364.
- [27] J.S. Lee, W. Zhou, F.H. Meng, D.W. Zhang, C. Otto, J. Feijen, Thermosensitive hydrogel-containing polymersomes for controlled drug delivery. *J. Control. Release* 146(3) (2010) 400-408.
- [28] L.G. Cima, Polymer Substrates for Controlled Biological Interactions. *J. Cell. Biochem.* 56(2) (1994) 155-161.
- [29] T.M. Allen, C.B. Hansen, D.E.L. Demenezes, Pharmacokinetics of Long-Circulating Liposomes. *Adv. Drug Deliv. Rev.* 16(2-3) (1995) 267-284.
- [30] S.M. Moghimi, J. Szebeni, Stealth liposomes and long circulating nanoparticles: critical issues in pharmacokinetics, opsonization and protein-binding properties. *Prog. Lipid Res.* 42(6) (2003) 463-478.
- [31] H. Takeuchi, H. Kojima, H. Yamamoto, Y. Kawashima, Evaluation of circulation profiles of liposomes coated with hydrophilic polymers having different molecular weights in rats. *J. Control. Release* 75(1-2) (2001) 83-91.
- [32] S.A. Johnstone, D. Masin, L. Mayer, M.B. Bally, Surface-associated serum proteins inhibit the uptake of phosphatidylserine and poly(ethylene glycol) liposomes by mouse macrophages. *Biochim. Biophys. Acta-Biomembr.* 1513(1) (2001) 25-37.
- [33] S.I. Jeon, J.D. Andrade, Protein Surface Interactions in the Presence of Polyethylene Oxide .2. Effect of Protein Size. *J. Colloid Interface Sci.* 142(1) (1991) 159-166.
- [34] G. Montesano, R. Bartucci, S. Belsito, D. Marsh, L. Sportelli, Lipid membrane expansion and micelle formation by polymer-grafted lipids: Scaling with polymer length studied by spin-label electron spin resonance. *Biophys. J.* 80(3) (2001) 1372-1383.

- [35] C. Larsen, Dextran prodrugs - structure and stability in relation to therapeutic activity. *Adv. Drug Deliv. Rev.* 3 (1989) 103-154.
- [36] H. Maeda, J. Wu, T. Sawa, Y. Matsumura, K. Hori, Tumor vascular permeability and the EPR effect in macromolecular therapeutics: a review. *J. Control. Release* 65(1-2) (2000) 271-284.
- [37] C.J. Rijcken, C.J. Snel, R.M. Schiffelers, C.F. van Nostrum, W.E. Hennink, Hydrolysable core-crosslinked thermosensitive polymeric micelles: Synthesis, characterisation and in vivo studies. *Biomaterials* 28(36) (2007) 5581-5593.
- [38] D.B. Kirpotin, D.C. Drummond, Y. Shao, M.R. Shalaby, K.L. Hong, U.B. Nielsen, J.D. Marks, C.C. Benz, J.W. Park, Antibody targeting of long-circulating lipidic nanoparticles does not increase tumor localization but does increase internalization in animal models. *Cancer Res.* 66(13) (2006) 6732-6740.
- [39] A. Gabizon, R. Catane, B. Uziely, B. Kaufman, T. Safra, R. Cohen, F. Martin, A. Huang, Y. Barenholz, Prolonged Circulation Time and Enhanced Accumulation in Malignant Exudates of Doxorubicin Encapsulated in Polyethylene-Glycol Coated Liposomes. *Cancer Res.* 54(4) (1994) 987-992.
- [40] M.V. Pimm, S.J. Gribben, K. Bogdan, F. Hudecz, The Effect of Charge on the Biodistribution in Mice of Branched Polypeptides with a Poly(L-Lysine) Backbone Labeled with I-125, in-111 or Cr-51. *J. Control. Release* 37(1-2) (1995) 161-172.
- [41] D.A. Christian, O.B. Garbuzenko, T. Minko, D.E. Discher, Polymer Vesicles with a Red Cell-like Surface Charge: Microvascular Imaging and in vivo Tracking with Near-Infrared Fluorescence. *Macromol. Rapid Commun.* 31(2) (2010) 135-141.
- [42] S.D. Troster, J. Kreuter, Contact Angles of Surfactants with a Potential to Alter the Body Distribution of Colloidal Drug Carriers on Poly(Methyl Methacrylate) Surfaces. *Int. J. Pharm.* 45(1-2) (1988) 91-100.
- [43] L. Illum, S.S. Davis, The Organ Uptake of Intravenously Administered Colloidal Particles Can Be Altered Using a Non-Ionic Surfactant (Poloxamer-338). *FEBS Lett.* 167(1) (1984) 79-82.

## Conclusions and Future Perspectives

Polymersomes have received great attention as extremely interesting systems for various applications in the past decade. The increasing number of publications on polymersomes demonstrates such growing popularity (2000 papers mostly published during the last 5 years). Polymersomes are able to encapsulate hydrophilic, hydrophobic and amphiphilic molecules like any other vesicular structure, but their membrane tunability and superior stability are unique and undoubtedly beneficial for potential applications in drug delivery, gene therapy and protein delivery as well as medical diagnostics and nanoreactor technology. Polymersomes based on biodegradable di-block copolymers were developed for the controlled delivery of model lipophilic or hydrophilic drugs in the study. Release of model drugs from the polymersomes can be modulated by either using different block copolymer compositions for the formation of polymersomes or introducing stimuli-sensitive hydrogels in the polymersomes. The biodegradable polymersomes have long circulating times and an excellent colloidal stability in blood, yielding strong accumulation in tumor tissues in mice.

Recently, stimuli-responsive polymersomes of which the membrane permeability or the stability of the membrane can be changed by external stimuli have received a lot of attention. The design of these types of polymersomes remains a very interesting research area. Controlled release of drugs at the site of action will enhance the efficacy and reduce the side effects. The next generation of polymersomes will be polymersomes which selectively recognize specific cells or receptors within the biological system. The combination of the use of stimuli-responsive materials and targeting moieties will lead to polymersomes which can be targeted to the site of action and which will deliver the drug at this site by an external stimulus. As one of the candidates, peptide-containing polymersomes that are modified with an anti-epidermal growth factor receptor antibody has been reported in this thesis. These polymersomes can be selectively taken up by cancer cells via antibody-mediated endocytosis and subsequently release the therapeutic drug inside the cells via membrane destabilization of the polymersomes in the lysosomal compartments. The membrane destabilization will take place via cleavage by lysosomal enzymes of the peptide sequence between the hydrophilic and hydrophobic blocks of the amphiphilic block polymer, which forms the membrane.

However, it should be noted that extensive preclinical evaluations are required for these types of polymersomes before they can be considered to be used in patients. Subjects which have to be evaluated are the pharmacokinetics of drug loaded polymersomes, effect of the surface-located targeting molecules on the opsonization process and blood circulation times as well as the efficacy and toxicity of the polymersomes in particular after repeated administration. Mechanistic studies of the intracellular drug release from the polymersomes are also required to further unravel the kinetics of intracellular polymersome destabilization and intracellular drug release.

## Summary

In this thesis, the development and characterization of biodegradable and/or enzyme-triggered destabilizable polymersomes (Ps) for controlled and targeted drug delivery are presented. In **Chapter 1**, a general introduction, the aim of the study and structure of the thesis are given. Scientific background information on the criteria for the formation of Ps and methods for their characterization are discussed in **Chapter 2**. In this chapter, also the recent progress on and challenges for the design of biodegradable and/or stimuli-sensitive Ps in the field of drug delivery are reviewed.

In **Chapter 3**, the preparation of biodegradable Ps based on methoxy poly(ethylene glycol)-*b*-poly(*D,L*-lactide) (mPEG-PDLLA), methoxy poly(ethylene glycol)-*b*-poly( $\epsilon$ -caprolactone) (mPEG-PCL) or a mixture of the block copolymers in a weight ratio of 50:50 (abbreviated as Ps (L), Ps (C) and Ps (LC), respectively) is described. Oregon Green<sup>®</sup> 488 Labeled Paclitaxel (Flutax) was loaded as a model drug by dissolving block copolymers and Flutax in THF and injecting the THF solution into an aqueous phase. Flutax loaded Ps (Flutax-Ps) with a size less than 150 nm were obtained and the entrapment efficiencies of Flutax were higher than 55 % at a weight ratio of polymersomes to Flutax of 10. A sustained and complete release of Flutax was observed for Flutax-Ps (L) over one month, while Flutax was released much slower from Ps (C) (49.9 % after one month). The release rate of Flutax from Ps (LC) is in between those of Ps (L) and Ps (C). Flutax-Ps (L) cause about 67 % reduction in the viability of SKBR3 cells at a Flutax concentration of 5  $\mu\text{g/ml}$ , whereas empty Ps (L) show a low cell toxicity (10 %).

Hydrogel-containing Ps (Hs, hydrosomes) are reported in **Chapter 4**. PNIPAAm-containing Ps (N/Ps) were prepared by injecting a THF solution of mPEG-PDLLA and PNIPAAm into water to incorporate a PNIPAAm solution into Ps. At 37 °C, Hs with an average diameter of 127 nm were obtained. Confocal laser scanning microscopy (CLSM) and fluorescence correlation spectroscopy (FCS) of N/Ps revealed co-localization of the PNIPAAm and the Ps. For CLSM, dual-labeled N/Ps (rhodamine B (RB) in the membrane and fluorescein-conjugated PNIPAAm (FITC-N) in the aqueous core) were applied. Micron-sized giant Ps with a diameter of 5-10  $\mu\text{m}$  containing FITC-N were prepared using  $\text{CHCl}_3$  as the organic phase. The presence of FITC-N in these giant Ps as well as the phase separation of the internal FITC-N solution above the lower critical solution temperature (LCST) was also shown by CLSM. In the presence of the hydrogel

in the Ps, a sustained release of fluorescein isothiocyanate tagged dextran (FITC-dextran (MW 4000 g/mol), FD4) up to 30 d with a low initial burst effect was obtained while the release from bare Ps was completed after 6 d. The hydrogel formation of a PNIPAAm solution in Ps was further investigated by using time resolved fluorescence studies. The results of time-resolved fluorescence as well as the time-resolved fluorescence anisotropy of FITC-N in Ps as a function of temperature are given in **Chapter 5**. FITC-N encapsulated in Ps (FITC-N/Ps) shows a decrease of the rotational motion upon increasing the temperature. The long rotational correlation time ( $\phi_2$ ) of FITC-N increases 3 fold when raising the temperature from 15 °C to 40 °C, reflecting a reduced rotational mobility as a result of coil to globule transition. The residual anisotropy ( $r_\infty$ ) of FITC-N/Ps increases from 0.11 to 0.21, indicating that a transition from coil to globule takes place and the transition is followed by possible phase separation and hydrogel formation.

As presented in **Chapter 6**, novel peptide-containing Ps (Ps (pep)) have been developed and characterized. A peptide sequence, Phe-Gly-Leu-Phe-Gly (FGLFG) was introduced in between mPEG and PDLLA (mPEG-pep-PDLLA) and Ps (pep) with an average diameter of about 124 nm were prepared by injecting a THF solution of the block copolymer into DI water. Ps (pep) can be destabilized by the presence of lysosomal enzyme cathepsin B (Cath B) as a result of the enzymatic hydrolysis of the peptide linker. A gradual decrease in kilo counts per second (Kcps) of the Ps (pep) over 7 d was observed after incubation of the Ps (pep) dispersions with 5 units/ml of Cath B at pH 5.5 and 37 °C. The size distribution became also bimodal indicating that aggregation and precipitation of Ps (pep) occurred by disintegration of the Ps (pep). Acridine orange (AO) was encapsulated in Ps (pep) as a model drug and rapid release of AO triggered by Cath B degradation of Ps (pep) was observed at pH 5.5. The surface of Ps (pep) was further modified by coupling with anti-epidermal growth factor receptor antibody (abEGFR) to enhance their interaction with cells. The abEGFR immobilized Ps (pep) (abEGFR-Ps (pep)) were endocytosed more efficiently by SKBR3 cells than Ps (pep) without abEGFR. FD40 (FITC-dextran (MW 40,000 g/mol)) was encapsulated in the Ps (pep) and intracellular release of FD40 was observed suggesting that disruption of the Ps (pep) membranes also took place in the cells.

In **Chapter 7**, the results of *in vivo* studies of Ps prepared from PEG-PDLLA in tumor-bearing mice are compared with those of stealth liposomes. The effects of the surface charge of the Ps on circulation kinetics, organ distribution and tumor accumulation were evaluated. The Ps

were dually labeled by encapsulating  $^3\text{H}$ -dextran (70,000 g/mol) in the aqueous core and by post-coupling of  $^{14}\text{C}$ -thioglycolic acid onto acrylated PEG chains of the Ps. Stealth liposomes (103 nm, -6 mV) based on dipalmitoyl phosphatidylcholine (DPPC)/cholesterol with 7.5 % of PEG distearoyl phosphatidylethanolamine (PEG-DSPE) were prepared for the comparison. A substantial longer half lifetime ( $\tau_{1/2}$ ) (47.3 h) and a reduced liver uptake (27.9 % of injected dose (% ID)) of Ps with a zeta potential of -7.6 mV were observed as compared to those of stealth liposomes (10.6 h, 39.8 % ID). As a result of their longer circulation times, a high tumor accumulation of 18.6 % ID was obtained for these Ps after 3 d circulation, while only 11.2 % ID of stealth liposomes accumulated in the tumors because of their relatively short  $\tau_{1/2}$ . By increasing the zeta potential on the Ps, more rapid clearance of Ps from the blood circulation was found due to an enhanced uptake by the liver. Co-localization of the two labels of Ps was observed during circulation indicating that dual labeled Ps were colloidally stable in blood without leakage of  $^3\text{H}$ -dextran.



## Samenvatting

In dit proefschrift worden de ontwikkeling en karakterisering beschreven van biodegradeerbare en/of door enzymen destabiliseerbare polymersomen (Ps) voor gecontroleerde en gerichte medicijnafgifte. **Hoofdstuk 1** bevat een algemene inleiding, het doel van de studie en de structuur van het proefschrift. Wetenschappelijke achtergrondinformatie betreffende de voorwaarden voor de vorming van Ps en methoden voor hun karakterisering worden behandeld in Hoofdstuk 2. In dit hoofdstuk worden ook recente ontwikkelingen en toekomstige uitdagingen besproken betreffende het ontwerp van biodegradeerbare en/of stimulus gevoelige Ps voor medicijnafgifte.

**Hoofdstuk 3** behandelt de synthese van biodegradeerbare Ps gebaseerd op methoxy poly(ethyleen glycol)-b-poly(*D,L*-lactide) (mPEG-PDLLA), methoxy poly(ethyleen glycol)-b-poly( $\epsilon$ -caprolacton) (mPEG-PCL) of een combinatie van deze blokcopolymeren met een gewichtsverdeling van 50:50 (respectievelijk afgekort als Ps (L), Ps (C) en Ps (LC)). Oregon green<sup>®</sup> 488 gelabeld PTX (Flutax) werd geïncorporeerd als model medicijn door de blok copolymeren en Flutax in THF op te lossen en de THF oplossing te injecteren in een waterfase. Er werden Flutax-beladen Ps verkregen (Flutax-Ps) met afmetingen kleiner dan 150 nm, en meer dan 55 % van het aangeboden Flutax werd opgenomen (gewichtsverhouding polymersomen/Flutax 10). Een constante en volledige afgifte van Flutax werd gevonden voor Flutax-Ps (L) gedurende 1 maand terwijl Flutax veel langzamer werd afgegeven vanuit Ps (C) (49.9 % na 1 maand). De afgiftesnelheid van Flutax uit Ps (LC) ligt tussen die van Ps (L) en Ps (C) in. Flutax-Ps (L) veroorzaken een afname van ongeveer 67 % in de levensvatbaarheid van SKBR3 cellen bij een Flutax concentratie van 5  $\mu$ g/ml terwijl ongeladen Ps (L) een lage cel toxiciteit laten zien (10 % afname).

Hydrogel-bevattende Ps (Hs, hydrosomen) worden besproken in **Hoofdstuk 4**. PNIPAAm-bevattende Ps (N/Ps) werden gemaakt door een THF oplossing van mPEG-PDLLA en PNIPAAm te injecteren in water om zo de PNIPAAm oplossing in Ps te incorporeren. Bij 37 °C werden Hs met een gemiddelde diameter van 127 nm verkregen. Confocale laser scanning microscopie (CLSM) en fluorescentie correlatie microscopie (FCS) van N/Ps toonden aan dat colocalisatie van PNIPAAm en de Ps optrad. Voor de CLSM metingen werden tweevoudig gelabelde N/Ps (rhodamine B (RB) in het membraan en FITC-N in de waterrijke kern) gebruikt.

FITC-N bevattende reuzen-Ps met een diameter van 5-10  $\mu\text{m}$  werden verkregen door  $\text{CHCl}_3$  als organische fase te gebruiken. De aanwezigheid van FITC-N in deze reuzen-Ps alsmede de fase scheiding van de interne FITC-N oplossing boven de laagste kritische oplossingstemperatuur (LCST) werden ook aangetoond met CLSM. In aanwezigheid van de hydrogel in de Ps werd een constante afgifte van fluoresceïne isothiocyanaat gelabeld dextraan (FD4, FITC-dextraan (MW 4000 g/mol)) bereikt gedurende 30 dagen met een laag initieel ‘burst’ effect, terwijl de afgifte vanuit ongeladen Ps volledig was na 6 dagen. De hydrogel vorming van een PNIPAAm oplossing in Ps werd verder onderzocht met behulp van tijdsopgeloste fluorescentie experimenten. De resultaten van de tijdsopgeloste fluorescentie evenals van de tijdsopgeloste fluorescentie anisotropie van FITC-gelabelde PNIPAAm (FITC-N) in Ps als functie van de temperatuur worden gepresenteerd in **Hoofdstuk 5**. FITC-N opgenomen in Ps (FITC-N/Ps) vertoont een afname van de rotatiebeweging als de temperatuur stijgt. De lange rotatie correlatie tijd ( $\phi_2$ ) van FITC-N verdrievoudigt als de temperatuur stijgt van 15 °C naar 40 °C. Dit wijst op een verminderde rotatiemobiliteit van FITC-N als gevolg van een overgang van een ‘coil’ naar een ‘globule’ conformatie. De resterende anisotropie ( $r_\infty$ ) van FITC-N/Ps neemt toe van 0.11 tot 0.21 hetgeen aantoont dat er een overgang van ‘coil’ naar ‘globule’ optreedt en dat de overgang mogelijk gevolgd wordt door fase scheiding en hydrogel vorming.

**Hoofdstuk 6** behandelt de ontwikkeling en karakterisering van nieuwe peptide-bevattende Ps (Ps (pep)). Een peptide sequentie, Phe-Gly-Leu-Phe-Gly (FGLFG), werd tussen mPEG en PDLA geplaatst (mPEG-pep-PDLA) en Ps (pep) met een gemiddelde diameter van ongeveer 124 nm werden verkregen door een THF oplossing van het blok copolymeer in demiwater te injecteren. Ps (pep) kunnen worden gedestabiliseerd door de aanwezigheid van het lysozomaal enzym cathepsin B (Cath B) als gevolg van de enzymatische splitsing van de peptide linker. Een geleidelijke afname in kilo counts per seconde (Kcps) van de Ps (pep) gedurende 7 d werd gevonden na incubatie van de Ps (pep) dispersies met 5 units/ml Cath B bij pH 5.5 en 37 °C. De deeltjesgrootte verdeling werd ook bimodaal wat aangeeft dat aggregatie en precipitatie van Ps (pep) optrad als gevolg van desintegratie van de Ps (pep). Acridine orange (AO) werd opgenomen in Ps (pep) als model medicijn en een snelle afgifte van AO werd waargenomen als gevolg van de door Cath B geïnduceerde degradatie van Ps (pep) bij pH 5.5. Het oppervlak van Ps (pep) werd verder gemodificeerd door koppeling met anti-epidermaal groeifactor receptor antilichaam (abEGFR) om de interactie van de Ps met de cellen te verbeteren. De Ps (pep) met

gekoppeld abEGFR (abEGFR-Ps (pep)) werden efficiënter opgenomen in SKBR3 cellen dan Ps (pep) zonder abEGFR. FD40 (FITC-dextraan, MW 40,000 g/mol) werd opgenomen in de Ps (pep) waarna er een intracellulaire afgifte van FD40 werd waargenomen, wat suggereert dat beschadiging van de Ps (pep) membranen ook in de cellen optrad.

In **Hoofdstuk 7** worden de resultaten van *in vivo* experimenten met Ps gemaakt van PEG-PDLLA in muizen met tumoren vergeleken met die van stealth liposomen. De effecten van de oppervlaktelading van Ps op de circulatie kinetiek, de verdeling over organen en de ophoping in tumoren werden onderzocht. De Ps werden tweevoudig gelabeld door <sup>3</sup>H-dextraan (MW 70,000 g/mol) in de waterrijke kern op te nemen en door koppeling van <sup>14</sup>C-thioglycolzuur aan geäcryleerde PEG ketens van de Ps. Stealth liposomen (103 nm, -6 mV) gebaseerd op dipalmitoyl phosphatidylcholine (DPPC)/cholesterol met 7.5 % PEG distearoyl phosphatidylethanolamine (PEG-DSPE) werden gemaakt als vergelijkingsmateriaal. Een duidelijke langere halfwaardetijd ( $\tau_{1/2}$ ) van 47.3 uren en een verminderde opname door de lever (27.9 % van de geïnjecteerde dosis (% ID)) werden waargenomen bij gebruik van Ps met een zeta potentiaal van -7.6 mV vergeleken met die van stealth liposomen (10.6 uren, 39.8 % ID). Als gevolg van hun langere circulatietijd werd een hogere opname in de tumor (18.6 % ID) gevonden voor deze Ps na 3 d circulatie terwijl slechts 11.2 % ID stealth liposomen terechtkwam in de tumoren vanwege hun relatief korte  $\tau_{1/2}$ . Bij verhoging van de zeta potentiaal van de Ps werd een snellere verwijdering van Ps uit de bloedsomloop waargenomen als gevolg van een verhoogde opname door de lever. Er werd co-lokalisatie van de twee labels van Ps in de bloedsomloop waargenomen, wat aangeeft dat de tweevoudig gelabelde Ps colloïdaal stabiel waren in bloed en dat er geen lekkage van <sup>3</sup>H-dextraan plaats vond.

## Acknowledgements

In 2006, I started my PhD study in the group of Polymer Chemistry and Biomaterials (PBM) of the University of Twente. I still remember how my heart was fluttering with a new life, job, friends and colleagues in the Netherlands. Four years have flown like an arrow and now time almost comes to the end of my PhD period. This thesis includes my four-year research work and each piece of work has been accomplished with the contribution and support of many people. It is very pleasant that I have the opportunity to express my gratitude for all of them.

First of all, I would like to express my immeasurable gratitude to Prof. Jan Feijen, my promoter as well as daily supervisor, for giving me the opportunity to pursue my PhD at the PBM group. I cannot emphasize enough how much you are important to me. I deeply appreciate your guidance and supervision. Your intellectual insights, the depth and breadth of your knowledge have always impressed me and taught me how to really carry out research. You are one of the greatest scientists I ever knew. As a supervisor, you are always very active and supportive. I was able to discuss research plans, results and manuscripts with you when I wanted. You are always pleasant to travel all around the Netherlands with me for our external collaborations. I could not forget the time we smoked and talked together in your car. Thank you very much for your trust in me and for your continuous support. Of course, my PhD thesis could not be completed without you. I wish you all the best with your life and family and I hope we will have the opportunity to meet each other again in the future.

My special gratefulness goes to Fenghua Meng (my former supervisor) and Wei Zhou (former PhD student of PBM group). You have developed and characterized novel biodegradable polymersomes, allowing me to continuously investigate them during my PhD. I did enjoy our discussions and it really helped a lot on my research work. Fenghua, I still remember my first night in the Netherlands, which was rainy and gloomy. You and your husband, Prof. Zhiyuan Zhong, picked me up from Hengelo train station. You gave me very kind words, ride to the campus and even something to eat. It was very kind of you!! I really hope that I visit China to see you and your family.

I would like to express my sincere thanks to the scientific staff of our group. Prof. Johan Engbersen and Prof. Dirk Grijpma, you are always enthusiastic about my research and asking critical questions that help me to improve it. Especially, I would like to thank Prof. Johan

Engbersen for kindly agreeing to be a member of my PhD defense committee. Piet Dijkstra and Andre Poot, thank you for your help whenever I asked any questions.

I am also thankful to the members of my PhD committee, Prof. Jurriaan Huskens, Prof. Wim E. Hennink, Prof. Cor E. Koning, Prof. Roeland J. M. Nolte, Prof. Leo H. Koole, Dr. Cees Otto and Prof. Johan Engbersen for the precious time for reading the thesis and for their valuable contributions.

Some parts of the work presented in this thesis could not have been done without the contributions of my collaborators. I would like to thank Dianwen Zhang and Cees Otto (Biophysical Engineering Group, University of Twente), co-authors of Chapter 4, for performing fluorescence correlation spectroscopy and for your effort to increase the quality of the manuscripts. I am thankful to Prof. Herbert van Amerongen and Rob B. M. Koehorst (Laboratory of Biophysics, Wageningen University), co-authors of Chapter 5, for your collaboration on Time-Resolved Fluorescence and Fluorescence Anisotropy. Tom Groothuis (co-author of Chapter 6) and Wilma Petersen from the Nanobiophysics group at the University of Twente, thank you very much for your help on the cell experiments and fluorescence microscopy. I learned a lot on cell biology from you. Thank you, Claudia Cusan (co-author of Chapter 6, DSM Pharmaceutical Products, Innovative Synthesis & Catalysis), for preparing poly(ethylene glycol)-peptide conjugate. I am sure that we will have a great paper together. I would also like to thank co-authors of Chapter 7, Prof. Wim E. Hennink, Raymond M. Schiffelers, Ebel Pieters (Utrecht Institute for Pharmaceutical Sciences at Utrecht University) and especially Marc Ankoné (BMC and BST, University of Twente). I appreciate your contributions and guidance on the animal study using radioactive molecules. We have nicely submitted our work as a special issue in *Journal of Controlled Release*. Thank you, Mark Smithers (MESA<sup>+</sup>, University of Twente) for TEM measurements and Clemens Padberg (MTP, University of Twente) for GPC analysis. I would like to express my special gratitude to Martin Bennink (Nanobiophysics Group, University of Twente) for coordinating my PhD project.

There are also many people, who I should not forget. Thank you so much, Karin. You are one of the best persons I ever met. You are always kindly helping me out not only in the administration work, but also for my personal concerns. You come to work very early and go home rather late because you have so many things to do, but you never complained when I asked for anything. Thanks Zlata, you have done a very good job in handling chemicals. Hetty and

Anita, thank you for helping with financial and IT problems, AFM and GPC measurements. Sytze Buwalda and Jos Wennink, thank you very much for being my paranymphs and for the translation of the Samenvatting. Niels, my former officemate, it was always pleasant to talk with you and thank you for translating my Dutch mails. Thank you, Erhan and Ferry for your help and guidance for my thesis and for preparing my PhD defense. Erwin, thank you very much for your nice artwork. You made a beautiful 3D image of the polymersomes discussed in Chapter 2. I would like to thank all the former and present group members for their support and company during coffee break and many parties, especially Martin, Hans, Vincent, Mark, Sigrid, Di, Dewi, Marloes, Chao, Rong, Janine, Gert-Jan, Xiaolin, Hongzhi, Sandra, Andries and Guoying.

Marc and Arkadiy, my friends, I could never forget you smoking, drinking and chatting together. I will miss you guys. Please come to Korea. I will make a great time for you. Hao and Lanti, my good friends, we helped each other a lot and I did enjoy the time with the two of you. You are my best Chinese friends. Dae June, my best friend, we know each other for 15 years, almost half of my life. I was happy to have you here in the Netherlands with me. We have encouraged each other in a foreign country-life and relied on one another pretty much. I believe that we will share our life to the end. Thank you very much and I give my best wishes for your PhD and bright future.

I would really love to give my special gratefulness to Prof. Ki Dong Park and Piet Dijkstra for introducing me to the PBM group. You always gave me kind advices, thoughtful suggestions and constant help for any of the problems in my life and career. I always feel like you are my fathers.

Finally, I deeply thank my parents, Tae Min Lee and Yeon Ju Kim, and my younger sister, Goun Lee, for their endless love, support, understanding and encouragement. I dedicate this thesis to my wife, Soo Hyun Lim, and my little princess, Eun Ji Lee.

Jung Seok Lee

May, 2011

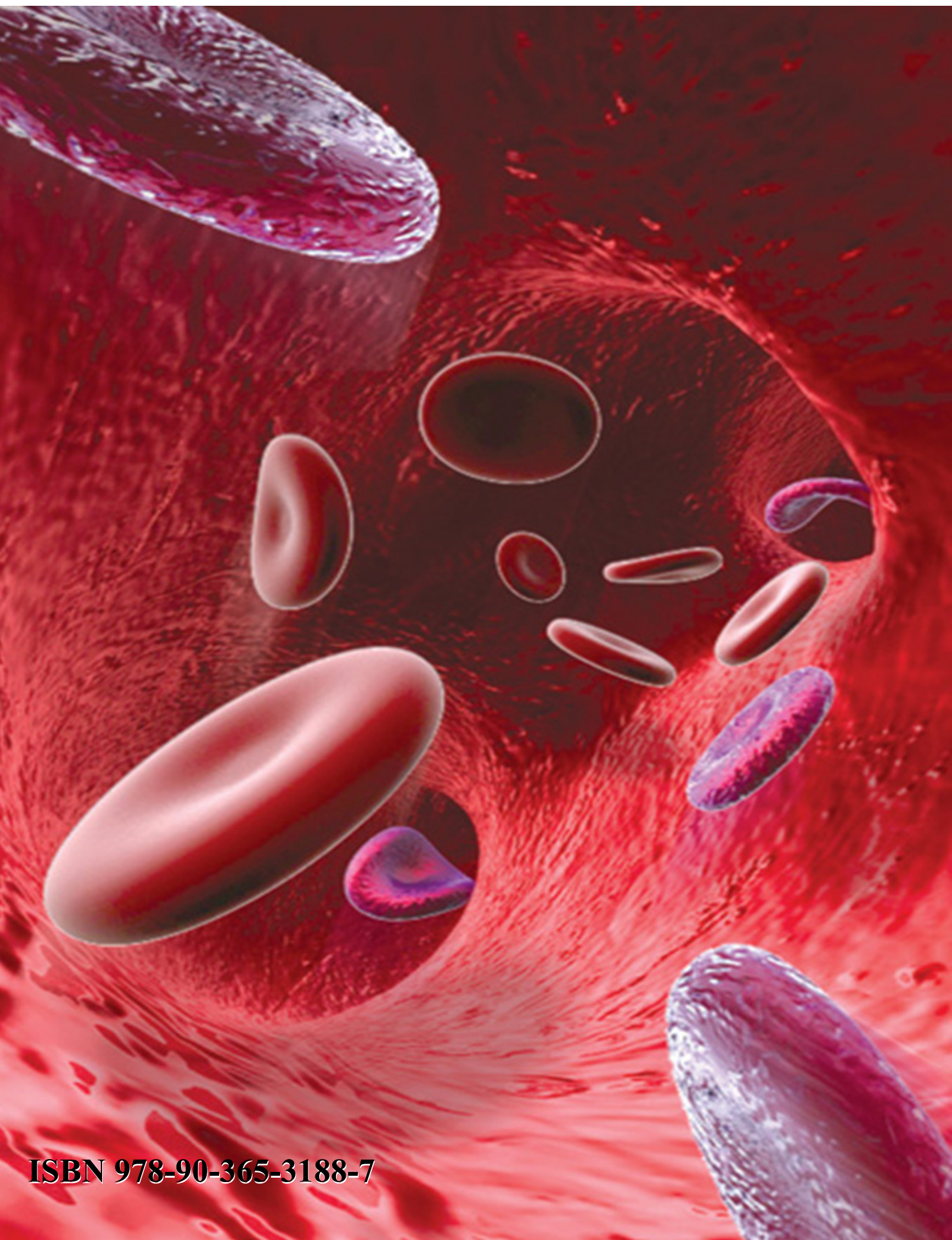
Enschede

## *Curriculum Vitae*

Jung Seok Lee was born on the 12th of December 1978 in Mokpo, South Korea and lived there until he graduated Mokpo High School. From 1997, he studied Applied Chemistry at Ajou University in Suwon, South Korea. In 2004, he received a Bachelor degree and continued studying Polymer Chemistry in the Department of Molecular Science and Technology at the same university under the supervision of Prof. Ki Dong Park. He worked on heparin conjugated polymeric micelles for controlled delivery of antiphlogistic drugs and growth factors and obtained his Master degree of Materials and Chemistry in 2006. Thereafter, he joined the Polymer Chemistry and Biomaterials group at the University of Twente (Enschede, The Netherlands) to pursue his PhD degree under the supervision of Prof. Jan Feijen. His research work has been directed to the development of novel polymeric nanocarriers for drug delivery systems. He is experienced in the design and synthesis of novel biodegradable and/or stimuli-sensitive polymeric biomaterials and the preparation of nanocarriers and 3D networks with drugs or bioactive molecules. Pharmacokinetic studies, cell experiments and animal studies using radioactive labels have been carried out in his PhD projects. He is the author of 6 publications and 2 patents. Moreover, 1 review and 4 articles have been submitted or will be submitted shortly.







**ISBN 978-90-365-3188-7**